Università degli Studi della Calabria

Facoltà di Farmacia e Scienze della Nutrizione e della Salute
Dipartimento Farmaco-Biologico (MED/04 PATOLOGIA GENERALE)

Dottorato di Ricerca in "Biochimica Cellulare ed Attività dei Farmaci in Oncologia" (XIX ciclo)

IGF-I regulating aromatase expression through SF-1 supports estrogen-dependent tumor Leydig cell proliferation

Docente Tutor
Ch.mo Prof. Vincenzo PEZZI

Coordinatore
Ch.mo Prof. Sebastiano ANDO'

Dottoranda
D.ssa Rosa SIRIANNI

Anno Accademico 2005-2006

INDEX

Scientific Publications

Differential expression of steroidogenic factor-1/adrenal 4 binding protein and liver receptor homolog-1 (LRH-1)/fetoprotein transcription factor in the rat testis: LRH-1 as a potential regulator of testicular aromatase expression.

Corticotropin-releasing hormone directly stimulates cortisol and the cortisol biosynthetic pathway in human fetal adrenal cells.

Corticotropin-releasing hormone (CRH) and urocortin act through

type 1 CRH receptors to stimulate dehydroepiandrosterone sulfate production in human fetal adrenal cells.

Antiestrogens upregulate estrogen receptor beta expression and inhibit adrenocortical H295R cell proliferation.

The AP-1 complex: a negative regulator of CYP17 transcription in adrenal cells.

IGF-I regulating aromatase expression through SF-1, supports estrogen dependent tumor Leydig cell proliferation.

Summary

Aim of this study was to investigate the role of estrogens in Leydig cell tumor proliferation. We used rat R2C Leydig tumor cells and testicular samples from Fischer rats with a developed Leydig tumor (FRTT). Both experimental models express high levels of aromatase and Estrogen Receptor alpha (ERα). Treatment with exogenous E2 induced proliferation of R2C cells and upregulation of cell cycle regulators cyclin D1 and E, that were blocked by addition of antiestrogens. These observations leaded us to suppose an E2/ERα dependent mechanism for Leydig cell tumor proliferation. Determining the molecular mechanism responsible for aromatase overexpression, we found that total and phosphorylated levels of transcription factors CREB and SF-1 were higher in tumor samples. Moreover, we found that R2C cells produce also high levels of IGF-I that increased aromatase mRNA, protein and activity as a consequence of increased total and phosphorylated SF-1 levels and that specific inhibitors for IGF-I receptor, Protein Kinase C and Phosphoinositol-3-kinase determined a reduction in SF1 and consequently in aromatase expression and activity. The same inhibitors were also able to inhibit the IGF-1 dependent-SF-1 recruitment to the aromatase PII promoter as shown with ChIP assays. We conclude that one of the molecular mechanims determining Leydig cell tumorogenesis is an excessive estrogen production stimulating a short autocrine loop determining cell proliferation. In addition, cell produced IGF-I amplifies estrogen signaling through a SF-1-dependent up-regulation of aromatase expression. The finding of this new molecular mechanism will be helpful in defining new therapeutic approaches of Leydig cell tumor.

Introduction

1. The testis

1.1 Anatomy

In mammalian species both testicular compartments consist of a variety of different cell types (1). The Sertoli cells comprise the main structural component of the seminiferous epithelium. They are responsible for the physical support of the germ cells, in addition to providing nutrients and growth factors. The germ cells are sequentially organised into several layers signifying the respective mitotic or meiotic processes and spermatid development. Each seminiferous tubule is surrounded by mesenchymal cells. Among these are the peritubular myoid cells whose contractile elements generate peristaltic waves along the tubules, but do not present a tight diffusion barrier. The interstitium is populated by androgen-producing Leydig cells which are heterogeneous in respect to their physiological and structural features. Vascular smooth muscle cells, macrophages and endothelial cell types are also located in the interstitial space of the testis. The physiological role of macrophages has long been underestimated. In the rat, the number of macrophages is one quarter of the number of Leydig cells and the presence of macrophages is crucial for (re)population of Leydig cells during development and after experimental depletion (2;3). Immune cells, known to secrete a number of growth factors and cytokines, are part of the intratesticular communication pathways (4).

1.2 Testicular function and its regulation

Testes are components of both the reproductive system (being gonads) and the endocrine system (being endocrine glands). The respective functions of the testicles are:

1. producing sperm (spermatozoa)
2. producing male sex hormones

These two functions occur in separate compartments within the testis: 1. the seminiferous tubules produce sperm and 2. the interstitial cells (i.e., Leydig cells) synthesize androgens (**Fig. 1**).

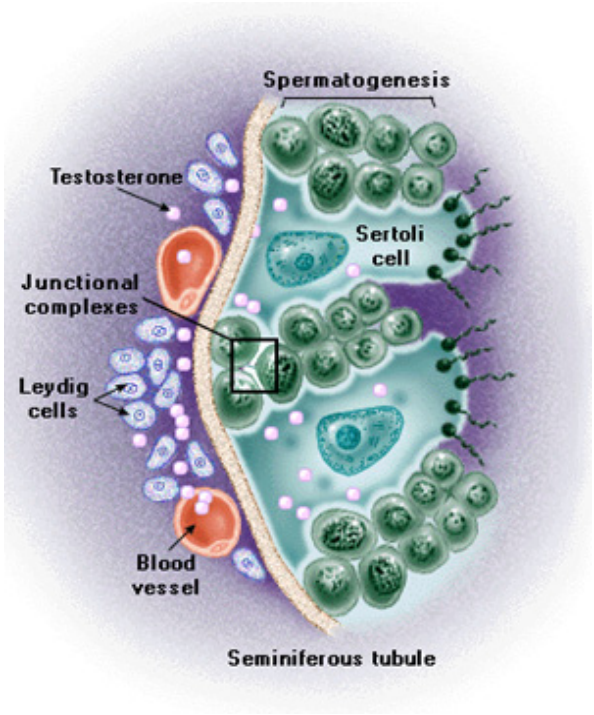

Figure 1. Schematic representation of functions of the testis.

Both functions of the testis, sperm-forming and endocrine, are under control of gonadotropic hormones produced by the anterior pituitary: luteinizing hormone (LH) and follicle-stimulating hormone (FSH).

Synthesis and release of both FSH and LH is regulated by a single gonadotropin releasing hormone (GnRH) also referred to as LHRH. GnRH is a decapeptide secreted from hypothalamic neurons into the hypothalamic/hypophysial portal vessels. LH and FSH secretion is subject to negative feedback control by the testis. At least two products of the testis are involved. LH acts to stimulate Leydig cells to produce testosterone which, in turn, inhibits further secretion of LH by inhibition of GnRH release from the hypothalamus. Testosterone also decreases the responsiveness of the pituitary to GnRH (**Fig. 2**).

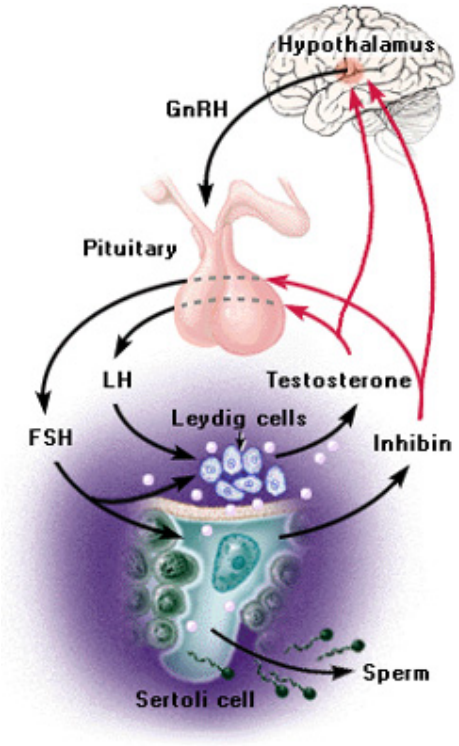

Figure 2. Hypothalamic-Pituitary-Testicular axis.

LH, through specific receptors found on the surface of Leydig cells, controls the production and secretion of testosterone (5;6). The interaction of LH with its receptor, a seven transmembrane domain G protein coupled receptor, initiates signalling through the cyclic AMP pathway through GTP binding proteins (7;8). Signal transduction occurs through the protein kinase A pathway as its principal signal transduction mechanism.

The testis is also able to produce growth factors that can act with an autocrine/paracrine manner (9). Some factors induce specific differentiation steps, while others act primarily as environmental or survival factors. Insulin-like growth factor (IGF) family which includes three structurally related peptides: insulin, IGF-I (also called somatomedin C) and IGF-II belongs to the second group of factors. The receptor for IGF-I has been found on most testicular cell types, including rat and human Sertoli cells, Leydig cells and pachytene spermatocytes (4;10-12), indicating a more general role such as the stimulation of

steroidogenesis in Leydig cells (13-16). IGF-I is produced locally in the testis, in Sertoli, Leydig and peritubular cells derived from the immature rat testis and cultured in vitro (17;18). The crucial role of IGF-I in the development and function of Leydig cells was highlighted by studies on IGF-I gene knock-out mice (19;20). The failure of adult Leydig cells to mature and the reduced capacity for T production is caused by deregulated expression of testosterone (T) biosynthetic and metabolizing enzymes (21). Expression levels of all mRNA species associated with T biosynthesis were lower in the absence of IGF-I.

1.3 Steroid production

The pathway of testosterone synthesis from cholesterol and the conversion of testosterone to active androgen and estrogen metabolites is shown in **Figure 3**. The mobilization of cellular sources of cholesterol is achieved through the action of cholesterol ester hydrolase and subsequently, this is converted to pregnenolone by the enzyme cholesterol side-chain cleavage termed cytochrome P450SCC (22). The conversion of cholesterol to pregnenolone is a key step at which regulation of androgen production within the Leydig cells occurs. Availability of cholesterol substrate can be rate-limiting and the intracellular trafficking of cholesterol across mitochondrial membranes is dependent on the steroidogenic acute regulatory protein (STAR) (23-25). The role of this protein has been well demonstrated in patients with mutations in the gene encoding STAR in the disorder termed congenital lipoid adrenal hyperplasia wherein the mitochondria from the adrenals and gonads of these patients are unable to convert cholesterol to pregnenolone (26). Further, the results of studies involving targeted disruption of the mouse gene encoding STAR support the data derived from human studies (27).

Intracellular transport of steroid substrates involved in androgen production is the transport of cholesterol into the mitochondrion to form pregnenolone and the transport of pregnenolone to smooth endoplasmic reticulum for the remainder of the steps in the production of testosterone. Pregnenolone may progress to testosterone production through two pathways. It can be converted to progesterone through the enzyme 3β-hydroxysteroid

dehydrogenase (the Δ4 pathway) or can be hydroxylated at the 17α position by the enzyme 17α-hydroxylase to form 17α-hydroxypregnenolone (the Δ5 pathway). The relative importance of these two pathways vary with the species and the physiological status of the male (28). The further conversion of 17α-hydroxypregnenolone through the Δ5 pathway involves the formation of the C19 steroid dehydroepiandrosterone catalyzed by the enzyme 17,20 lyase and both steps appear to be catalyzed by a single microsomal enzyme cytochrome P450c17 encoded by a single copy gene (29;30). The conversion of dehydroepiandrosterone to androstenediol is mediated by a microsomal enzyme 17β-hydroxysteroid dehydrogenase encoded by a single gene (31;32). The conversion of substrates from the Δ5 to the Δ4 pathway are catalyzed by the enzyme 3β-hydroxysteroid dehydrogenase (33). In the Δ4 pathway 17α-hydroxyprogesterone proceeds through the action of cytochrome P450c17 to androstenedione and testosterone. Testosterone can be converted to a dihydrotestosterone by the enzyme 5α-reductase (34) or can be metabolised to 17β-estradiol by the enzyme aromatase (35).

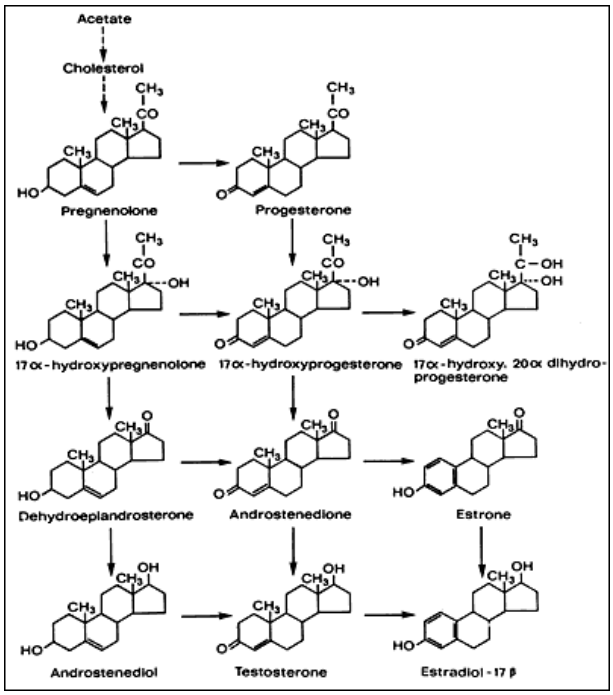

Figure 3. Steps in steroidogenesis leading to androgens and estrogens production.

2. Estrogen biosynthesis and action

2.1 The aromatase gene: structure and regulation

In males, estrogens derive from circulating androgens. Aromatization of the C19 androgens, testosterone and androstenedione, to form estradiol and estrone, respectively, is the key step in estrogen biosynthesis, which is under the control of the aromatase enzyme. The aromatase enzyme is a P450 mono-oxygenase enzyme complex present in the smooth endoplasmic reticulum which acts through three consecutive hydroxylation reactions, whose final effect is the aromatization of the A ring of androgens (**Fig. 4**).

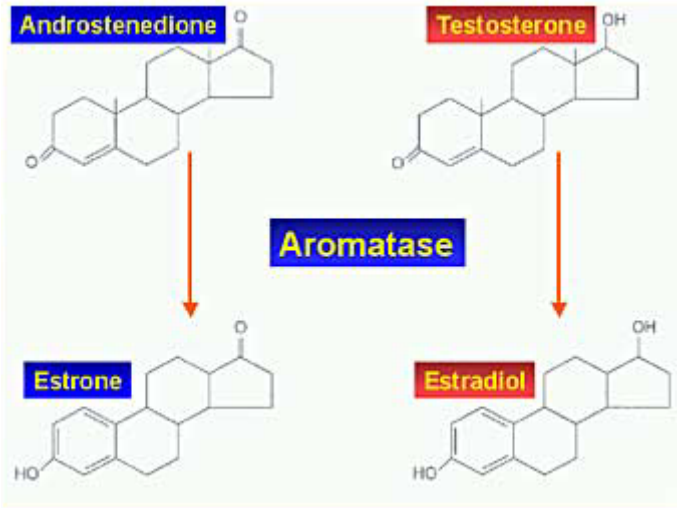

Figure 4: Biochemical pathway of testosterone conversion into estrogens.

P450 aromatase is the product of the CYP19 gene which consists of at least 16 exons and is located on chromosome 15 in humans (36;37) (**Fig. 5**). Analysis of transcript and genomic sequences indicates that the tissue-specific expression of P450arom is regulated in part by alternatively spliced untranslated first exons (38;39). The proximal promoter PII

regulates P450arom expression in mammalian gonads (40;41) as well as in Leydig cell tumors (42). Promoter PII activity (fig. 5) is regulated by cyclic AMP and requires the transcription factors cAMP responsive element binding protein (CREB), cAMP response element modulator (CREM) and steroidogenic factor-1 (SF-1). SF-1 belongs to the nuclear orphan receptor superfamily and regulates steroidogenic gene transcription.

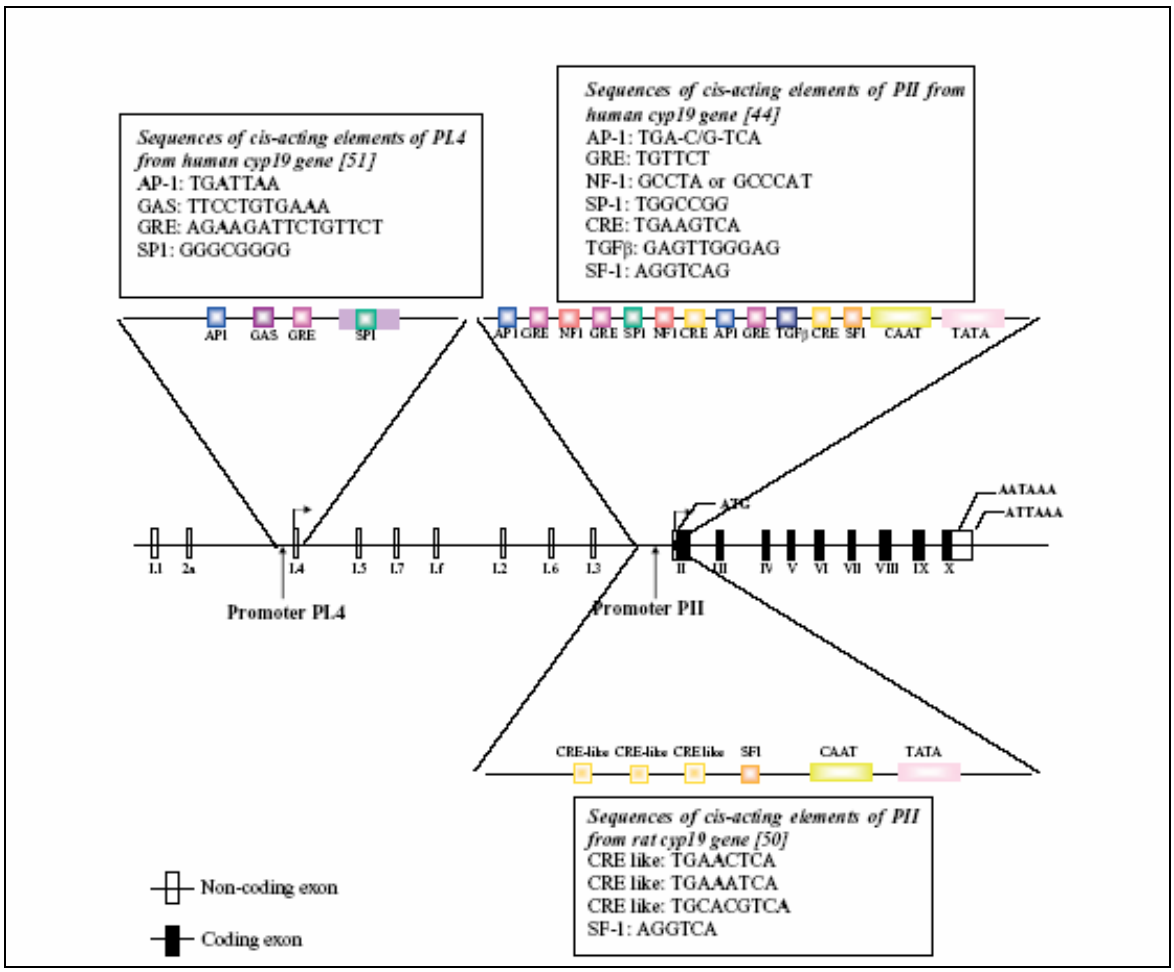

Figure 5: Structure of the human Cyp19 gene showing the various untranslated first exons and their corresponding promoters. The region around promoter PI.4 and PII from human and PII from rat are expanded to show the identified response elements. Sequences of these are shown in boxes.

2.2 The Estrogen Receptors (ERs)

Estrogens actions are mediated through the specific binding to nuclear estrogen receptors (ERs), which are ligand-inducible transcription factors regulating the expression of target genes after hormone binding. Two subtypes of ERs have been described: estrogen receptor α (ERα) and the more recently discovered estrogen receptor β (ERβ). The two ER (α and β) proteins have a high degree of homology at the amino acid level (**Fig. 6**).

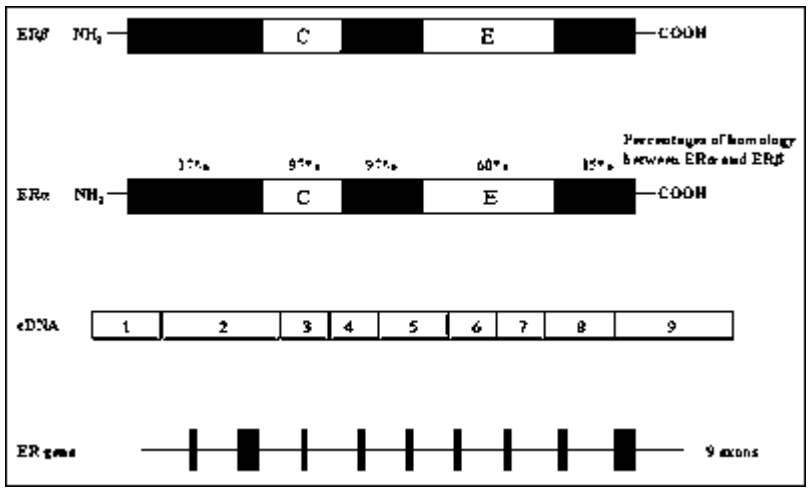

Figure 6: ERs genes and their products.

While it is clear that estrogens regulate transcription via a nuclear interaction after binding their receptors, a non-genomic action of estrogens has been recently demonstrated, suggesting that a different molecular mechanism accounts for some estrogen actions. In vitro studies showed a very short latency time between the administration of estrogens and the appearance of biological effects. These actions are thought to be mediated through cell-surface receptors, which are not believed to act via a transcriptional mechanism (43).

2.3 Distribution of ERs and aromatase in the male reproductive system

ERs and the aromatase enzyme are widely expressed in the male reproductive tract in both animals and humans, implying that estrogen biosynthesis occurs in the male reproductive

tract and that both locally produced and circulating estrogens may interact with ERs in an intracrine/paracrine and/or endocrine fashion (43). The concept of a key estrogen action in the male reproductive tract is strongly supported by the fact that male reproductive structures are able to produce and respond to estrogens (44).

In particular in the adult rodent testisERα is expressed in the Leydig cells of both adult rats and mice (45) but not in Sertoli cells. Knowledge of the distribution of ERα is of great importance in understanding estrogen action on the male reproductive tract. ERα is highly expressed in the proximal reproductive ducts (rete testis, efferent ductules, proximal epididymis) and its expression progressively decreases distally (corpus and cauda of the epidydimis, vas deferens). The highest degree of ERα expression is seen in the efferent ductules of the rat (46) and accounts for one of the most well-documented estrogenic actions on male reproductive system, that of fluid reabsorption from the efferent ductules. It has to be remarked that the concentration of ERα in the male reproductive tract is opposite to that of ERβ, which is more concentrated in the distal tract (**Table 1**).

Table 1. ERs and Aromatase distribution in the adult rodent testis.

	ERα	**ERβ**	**Aromatase**
Leydig cells	+/-	+/-	+++
Sertoli cells	-	+	+
Germ cells	+/-	++	++++
Spermatogonia	-	+	+ (?)
Pachytene Spermatocytes	-/+	+	+
Round Spermatids	-/+	+	++
Spermatozoa	+ (?)	+ (?)	+
efferent ductules	++++	+	- (?)

ERβ is expressed in Leydig, Sertoli and germ cells in adult rodents (44;47-49) and has also been detected in primate germ cells (50). There is now considerable evidence that germ cells contain both ERβ and aromatase (44;50).

By adulthood, rodent Leydig cells show higher aromatase activity compared to every other age and in comparison to Sertoli cells (51). Aromatase is also expressed at high levels in germ cells throughout all stages of maturation, and its expression appears to increase as the germ cell becomes a mature spermatid.

2.4 Aromatase over-expression in rodents

Recently a transgenic line of mice overexpressing aromatase enzyme (AROM+) has been developed (52;53). These mice show highly elevated serum estradiol concentrations, with a reciprocal decrease in testosterone concentrations. About half of these male mice were infertile and/or had enlarged testis and showed Leydig cell hyperplasia and Leydig cell tumors (54) while the female of these mice revealed mammary glands hyperplasia associated with an altered expression of proteins involved in apoptosis, cell cycle, growth and tumor suppression (55).

2.5 Exposure to excess estrogens in animals

In order to evaluate the effect of estrogen excess on the reproductive tract, several studies have been performed in various animal species treated with diethylstilbestrol, a synthetic estrogenic compound. In male mice, the critical period for Müllerian duct formation is day 13 post-coitus. Prenatal exposure of fetal male mice to DES caused a delay in Müllerian duct formation by approximately two days as well as incomplete Müllerian duct regression with a female-like differentiation of the non-regressed caudal part (56). An increase in the expression of anti-Müllerian-Hormone (AMH) mRNA in male mice fetuses exposed to DES has also been demonstrated. This increase was not accompanied by a regression of the ducts. This data was interpreted to suggest that the asynchrony in the timing of Müllerian duct formation, with respect to the critical period of Müllerian duct regression, led to the persistence of Müllerian duct remnants at birth in male mice. Moreover DES

exposure did not impair embryonal genetic development, but increased ERs number, and slightly prolonged the gestation time (cesarean sections were performed to rescue the litter and revealed no difference in size of fetuses from control and DES treated mothers). The timing of DES exposure is crucial to the induction of abnormalities of Müllerian duct development and regression (56).

Many studies in rodents suggest that inappropriate exposure to estrogen in utero and during the neonatal period impairs testicular descent, efferent ductule function, the hypothalamic-pituitary-gonadal axis, and testicular function (44). The latter effect can be a direct consequence of exposure to excess estrogen, as well as a secondary effect due to perturbations in circulating hormones or the ability of the efferent ductules to reabsorb fluid. Some studies show that low dose estrogenic substances given during puberty can actually stimulate the onset of spermatogenesis, likely due to stimulatory effects on FSH (57), highlighting the fact that the effects of excess estrogen on male fertility are often complex. The effects of excess estrogen in the neonatal period can impact upon the testis into adulthood, with permanent changes in testis function and spermatogenesis (44).

2.6 Exposure to excess estrogens in humans

The clinical use of diethylstilbestrol (DES) by pregnant women in order to prevent miscarriage resulted in an increased incidence of genital malformations in their sons (58). DES may have an effect on sex differentiation in men, as is the case in rodents (56). The risk of testicular cancer among men exposed to DES in utero has been a controversial issue and several meta-analyses showed no increased risk (59). However more direct evidence will be necessary in order to fully understand this issue.

While various studies suggest that environmental estrogens affect male fertility in animal models, the implications for human spermatogenesis are less clear (60). It has been demonstrated that male mice whose mothers have consumed a 29 ng/g dose of bisphenol A for seven days during pregnancy had a 20% lower sperm production as compared to control males (61). Various abnormalities in reproductive organs have also been described in males exposed to bisphenols (i.e. a significant decrease in the size of the epididymis and

seminal vesicles and an increase in prostate gland volume), suggesting that bisphenols interfere with the normal development of the Wolffian ducts in a dose-related fashion. Exogenous estrogens could interfere with the development of the genital structures if administered during early organogenesis, by leading to both an impairment of gonadotropin secretion and by creating an imbalance in the androgen to estrogen ratio, which may account for impaired androgen receptor stimulation or inhibition according to the dose, the cell type and age (58;62-64).

An excess of environmental estrogens has been suggested as a possible cause of impaired fertility in humans (65-67). A progressive decline in sperm count has been reported in some Western countries during the past 50 years, suggesting a possible negative effect of environmental contaminants on male reproductive function (58;62;66;68). Data concerning the role of estrogens in male reproductive structure development remains conflicting. Animal studies suggest that exposure to estrogen excess may negatively affect the development of reproductive male organs. These effects, however, are considered to be the result of an impaired hypothalamic-pituitary function as a consequence of estrogen excess and of the concomitant androgen deficiency (63;64). Much of the knowledge on excess estrogen exposure and human fertility depends upon animal data and the validity of these concepts to humans has not been established.

3. Testicular cancer

Although cancer of the testes is rare, accounting for only about 1 percent of all cancers in men of all ages and about 5 percent of all male genitourinary system cancers, it is the most common cancer in men between the ages of 15 and 35, and the second most common malignancy in men ages 35 to 39 (69-72).

Because the incidence of testicular cancer has risen markedly in the past 20 years, numerous studies are being conducted to explore possible environmental causes, including the mother's diet during her pregnancy as well as her use of diethlstilbestrol (DES) to prevent miscarriage. Researchers are also looking at the increasing presence of estrogen-

mimicking pollutants in the environment. The most consistent occupational association has been the elevated rate among men in professional and white-collar occupation, which may be linked to an increased risk observed with lower levels of exercise. Other possible causes include hereditary factors, genetic anomalies, congenital defects involving the reproductive tract, testicular injury, and atrophy of the testes. Viral infections such as mumps, which cause inflammation of the testes, have not been proven to cause cancer.

Testicular cancer comprises a number of different diseases. Nearly all of the main cell types in the testis can undergo neoplastic transformation, but germ cell-derived tumors constitute the vast majority of cases of testicular neoplasms. Ninety-five percent of testicular cancers arise from sperm-forming, or germ cells and are called germinal tumors. The remaining 5 percent are nongerminal tumors. About 40 percent of germinal tumors are categorized as seminomas. Several other types of germinal tumors are referred to collectively as non-seminomas. Somatic cell tumors, known as sex cord-stromal neoplasms and Leydig cell tumors are relatively rare. However, being derived from endocrine active cells, they have endocrine manifestations.

3.1 Leydig cell hyperplasia and tumors

Although Leydig cells in adult men are considered to be a terminally differentiated and mitotically quiescent cell type, in various disorders of testicular function, focal or diffuse Leydig cell hyperplasia is very common. Micronodules of Leydig cells are frequently seen in certain conditions associated with severe decrease of spermatogenesis or germinal aplasia, such as the so-called Sertoli-cell-only syndrome (Del Castillo syndrome), cryptorchidism, or Klinefelter's syndrome (73). A term "Leydig cell adenoma" is used when the size of a nodule exceeds several fold the diameter of a seminiferous tubule. It is unknown whether Leydig cell adenomas can progress further to form overt Leydig cell tumors, but even if it was the case, it is exceedingly rare. Morphological heterogeneity of hyperplastic Leydig cells is noticeable in some cases.

The mechanism of Leydig cell hyperplasia in the human male is still poorly understood. The disruption of hypothalamo-pituitary-testicular axis leading to an excessive stimulation

of Leydig cells by LH can play a central role (73). However, molecular pathways remain largely unknown in the vast majority of cases. In a small subset of cases structural changes of the LH receptor (74;75) and G proteins (76;77) were detected. Constitutively activating mutations of LH receptor cause early Leydig cell hyperplasia and precocious puberty (74;78). Similarly, constitutively activating mutations of Gs-protein in Leydig cells lead into hyperplasia and endocrine hyperactivity (77;79). However, Leydig cell hyperplasia is distinct from tumors that are usually solitary, and the role of the LH receptor and G protein mutations in the tumorigenesis may be limited to few cases (75;77). Leydig cell hyperplasia and adenomas can be easily induced in rodents by administration of estrogens, gonadotropins and a wide range of chemical compounds. Whether or not humans would be similarly susceptible to environmental effects remains to be elucidated.

Leydig cell tumors account for one to three percent of testicular neoplasms and occur in all age groups (79-81). Approximately 20 % are found before the age of 10, most often between five and ten years of age. Precocious puberty is the presenting symptom in these cases. Tumors produce androgens, mainly testosterone in a gonadotropin independent manner, and therefore LH and FSH remain low in spite of external signs of puberty. Approximately 10 % of the boys also have gynecomastia that is caused by estrogens produced in excess due to aromatase activity. In adults, gynecomastia is found in approximately 30 % of patients (81). The excessive androgen secretion rarely causes notable effects in adults.

Leydig cell tumors are always benign in children and can be treated with surgical enucleation when the tumor is encapsulated (71), whereas in adults malignant tumors have been found in 10-15 % of patients, and inguinal orchidectomy remains the treatment of choice (80). The presence of cytologic atypia, necrosis, angiolymphatic invasion, increased mitotic activity, atypical mitotic figures, infiltrative margins, extension beyond testicular parenchyma, and DNA aneuploidy are associated with metastatic behavior in Leydig cell tumors (81;82). Malignant tumors are hormonally active only in exceptional cases. Benign tumors can be treated by orchidectomy, whereas an additional retroperitoneal lymphadenectomy should be considered when the gross or histological features suggest

malignancy (82). Malignant tumors have not responded favorably to conventional chemotherapy and irradiation (82). Survival time has ranged from 2 months to 17 years (median, 2 years), and metastases have been detected as late as nine years after the diagnosis (81;82). Therefore follow-up of patients with malignant Leydig cell tumors has to be life-long. The remaining testis may be irreversibly damaged by longstanding high estrogen levels, resulting in both permanent infertility and hypoandrogenism (81-83).

Specific aim

Whereas the effects of estrogen on mammary gland tumorogenesis in human and in rodents is well known, the role of aromatase overexpression and in situ estrogen production in testicular tumorogenesis is not clearly defined. In this study we have investigated the molecular mechanisms causing aromatase overexpression and the effect of estradiol (E2) overproduction on rat Leydig cell tumor proliferation. As experimental model we used rat R2C Leydig tumor cell line and to validate our in vitro data in an in vivo model we used Leydig cell tumors from old Fisher rat testes in which the incidence of the spontaneous neoplasm is exceptionally high in aged animals (84).

We investigated the role of IGF-I a peptide also demonstrated to have a role in testicular growth and development, control of Leydig cell number (9). A previous study showed that in IGF-I gene knock-out mice (19;20) adult Leydig cells fail to mature, as a consequence these animals have a reduced capacity for testosterone (T) production caused by deregulated expression of T biosynthetic and metabolizing enzymes (21). Expression levels of all mRNA species associated with T biosynthesis were lower in the absence of IGF-I. However, this study did not investigate the effect on aromatase expression, even though an effect could be supposed.

Starting from these findings, in this study we investigated if a testicular overproduction of IGF-I could be one of the mechanisms determining aromatase overexpression in rat tumor Leydig cells through the activation of specific transcriptional factors. The high related Leydig cells E2 production through an autocrine/paracrine mechanism mediated by their own receptors, could contribute to the hormone dependence of testicular tumorogenesis stimulating Leydig tumor cell proliferation.

Materials and Methods

Cell cultures and animals.

TM3 cells (mouse Leydig cell line) were cultured in D-MEM/F-12 medium supplemented with 5% HS, 2.5% FBS and antibiotics (Invitrogen, S.R.L., San Giuliano Milanese, Italy); R2C cells (rat Leydig tumor cell line) were cultured in Ham/F-10 medium supplemented with 15% HS, 2.5% FBS and antibiotics (Invitrogen, S.R.L., San Giuliano Milanese, Italy). Male Fischer 344 rats (a generous gift of Sigma-Tau Pomezia, Italy), 6 (FRN) and 24 (FRT) months of age were used for studies. 24 months old animals presented spontaneously developed Leydig cell tumors absent in younger animals. Testes of all animals were surgically removed by qualified, specialized animal care staff in accordance with the Guide for Care and Use of Laboratory Animals (National Institutes of Health) and used for experiments.

Aromatase activity assay.

The aromatase activity in subconfluent R2C cell culture medium was measured by tritiated water-release assay using 0.5 μM [1β-^{3}H(N)]androst-4-ene-3,17-dione (DuPont NEN, Boston, MA, USA) as a substrate (85). Incubations were performed at 37 °C for 2 h under a 95%:5% air/CO2 atmosphere. Obtained results were expressed as pmol/h and normalized to milligram of protein (pmol/h per mg protein).

Radioimmunoassay.

Prior to experiments, TM3 cells were maintained overnight in DME/F12 medium and R2C cells in Ham/F-10 (medium only). The Estradiol content of medium recovered from each well was determined against standards prepared in low serum medium using a radioimmunoassay kit (DSL 43100; Diagnostic System Laboratories, Webster, TX, USA). Results assay were normalized to the cellular protein content per well and expressed as pmol per mg cell protein. IGF-I content in medium recovered from each well of R2C and TM3 cells was determined following extraction and assay protocols provided with the mouse/rat IGF-I radioimmunoassay kit (DSL 2900; Diagnostic System Laboratories, Webster, TX, USA).

Chromatin Immunoprecipitation (ChIP).

This assay was performed using the ChIP assay kit from Upstate (Lake Placid, NY) with minor modifications in the protocol. R2C cells were grown in 100 mm plates. Confluent cultures (90 %) were treated for 24 h with AG1024 (Sigma St Louis, MO, USA), PD98059 (Calbiochem, VWR International S.R.L. Milano), LY294002 (Calbiochem, VWR International S.R.L. Milano), GF109203X (Calbiochem, VWR International S.R.L. Milano) or for increasing times with 100 ng/ml IGF-I (Sigma St Louis, MO, USA) or left untreated. Following treatment DNA/protein complexes were crosslinked with 1 % formaldehyde at 37 °C for 10 min. Next, cells were collected and resuspended in 400 µl of SDS lysis buffer (Upstate Technology, Lake Placid, NJ) and left on ice for 10 min. Then, cells were sonicated four times for 10 sec at 30 % of maximal power and collected by centrifugation at 4 °C for 10 min at 14 000 rpm. Of the supernatants 10 µl were kept as input (starting material, to normalize results) while 100 µl were diluted 1:10 in 900 µl of ChIP dilution buffer (Upstate Technology, Lake Placid, NJ) and immunocleared with 80 µl of sonicated salmon sperm DNA protein A agarose (Upstate) for 6 h at 4 °C. Immunocomplex was formed using 1 µl of 1:5 dilution of specific antibody anti-SF-1 (provided by Prof. Ken-ichirou Morohashi, Division for Sex Differentiation, National Institute for Basic Biology, National Institutes of Natural Sciences, Myodaiji-cho, Okazaki, Japan) overnight at 4 °C. Immunoprecipitation with salmon sperm DNA protein A agarose was continued at 4 °C until the day after. DNA/protein complexes were reverse crosslinked overnight at 65 °C. Extracted DNA was resuspended in 20 µl of TE buffer. 3 µl volume of each sample and input were used for PCR using CYP19 promoter II specific primers. The PCR conditions were 1 min at 94 °C, 1 min at 50 °C and 2 min at 72 °C for 30 cycles using the following primers: forward, 5'-TCAAGGGTAGGAATTGGGAC-3'; reverse, 5'-GGTGCTGGAATGGACAGATG-3'. Amplification products were analyzed on a 1 % agarose gel and visualized by ethidium bromide staining. In control samples, non immune rabbit IgG was used instead of specific antibodies.

Real-time RTPCR.

Prior to experiments, cells were maintained overnight in low serum medium. Cells were then treated or the indicated times and RNA was extracted from cells using the TRiazol RNA isolation system (Invitrogen). TRiazol was also used to homogenize total tissue of normal (FRNT) and tumor (FRTT) Fisher rat testes for RNA extraction. Each RNA sample was treated with DNase I (Ambion, Austin, TX), and purity and integrity of the RNA was confirmed spectroscopically and by gel electrophoresis prior to use. One µg of total RNA was reverse transcribed in a final volume of 30 µl using the ImProm-II Reverse transcription system kit (Promega, Promega Italia S.R.L. Milano, Italy), cDNA was diluted 1:3 in nuclease free water, aliquoted and stored at –20°C. Primers for the amplification were based on published sequences for the rat CYP19, rat CREB and rat SF-1 genes. The nucleotide sequences of the primers for CYP19 were: forward 5'-GAGAAACTGGAAGACTGTATGGAT-3' and reverse 5'-ACTGATTCACGTTCTCCTTTGTCA-3'. For CREB amplification were used the following primers: forward 5'-AATATGCACAGACCACTGATGGA-3' and reverse 5'-TGCTGTGCGAATCTGGTATGTT-3'; for SF-1 amplification primers have been previously published (86). PCR reactions were performed in the iCycler iQ Detection System (Biorad Hercules, CA, USA), using 0.1 µM of each primer, in a total volume of 30 µL reaction mixture following the manufacturer's recommendations. SYBR Green Universal PCR Master Mix (Biorad Hercules, CA, USA) with the dissociation protocol was used for gene amplification, negative controls contained water instead of first-strand cDNA. Each sample was normalized on the basis of its 18S ribosomal RNA content. The 18S quantification was performed using a TaqMan Ribosomal RNA Reagent kit (Applied Biosystems, Applera Italia, Monza, Milano, Italy) following the method provided in the TaqMan Ribosomal RNA Control Reagent kit (Applied Biosystems, Applera Italia, Monza, Milano, Italy). The relative gene expression levels were normalized to a calibrator that was chosen to be the basal, untreated sample. Final results were expressed as *n*-fold differences in gene expression relative to 18S rRNA and calibrator, calculated following the ΔΔCt method, as follows:

$$n\text{-fold} = 2^{-(\Delta Ctsample - \Delta Ctcalibrator)}$$

where ΔCt values of the sample and calibrator were determined by subtracting the average Ct value of the 18S rRNA reference gene from the average Ct value of the different genes analyzed.

Western-blot analysis

R2C and TM3 cells or total tissue of FRNT and FRTT were lysed in ice-cold Ripa buffer containing protease inhibitors (20 mM Tris, 150 mM NaCl, 1% Igepal, 0.5% sodium deoxycholate, 1 mM EDTA, 0·1% SDS, 1 mM PMSF, 0.15 units/ml aprotinin and 10 μM leupeptin) for protein extraction. The protein content was determined by Bradford method (87). The proteins were separated on 11% SDS/polyacrylamide gel and then electroblotted onto a nitrocellulose membrane. Blots were incubated overnight at 4 °C with 1. anti-human P450 aromatase antibody (1:50) (Serotec, Oxford, UK, MCA 2077), 2. anti-ERα (F-10) antibody (1:500) (Santa Cruz Biotechnology, Santa Cruz, CA, USA, sc8002), 3. anti-ERβ (H-150) (1:1000) (Santa Cruz Biotechnology, Santa Cruz, CA, USA, sc8974), 4. anti-cyclin D1 (M-20) antibody (1:1000) (Santa Cruz Biotechnology, Santa Cruz, CA, USA, sc718), 5. anti-cyclin E (M-20) antibody (1:1000) (Santa Cruz Biotechnology, Santa Cruz, CA, USA, sc481), 6. anti-CREB antibodies (1:1000) (48H2, Cell Signaling Technology, Celbio, Milan, Italy) and (1:1000) (AHO0842Biosource Inc. Camarillo CA USA); 7. anti-pCREB ser133 (87G3) (1:1000) (Cell Signaling Technology, Celbio, Milan, Italy) or anti-pCREB Ser129/133 (1:1000) (Biosource Inc. Camarillo CA USA, 44-297G), 8. anti SF-1 (1:1000) provided by Prof. Ken-ichirou Morohashi, Division for Sex Differentiation, National Institute for Basic Biology, National Institutes of Natural Sciences, Myodaiji-cho, Okazaki, Japan), 9. anti-pSF-1 (1:1000) provided by Dr Holly A. Ingraham Department of Physiology, University of California, San Francisco, San Francisco, California 94143-0444, USA), 10. anti-actin (C-2) antibody (1:1000) (Santa Cruz Biotechnology, Santa

Cruz, CA, USA, sc8432). Membranes were incubated with horseradish peroxidase (HRP)-conjugated secondary antibodies (Amersham Pharmacia Biotech, Piscataway, NJ) and immunoreactive bands were visualized with the ECL western blotting detection system (Amersham Biosciences, Cologno Monzese, Italy). To assure equal loading of proteins membranes were stripped and incubated overnight with β-actin antiserum.

Cell-proliferation assay.

For proliferative analysis a total of $1x10^5$ cells were seeded onto 12-well plates in complete medium and let grow for 2 days. Prior to experiments, cells were maintained overnight in Ham/F-10 medium and the day after treated with ICI 182780, a gift from Astra-Zeneca (Basiglio, Milano, Italy), 4-hydroxytamoxifen (OHT) (Sigma St Louis, MO, USA) and Letrozole, a gift from Novartis Pharma AG (Basel, Switzerland) and 17β-estradiol (E2) (Sigma St Louis, MO, USA). Control (basal) cells were treated with the same amount of vehicle alone (DMSO) that never exceeded the concentration of 0.01% (v/v). [^{3}H]Thymidine incorporation was evaluated after a 24-h incubation period with 1 μCi [^{3}H]thymidine (PerkinElmer Life Sciences, Boston, MA, USA) per well. Cells were washed once with 10% trichloroacetic acid, twice with 5% trichloroacetic acid and lysed in 1 ml 0.1 M NaOH at 37°C for 30 min. The total suspension was added to 10 ml optifluor fluid and was counted in a scintillation counter.

Data Analysis and Statistical Methods.

Pooled results from triplicate experiments were analyzed using one-way ANOVA with Student-Newman-Keuls multiple comparison methods, using SigmaStat version 3.0 (SPSS, Chicago, IL).

Results

Estradiol induces Leydig cell tumor proliferation through an autocrine mechanism. We performed our study utilizing as model system R2C Leydig tumor cells. These cells have been demonstrated to have high aromatase expression and, consequently, activity (42), while we used another Leydig cell line, TM3 cells, as a normal control. We also analyzed testes from older and younger Fischer rats. Aged animals have a high incidence of spontaneous neoplasm of Leydig cells (84;88), a phenomenon not observed in younger animals, allowing us to use them as a good *in vivo* model to confirm results obtained in cell lines. Our first step was to measure estradiol content in culture medium of R2C and TM3 cells maintained in culture for increasing time. While E2 levels in TM3 medium were extremely low (data not shown) in R2C cells E2 levels after 24 h were 0.5 pmol/mg protein and increased by 7-fold at 96 h (Fig. 1A). This production was dependent on high constitutive active aromatase activity, since the presence of aromatase inhibitor Letrozole was able to decrease E2 production at all time points tested (Fig. 1B). E2 levels after 24 h treatment with Letrozole were still detectable, but were completely knock down when we removed the medium after 24 h and renewing the treatment for an additional 24 h. The same effect was maintained for the other two time points investigated (Fig. 1B).

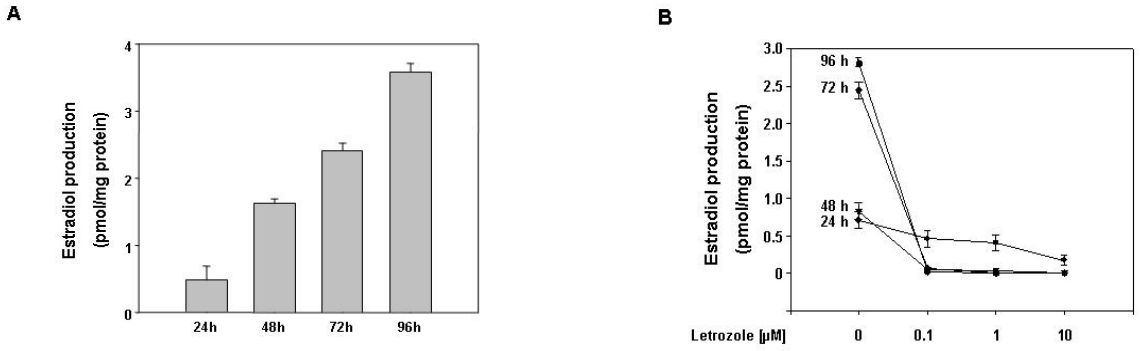

Figure 1. E2 production in R2C cells. (**A**) Cells were cultured for the indicated times in serum free medium. (**B**) Cells were treated for the indicated times in HAM-F10 in the absence (-) or presence of aromatase inhibitor Letrozole (0.1, 1, 10 µM). Every 24h, before renewing treatment, cell culture medium was removed and analyzed for steroid content. E2 content was determined by RIA and normalized to the cell culture well protein content. Data represent the mean ± SEM of values from three separate cell culture wells expressed as pmol/mg protein.

Once estradiol is produced it can exert its actions binding to specific receptors, the estrogen receptors α e β (ERα and ERβ). Analysis of the two receptor protein isoforms in our models demonstrated that tumor Leydig cells express both isoform of ERs (Fig. 2). Particularly the α isoform seems to be more expressed in R2C cells respect to TM3 and in FRTT respect to the its control FRNT (Fig. 2A) where ERβ is more expressed (Fig. 2B). In R2C as well as in FRTT was observed an increase in ERα/ERβ ratio (Fig. 2E). Moreover aromatase protein content is extremely high in tumoral samples (54) (Fig. 2C).

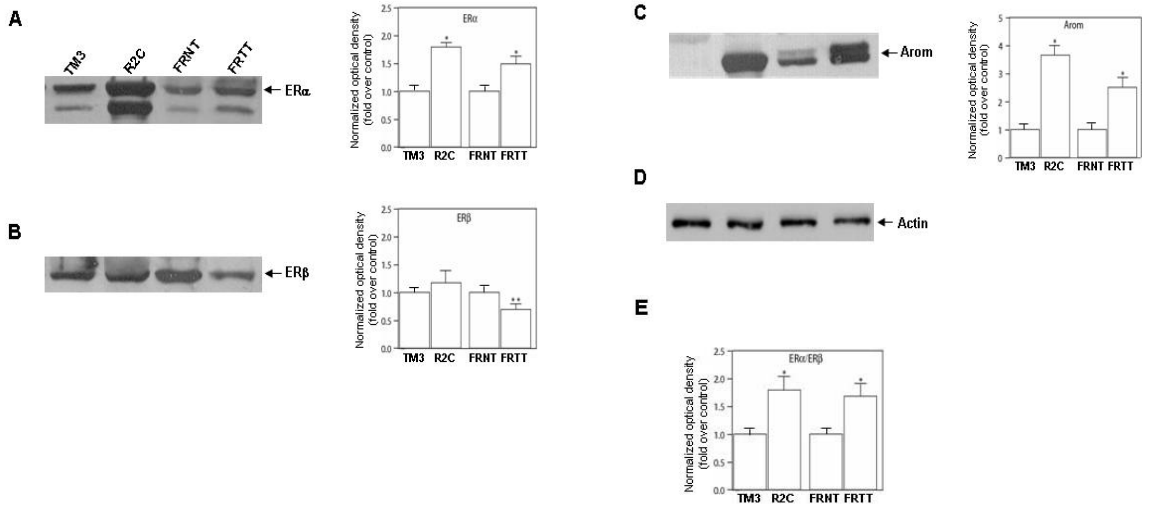

Figure 2. Expression of estrogen receptors and Aromatase in R2C cells. ERα (**A**) ERβ (**B**) and aromatase (**C**) western blot analysis was performed on 50 μg of total proteins extracted from TM3 and R2C cells or from total tissue of normal (FRNT) and tumor (FRTT) Fisher rat testes. Results are representative of three independent experiments. β-actin (**D**) was used as loading control. Graphs depicted near western blots were obtained by averaging densitometric analyses of the three independent experiments. Protein expression in each lane was normalized to the β-actin content, and expressed as fold over control. (**E**) Graph was obtained calculating ERα/ERβ ratio of normalized optical density. (*,$P < 0.001$ and **,$P < 0.05$ compared with basal).

Our next experiments demonstrated that estrogen receptors are required for proliferation through a short autocrine loop maintained by endogenous E2 production in Leydig tumor cells. For instance, the use of both antiestrogens OHT and ICI and the use of aromatase inhibitor Letrozole determined a dose-dependent inhibition of cell proliferation (Fig. 3A). Among the different doses tested the highest dose of OHT (10 μM) was able to inhibit cell proliferation by 90%, ICI 10 μM by 86% and letrozole by 70%. In the same vein, starving

cells for prolonged time and changing the medium every day in order to remove local E2 production, we found that addition of 1, 10 and 100 nM E2 stimulated Leydig tumor cell proliferation (Fig. 3B), and partially abrogated the inhibition induced by Letrozole (Fig. 3C).

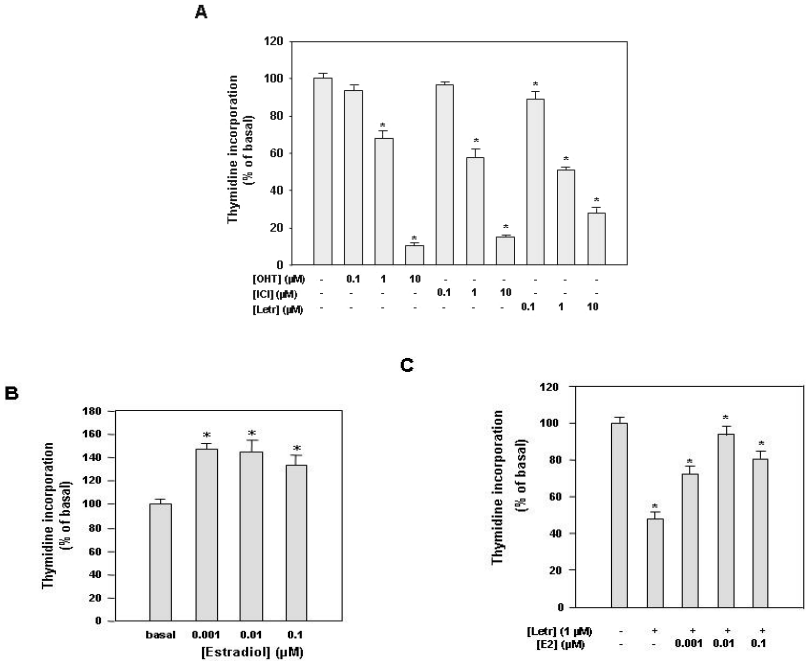

Figure 3. Effects of antiestrogens, aromatase inhibitor Letrozole and estradiol on R2C cell proliferation. (**A**) Cells were treated for 96h in HAM-F10 in the absence (-) or presence of antiestrogens hydroxytamoxifen (OHT) or ICI 182,760 (ICI) or aromatase inhibitor Letrozole at the indicated concentrations. (**B**) Cells were cultured for 48h in serum-free HAM-F10, every 24 h cell culture medium was removed and renewed. Cells were then treated for 24 h with estradiol at the indicated concentrations. (**C**) Cells were cultured for 24h in serum-free HAM-F10, cells were then treated for 48 h with letrozole (1μM) changing the culture medium and renewing treatment every 24h. For additional 24h cells were treated with letrozole (1μM) in combination with estradiol at the indicated concentrations. Proliferation was evaluated by [3H] Thymidine incorporation analysis. Values expressed as percent of untreated (basal) cells (100%) represent the mean ± SEM of three independent experiments each performed in triplicate. (*) $P < 0.05$ compared with basal cells.

The stimulatory effect of E2 was concomitant with the increased levels of cell cycle regulator cyclin D1 and E, whose expression was inhibited by pure antiestrogen ICI (Fig. 4). All these results address how the classic E2/ERalpha signalling may control Leydig cell tumor growth and proliferation similarly to what observed in other estrogen-dependent tumors.

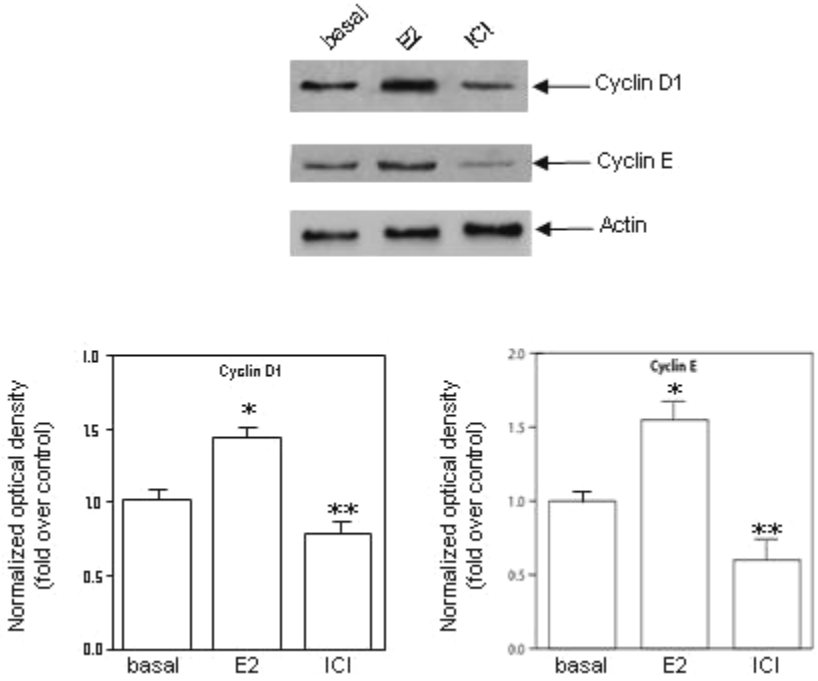

Figure 4. R2C cells were cultured for 48h in serum-free HAM-F10, every 24 h cell culture medium was removed and renewed. Cells were then treated for 24 h in the absence (basal) or in the presence with estradiol (1nM) and ICI (1μM) before extracting total proteins. Western blot analysis of Cyclin D1 and Cyclin E was performed on 50 μg of total proteins extracted from R2C cells. Blots are representative of three independent experiments with similar results. β-actin was used as loading control. Graphs depicted below western blots were obtained by averaging densitometric analyses of the three independent experiments. Protein expression in each lane was normalized to the β-actin content, and expressed as relative fold over basal. (*,$P < 0.05$ and **,$P < 0.01$ compared with basal).

Aromatase overexpression is determined by constitutive activation of transcription factors SF-1 and CREB.

Aromatase gene transcription in rat Leydig cells is driven by the PII promoter, which is principally regulated through three CRE-like sites and one NRE site binding SF-1 and LRH-1 (42;86). Constitutive active levels of CREB have been previously demonstrated in R2C cells (89). Here we confirmed these data and demonstrated high phosphorylated status of CREB together with enhanced phosphorylation of SF-1 in FRTT (Fig. 5). Furthermore we demonstrated the presence of high expression levels of SF-1 with the protein present in a phosporylated status in R2C but not in TM3.

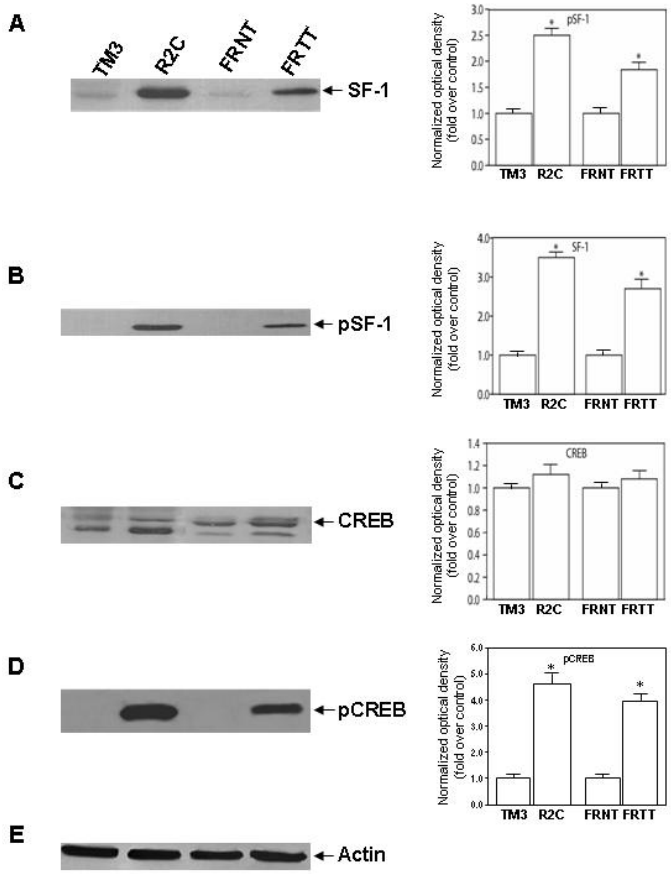

Figure 4. Expression of total and phosphorylated forms of SF-1 and CREB. Western blot analysis was performed on 50 μg of total proteins extracted from TM3 and R2C cells or from total tissue of normal (FRNT) and tumor (FRTT) Fisher rat testes. Blots are representative of three independent experiments with similar results. β-actin was used as loading control. Graphs depicted near western blots were obtained by averaging densitometric analyses of the three independent experiments. Protein expression in each lane was normalized to the β-actin content, and expressed as relative difference from controls. (*,$P < 0.001$ compared with basal).

IGF-I is produced by R2C cells and induces aromatase expression through PI3K- and PKC- mediated activation of SF-1.

Starting from previous findings demonstrating that SF-1 and CREB are activated by IGF-I and lead to an increase in StAR transcription and then steroidogenesis (90;91), we investigated the role of this factor locally produced in the testis in regulation of aromatase. Determination of IGF-I content in TM3 and R2C culture medium by RIA revealed a

significant difference in the growth factor production with R2C cells producing about 4-fold higher IGF-I (Fig. 5).

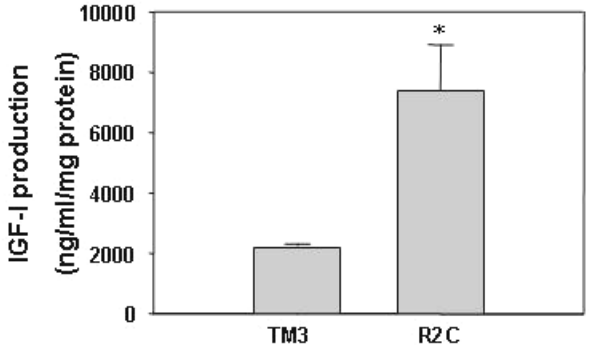

Figure 5. IGF-I production in Leydig cells. IGF-I levels in culture medium of TM3 and R2C cells by RIA. TM3 and R2C cells were cultured for 24 h in serum free medium and IGF-I content was normalized to the cell culture well protein content. Data represent the mean ± SEM of values from three separate cell culture wells expressed as pmol/mg protein. (*) P< 0.01 compared with basal conditions.

Upon binding to its receptor, IGF-IR, IGF-I activates three major transductional pathways: Ras/Raf/MAPK, PI3K/AKT, PLC/PKC, to demonstrate involvement of IGF-I transductional pathways in modulating aromatase expression in Leydig cell tumors, we used specific inhibitors: of IGF-I receptor (IGF-IR) [AG1024 (AG)], of ERK1/2 [PD98059 (PD)], of PI3K [LY294002 (LY)] and of PKC [GF109203X (GFX)]. IGF-I receptor inhibitor was able to inhibit aromatase activity in R2C cells by 85%, LY determined 65 % inhibition, PD 35 % and GFX 61 % (Fig. 6).

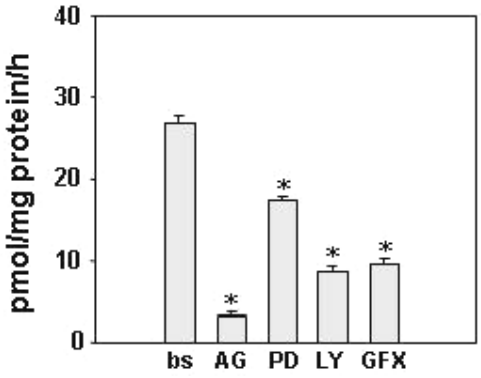

Figure 6. Aromatase activity in R2C cells in response to inhibitors of IGF-I pathways. Cells were treated with AG (20μM), LY (10 μM), PD (20 μM) and GFX (20 μM). Aromatase activity was assessed by using the modified tritiated water method. Results obtained are expressed as pmoles of $[^3H]H_2O$ released per hour and are normalized to the well protein content (pmol/h/mg protein). Values represent the mean ± SEM of three independent experiments each performed with triplicate samples. * P < 0.01 compared to basal.

The same inhibitory pattern was observed also on aromatase mRNA (fig. 7A) and protein content (Fig. 8). Parallely all of the different inhibitors but PD were able to reduce SF-1 mRNA, while CREB remained unchanged (Fig. 7). For SF-1 inhibition was 75% with AG, 90 % with LY and 80 % with GFX (Fig. 7). Analysis of protein levels by western blot confirmed the data on mRNA (Fig. 8). Treatments with increasing doses of AG, LY and GFX but not PD were able to induce a dose-dependent inhibition of total and phosphorylated levels of SF-1, on the other hand CREB was not affected by the presence of any of the inhibitors (Fig. 8).

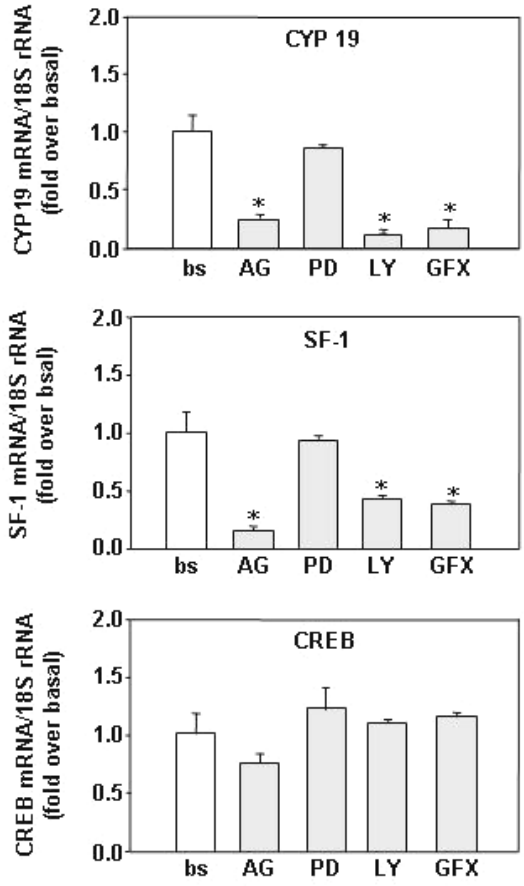

Figure 7. Effects of inhibitors of IGF-I pathways on mRNA expression of CYP19, SF-1 and CREB in R2C cells. Total RNA was extracted from R2C cells untreated (bs) or treated for 24h with AG (20μM), LY (10 μM), PD (20 μM) and GFX (20 μM). Real time RT-PCR was used to analyze mRNA levels of CYP19, SF-1, and CREB. Data represent the mean ± SEM of values from three separate RNA samples. Each sample was normalized to its 18S ribosomal RNA content. Final results are expressed as n-fold differences of gene expression relative to calibrator (basal) calculated with the ΔΔCt method. * $P < 0.001$ compared to basal.

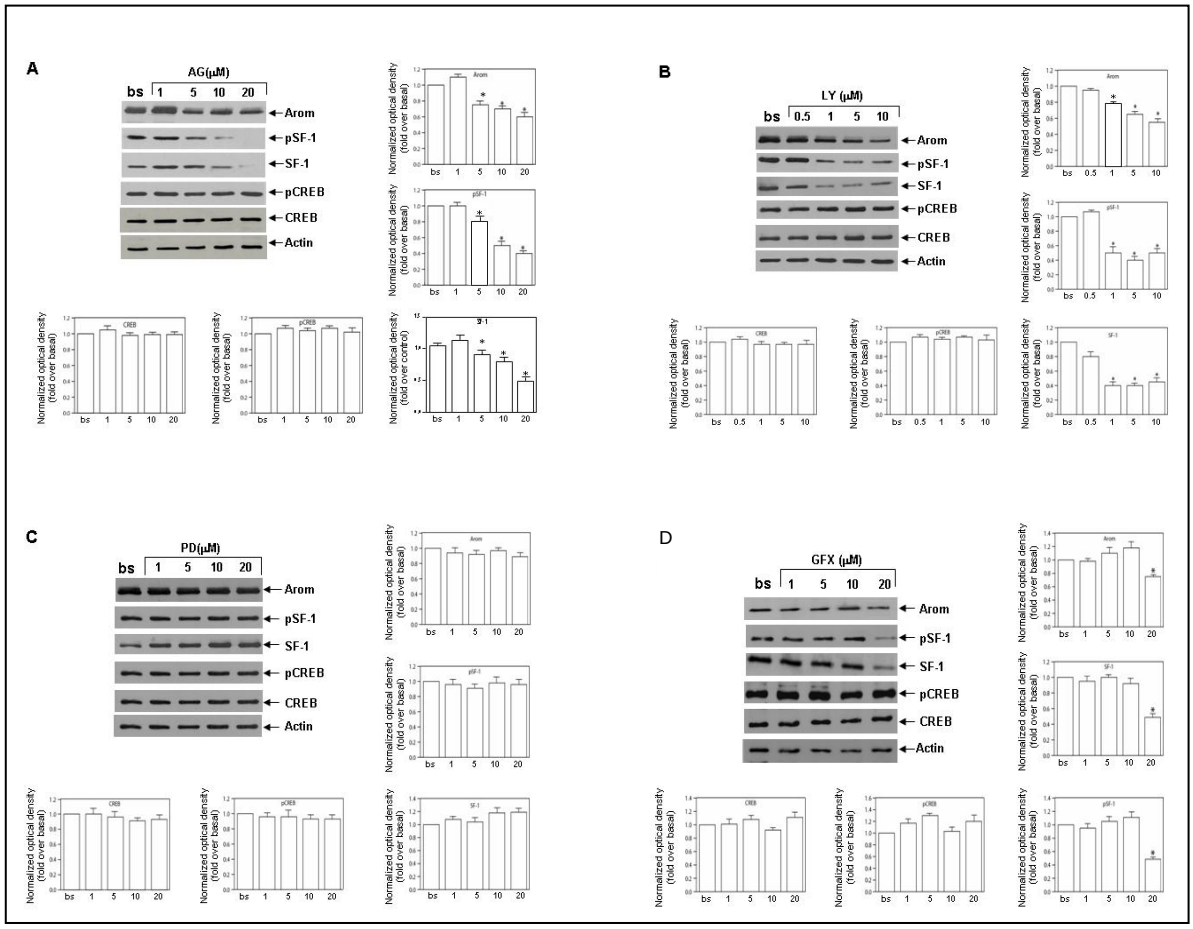

Figure 8. Effects of inhibitors of IGF-I pathways on expression of Aromatase, total and phosphorylated forms of SF-1 and CREB in R2C cells. Western blot analyses were performed on 50 μg of total proteins extracted from R2C cells untreated (bs) or treated for 24h with the indicated doses of AG (**A**), LY (**B**), PD (**C**) and GFX (**D**). Blots are representative of three independent experiments with similar results. β-actin was used as loading control. Graphs depicted near western blots were obtained by averaging densitometric analyses of the three independent experiments. Protein expression in each lane was normalized to the β-actin content, and expressed as relative difference from basal. (*,$P < 0.01$ compared with basal).

IGF-I induces aromatase expression and activity in R2C cells. To further demonstrate the prevalent role of SF-1 in IGF-I induced aromatase expression in Leydig cell tumor, we monitored the effect of IGF-I on CYP19 and SF-1 expression. Addition of exogenous amounts of IGF-I were able to induce aromatase activity by 1.8-fold (Fig. 9A). A significant effect of IGF-I treatment was seen also on CYP19 mRNA levels (Fig. 9B). IGF-I was able to induce a significant increase of 2- and 3.8-fold in aromatase mRNA at 12h and 24h, respectively (Fig. 9B). Aromatase protein levels under the same treatments reflected mRNA data (Fig. 9C). Analysis of expression levels of total and phosphorylated forms of transcription factors SF-1 and CREB showed an increase in SF-1 and pSF-1 in the

presence of IGF-I after 4h while no difference was observed for CREB at any of the investigated times (Fig. 9C).

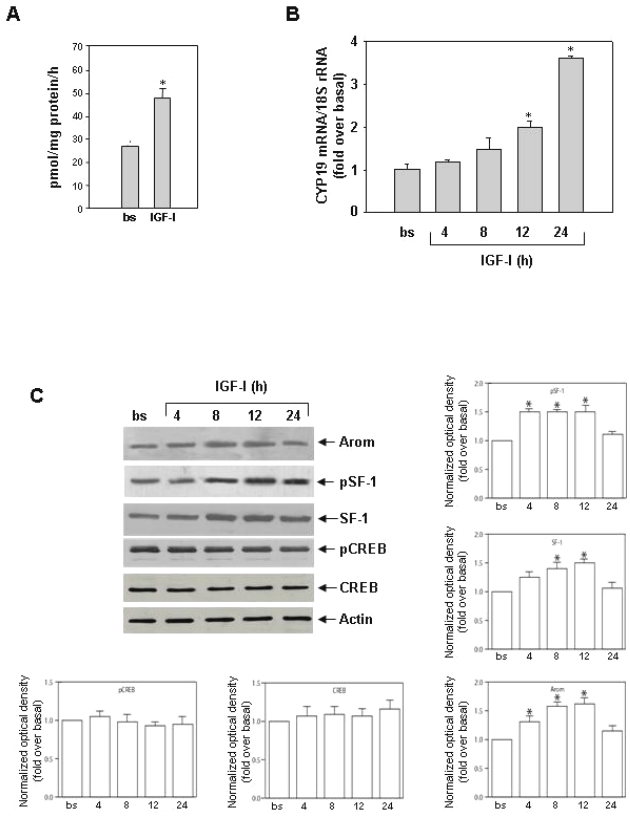

Figure 9. Aromatase activity and expression in R2C cells in response to IGF-I. (A) Cells were treated with IGF-I (100 ng/ml) for 24h. Aromatase activity was assessed by using the modified tritiated water method. Results obtained are expressed as pmoles of [3H]H2O released per hour and are normalized to the well protein content (pmol/h/mg protein). Values represent the mean ± SEM of three independent experiments each performed with triplicate samples. *P<0.05 compared to basal. (B) Total RNA was extracted from R2C cells untreated (bs) or treated for the indicated times with IGF-I (100 ng/ml). Real time RT-PCR was used to analyze mRNA levels of CYP19. Data represent the mean ± SEM of values from three separate RNA samples. Each sample was normalized to its 18S ribosomal RNA content. Final results are expressed as n-fold differences of gene expression relative to calibrator (basal) calculated with the ΔΔCt method. *P<0.01 and **P<0.001compared to basal. (C) Western blot analyses were performed on 50 µg of total proteins extracted from R2C cells untreated (basal) or treated for the indicated times with IGF-I (100 ng/ml). Blots are representative of three independent experiments with similar results. β-actin was used as loading control. Graphs depicted below western blots were obtained by averaging densitometric analyses of the three independent experiments.. Protein expression in each lane was normalized to the β-actin content, and expressed as relative difference from controls. (*,P < 0.01 compared with basal).

Changes in IGF-I pathway activation status lead to changes in SF-1 binding to the aromatase PII promoter.

Finally we performed CHIP assay to investigate how IGF-I stimulation influence per se binding of transcription factors to the aromatase PII promoter. We evidenced how in basal condition all the different inhibitors but not PD reduced the amount of bound SF-1

reflecting changes in SF-1 protein amount (Fig. 10 A). The increase in SF-1 protein content seen under IGF-I treatment (Fig. 9C) reflected an increase in SF-1 binding to the PII promoter (Fig. 10B).

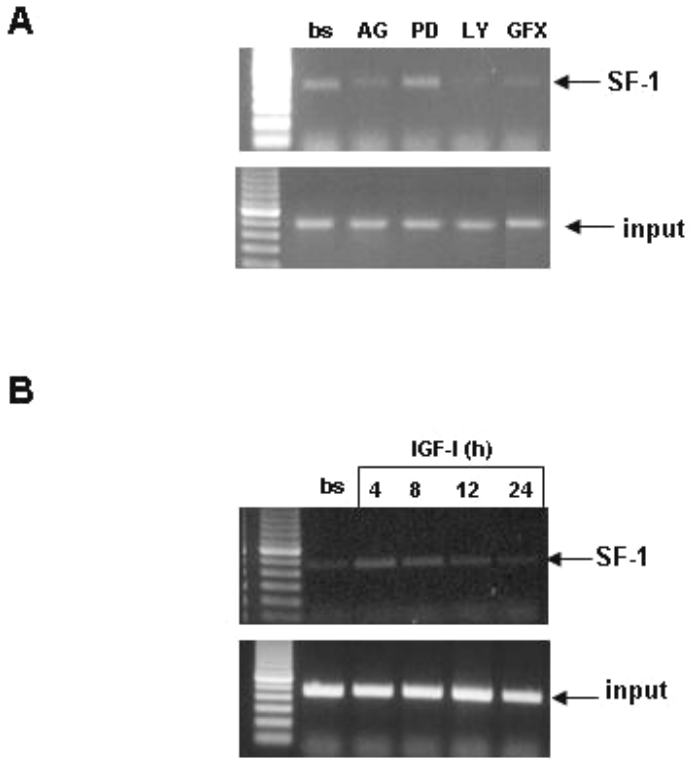

Figure 10. IGF-I increases SF-1 recruitment to the aromatase PII promoter through PI3K and PKC. (A) R2C cells were incubated for 24 h with AG (20μM), LY (10 μM), PD (20 μM) and GFX (20 μM). Untreated cells (basal, bs) were treated with the same amount of vehicle alone (DMSO) that never exceeded 0·01% (v/v). (B) R2C cells were incubated for the indicated times with IGF-I (100 ng/ml). *In vivo* binding of SF-1 to the aromatase PII promoter was examined using ChIP assay. Immunoprecipitated (SF-1) and total (10% input) DNA were subject to PCR using specific primers. Similar results were obtained in two additional experiments.

Discussion

Discussion

The current study was aimed to explain the molecular mechanism responsible for aromatase overexpression in tumor Leydig cells with a consequent excess of estradiol *in situ* production sustaining tumor cell growth and proliferation.

Mammalian testis is capable of estrogen synthesis, whose production is regulated by different factors at different ages. In mature animals, aromatization of testosterone to estradiol is enhanced by LH/chorionic gonadotropin (CG) and not by FSH. The site of this synthesis appears to be age-dependent, at least in some species, such as the rat (92). Leydig cells are an elective target site of LH/CG which controls testosterone biosynthesis as well as its conversion to estradiol through aromatase activity. Leydig cell is also known to be the site of estrogen synthesis in several species, including mice (93), humans (94), suine (95), and sheep (96). Alterations in local estrogen synthesis may have significant consequences in malignancy of these cells. In the present study we observed that manteinance of R2C cells in the absence of serum induces a cospicous release of E2 from cellular storage in a time dependent manner. This synthesis was abrogated by treatment with Letrozole, an aromatase inhibitor, addressing how estrogen production is dependent on high constitutive aromatase activity. A strongly increased aromatase expression was observed in R2C cells respect to the normal cell line control TM3 as well as in FRTT respect to FRNT. These findings concord with a previous study on human tissues showing that the increase in estrogen synthesis, as a consequence of a more intense aromatase activity, is higher in Leydig cell tumor fraction than in normal tissue surrounding the tumor of the same patient (97).

Mediators of the physiological effects of estrogens are the estrogen receptors (ER) α and β. ERα appears to be confined to Leydig cells in testicular tissue (45), while ERβ has been detected immunohistochemically in several rat testicular cell types, including Sertoli cells, germ cells, and peritubular cells (98). An enhanced expression of ERα, resulting in an increased ERα/ERβ, ratio was observed in R2C compared to TM3 cell line as well as in FRTT respect to FRNT. This is in agreement with previous reports demonstrating that

transgenic mice overexpressing aromatase have an enhanced occurrence of breast and Leydig cell tumors together with an enhanced expression of ERα in the tumoral tissue (54). The latter findings address reasonably how an estrogen short autocrine loop may be involved in breast and testicular tumorogenesis in the presence of an excess of locally produced estradiol. Indeed, an arrest of cell growth was observed following abrogation of local E2 production with Letrozole or after addition of ERα inhibitors ICI or OHT. Besides, only after remotion of medium every day along with prolonged R2C starvation abolishing local steroid production, we observed how exogenous E2 was able to display proliferative effects.

One mechanism through which estrogens induce cell proliferation is by increasing protein levels of G1 regulatory cyclins A, B1, D1, D3, and E in target cells (99). In our study we showed that the expression of two of the most important regulators of Leydig cell cycle, cyclin D1 and E can be increased by E2 and downregulated by treatment with antiestrogens. These data further confirm that aromatase overexpression and the consequent E2 production may be the cause of altered cell cycle regulation of Leydig tumor cells.

In the attempt to explain the molecular mechanism determining aromatase overexpression in our tumor cell line, we focused our attention on expression levels of transcription factors identified as crucial regulators of aromatase gene expression: CREB and SF-1. In the adult testis SF-1 is predominantly expressed in Leydig cells (100). The increase of total and/or phosphorylated protein can potentiate SF-1 transcriptional activity (101). In R2C cells and in FRTT compared to the normal controls we found higher SF-1 phosphorylated protein levels as a consequence of elevated protein content. Total CREB levels were similar in all samples but highly phosphorylated in tumor samples. Starting from these observations we investigated which pathways could be involved in the activation of these transcription factors.

The most important signal that initiates steroidogenesis in Leydig cells is the binding of LH to the LH receptor (102). It has been demonstrated that LH/LHreceptor signaling pathway is constitutively active in R2C cells and makes the phenotype of these cells

constitutively steroidogenic (103). For instance in the presence of a specific PKA inhibitor, constitutive synthesis of *Star* mRNA and steroids were significantly inhibited (104). These observations fit well with our findings evidencing how the presence of PKA inhibitor determined a strong decrease in aromatase activity together with a drop in CREB phosphorylation (data not shown). In the presence of a specific PKC inhibitor no effects were elicited on phosphorylation of CREB, while SF-1 dropped dramatically.

It has been shown that CREB in mouse Leydig cells can be phosphorylated also through the PKC pathway, activated by IGF-I (103). In this study we have revealed that R2C tumor Leydig cells release higher levels of IGF-I in the culture medium respect to TM3 cells. However, the exposure to IGF-I as well as the treatment with inhibitors of IGF-I signalling did not affect CREB phosphorylative status but decreased SF-1 phosphorylation, postulating a separate mechanism controlling CREB and SF-1 activation in modulating aromatase activity.

These findings led us to suppose that the IGF-I derived from tumor Leydig cells could act through an autocrine mechanism in activating aromatase expression. IGF-I receptors have previously been identified in Leydig cells of several species (10;105-107). It has been hypothesized that changes in IGF-RI expression can influence tumor cell progression. However in our cellular models, we did not reveal differences in IGF-RI expression between normal and tumor cells (data not shown), indicating that IGF-I level may be the determining factor in potentiating IGF-I signalling. A previous study investigating the effects of long term IGF-I treatment on Leydig cells did not reveal alterations in DNA synthesis, indicating that IGF-I may act as a differentiation factor rather than a mitogenic factor (12). In fact, expression levels of all mRNA species associated with T biosynthesis were shown to be lower in the absence of IGF-I, while treatment with IGF-I/insulin has been found to stimulate steroidogenesis and StAR expression in Leydig cells through a process that does not require cAMP signaling (9;107;108). In the same vein we may reasonable hypothesize that IGF-I could sustain, through an autocrine/paracrine mechanism, the elevated aromatase expression/activity in tumor Leydig cells. To verify this hypothesis we studied the various signalling pathways initiated by IGF-I through IGF-

IR. Binding of IGF-I to its receptor causes receptor autophosphorylation and the activation of intrinsic tyrosine kinase that acts on various substrates including the insulin receptor substrate (IRS) and Shc adaptor proteins. These activated proteins recruit other factors, leading to activation of multiple signalling pathways including the phosphatidyl inositol 3-kinase (PI3K)/Akt and the mitogen-activated protein (MAP) kinase cascade. In addition, it has been shown that IGF-I can activate also the phospholipase C (PLC)/protein kinase C (PKC) pathway (90;109). To demonstrate a role for IGF-I in mediating aromatase activation we used specific inhibitors for IGF-I signaling [AG1024 (AG)], ERK1/2 [PD98059 (PD)], PI3K [LY294002 (LY)] and PKC [GF109203X (GFX)] and showed a reduction of aromatase activity with all of them. Together these data confirm a role for IGF-I in mediating aromatase activation in tumor Leydig cells. All of the different inhibitors but PD were able to produce a similar inhibitory pattern on both aromatase and SF-1 mRNA and protein expression. Furthermore by ChIP assay we evidenced that SF-1 binding to the aromatase promoter II that was reduced by AG, LY, GFX but not by PD indicating a central role of this transcription factor in regulating aromatase gene transcription in tumor Leydig cells. This is the first report of a direct link between SF-1 transcription and IGF-I signalling pathway in regulating aromatase expression.

Furthermore, addition of IGF-I itself was able to increase aromatase activity and expression. These events were due to an increase in the amount of total and phosphorylated SF-1 levels whose binding to the aromatase promoter was shown to be rapidly augmented. So we postulate that an enhanced endogenous IGF-I local production may contribute to maintain an elevated aromatase activity sustained by a direct stimulatory effect of SF-1. For instance the inhibition of IGF-I signalling through inhibition of either PI3K/AKT and PLC/PKC pathways were able to block SF-1 expression and protein phoshorylation. Particularly treatment with AG blocked SF-1 phosphorylation more efficiently than the separate treatment of PI3K or PKC, addressing how both pathways may synergize in upregulating SF-1 activity. In the presence of PD, SF-1 expression remained unchanged together with unaffected aromatase mRNA and protein levels. Importantly aromatase activity appeared decreased in the presence of PD suggesting a potential stimulatory role of

ERK1/2 on the enzyme at a post-transcriptional level. From our findings then emerges a double mechanism inducing enhanced expression of aromatase: 1. a constitutive activation of LH/cAMP/PKA pathway which determines CREB activation; 2. an enhanced IGF-I signaling potentiating SF-1 action. The enhanced expression of SF-1 may be maintained by the lack of DAX-1 (Dosage-Sensitive Sex Reversal, Adrenal Hypoplasia Congenita, Critical Region on the X Chromosome, Gene-1) in R2C cells (89). DAX-1 is a specific co-repressor of SF-1 (60-64) and inhibits StAR expression and steroidogenesis by 40-60% when overexpressed in R2C cells (89). The lack of DAX-1 expression in R2C cells may be due to the constitutive active PKA signalling, in fact since in a mouse Leydig cell line was shown a marked decrease of DAX-1 mRNA within 3 h after addition of LH or forskolin (110). Then, the activation of LH/LHr/PKA pathway at the same time decreases DAX-1 expession and promotes SF-1 activity.

Remains to explain which molecular mechanism(s) is responsible for the elevated IGF-I production in tumor Leydig cells. In vivo, administration of hCG increases IGF-I mRNA levels in rat Leydig cells (111). LH deprival determines a decrease in the BrdU incorporation as well as a decrease in mRNA levels of IGF-I and IGF-I receptor. These observations together with our data showing a decrease in IGF-I basal production after treatment with a PKA inhibitor (data not shown) suggest the possibility that LH can mediate its proliferative effects also by regulating IGF-I and its receptor in Leydig cells and that the altered LH/LHreceptor activated pathway in R2C cells could be the cause of oIGF-I overproduction (112).

Moreover the observation that in murine Leydig cells IGF-I is able to increase the LHr mRNA stability (113) together with data showing that the presence of an IGF-I antibody reduced the steroidogenic responsiviness to LH/hCG (114) suggest also the possibility of an IGF-I action in sustaining LH/LHr signalling. If the constitutive activation of LH/LHr/PKA signalling in R2C cells may be involved in upregulation of IGF-I expression remains also to be explored.

In conclusion, in this study we demonstrated that in tumor Leydig cells aromatase overexpression determines an excessive local estradiol production able to stimulate the

expression of genes involved in cycle regulation and sustaining cell proliferation. Aromatase overexpression appears to be induced by the combined enhanced LH/LHr and IGF-I signalling (Fig. 11).

Particularly, LH/LHr signaling determines a constitutive active CREB phosphorylation on aromatase gene promoter while IGF-I overproduction stimulates through an autocrine mechanism SF-1 binding on the same promoter. The observation that antiestrogens and aromatase inhibitors as well as IGF-I signalling blockers are able to reduce R2C proliferation opens new perspectives on the adjuvant therapeutic approach of testicular cancer.

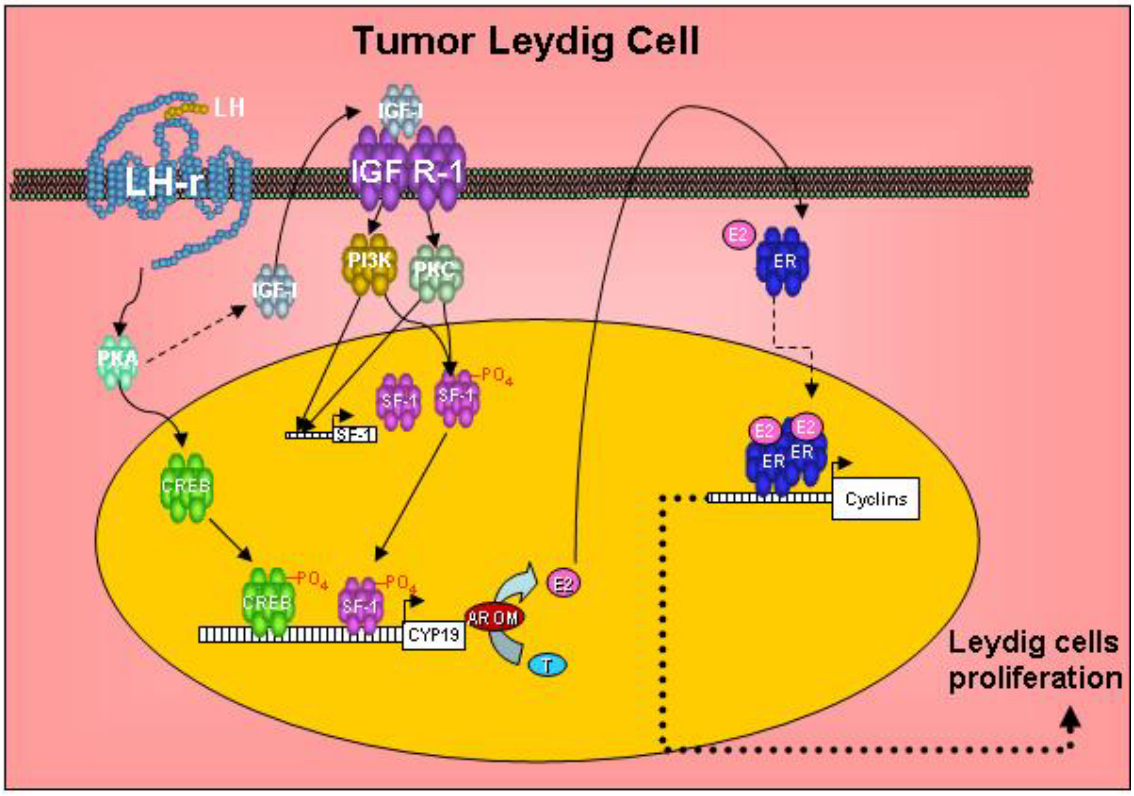

Figure 11. Schematic model showing the mechanism of tumor Leydig cell proliferation.

References

1. **De Kretser DM, Kerr JB** 1994 The cytology of the testis. ThePhysiology of Reproduction. E Knobil & JD Neill. New York: Raven Press ed.; 1177-1290

2. **Gaytan F, Bellido C, Aguilar E, van Rooijen N** 1994 Requirement for testicular macrophages in Leydig cell proliferation and differentiation during prepubertal development in rats. J Reprod Fertil 102:393-399

3. **Gaytan F, Bellido C, Morales C, Reymundo C, Aguilar E, van Rooijen N** 1994 Effects of macrophage depletion at different times after treatment with ethylene dimethane sulfonate (EDS) on the regeneration of Leydig cells in the adult rat. J Androl 15:558-564

4. **Borland K, Mita M, Oppenheimer CL, Blinderman LA, Massague J, Hall PF, Czech MP** 1984 The actions of insulin-like growth factors I and II on cultured Sertoli cells. Endocrinology 114:240-246

5. **De Kretser DM, Catt KJ, Paulsen CA** 1971 Studies on the in vitro testicular binding of iodinated luteinizing hormone in rats. Endocrinology 88:332-337

6. **Loosfelt H, Misrahi M, Atger M, Salesse R, Vu Hai-Luu Thi M, Jolivet A, Guiochon-Mantel A, Sar S, Jallal B, Garnier J, al. e** 1989 Cloning and sequencing of porcine LH-hCG receptor cDNA: variants lacking transmembrane domain. Science 245:525-528

7. **Dufau ML** 1988 Endocrine Regulation and Communicating Functions of the Leydig Cell. Annual Review of Physiology 50:483-508

8. **Dufau ML, Dufau ML, Tsuruhara T, Horner KA, Podesta E, Catt KJ** 1977 Intermediate role of adenosine 3':5'-cyclic monophosphate and protein kinase during gonadotropin-induced steroidogenesis in testicular interstitial cells. Proc Natl Acad Sci U S A 74:3419-3423

9. **Saez JM** 1994 Leydig cells: endocrine, paracrine, and autocrine regulation. Endocr Rev 15:574-626

10. **Vannelli BG, Barni T, Orlando C, Natali A, Serio M, Balboni GC** 1988 Insulin-like growth factor-I (IGF-I) and IGF-I receptor in human testis: an immunohistochemical study. Fertil Steril 49:666-669

11. **Handelsman DJ, Spaliviero JA, Scott CD, Baxter RC** 1985 Identification of insulin-like growth factor-I and its receptors in the rat testis. Acta Endocrinol 109:543-549

12. **Lin T, Haskell J, Vinson N, Terracio L.** 1986 Characterization of insulin and insulin-like growth factor I receptors of purified Leydig cells and their role in steroidogenesis in primary culture: a comparative study. Endocrinology 119:1641-1647

13. **Tres LL, Smith EP, Van Wyk JJ, Kierszenbaum AL** 1986 Immunoreactive sites and accumulation of somatomedin-C in rat Sertoli-spermatogenic cell co-cultures. Experimental Cell Research 162:33-50

14. **Lin T, Haskell J, Vinson N, Terracio L** 1986 Direct stimulatory effects of insulin-like growth factor-I on Leydig cell steroidogenesis in primary culture. Biochemical and Biophysical Research Communications 137:950-956

15. **Benahmed M, Morera AM, Chauvin MC, de Peretti E** 1987 Somatomedin C/insulin-like growth factor 1 as a possible intratesticular regulator of Leydig cell activity. Molecular and Cellular Endocrinology 50:69-77

16. **Kasson BG, Hsueh AJW** 1987 Insulin-like growth factor-I augments gonadotropin-stimulated androgen biosynthesis by cultured rat testicular cells. Molecular and Cellular Endocrinology 52:27-34

17. **Casella SJ, Smith EP, van Wyk JJ, Joseph DR, Hynes MA, Hoyt EC, Lund PK** 1987 Isolation of rat testis cDNAs encoding an insulin-like growth factor I precursor. DNA 6:325-330

18. **Zhou J, Bondy C** 1993 Anatomy of the insulin-like growth factor system in the human testis. Fertil Steril 60:897-904

19. **Baker J, Hardy MP, Zhou J, Bondy C, Lupu F, Bellve AR, Efstratiadis A.** 1996 Effects of an Igf1 gene null mutation on mouse reproduction. Mol Endocrinol 10:903-918

20. **Liu JP, Baker J, Perkins AS, Robertson EJ, Efstratiadis A.** 1993 Mice carrying null mutations of the genes encoding insulin-like growth factor I (Igf-1) and type 1 IGF receptor (Igf1r). Cell 75:59-72

21. **Wang GM, O'Shaughnessy PJ, Chubb C, Robaire B, Hardy MP** 2003 Effects of Insulin-Like Growth Factor I on Steroidogenic Enzyme Expression Levels in Mouse Leydig Cells. Endocrinology 144:5058-5064

22. **Chung BC, Matteson KJ, Voutilainen R, Mohandas TK, Miller WL** 1986 Human Cholesterol Side-Chain Cleavage Enzyme, P450scc: cDNA Cloning, Assignment of the Gene to Chromosome 15, and Expression in the Placenta. PNAS 83:8962-8966

23. **Pollack SE, Furth EE, Kallen CB, Arakane F, Kiriakidou M, Kozarsky KF, Strauss JF, III** 1997 Localization of the Steroidogenic Acute Regulatory Protein in Human Tissues. Journal of Clinical Endocrinology Metabolism 82:4243-4251

24. **Stocco DM, Clark BJ** 1996 Regulation of the acute production of steroids in steroidogenic cells. Endocr Rev 17:221-244

25. **Clark BJ, Wells J, King SR, Stocco DM** 1994 The purification, cloning, and expression of a novel luteinizing hormone-induced mitochondrial protein in MA-10 mouse Leydig tumor cells. Characterization of the steroidogenic acute regulatory protein (StAR). J Biol Chem 269:28314-28322

26. **Lin D, Sugawara T, Strauss JF, III, Clark BJ, Stocco DM, Saenger P, Rogol A, Miller WL** 1995 Role of steroidogenic acute regulatory protein in adrenal and gonadal steroidogenesis. Science 267:1828-1831

27. **Caron KM, Soo SC, Wetsel WC, Stocco DM, Clark BJ, Parker KL** 1997 Targeted disruption of the mouse gene encoding steroidogenic acute regulatory protein provides insights into congenital lipoid adrenaláhyperplasia. PNAS 94:11540-11545

28. **Weusten JJ, Smals AG, Hofman JA, Kloppenborg PW, Benraad TJ** 2006 Early time sequence in pregnenolone metabolism to testosterone in homogenates of human and rat testis. Endocrinology 120:1909-1913

29. **Matteson KJ, Picado-Leonard J, Chung BC, Mohandas TK, Miller W** 1986 Assignment of the gene for adrenal P450c17 (steroid 17 alpha-hydroxylase/17,20 lyase) to human chromosome 10. J Clin Endocrinol Metab 63:789-791

30. **Chung BC, Picado-Leonard J, Haniu M, Bienkowski M, Hall PF, Shively JE, Miller WL** 1987 Cytochrome P450c17 (Steroid 17alpha -hydroxylase/17,20 Lyase): Cloning of Human Adrenal and Testis cDNAs Indicates the Same Gene is Expressed in Both Tissues. PNAS 84:407-411

31. **Inano H, Ishii-Ohba H, Sugimoto Y, Ohta Y, Morikawa T, Yoshida M, Tamaoki B** 1990 Purification and properties of enzymes related to steroid hormone synthesis. Ann N Y Acad Sci 595:17-25

32. **Luu-The V, Labrie C, Simard J, Lachance Y, Zhao HF, Couet J, Leblanc G, Labrie F** 1990 Structure of two in tandem human 17 beta-hydroxysteroid dehydrogenase genes. Mol Endocrinol 4:268-275

33. **Lorence MC, Corbin CJ, Kamimura N, Mahendroo MS, Mason JI** 1990 Structural analysis of the gene encoding human 3 beta-hydroxysteroid dehydrogenase/delta 5----4-isomerase. Mol Endocrinol 4:1850-1855

34. **Andersson S, Russell DW** 1990 Structural and Biochemical Properties of Cloned and Expressed Human and Rat Steroid 5 {alpha}-Reductases. PNAS 87:3640-3644

35. **Chen SA, Besman MJ, Sparkes RS, Zollman S, Klisak I, Mohandas T, Hall PF, Shively JE** 1988 Human aromatase: cDNA cloning, Southern blot analysis, and assignment of the gene to chromosome 15. DNA 7:27-38

36. **Faustini-Fustini M, Rochira V, Carani C** 1999 Oestrogen deficiency in men: where are we today? Eur J Endocrinol 140:111-129

37. **Simpson ER, Mahendroo MS, Means GD, Kilgore MW, Hinshelwood MM, Lorence S, Amarneh B, Ito Y, Fisher CR, Michael MD** 1994 Aromatase cytochrome P450, the enzyme responsible for estrogen biosynthesis. Endocr Rev 15:342-355

38. **Conley A, Hinshelwood M** 2001 Mammalian aromatases. Reproduction 121:685-695

39. **Simpson ER, Michael MD, Agarwal VR, Hinshelwood MM, Bulun SE, Zhao Y** 1997 Cytochromes P450 11: expression of the CYP19 (aromatase) gene: an unusual case of alternative promoter usage. FASEB J 11:29-36

40. **Hickey GJ, Krasnow JS, Beattie WG, Richards JS** 1990 Aromatase cytochrome P450 in rat ovarian granulosa cells before and after luteinization: adenosine 3',5'-monophosphate-dependent and independent regulation. Cloning and sequencing of rat aromatase cDNA and 5' genomic DNA. Mol Endocrinol 4:3-12

41. **Means GD, Kilgore MW, Mahendroo MS, Mendelson CR, Simpson ER** 1991 Tissue-specific promoters regulate aromatase cytochrome P450 gene expression in human ovary and fetal tissues. Mol Endocrinol 5:2005-2013

42. **Young M, McPhaul MJ** 1998 A Steroidogenic Factor-1-Binding Site and Cyclic Adenosine 3',5'-Monophosphate Response Element-Like Elements Are Required for the Activity of the Rat Aromatase Promoter in Rat Leydig Tumor Cell Lines. Endocrinology 139:5082-5093

43. **Gruber CJ, Tschugguel W, Schneeberger C, Huber JC** 2002 Production and Actions of Estrogens. N Engl J Med 346:340-352

44. **O'Donnell L, Robertson KM, Jones ME, Simpson ER** 2001 Estrogen and Spermatogenesis. Endocr Rev 22:289-318

45. **Fisher JS, Millar MR, Majdic G, Saunders PT, Fraser HM, Sharpe RM** 1997 Immunolocalization of oestrogen receptor-a within the testis and excurrent ducts of the rat and marmoset monkey from perinatal life to adulthood. J Endocrinol 153:485-495

46. **Hess RA, Bunick D, Lee KH, Bahr J, Taylor JA, Korach KS, Lubahn DB** 1997 A role for oestrogens in the male reproductive system. Nature 390:509-512

47. **Carreau S, Bourguiba S, Lambard S, Galeraud-Denis I, Genissel C, Levallet J** 2002 Reproductive system: aromatase and estrogens. Molecular and Cellular Endocrinology 193:137-143

48. **van Pelt AMM, de Rooij DG, van der Burg B, van der Saag PT, Gustafsson JA, Kuiper GGJM** 1999 Ontogeny of Estrogen Receptor-{beta} Expression in Rat Testis. Endocrinology 140:478-483

49. **Pelletier G, Labrie C, Labrie F** 2000 Localization of oestrogen receptor alpha, oestrogen receptor beta and androgen receptors in the rat reproductive organs. J Endocrinol 165:359-370

50. **Shughrue PJ, Lane MV, Scrimo PJ, Merchenthaler I** 1998 Comparative distribution of estrogen receptor-[alpha] (ER-[alpha]) and [beta] (ER-[beta]) mRNA in the rat pituitary, gonad, and reproductive tract. Steroids 63:498-504

51. **Levallet J, Bilinska B, Mittre H, Genissel C, Fresnel J, Carreau S** 1998 Expression and immunolocalization of functional cytochrome P450 aromatase in mature rat testicular cells. Biol Reprod 58:919-926

52. **Li X, Nokkala E, Yan W, Streng T, Saarinen N, Warri A, Huhtaniemi I, Santti R, Makela S, Poutanen M** 2001 Altered Structure and Function of Reproductive Organs in Transgenic Male Mice Overexpressing Human Aromatase. Endocrinology 142:2435-2442

53. **Streng T, Li X, Lehtoranta M, Makela S, Poutanen M, Talo A, Tekmal RR, Santti R** 2002 Infravesical obstruction in aromatase over expressing transgenic male mice with increased ratio of serum estrogen-to-androgen concentration. J Urol 168:298-302

54. **Fowler KA, Gill K, Kirma N, Dillehay DL, Tekmal RR** 2000 Overexpression of Aromatase Leads to Development of Testicular Leydig Cell Tumors : An in Vivo Model for Hormone-Mediated TesticularCancer. Am J Pathol 156:347-353

55. **Kirma N, Gill K, Mandava U, Tekmal RR** 2001 Overexpression of Aromatase Leads to Hyperplasia and Changes in the Expression of Genes Involved in Apoptosis, Cell Cycle, Growth, and Tumor Suppressor Functions in the Mammary Glands of Transgenic Mice. Cancer Res 61:1910-1918

56. **Visser JA, McLuskey A, Verhoef-Post M, Kramer P, Grootegoed JA, Themmen APN** 1998 Effect of Prenatal Exposure to Diethylstilbestrol on Mullerian Duct Development in Fetal Male Mice. Endocrinology 139:4244-4251

57. **Atanassova N, McKinnell C, Turner KJ, Walker M, Fisher JS, Morley M, Millar MR, Groome NP, Sharpe RM** 2000 Comparative Effects of Neonatal Exposure of Male Rats to Potent and Weak (Environmental) Estrogens on Spermatogenesis at Puberty and the Relationship to Adult Testis Size and Fertility: Evidence for Stimulatory Effects of Low Estrogen Levels. Endocrinology 141:3898-3907

58. **Toppari J, Skakkebaek NE** 1998 Sexual differentiation and environmental endocrine disrupters. Baillieres Clin Endocrinol Metab 12:143-156

59. **Raman-Wilms L, Tseng AL, Wighardt S, Einarson TR, Koren G** 1995 Fetal genital effects of first-trimester sex hormone exposure: a meta-analysis. Obstet Gynecol 85:141-149

60. **Akingbemi BT, Hardy MP** 2001 Oestrogenic and antiandrogenic chemicals in the environment: effects on male reproductive health. Ann Med 33:391-403

61. **vom Saal FS, Cooke PS, Buchanan DL, Palanza P, Thayer KA, Nagel SC, Parmigiani S, Welshons WV** 1998 A physiologically based approach to the study of bisphenol A and other estrogenic chemicals on the size of reproductive organs, daily sperm production, and behavior. Toxicol Ind Health 14:239-260

62. **Cheek AO, McLachlan JA** 1998 Environmental hormones and the male reproductive system. J Androl 19:5-10

63. **McLachlan JA, Newbold RR, Bullock B** 1975 Reproductive tract lesions in male mice exposed prenatally to diethylstilbestrol. Science 190:991-992

64. **Wilson JD** 1999 The Role of Androgens in Male Gender Role Behavior. Endocr Rev 20:726-737

65. **Sharpe RM** 1993 Declining sperm counts in men--is there an endocrine cause**?** J Endocrinol 136:357-360

66. **Toppari J, Larsen JC, Christiansen P, Giwercman A, Grandjean P, Guillette LJ Jr, Jegou B, Jensen TK, Jouannet P, Keiding N, Leffers H, McLachlan JA, Meyer O, Muller J, Rajpert-De Meyts E, Scheike T, Sharpe R, Sumpter J, Skakkebaek NE** 1996 Male reproductive health and environmental xenoestrogens. Environ Health Perspect 104:741-803

67. **Pflieger-Bruss S, Schuppe HC, Schill WB** 2004 The male reproductive system and its susceptibility to endocrine disrupting chemicals. Andrologia 36:337-345

68. **Sharpe RM, Skakkebaek NE** 1993 Are oestrogens involved in falling sperm counts and disorders of the male reproductive tract? Lancet 341:1392-1395

69. **Borer JG, Tan PE, Diamond DA** 2000 The spectrum of Sertoli cell tumors in children. Urol Clin North Am 27:529-541

70. **Harms D, Kock LR** 1997 Testicular juvenile granulosa cell and Sertoli cell tumours: a clinicopathological study of 29 cases from the Kiel Paediatric Tumour Registry. Virchows Archiv V430:301-309

71. **Rushton HG, Belman AB** 1993 Testis-sparing surgery for benign lesions of the prepubertal testis. Urol Clin North Am 20:27-37

72. **Kaplan GW, Cromie WJ, Kelalis PP, Silber I, Tank ES Jr** 1986 Gonadal stromal tumors: a report of the Prepubertal Testicular Tumor Registry. J Urol 136:300-302

73. **Holm M, Rajpert-De Meyts E, Andersson AM, Skakkebaek NE** 2003 Leydig cell micronodules are a common finding in testicular biopsies from men with impaired spermatogenesis and are associated with decreased testosterone/LH ratio. J Pathol 199:378-386

74. **Shenker A, Laue L, Kosugi S, Merendino JJ, Minegishi T, Cutler GB** 1993 A constitutively activating mutation of the luteinizing hormone receptor in familial male precocious puberty. Nature 365:652-654

75. **Liu G, Duranteau L, Carel JC, Monroe J, Doyle DA, Shenker A** 1999 Leydig-Cell Tumors Caused by an Activating Mutation of the Gene Encoding the Luteinizing Hormone Receptor. N Engl J Med 341:1731-1736

76. **Iiri T, Herzmark P, Nakamoto JM, Van Dop C, Bourne HR** 1994 Rapid GDP release from Gs[alpha] in patients with gain and loss of endocrine function. Nature 371:164-168

77. **Villares Fragoso MC, Latronico AC, Carvalho FM, Zerbini MC, Marcondes JAM, Araujo LMB, Lando VS, Frazzatto ET, Mendonca BB, Villares SM** 1998 Activating Mutation of the Stimulatory G Protein (gsp) as a Putative Cause of Ovarian and Testicular Human Stromal Leydig Cell Tumors. Journal of Clinical Endocrinology Metabolism 83:2074-2078

78. **Themmen AP, Brunner HG** 1996 Luteinizing hormone receptor mutations and sex differentiation. Eur J Endocrinol 134:533-540

79. **Dilworth JP, Farrow GM, Oesterling JE** 1991 Non-germ cell tumors of testis. Urology 37:399-417

80. **Rich MA, Keating MA** 2000 Leydig cell tumors and tumors associated with congenital adrenal hyperplasia. Urol Clin North Am 27:519-528

81. **Kim I, Young RH, Scully RE** 1985 Leydig cell tumors of the testis. A clinicopathological analysis of 40 cases and review of the literature. Am J Surg Pathol 9:177-192

82. **Bertram KA, Bratloff B, Hodges GF, Davidson H** 1991 Treatment of malignant Leydig cell tumor. Cancer 68:2324-2329

83. **Cheville JC, Sebo TJ, Lager DJ, Bostwick DG, Farrow GM** 1998 Leydig cell tumor of the testis: a clinicopathologic, DNA content, and MIB-1 comparison of nonmetastasizing and metastasizing tumors. Am J Surg Pathol 22:1361-1367

84. **Coleman GL, Barthold W, Osbaldiston GW, Foster SJ, Jonas AM** 1977 Pathological changes during aging in barrier-reared Fischer 344 male rats. J Gerontol 32:258-278

85. **Lephart ED, Simpson ER.** 1991 Assay of aromatase activity. Methods Enzymol 206:477-483

86. **Pezzi V, Sirianni R, Chimento A, Maggiolini M, Bourguiba S, Delalande C, Carreau S, Ando S, Simpson ER, Clyne CD** 2004 Differential Expression of Steroidogenic Factor-1/Adrenal 4 Binding Protein and Liver Receptor Homolog-1 (LRH-1)/Fetoprotein Transcription Factor in the Rat Testis: LRH-1 as a Potential Regulator of Testicular Aromatase Expression. Endocrinology 145:2186-2196

87. **Bradford MM** 1976 A rapid and sensitive method for thequantitation of microgram quantities of protein utilizing theprinciple of protein-dye binding. Analytical Biochemistry 72:248-254

88. **Jacobs BB, Huseby RA** 1967 Neoplasms occurring in aged Fischer rats, with special reference to testicular, uterine and thyroid tumors. J Natl Cancer Inst303-309

89. **Jo Y, Stocco DM** 2004 Regulation of Steroidogenesis and Steroidogenic Acute Regulatory Protein in R2C Cells by DAX-1 (Dosage-Sensitive Sex Reversal, Adrenal Hypoplasia Congenita, Critical Region on the X Chromosome, Gene-1). Endocrinology 145:5629-5637

90. **Manna PR, Chandrala SP, King SR, Jo Y, Counis R, Huhtaniemi IT, Stocco DM** 2006 Molecular Mechanisms of Insulin-like Growth Factor-I Mediated Regulation of the Steroidogenic Acute Regulatory Protein in Mouse Leydig Cells. Mol Endocrinol 20:362-378

91. **LaVoie HA, Garmey JC, Veldhuis JD** 1999 Mechanisms of Insulin-Like Growth Factor I Augmentation of Follicle-Stimulating Hormone-Induced Porcine Steroidogenic Acute Regulatory Protein Gene Promoter Activity in Granulosa Cells. Endocrinology 140:146-153

92. **Pomerantz D** 1980 Developmental Changes in the Ability of Follicle Stimulating Hormone to Stimulate Estrogen Synthesis in vivo by the Testis of the Rat. Biol Reprod 23:948-954

93. **Kmicikiewicz I, Krezolek A, Bilinska B** 1997 The effects of aromatase inhibitor on basal and testosterone-supplemented estradiol secretion by Leydig cells in vitro. Exp Clin Endocrinol Diabetes 105:113-118

94. **Payne AH, Kelch RP, Musich SS, Halpern ME** 1976 Intratesticular site of aromatization in the human. J Clin Endocrinol Metab 42:1081-1087

95. **Raeside JI, Renaud RL** 1983 Estrogen and androgen production by purified Leydig cells of mature boars. Biol Reprod 28:727-733

96. **Bilinska B, Lesniak M, Schmalz B** 1997 Are ovine Leydig cells able to aromatize androgens?. Reprod Fertil Dev 9:193-199

97. **Valensi P, Coussieu C, Pauwles A, Attali JR, Kemeny JL, Amouroux J, Sebaoun J** 1987 Feminizing Leydig cell tumor: endocrine and incubation studies. J Endocrinol Invest 10:187-193

98. **Saunders PT, Fisher JS, Sharpe RM, Millar MR** 1998 Expression of oestrogen receptor beta (ER beta) occurs in multiple cell types, including some germ cells, in the rat testis. J Endocrinol 156:R13-R17

99. **Prall OWJ, Sarcevic B, Musgrove EA, Watts CKW, Sutherland RL** 1997 Estrogen-induced Activation of Cdk4 and Cdk2 during G1-S Phase Progression Is Accompanied by Increased Cyclin D1 Expression and Decreased Cyclin-dependent Kinase Inhibitor Association with Cyclin E-Cdk2. J Biol Chem 272:10882-10894

100. **Hatano O, Takayama K, Imai T, Waterman MR, Takakusu A, Omura T, Morohashi K** 1994 Sex-dependent expression of a transcription factor, Ad4BP, regulating steroidogenic P-450 genes in the gonads during prenatal and postnatal rat development. Development 120:2787-2797

101. **Desclozeaux M, Krylova IN, Horn F, Fletterick RJ, Ingraham HA** 2002 Phosphorylation and Intramolecular Stabilization of the Ligand Binding Domain in the Nuclear Receptor Steroidogenic Factor 1. Mol Cell Biol 22:7193-7203

102. **Dufau ML, Winters CA, Hattori M, Aquilano D, Baranao JL, Nozu K, Baukal A, Catt KJ** 1984 Hormonal regulation of androgen production by the Leydig cell. J Steroid Biochem 20:161-173

103. **Jo Y, King SR, Khan SA, Stocco DM** 2005 Involvement of Protein Kinase C and Cyclic Adenosine 3',5'-Monophosphate-Dependent Kinase in Steroidogenic Acute Regulatory Protein Expression and Steroid Biosynthesis in Leydig Cells. Biol Reprod 73:244-255

104. **Rao RM, Jo Y, Leers-Sucheta S, Bose HS, Miller WL, Azhar S, Stocco DM** 2003 Differential Regulation of Steroid Hormone Biosynthesis in R2C and MA-10 Leydig Tumor Cells: Role of SR-B1-Mediated Selective Cholesteryl Ester Transport. Biol Reprod 68:114-121

105. **Saez JM, Chatelain PG, Perrard-Sapori MH, Jaillard C, Naville D** 1988 Differentiating effects of somatomedin-C/insulin-like growth factor I and insulin on Leydig and Sertoli cell functions. Reprod Nutr Dev 28:989-1008

106. **Nagpal ML, Wang D, Calkins JH, Chang WW, Lin T.** 1991 Human chorionic gonadotropin up-regulates insulin-like growth factor-I receptor gene expression of Leydig cells. Endocrinology 129:2820-2826

107. **Gelber SJ, Hardy MP, Mendis-Handagama SM, Casella SJ** 1992 Effects of insulin-like growth factor-I on androgen production by highly purified pubertal and adult rat Leydig cells. J Androl 13:125-130

108. **Lin T, Wang D, Hu J, Stocco DM** 1998 Upregulation of human chorionic gonadotrophin-induced steroidogenic acute regulatory protein by insulin-like growth factor-I in rat Leydig cells. Endocrine 8:73-78

109. **Kojima I, Mogami H, Shibata H, Ogata E** 1993 Role of calcium entry and protein kinase C in the progression activity of insulin-like growth factor-I in Balb/c 3T3 cells. J Biol Chem 268:10003-10006

110. **Song KH, Park YY, Park KC, Hong CY, Park JH, Shong M, Lee K, Choi HS** 2004 The Atypical Orphan Nuclear Receptor DAX-1 Interacts with Orphan Nuclear Receptor Nur77 and Represses Its Transactivation. Mol Endocrinol 18:1929-1940

111. **Moore A, Chen CL, Davis JR, Morris ID** 1993 Insulin-like growth factor-I mRNA expression in the interstitial cells of the rat testis. J Mol Endocrinol 11:319-324

112. **Sriraman V, Rao VS, Sairam MR, Rao AJ** 2000 Effect of deprival of LH on Leydig cell proliferation: involvement of PCNA, cyclin D3 and IGF-1. Molecular and Cellular Endocrinology 162:113-120

113. **Zhang FP, El-Hafnawy T, Huhtaniemi I** 1998 Regulation of Luteinizing Hormone Receptor Gene Expression by Insulin-Like Growth Factor-I in an Immortalized Murine Leydig Tumor Cell Line (BLT-1). Biol Reprod 59:1116-1123

114. **Le Roy C, Lejeune H, Chuzel F, Saez JM, Langlois D** 1999 Autocrine regulation of Leydig cell differentiated functions by insulin-like growth factor I and transforming growth factor beta. J Steroid Biochem Mol Biol 69:379-384

0013-7227/04/$15.00/0
Printed in U.S.A.

Endocrinology 145(5):2186–2196

doi: 10.1210/en.2003-1366

Differential Expression of Steroidogenic Factor-1/Adrenal 4 Binding Protein and Liver Receptor Homolog-1 (LRH-1)/Fetoprotein Transcription Factor in the Rat Testis: LRH-1 as a Potential Regulator of Testicular Aromatase Expression

VINCENZO PEZZI, ROSA SIRIANNI, ADELE CHIMENTO, MARCELLO MAGGIOLINI, SONIA BOURGUIBA, CHRISTELLE DELALANDE, SERGE CARREAU, SEBASTIANO ANDÒ, EVAN R. SIMPSON, AND COLIN D. CLYNE

Departments of Pharmaco-Biology and Cell Biology (V.P., R.S., A.C., M.M., S.A.), University of Calabria, Arcavacata di Rende 87036 (CS), Italy; Prince Henry's Institute of Medical Research (E.R.S., C.D.C.), Melbourne, Victoria 3168, Australia; and Department of Biochemistry (S.B., C.D., S.C.), University, Unité Pour Recherche Enseignement Supérieur Equipe Associeé 2608, USC Institut National de la Recherche Agronomique, 14032-Caen, France

Aromatase converts testicular androgens to estrogens, which are essential for male fertility. Aromatase expression in testis occurs via transcription from promoter II, and requires the presence of a nuclear receptor half-site that binds the orphan receptor steroidogenic factor-1 [SF-1 (nuclear receptor 5A1)] to mediate basal and (in part) cAMP-induced transcription. We hypothesized that liver receptor homolog-1 (LRH-1) (nuclear receptor 5A2), a receptor closely related to SF-1, could also play a role in regulating aromatase expression in the testis. We demonstrate expression of LRH-1 in adult rat and immature mouse Leydig cells (LHR-1 > SF-1) as well as in pachytene spermatocytes and round spermatids but not in Sertoli cells, which in contrast, express high levels of SF-1. In transient transfection assays using TM3 Leydig cells and TM4 Sertoli cells, a rat promoter II luciferase reporter construct was stimulated by cotransfection of LRH-1 expression vector. Mutation analysis showed that induction by LRH-1 in TM3 and TM4 cells requires an AGGTCA motif at position −90, to which LRH-1 bound in gel shift analysis. We therefore provide evidence that LRH-1 plays an important role in the regulation of aromatase expression in Leydig cells. The colocalization of LRH-1 and aromatase to multiple testis cell types suggests that LRH-1 may have important effects on estrogen production, testis development, spermatogenesis, and testicular carcinogenesis. (*Endocrinology* 145: 2186–2196, 2004)

GONADOTROPINS AND TESTOSTERONE, together with numerous intratesticular factors, play a crucial role in the development and maintenance of spermatogenesis in the mammalian testis (1, 2). However, several lines of evidence have conclusively shown that estrogens are also produced in the male genital tract and contribute significantly in regulating testicular functions and development (3, 4). The biosynthesis of estrogens from androgens is catalyzed by the microsomal enzymatic complex termed aromatase, which is composed of two polypeptides: a ubiquitous, nonspecific flavoprotein reduced nicotinamide adenine dinucleotide phosphate (NADPH)-cytochrome P450 reductase; and a specific form of cytochrome P450 (P450arom encoded by the *CYP19* gene) expressed in several tissues such as placenta, adipose tissue, skin, brain, and gonads (5).

In the rat testis, there is an age-related pattern of aromatase activity. Activity is present mainly in Sertoli cells of immature animals and in Leydig cells of adults (6). In pig, ram, and human, however, aromatase is mainly present in Leydig cells (7). In germ cells, the amount of P450arom mRNA changes with the stage of maturation: it is twice as high in pachytene spermatocytes (PS) than in round spermatids (RS), and 20-fold higher in RS than in spermatozoa (8). Conversely, aromatase activity appears to be 4- to 5-fold higher in spermatozoa than in either PS or RS (4). Similar patterns of aromatase expression have been reported in mouse Leydig, Sertoli, and germs cells (9). Moreover, the presence of aromatase in Leydig cells of primates and humans is well established (7), and we have recently identified aromatase expression in ejaculated human spermatozoa (10).

Aromatase expression is regulated by tissue-specific promoters (11–14). A promoter proximal to the translation start site, termed promoter II (PII), regulates the expression of P450arom in ovaries of several species (15, 16), in fetal gonads (13) and in two rat Leydig tumor cells (R2C and H540) (17, 18). Recently we have demonstrated that PII is the principal promoter that is active in rat Sertoli, Leydig, and germ cells

Abbreviations: AD4BP, Adrenal 4 binding protein; CPF, CYP7A promoter binding factor; CRE, cAMP response element; Ct, threshold cycle; DAX-1, dosage-sensitive sex reversal adrenal hypoplasia congenita critical region on the X chromosome, gene 1; FSK, forskolin; FTF, fetoprotein transcription factor; LRH-1, liver receptor homolog-1; MBF-1, multiprotein-bridging factor-1; NRE, nuclear receptor element; PII, promoter II; PS, pachytene spermatocytes; RS, round spermatids; SF-1, steroidogenic factor 1; SHP, short heterodimer partner; ST, seminiferous tubules; ttp, transcripted translated protein.

***Endocrinology* is published monthly by The Endocrine Society (http://www.endo-society.org), the foremost professional society serving the endocrine community.**

(19). This promoter contains several cAMP response element (CRE)-like motifs that mediate the effects of the cAMP transduction pathway that potentiates aromatase expression and activity. Basal and, in part, cAMP-induced transcription of *CYP19* also requires the presence of a nuclear receptor half site [nuclear receptor element (NRE)] located at −90 relative to the start of transcription of the rat gene that has been proposed to bind the orphan nuclear receptor steroidogenic factor-1 [SF-1 (nuclear receptor 5A1)] (19, 20). However, the intratesticular sites of expression of SF-1 and aromatase do not correlate; in adult rats, SF-1 is mainly expressed in Sertoli cells (21), whereas aromatase is mainly in Leydig and germ cells. In seeking an alternative factor that might account for aromatase expression in these SF-1 negative sites, we have focused the present study on the liver receptor homolog-1 (LRH-1).

LRH-1 [nuclear receptor 5A2, also known as CYP7A promoter binding factor (CPF), α-fetoprotein transcription factor (FTF), and hB1f (22–25)] and SF-1 are the two mammalian homologues of the Drosophila nuclear receptor Fushi tarazu F1 (26) and share common DNA binding and transactivation properties. LRH-1 is expressed at high levels in liver, where it regulates expression of genes involved in cholesterol metabolism and bile acid synthesis including cholesterol 7α-hydroxylase (CYP7A) (27, 28), sterol 12α-hydroxylase (CYP8B1) (29), and the cholesteryl ester transfer protein (30). Initially, LRH-1 expression was thought to be limited only to the nonsteroidogenic tissues pancreas, intestine, and colon (31). Recently, however, LRH-1 was shown to be expressed in horse and rat ovary (32–34); whereas, in collaboration with Rainey and co-workers (35), we have quantified mRNA levels of SF-1 and LRH-1 in different human steroidogenic tissues, showing high expression in the human ovary and testis. We also described the effect of LRH-1 on transcription of the genes encoding the enzymes involved in steroidogenesis, suggesting that this transcription factor may play a role not only in bile acid production but also in steroidogenesis (35). Our recent results (36), suggesting that LRH-1 regulates aromatase gene transcription in preadipocytes acting on aromatase PII, led us to hypothesize a role for this factor in regulation of *CYP19* gene in the testis. In the current study, we demonstrate expression of LRH-1 in several rat testicular cell types and investigate the role of LRH-1 in regulating aromatase expression in these cells.

Materials and Methods

Plasmids

PII-688 is a *CYP19* PII/luciferase construct containing −688/+94 of rat *CYP19* PII inserted upstream of the firefly luciferase gene in the reporter vector pGL2-Basic (Promega, Madison, WI). The nuclear receptor half site (NRE) at position −90 within this construct was mutated by PCR-directed mutagenesis (AGGTCA→AtaTCA) to produce pII-688mNRE. Both these plasmids were generously provided by Michael McPhaul (University of Texas Southwestern Medical Center, Dallas, TX). For all transfections, empty pGL2-Basic was used as the control vector to measure basal activity. The coding region of mouse LRH-1 (provided by Dr. David Mangelsdorf, UT Southwestern Medical Center) and mouse SF-1 (provided by Dr. William Rainey, UT Southwestern Medical Center) were inserted into pcDNA3.1 zeo (Invitrogen, Carlsbad, CA) eukaryotic expression vector and used for transfections and *in vitro* transcription/translation reactions.

Cell culture and transfection

Primary cultures of purified adult rat Leydig cells, Sertoli cells, and testicular mixed germ cells (enriched PS or RS, respectively) were established as described previously (37, 38). All animal studies were conducted in accordance with the Guide for Care and Use of Laboratory Animals (National Institutes of Health). TM3 and TM4 cells (immature mouse Leydig and Sertoli cell lines) were cultured in DMEM/Ham's F12 (Invitrogen, S.R.L., San Giuliano Milanese, Italy) supplemented with 5% NU Serum (Collaborative Biom, Bedford, MA) and antibiotics in a 24-well plate. For transfection experiments, Fugene6 (Roche, Indianapolis, IN) was used, as directed by the manufacturer, to transfect the reporter plasmid and the indicated amounts of expression vectors. pcDNA3.1 Zeo empty vector was used to ensure constant amounts of DNA per well for each transfection. To normalize luciferase activity, cells were co-transfected with 50 ng/well of TK Renilla luciferase plasmid (Promega). Where indicated, cells were treated with forskolin (FSK) (10 μM) for the indicated time, 18–24 h after the beginning of transfection, and then assayed for activity using the Dual Luciferase assay system (Promega).

RNA extraction, cDNA synthesis, and real-time RT-PCR

The RNAgents total RNA isolation system (Promega, Charbonnieres, France) was used to extract total RNA from primary cells. Total cellular RNA was extracted from TM3 and TM4 cells using Total RNA Isolation System kit (Promega). All RNA was treated with DNase (Ambion, Austin, TX), and purity and integrity of the RNA was confirmed spectroscopically and by gel electrophoresis before use. Four micrograms of total RNA were reverse transcribed in a final vol of 100 μl using the High Capacity cDNA Archive Kit (Applied Biosystems, Foster City, CA) and stored at −20 C. Primers for the amplification were based on published sequences for the rat and mouse LRH-1 and SF-1. The nucleotide sequences of the primers are shown in Table 1.

PCRs were performed in the ABI Prism 7000 Sequence Detection System (Applied Biosystems) in a total vol of 30 μl reaction mixture, following the manufacturer's recommendations, using the SYBR Green Universal PCR Master Mix 2 × (Applied Biosystems) and 0.1 μM of each primer using the dissociation protocol. Negative controls contained water instead of first-strand cDNA. Each sample was normalized on the basis of its 18S ribosomal RNA content. The 18S quantification was performed using a TaqMan Ribosomal RNA Reagent kit (Applied Biosystems), following the method provided in the TaqMan Ribosomal RNA Control Reagent kit (Applied Biosystems). The relative SF1 and LRH-1 gene expression levels were normalized to a calibrator that was chosen to be the sample with the highest threshold cycle (Ct). Final results, expressed as *n*-fold differences in orphan nuclear receptor gene expression relative to 18S rRNA and calibrator, were

TABLE 1. Oligonucleotide primer sequences

Gene	Oligonucleotide	Sequence (5′-3′)	PCR product size (bp)
Mouse SF-1 (AF511594)	Upper primer	GTCTCAAGTTCCTCATCCTCTTCAG	74
	Lower primer	CCTGGGCGTCCTTTACGA	
Rat SF-1 (NM_053344)	Upper primer	GTCTCAAGTTCCTCATCCTCTTCAG	74
	Lower primer	CCTGGGCGTCCTTTACCA	
Mouse LRH-1 (NM_030676)	Upper primer	CCCTGCTGGACTACACGGTTT	74
	Lower primer	CGGGTAGCCGAAGAAGTAGCT	
Rat LRH-1 (NM_021742)	Upper primer	AAAGCTGAGCGCGTTTGG	67
	Lower primer	CCCACTCAACAATGGAGAACAG	

calculated following the ΔΔCt method, determined as follows: n-fold = $2^{-(\Delta Ct_{sample} - \Delta Ct_{calibrator})}$, where ΔCt values of the sample and calibrator are determined by subtracting the average Ct value of the nuclear receptor gene from the average Ct value of the 18S rRNA reference gene. Before using the ΔΔCt method for relative quantification, we perform validation experiments to demonstrate that efficiencies of target and reference are approximately equal, following instructions of Applied Biosystems [http://docs.appliedbiosystems.com/pebiodocs/04303859.pdf (page 14)].

Western blot analysis

Nuclear extracts were prepared from cultured cells as previously described (39). Briefly, cells plated into 60-mm^2 dishes were scraped into 1.5 ml cold PBS. Cells were pelleted for 10 sec and resuspended in 400 μl cold buffer A (10 mM HEPES-KOH, pH 7.9, at 4 C; 1.5 mM $MgCl_2$; 10 mM KCl; 0.5 mM dithiothreitol; 0.2 mM phenylmethylsulfonylfluoride) by flicking the tube. The cells were allowed to swell on ice for 10 min and then vortexed for 10 sec. Samples were centrifuged for 10 sec, and the supernatant fraction was discarded. The pellet was resuspended in 50 μl cold buffer C (20 mM HEPES-KOH, pH 7.9; 25% glycerol; 1.5 mM $MgCl_2$; 420 mM NaCl; 0.2 mM EDTA; 0.5 mM dithiothreitol; 0.2 mM phenylmethylsulfonylfluoride) and incubated in ice for 20 min for high-salt extraction. Cellular debris was removed by centrifugation for 2 min at 4 C, and the supernatant fraction (containing DNA binding proteins) was stored at −70 C. The yield was determined by the Bradford method. The proteins (50 μg) were separated on sodium dodecyl sulfate-polyacrylamide (12%) gel and then electroblotted onto a nitrocellulose membrane. The blots were incubated overnight at 4 C with FTF-2 antiserum (polyclonal antibody generated against the mouse FTF extra DNA binding domain, provided by Dr. Luc Belanger, Laval University, Quebec Canada) or with anti-CPF antibody against the amino-terminal region of mouse LRH-1, (1:1000) (Santa Cruz Biotechnology, Inc., Santa Cruz, CA) or rabbit antiserum to adrenal 4 binding protein (Ad4BP)/SF-1 [Ad4BP is the bovine homolog of SF-1 (1:1000) kindly provided from Dr. Morohashi (National Institute for Basic Biology, myodaiji-cho, Okazaki, Japan)]. The antigen-antibody complexes were detected by incubation of the membranes at room temperature with antigoat (for CPF) or anti-rabbit for Ad4BP IgG coupled to peroxidase, developed using the ECL

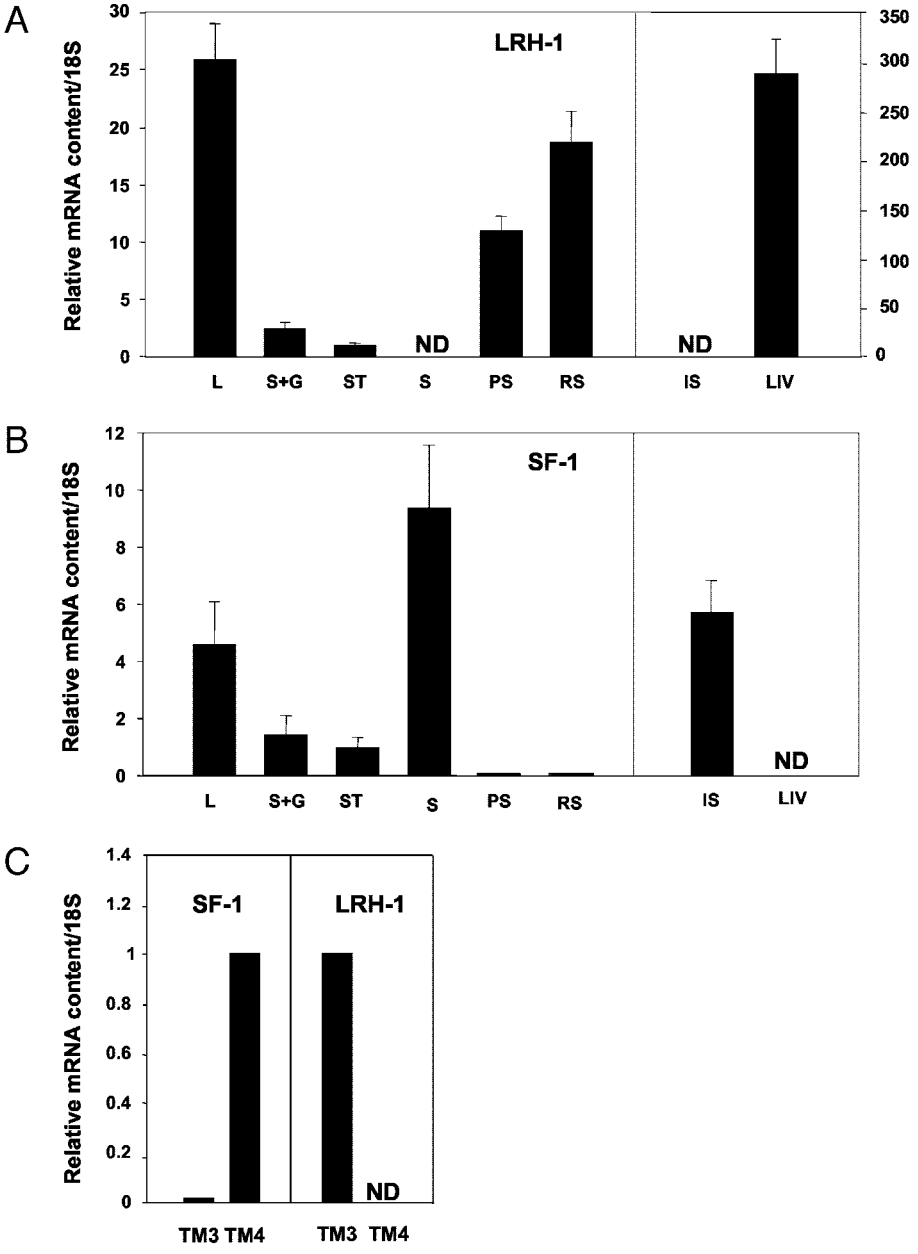

FIG. 1. Quantification of LRH-1 and SF1 transcript levels in purified rat testicular cells (primary cells). Real-time RT-PCR was used to quantify the level of LRH-1 (A) and SF-1 (B) mRNA in total RNA obtained from primary cultures of Leydig cells (L), Sertoli and germ cells (S+G), Sertoli cells (S), RS, PS isolated from adult rats, and in TM3 Leydig and TM4 Sertoli cells (C) as described in *Materials and Methods*. Total RNA from immature Sertoli (IS) cells was used as positive control for SF-1, whereas total RNA from rat Liver (LIV) was used as positive control for LRH-1. Data represent the mean ± SEM of three independent RNA samples obtained from testis of several adult rats or TM4 and TM3 cultures and are expressed as relative difference from the calibrator.

Plus Western blotting detection system (Amersham Biosciences, Cologno Monzese, Italy). *In vitro* transcribed and translated LRH-1 and SF-1 proteins were synthesized from the expression vectors described above using T7 polymerase in the rabbit reticulocyte lysate system as directed by the manufacturer (Promega). These proteins were used as positive controls in the immunoblot and EMSA experiments. The specificity of each antibody was tested using antisera preabsorbed with excess amount of antigens.

Gel mobility shift assay

Nuclear extracts were prepared from TM3 and TM4 as previously described (39). *In vitro* transcribed and translated LRH-1 and SF-1 proteins were synthesized using T7 polymerase in the rabbit reticulocyte lysate system as directed by the manufacturer (Promega). The probe was generated by annealing single-stranded oligonucleotides (Sigma Genosys, Cambridge, UK) and labeling with [γ^{32}P] ATP and T4 polynucleotide kinase, followed by purification using Sephadex G50 spin columns (Amersham Pharmacia Biotech). The DNA sequences used as probe or as cold competitors are the following (the nucleotide motifs of interest are *underlined*): 5′-CAG GAC CTG AGT CTC CCA AGG TCA TCC TTG TTT GAC TTG TA-3′. The protein binding reactions were carried out in 20 μl buffer [20 mM HEPES, pH 8; 1 mM EDTA; 50 mM KCl; 10 mM DTT; 10% glycerol; 1 mg/ml BSA] with 50,000 cpm of labeled probe, 20 μg nuclear proteins or 2 μl of transcribed and translated *in vitro* SF-1 protein or LRH-1 protein, and 5 μg poly (dI-dC) (Roche). The mixtures were incubated at 4 C for 30 min in the presence or absence of unlabeled competitor oligonucleotides or *in vitro*-translated protein in the presence or absence of rabbit antiserum to Ad4BP/SF-1 or FTF-1 antiserum [rabbit immunized with the peptide CLTSAIQNIHSSASKGL; rat position 142–156 (22), provided by Dr. Luc Belanger, Laval University]. For FTF-1 the reaction mixture was incubated with this antibody at 4 C for 2 h before addition of labeled probe. The entire reaction mixture was electrophoresed through a 6% polyacrylamide gel in 0.25× Tris borate-EDTA for 3 h at 150 V. Gels were dried and subjected to autoradiography at −70 C.

Statistical analysis

Data were analyzed using STATPAC software (Minneapolis, MN).

Results

LRH-1 and SF-1 expression in various testicular cell types

To address the possible role of LRH-1 in the regulation of *CYP19* in rat testis, we first determined the expression profile of LRH-1 in various testicular cell types and compared it with expression levels of SF-1. To accomplish this, total RNA from primary cell cultures of Leydig cells, Sertoli cells, RS, PS, primary cocultures of Sertoli and germ cells, seminiferous tubules (ST) isolated from adult rats, and Sertoli cells isolated from immature animals were used to quantify transcript levels of both nuclear receptors using real-time RT-PCR (Fig. 1). LRH-1 was expressed at appreciable levels in mature Leydig cells as well as in PS and RS (~50% and 75% of the levels in Leydig cells, respectively, but was undetectable in Sertoli cells of any age (Fig. 1A). The relatively lower LRH-1 mRNA levels measured in coculture of Sertoli and germ cells and in ST reflects the diluted quantity of LRH-1 mRNA expressed in germ cells, and confirms that LRH-1 expression is present only in germ cells but not in Sertoli cells (Fig. 1A). In contrast, we observed high levels of SF-1 mRNA in immature and mature Sertoli cells as well as in mature Leydig cells; whereas in germ cells, the SF-1 mRNA was present at negligible levels (Fig. 1B). This is confirmed by the relatively lower SF-1 mRNA levels measured in coculture of Sertoli and germ cells and in ST (Fig. 1B). SF-1 was undetectable in rat liver, confirming the lack of cross-reactivity of the primers used in the assay. The data obtained for the somatic cells was confirmed using RNA isolated from immature mouse Leydig cell line (TM3) and Sertoli cell line (TM4): LRH-1 was undetectable in TM4 cells, where SF-1 expression was high, whereas TM3 showed an opposite pattern with high LRH-1 expression and almost undetectable expression of SF-1 (Fig. 1C). Thus, the two orphan receptors show overlapping, but distinct, patterns of expression within the rat testis: Leydig cells express both SF-1 and LRH-1 mRNA, whereas Sertoli cells and germ cells (PS and RS) exclusively express SF-1, and LRH-1 mRNA, respectively.

We confirmed this pattern of SF-1 and LRH-1 expression at the protein level by Western analysis using nuclear extracts from TM3/4 cells, as well as from isolated rat primary cells. As shown in Fig. 2A, bands of the expected size (64 kDa

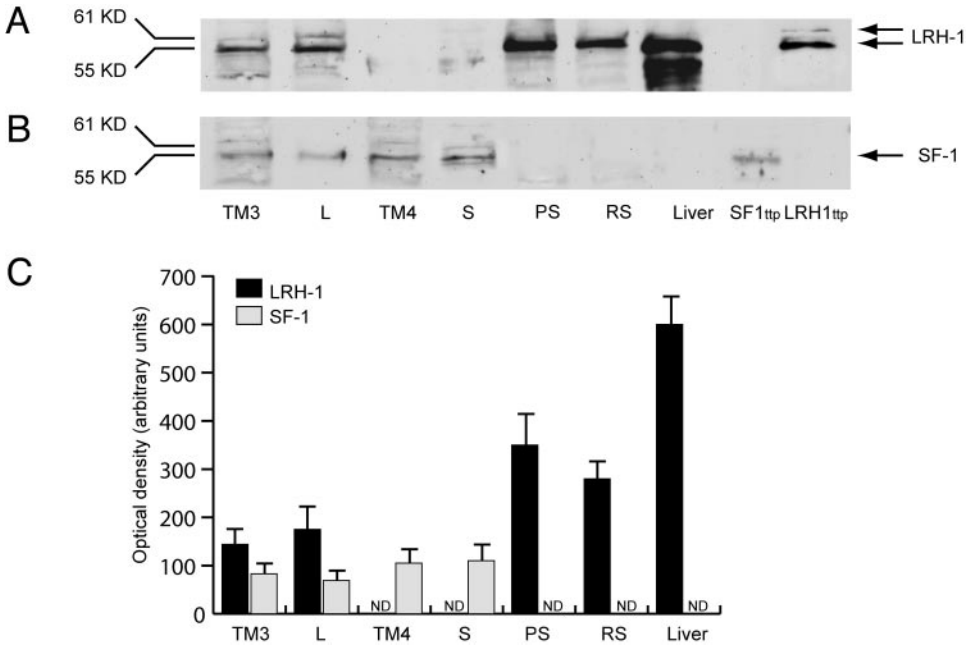

FIG. 2. Western blot analysis of LRH-1 and SF-1 expression testicular cells. LRH-1 (A) and SF-1 (B) proteins were examined by Western analysis using 50 μg nuclear extracts isolated from TM3 Leydig cells (TM3), primary cultured rat Leydig cells (L), TM4 Sertoli cells (TM4), primary cultured rat Sertoli cells, PS, and RS. Rat liver extract and *in vitro*-translated LRH-1/SF-1 (ttp) served as positive controls. The same nuclear extracts were run on two different gels, transferred to membranes, and one probed for LRH-1 and the other for SF-1. One representative experiment from three independent experiments is shown. C, The histograms represent the mean ± SEM of three separate Western analyses performed on different nuclear extract preparations in which band intensities were evaluated by OD. ND, Nondetectable.

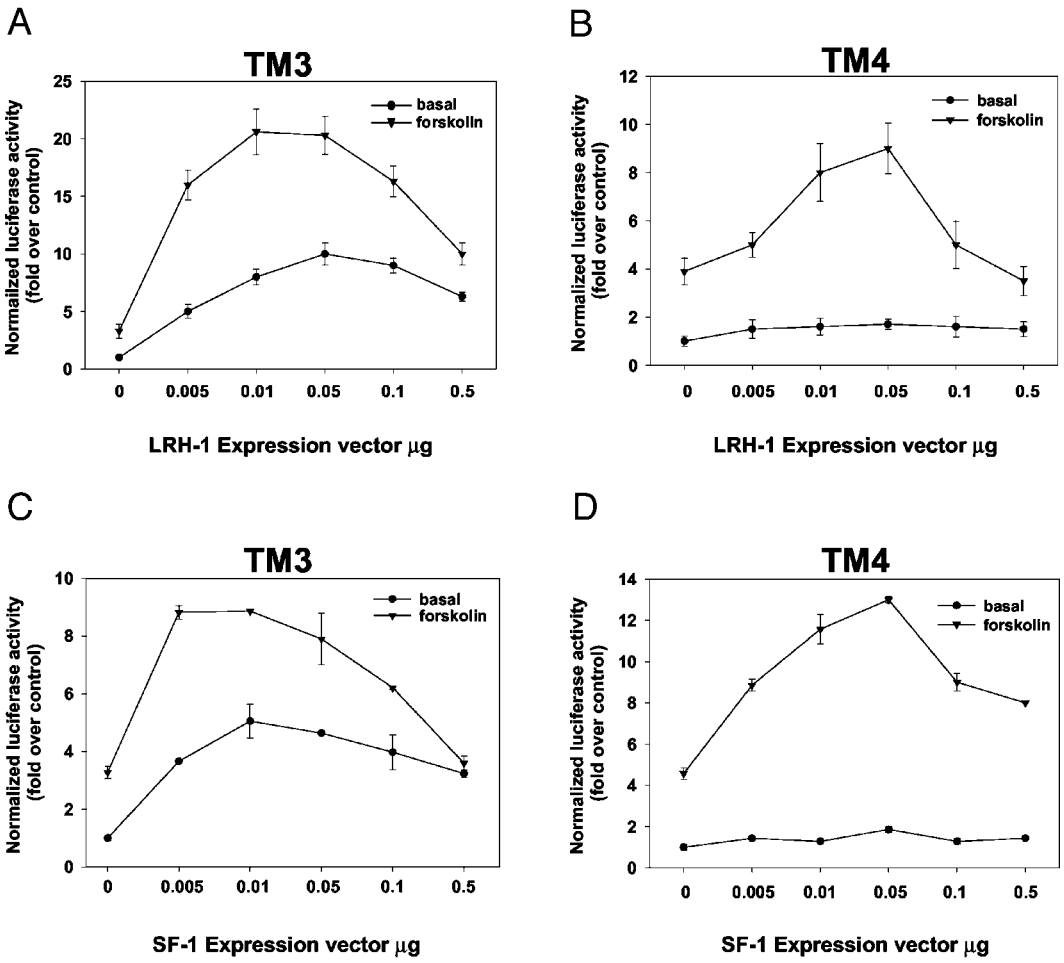

FIG. 3. LRH-1 and SF-1 induce aromatase PII reporter gene activity in TM3 and TM4 cells. TM3 (A–C) and TM4 (B–D) cells were transfected with 0.5 μg rat aromatase PII promoter and with empty pcDNA3.1zeo expression vector or the indicated amounts of LRH-1 (A and B) or SF-1 (C and D) expression plasmids, and a renilla luciferase reporter vector. The day after transfection, where indicated, cells were treated with FSK (10 μM). Twenty-four hours later, cells were lysed and assayed for luciferase activity. Luciferase signal was normalized to the renilla activity. Results represent the mean ± SD of pooled data from three to four independent experiments, each performed in triplicate.

and 56 kDa) were observed using TM3 Leydig cell nuclear extract and primary rat Leydig cells (TM3 and L) but not in TM4 Sertoli cells or primary rat Sertoli cells (TM4 and S). Strong expression was observed in rat PS and RS, consistent with the mRNA data above (Fig. 1). Strong expression was also observed in the positive control tissue, liver. Using *in vitro*-translated SF-1 and LRH-1 as the source of protein, no staining was observed for SF-1 [SF-1ttp (transcripted translated protein)], indicating an absence of cross-reactivity of the LRH-1 antibody with SF-1, whereas bands of the expected size were observed using *in vitro*-translated LRH-1 (LRH1ttp). Note that the 64-kDa protein corresponds to full-length LRH-1, whereas the shorter isoform presumably arises through use of an alternative in-frame initiator methionine at position 62. This isoform is 61 amino acids smaller than the full-length product and has a size of 56 kDa. Alternatively, two LRH-1 isoforms with different length of the A/B region (hB1F and hB1F-2) have been identified in human hepatocytes (25), both of which are recognized by the antibody used in this study.

A quite different pattern of expression was observed for SF-1 protein (Fig. 2B). SF-1 was detected at similar low levels in TM3 Leydig cells, primary rat Leydig cells, TM4 Sertoli cells (TM4), and primary rat Sertoli cells, but was completely absent from PS, RS, or liver. Again, *in vitro*-translated proteins confirmed the specificity of the SF-1 antibody (SF-1ttp and LRH1ttp). Densitometric analysis of Western blot data combined from three independent experiments indicated that SF-1 protein is expressed at similar low levels in TM3, TM4, and primary Leydig and Sertoli cells. Further, the relative levels of LRH-1 protein in purified germ cells is approximately 50% of that seen in the positive control tissue liver (Fig. 2C). Therefore, the intratesticular patterns of expression of LRH-1 and SF-1 proteins mirror that of their respective mRNAs, and are distinct: whereas Leydig cells express both SF-1 and LRH-1 protein, Sertoli cells uniquely express SF-1, and germ cells (PS and RS) uniquely express LRH-1. Moreover, LRH-1 protein is present in these testicular cell types at significant levels.

Regulation of CYP19 PII by LRH-1

Aromatase activity and *CYP19* mRNA expression in testis are strongly induced by LH in Leydig cells or by FSH in

Sertoli cells, both of which act through the cAMP pathway to induce transcription from PII. Basal and, in part, cAMP-induced transcription of *CYP19* has been shown to require SF-1 (40), which, in rat, binds to a nuclear receptor half site (NRE) located at −90 relative to the start of transcription. Because LRH-1 recognizes the same binding site as SF-1, we next assessed the potential of LRH-1 to induce transcription from PII.

TM3 and TM4 cells were cotransfected with the rat *CYP19* PII reporter construct and increasing concentrations of either LRH-1 or SF-1 expression vectors. Cells were then incubated in the presence or absence of the adenylyl cyclase activator FSK for 24 h. Transfected into TM3 cells, in the absence of stimulation, LRH-1 dose-dependently increased PII activity, reaching a maximum of 8-fold over basal at 0.05 μg plasmid (Fig. 3A). Treatment with FSK increased basal promoter activity 3-fold (over basal level at 0.05 μg); however, in the presence of this agent, LRH-1 strongly induced PII activity, reaching a maximum of 20-fold at only 0.01 μg LRH-1 (Fig. 3A). Transcription was inhibited at higher concentrations of LRH-1. Analogous transfection experiments using SF-1 instead of LRH-1 revealed a similar pattern, although the maximum levels of induction were lower (8-fold in the presence of FSK and 5 ng SF-1 plasmid) (Fig. 3C). Interestingly, in TM4 cells in basal conditions, neither LRH-1 nor SF-1 increased luciferase activity (Fig. 3, B and D). However, once activated by FSK, both LRH-1 and SF-1 further increased luciferase activity, reaching a maximum of 9-fold at 0.05 μg LRH-1 and 13-fold at 0.05 μg SF-1. Treatment with PKC activators alone or in combination with FSK was ineffective (data not shown).

We next investigated the contribution of the PII NRE to transcriptional regulation by FSK and LRH-1 (Fig. 4). TM3 (Fig. 4B) and TM4 (Fig. 4C) cells were transfected with LRH-1 and either a wild-type PII reporter construct (PII-688) or a promoter construct harboring a mutation in the NRE (AGGTCA→AtaTCA pII-688m, see Fig. 4A). Under control conditions, 0.05 μg/well of LRH-1 plasmid increased PII activity 8-fold in TM3 cells, and this stimulation was completely abolished when the NRE was mutated (Fig. 4B). FSK treatment increased the activity of pII-688 approximately 3-fold, and this induction was augmented by a further 5-fold by LRH-1 cotransfection (Fig 4B). Mutation of NRE did not significantly affect the ability of the promoter to respond to FSK; however, LRH-1 did not increase activity of pII-688m (Fig. 4B). Similar results were obtained performing the same experiments in TM4 cells (Fig. 4C); although, as before, LRH-1 did not increase transcription in the absence of FSK. These data suggest that the NRE is required for induction of PII by LRH-1 acting as a basal transcription factor, whereas cAMP-dependent transcription occurs through other mechanisms.

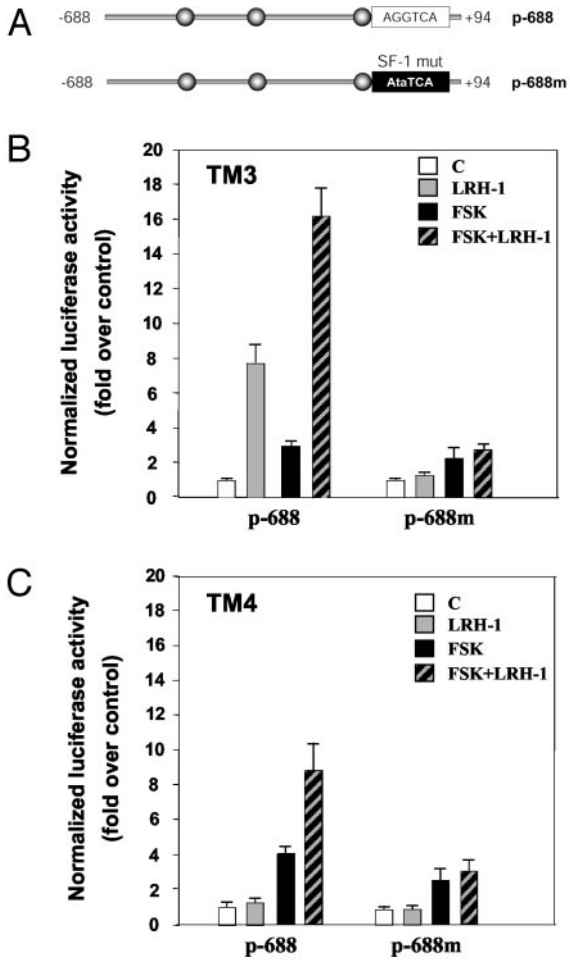

FIG. 4. LRH-1 induces aromatase PII activity via the −90 NRE. A, Schematic map of the rat P450arom proximal PII/luciferase construct containing 688/+94 of rat CYP19 PII inserted upstream of the firefly luciferase gene (p-688). Three putative CRE motifs (5′CRE at −335, 3′CRE at −231, and XCRE at −169) are indicated as *filled circles*. The AGGTCA NRE (−90) is indicated as a *rectangle*. The mutated NRE site (SF-1 mut) is present in p-688m (*black rectangle*). TM3 (B) and TM4 (C) cells were transfected with either p-688 or p-688m (both 0.5 μg/well) and with either an LRH-1 expression vector or the pcDNA3.1Zeo empty vector (both 0.05 μg/well). Twenty-four hours later, where indicated, cells were treated with 10 μM FSK for 24 h before being lysed and assayed for luciferase activity. Data were normalized to the coexpressed renilla luciferase expression vector. Results represent the mean ± SD of pooled data from at least three independent experiments, each performed in triplicate.

LRH-1 binds to the rat aromatase PII NRE

To demonstrate whether LRH-1 derived from TM3 cells is capable of binding to the PII NRE, a synthetic oligonucleotide probe encompassing this sequence was prepared and used in EMSA. In the presence of TM4 nuclear extract, a single distinct protein-DNA complex was formed (Fig. 5, lane 1). Formation of this complex was abolished by the addition of a 100-fold molar excess of nonradiolabeled wild-type probe (lane 2), but not by 100-fold molar excess of nonradiolabeled mutated probe (lane 3), confirming sequence-specific DNA binding. Similar binding profiles were observed using TM3 nuclear extracts (lanes 4–6), *in vitro* synthesized LRH-1 (lanes 7–9), and SF-1 (lanes 10–12). Because the use of a 6% polyacrylamide gel in EMSA does not permit discrimination of the different sizes of LRH-1 and SF-1 protein, as does Western analysis using a 12% sodium dodecyl sulfate-polyacrylamide gel, we confirmed the presence and identity of the two nuclear receptors using specific antibodies (Fig. 6). As before, a distinct band was observed using either TM3 or TM4 nuclear extracts, *in vitro* translated LRH-1 or SF-1 (lanes

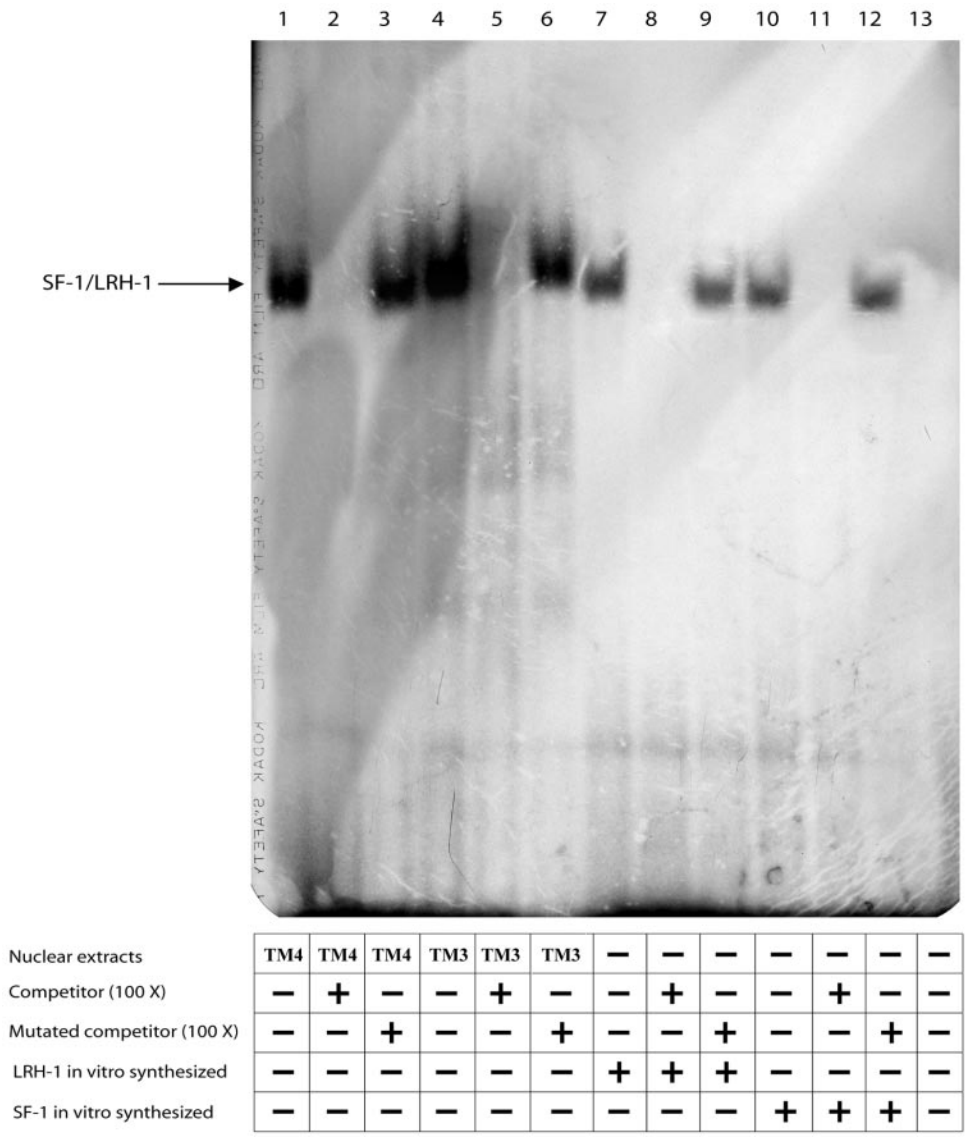

FIG. 5. Nuclear proteins from TM4 and TM3 cells bind to the aromatase PII NRE. TM4 (lanes 1–3) and TM3 (lanes 4–6) nuclear extracts or *in vitro* transcribed/translated mouse LRH-1 (lanes 7–9) and mouse SF1 (lanes 10–12) were incubated with radiolabeled probe encompassing the −90 NRE (AGGTCA) (40,000 cpm) in the presence or absence of nonradiolabeled (100×) competitor probe wild-type (lanes 2, 5, 8, and 11) or mutated (lanes 3, 6, 9, and 12). DNA/protein complexes were separated from free probe by gel electrophoresis. Lane 13 contains probe alone.

1–4). This band was recognized and supershifted by a specific LRH-1 antibody in TM3, but not TM4, nuclear extracts (lanes 5 and 6) or *in vitro*-translated LRH-1 (lane 7). In contrast, a specific SF-1 antibody recognized the DNA/protein complex in both TM3 and TM4 nuclear extracts (lanes 8 and 9), as well as using *in vitro*-translated SF-1 (lane 10). Nonspecific IgG had no effect (lanes 11 and 12). These data confirm the mRNA and protein data above and further support the conclusion that TM3 Leydig cells express both active LRH-1 and SF-1, whereas TM4 Sertoli cells express only SF-1. Finally, we confirmed the cell line EMSA experiments using, as the source of protein, nuclear extracts from primary cultures of rat Leydig and Sertoli cells (Fig. 7). Primary Leydig cell nuclear extracts produced a protein/DNA complex of mobility similar to that formed with TM3 cell extracts (lanes 1 and 2) or in *vitro*-translated LRH-1 (lane 5), whereas primary Sertoli cell nuclear extracts produced a complex of mobility similar to that formed with TM4 extracts (lanes 3 and 4). The LRH-1 antibody supershifted the binding activity from both TM3 and primary rat Leydig cell extracts (lanes 6 and 7) but not from TM4 or primary rat Sertoli cells (lanes 8 and 9). Thus, LRH-1 DNA binding activity is present in rat Leydig, but not Sertoli, cells.

Discussion

Estrogen is produced by the testis, from the fetal period throughout adulthood, and acts via estrogen receptors (ERs) to modulate transcription of specific genes. Both ERα and ERβ are found in the testis at all ages, suggesting a role for estrogen in testicular development and function. Targeted disruption of the genes encoding the ERα or aromatase indicates that estrogen is essential for normal male fertility (41, 42). On the other hand, estrogen excess stimulates Leydig cell hyperplasia in rodents and has been associated with cryptorchidism, testicular cancer, and impaired spermatogenesis (43). The molecular mechanisms controlling aromatase expression and the estrogen production in the different testicular cellular compartment are poorly understood. For this reason, it is particularly important to analyze this process.

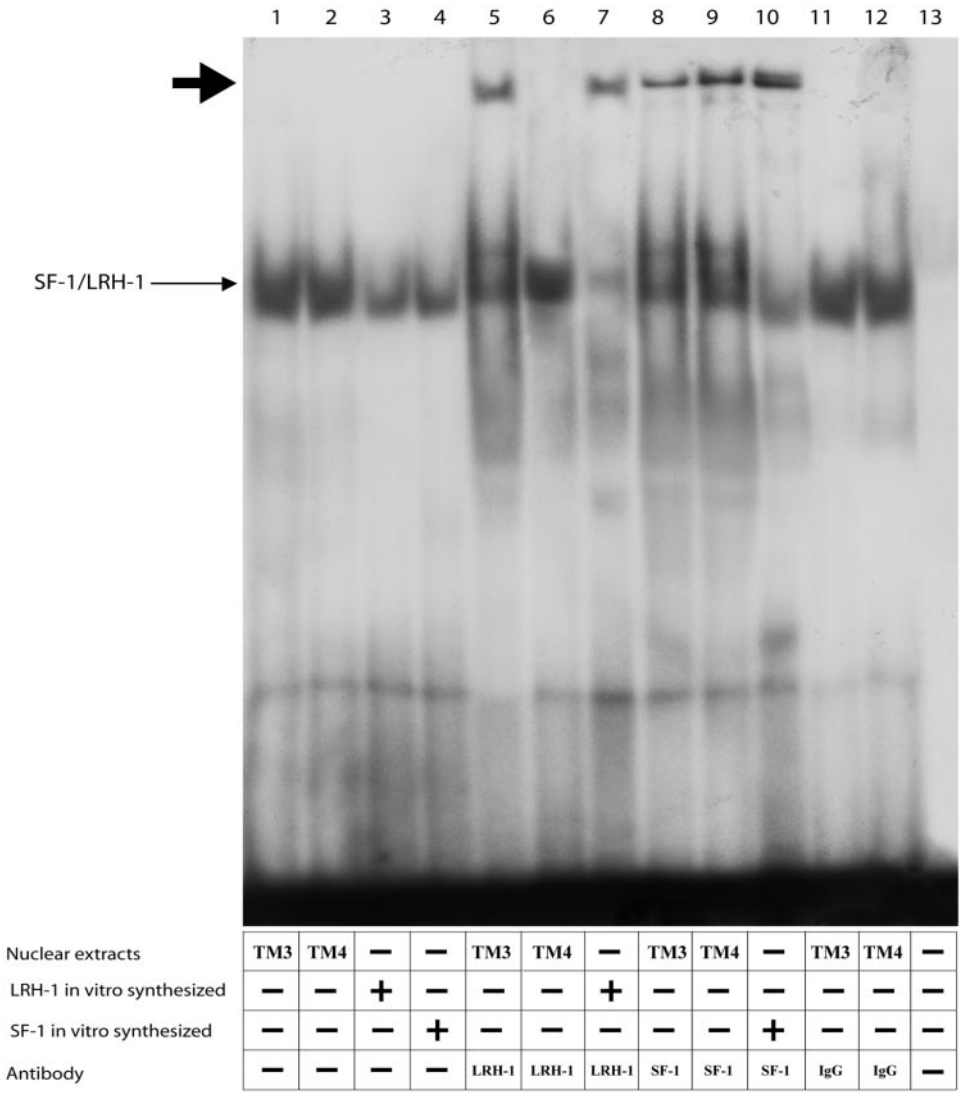

FIG. 6. Antibody supershift analysis of TM3 and TM4 nuclear extract NRE binding activity. TM3 (lanes 1, 5, 8, and 11) and TM4 (lanes 2, 6, 9, and 12) nuclear extracts or *in vitro* transcribed/translated mouse LRH-1 (lanes 3 and 7) and mouse SF1 (lanes 4 and 10) were incubated with radiolabeled probe encompassing the −90 SF1 motif (AGGTCA) (40,000 cpm) in the presence or absence of antibodies directed against either LRH-1 (lanes 5–7) or SF-1 (lanes 8–10) or nonspecific IgG (lanes 11 and 12). DNA/protein complexes were separated from free probe by gel electrophoresis. The *large solid arrow* indicates the SF-1 and LRH-1 supershifts. Lane 13 contains probe alone.

Previous studies have implicated SF-1 in regulating steroidogenic gene expression in Leydig cells (17, 18). Although aromatase is expressed in Leydig cells, it is also expressed in germ cells. Because germ cells do not express SF-1 (21), we hypothesized that other factors might regulate aromatase expression in the testis. Because LRH-1 is the closest relative of SF-1 and recognizes the same DNA response element, we have focused the current study on this protein. The first aim of this study was to investigate the cellular localization of LRH-1 in the testis. We show that LRH-1 mRNA and protein are expressed in Leydig and germ cells, but not in Sertoli cells, which, in contrast, express high levels of SF-1. Moreover, SF-1 is almost undetectable in germ cells. Quantitative real-time PCR revealed that LRH-1 mRNA is expressed approximately 5-fold higher than SF-1 in Leydig cells. Because LRH-1 can regulate many of the known SF-1 target genes in Leydig cells, including CYP11A, CYP17, 3βHSD, and StAR (35), we suggest that LRH-1 may regulate these and other genes *in vivo*. This is significant because SF-1 and LRH-1 are differentially regulated by other nuclear receptors such as dosage-sensitive sex reversal adrenal hypoplasia congenita critical region on the X chromosome, gene 1 (DAX-1) and short heterodimer partner (SHP) (unpublished observations). Our findings are consistent with immunostaining data reported previously by Morohashi and co-workers (21) showing a higher expression of SF-1 in Sertoli cells compared with Leydig cells in the prepubertal rat, decreased expression of SF-1 in Sertoli cells of mature animals, and constant expression in Leydig cells, with no detectable SF-1 expression in germ cells. Our data therefore indicate that LRH-1 could play a role in the regulation of estrogen-dependent testicular development and function, especially in those cellular types where SF-1 is expressed at very low concentration or not expressed (*e.g.* germ cells).

At least two steps of spermatogenesis are, in part, regulated by estrogen: germ cell number and spermatid maturation (4). However, the observations that mouse germ cells contain only ERβ but not ERα, and that ERβ knockout mice are fertile (44), raise questions as to the role of ERs in germ cells and point to a potential action of estrogen in germ cells via nonclassic receptors activating nongenomic pathways. In this scenario, the observation that male mice deficient in

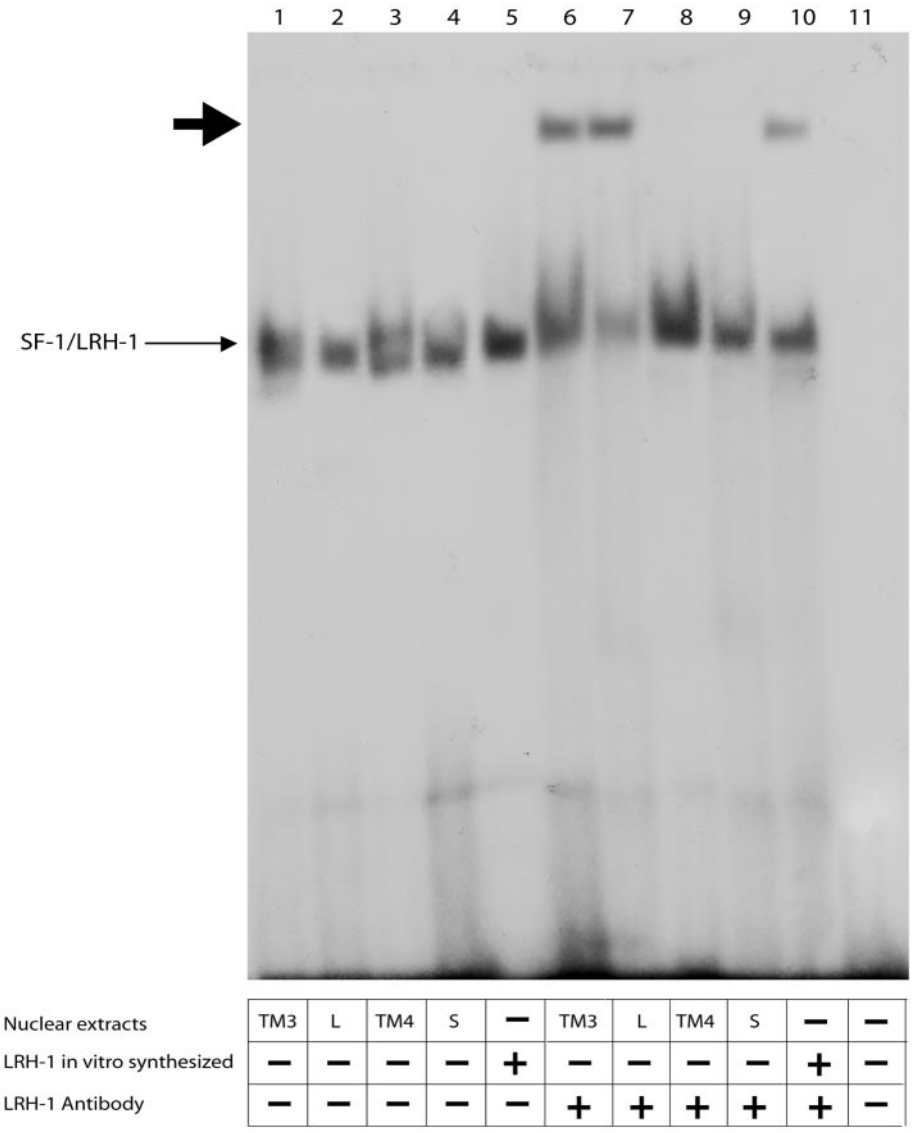

FIG. 7. LRH-1 DNA binding activity is present in primary rat Leydig but not Sertoli cell nuclear extracts. Nuclear extracts from TM3 (lanes 1 and 6), TM4 (lanes 3 and 8), primary Leydig (L) (lanes 2 and 7), Sertoli (S) (lanes 4 and 9) cell cultures or *in vitro* transcribed/translated mouse LRH-1 (lanes 5 and 10) were incubated with radiolabeled probe encompassing the −90 SF1 motif (AGGTCA) (40,000 cpm) in the presence or the absence of antibodies directed against LRH-1 (lanes 5–7). DNA/protein complexes were separated from free probe by gel electrophoresis. The *large solid arrow* indicates the LRH-1 supershift. Lane 11 contains probe alone.

aromatase by the age of 1 yr develop abnormal spermatogenesis with a blockage of germ cell maturation at the RS stage (42) suggests that the regulation of expression and activity of aromatase is probably the most important step determining the role of estrogen in spermatogenesis. Interestingly, the expression of LRH-1 (but not SF-1) in PS and RS leads us to hypothesize that this factor could regulate key genes involved in spermatogenesis including aromatase, and opens a new field that will require further investigation.

The current observation that SF-1, but not LRH-1, is expressed in Sertoli cells is consistent with our previous study (20), showing that SF-1 plays a pivotal role in the regulation of aromatase expression in Sertoli cells. In these cells, aromatase activity is highest in prepubertal rats, declines as Sertoli cells mature, and is hormonally regulated, principally by FSH (45). It has been proposed that estrogen may participate in the FSH-mediated mitogenic activity on Sertoli cells via induction of TGF-β (46, 47). However, several observations support the indication that estrogen also has negative effects on Sertoli cell differentiation and development (3). In fact, toward the end of the period of Sertoli cell proliferation, FSH-induced aromatase activity begins to decline. Thyroid hormone, which stimulates Sertoli cell differentiation (47), decreases aromatase activity (48, 49). We have recently demonstrated that the molecular mechanisms by which this inhibition occurs is through a competition of thyroid receptor β and SF-1 for the same regulatory site NRE (20), demonstrating the crucial role of this site in regulating aromatase expression.

Our transfection studies clearly demonstrate that, in TM3 Leydig cells, very low concentrations of LRH-1 induce basal aromatase promoter activity, as well as potentiate cAMP-induced transcription. By contrast, neither LRH-1 nor SF-1 modulates basal aromatase transcription in TM4 Sertoli cells, but both potentiate cAMP-induced transcription. These differences possibly reflect differences in coregulator expression between Leydig and Sertoli cells. The two members of the NR0B family of nuclear receptors, SHP and DAX-1, inhibit transcriptional activity of LRH-1 and SF-1, respectively. It is therefore possible that Sertoli cells express higher levels

of either or both of these receptors than Leydig cells, necessitating higher concentrations of cotransfected LRH-1 or SF-1 to overcome a tonic inhibitory action. This hypothesis has yet to be tested. Few other coregulators for LRH-1 have been identified; recently however, multiprotein-bridging factor-1 (MBF-1) has been shown to coactivate LRH-1, as well as LXR and PPARγ (50). Of the tissues examined, the site of highest expression of MBF-1 was the testis (50). MBF-1 also coactivates members of the CRE-binding protein/ATF-1 family of transcription factors (51). Because aromatase PII is regulated by cAMP through at least two CRE-like sequences that bind CRE-binding protein/ATF-1, it follows that MBF-1 may facilitate the synergistic activation of PII by LRH-1 and cAMP in the testis.

Our data support previous observations highlighting the importance of nuclear receptors in regulating aromatase gene expression in testis. The finding that, in DAX-1 knockout mice, aromatase is overexpressed selectively in Leydig cells (52) underscores the importance of this type of transcription factor in local testicular estrogen production *in vivo*. Although this Leydig cell phenotype of DAX-1 $-/-$ mice might seem to argue against a role for LRH-1 in Leydig cell aromatase expression *in vivo* (because DAX-1 antagonizes SF-1 action), DAX-1 has recently been shown to inhibit LRH-1 transcriptional activity as well as SF-1 (53). Indeed, we have found that DAX-1 is a very potent inhibitor of LRH-1-induced aromatase PII activity in Leydig cells (data not shown). This, together with the fact that LRH-1 is expressed at higher levels than SF-1 in Leydig cells, raises the possibility that the overexpression of aromatase in Leydig cells of DAX-1 $-/-$ mice arises through lack of repression of LRH-1, rather than SF-1.

Given that the DNA binding domains of SF-1 and LRH-1 are highly conserved, and both proteins recognize the same DNA sequence, the question arises as to the relative importance of each protein in testicular function. Both proteins are expressed in Leydig cells and therefore potentially share target genes; however, Sertoli cells and germ cells exclusively express SF-1 and LRH-1 respectively, suggesting cell-specific functions for each transcription factor. The critical role of SF-1 in testis development is clear from the dramatic phenotype of testicular agenesis seen in SF-1 $-/-$ mice (54). Knockout of LRH-1, however, is embryonic-lethal at an early stage (D. Russell, personal communication). Identification of the physiological roles of LRH-1 in the testis will therefore await the development of tissue-specific or conditional transgenic animals.

In conclusion, we have provided evidence that LRH-1 regulates aromatase expression in Leydig cells. Because the regulation of aromatase expression in testis has been investigated mainly in relation to SF-1 and DAX-1, future studies focusing on LRH-1 in addition to SF-1 would enhance our understanding of the mechanisms regulating the age-specific expression of aromatase in the testis. The roles of LRH-1 in testis maturation and testicular carcinogenesis also warrant further study.

Acknowledgments

We thank Dr. William E. Rainey for providing us the SF-1 plasmid, Dr. Michael Mc Phaul for aromatase PII gene reporter plasmids, Dr. David Mangelsdorf for the plasmid including the coding region of mouse LRH-1, Dr. K. Morohashi for the antibody Ad4BP, and Dr. Luc Belanger for the anti-FTF antibodies.

Received October 10, 2003. Accepted January 6, 2004.

Address all correspondence and requests for reprints to: Dr. Vincenzo Pezzi, Department of Pharmaco-Biology, University of Calabria, Arcavacata di Rende 87036 (CS), Italy. E-mail: v.pezzi@unical.it.

This work was supported by Ministero Università e Ricerca Scientifica e Tecnologica (Italy) 2001 Grant 2001063981, by the French Ministry of Education and Research, and by the National Health and Medical Research Council of Australia Grant 289318.

References

1. **Saez JM** 1994 Leydig cells: endocrine, paracrine, and autocrine regulation. Endocr Rev 15:574–626
2. **Sharpe RM** 1993 Experimental evidence for Sertoli-germ cell and Sertoli-Leydig cell interactions. In: Russel LD, Griswold MD, eds. The Sertoli cell. Clearwater, FL: Cache River Press; 391–438
3. **O'Donnell L, Robertson KM, Jones ME, Simpson ER** 2001 Estrogen and spermatogenesis. Endocr Rev 22:289–318
4. **Carreau S, Bourguiba S, Lambard S, Galeraud-Denis I, Genissel C, Levallet J** 2002 Reproductive system: aromatase and estrogens. Mol Cell Endocrinol 193:137–143
5. **Simpson ER, Mahendroo MS, Means GD, Kilgore MW, Hinshelwood MM, Graham-Lorence S, Amarneh B, Ito Y, Fisher CR, Michael MD, Mendelson CR, Bulun SE** 1994 Aromatase cytochrome P450, the enzyme responsible for estrogen biosynthesis. Endocr Rev 15:342–355
6. **Papadopoulos V, Carreau S, Szerman-Joly E, Drosdowsky MA, Dehennin L, Scholler R** 1986 Rat testis 17 β-estradiol: identification by gas chromatography-mass spectrometry and age related cellular distribution. J Steroid Biochem 24:1211–1216
7. **Carreau S, Genissel C, Bilinska B, Levallet J** 1999 Sources of oestrogen in the testis and reproductive tract of the male. Int J Androl 22:211–223
8. **Levallet J, Bilinska B, Mittre H, Genissel C, Fresnel J, Carreau S** 1998 Expression and immunolocalization of functional cytochrome P450 aromatase in mature rat testicular cells. Biol Reprod 58:919–926
9. **Nitta H, Bunick D, Hess RA, Janulis L, Newton SC, Millette CF, Osawa Y, Shizuta Y, Toda K, Bahr JM** 1993 Germ cells of the mouse testis express P450 aromatase. Endocrinology 132:1396–1401
10. **Aquila S, Sisci D, Gentile M, Middea E, Siciliano L, Ando S** 2002 Human ejaculated spermatozoa contain active P450 aromatase. J Clin Endocrinol Metab 87:3385–3390
11. **Choi I, Simmen RC, Simmen FA** 1996 Molecular cloning of cytochrome P450 aromatase complementary deoxyribonucleic acid from periimplantation porcine and equine blastocysts identifies multiple novel 5′-untranslated exons expressed in embryos, endometrium, and placenta. Endocrinology 137:1457–1467
12. **Lephart ED, Herbst MA, McPhaul MJ** 2003 Characterization of aromatase cytochrome P450 mRNA in rat perinatal brain, ovary, and a Leydig tumor cell line: evidence for the existence of brain specific aromatase transcripts. Endocrine 3:25–31
13. **Bulun SE, Rosenthal IM, Brodie AM, Inkster SE, Zeller WP, DiGeorge AM, Frasier SD, Kilgore MW, Simpson ER** 1994 Use of tissue-specific promoters in the regulation of aromatase cytochrome P450 gene expression in human testicular and ovarian sex cord tumors, as well as in normal fetal and adult gonads. J Clin Endocrinol Metab 78:1616–1621
14. **Hinshelwood MM, Corbin CJ, Tsang PC, Simpson ER** 1993 Isolation and characterization of a complementary deoxyribonucleic acid insert encoding bovine aromatase cytochrome P450. Endocrinology 133:1971–1977
15. **Hickey GJ, Krasnow JS, Beattie WG, Richards JS** 1990 Aromatase cytochrome P450 in rat ovarian granulosa cells before and after luteinization: adenosine 3′,5′-monophosphate-dependent and independent regulation. Cloning and sequencing of rat aromatase cDNA and 5′ genomic DNA. Mol Endocrinol 4:3–12
16. **Means GD, Kilgore MW, Mahendroo MS, Mendelson CR, Simpson ER** 1991 Tissue-specific promoters regulate aromatase cytochrome P450 gene expression in human ovary and fetal tissues. Mol Endocrinol 5:2005–2013
17. **Young M, Lephart ED, McPhaul MJ** 1997 Expression of aromatase cytochrome P450 in rat H540 Leydig tumor cells. J Steroid Biochem Mol Biol 63:37–44
18. **Young M, McPhaul MJ** 1998 A steroidogenic factor-1-binding site and cyclic adenosine 3′,5′-monophosphate response element-like elements are required for the activity of the rat aromatase promoter in rat Leydig tumor cell lines. Endocrinology 139:5082–5093
19. **Lanzino M, Catalano S, Genissel C, Ando S, Carreau S, Hamra K, McPhaul MJ** 2001 Aromatase messenger RNA is derived from the proximal promoter of the aromatase gene in Leydig, Sertoli, and germ cells of the rat testis. Biol Reprod 64:1439–1443
20. **Catalano S, Pezzi V, Chimento A, Giordano C, Carpino A, Young M,**

McPhaul MJ, Ando S 2003 Triiodothyronine (T3) decreases the activity of the proximal promoter (PII) of the aromatase gene in the mouse Sertoli cell line, TM4. Mol Endocrinol 17:923–934
21. **Hatano O, Takayama K, Imai T, Waterman MR, Takakusu A, Omura T, Morohashi K** 1994 Sex-dependent expression of a transcription factor, Ad4BP, regulating steroidogenic P-450 genes in the gonads during prenatal and postnatal rat development. Development 120:2787–2797
22. **Galarneau L, Pare JF, Allard D, Hamel D, Levesque L, Tugwood JD, Green S, Belanger L** 1996 The α1-fetoprotein locus is activated by a nuclear receptor of the Drosophila FTZ-F1 family. Mol Cell Biol 16:3853–3865
23. **Nitta M, Ku S, Brown C, Okamoto AY, Shan B** 1999 CPF: an orphan nuclear receptor that regulates liver-specific expression of the human cholesterol 7α-hydroxylase gene. Proc Natl Acad Sci USA 96:6660–6665
24. **Repa JJ, Mangelsdorf DJ** 1999 Nuclear receptor regulation of cholesterol and bile acid metabolism. Curr Opin Biotechnol 10:557–563
25. **Li M, Xie YH, Kong YY, Wu X, Zhu L, Wang Y** 1998 Cloning and characterization of a novel human hepatocyte transcription factor, hB1F, which binds and activates enhancer II of hepatitis B virus. J Biol Chem 273:29022–29031
26. **Lavorgna G, Ueda H, Clos J, Wu C** 1991 FTZ-F1, a steroid hormone receptor-like protein implicated in the activation of fushi tarazu. Science 252:848–851
27. **Goodwin B, Jones SA, Price RR, Watson MA, McKee DD, Moore LB, Galardi C, Wilson JG, Lewis MC, Roth ME, Maloney PR, Willson TM, Kliewer SA** 2000 A regulatory cascade of the nuclear receptors FXR, SHP-1, and LRH-1 represses bile acid biosynthesis. Mol Cell 6:517–526
28. **Lu TT, Makishima M, Repa JJ, Schoonjans K, Kerr TA, Auwerx J, Mangelsdorf DJ** 2000 Molecular basis for feedback regulation of bile acid synthesis by nuclear receptors. Mol Cell 6:507–515
29. **Castillo-Olivares A, Gil G** 2000 α 1-Fetoprotein transcription factor is required for the expression of sterol 12α-hydroxylase, the specific enzyme for cholic acid synthesis. Potential role in the bile acid-mediated regulation of gene transcription. J Biol Chem 275:17793–17799
30. **Luo Y, Liang CP, Tall AR** 2001 The orphan nuclear receptor LRH-1 potentiates the sterol-mediated induction of the human CETP gene by liver X receptor. J Biol Chem 276:24767–24773
31. **Lu TT, Repa JJ, Mangelsdorf DJ** 2001 Orphan nuclear receptors as eLiXiRs and FiXeRs of sterol metabolism. J Biol Chem 276:37735–37738
32. **Boerboom D, Pilon N, Behdjani R, Silversides DW, Sirois J** 2000 Expression and regulation of transcripts encoding two members of the NR5A nuclear receptor subfamily of orphan nuclear receptors, steroidogenic factor-1 and NR5A2, in equine ovarian cells during the ovulatory process. Endocrinology 141:4647–4656
33. **Liu DL, Liu WZ, Li QL, Wang HM, Qian D, Treuter E, Zhu C** 2003 Expression and functional analysis of liver receptor homologue 1 as a potential steroidogenic factor in rat ovary. Biol Reprod 69:508–517
34. **Falender AE, Lanz R, Malenfant D, Belanger L, Richards JS** 2003 Differential expression of steroidogenic factor-1 and FTF/LRH-1 in the rodent ovary. Endocrinology 144:3598–3610
35. **Sirianni R, Seely JB, Attia G, Stocco DM, Carr BR, Pezzi V, Rainey WE** 2002 Liver receptor homologue-1 is expressed in human steroidogenic tissues and activates transcription of genes encoding steroidogenic enzymes. J Endocrinol 174:R13–R17
36. **Clyne CD, Speed CJ, Zhou J, Simpson ER** 2002 Liver receptor homologue-1 (LRH-1) regulates expression of aromatase in preadipocytes. J Biol Chem 277:20591–20597
37. **Bourguiba S, Genissel C, Lambard S, Bouraima H, Carreau S** 2003 Regulation of aromatase gene expression in Leydig cells and germ cells. J Steroid Biochem Mol Biol 86:335–343
38. **Carreau S, Papadopoulos V, Drosdowsky MA** 1988 Stimulation of adult rat Leydig cell aromatase activity by a Sertoli cell factor. Endocrinology 122:1103–1109
39. **Andrews NC, Faller DV** 1991 A rapid micropreparation technique for extraction of DNA-binding proteins from limiting numbers of mammalian cells. Nucleic Acids Res 19:2499
40. **Michael MD, Kilgore MW, Morohashi K, Simpson ER** 1995 Ad4BP/SF-1 regulates cyclic AMP-induced transcription from the proximal promoter (PII) of the human aromatase P450 (CYP19) gene in the ovary. J Biol Chem 270:13561–13566
41. **Hess RA, Bunick D, Lee KH, Bahr J, Taylor JA, Korach KS, Lubahn DB** 1997 A role for oestrogens in the male reproductive system. Nature 390:509–512
42. **Robertson KM, O'Donnell L, Jones ME, Meachem SJ, Boon WC, Fisher CR, Graves KH, McLachlan RI, Simpson ER** 1999 Impairment of spermatogenesis in mice lacking a functional aromatase (cyp 19) gene. Proc Natl Acad Sci USA 96:7986–7991
43. **Abney TO** 1999 The potential roles of estrogens in regulating Leydig cell development and function: a review. Steroids 64:610–617
44. **Couse JF, Korach KS** 1999 Estrogen receptor null mice: what have we learned and where will they lead us? Endocr Rev 20:358–417
45. **Dorrington JH, Khan SA** 1993 Steroid production, metabolism and release by Sertoli cells. In: Russel LD, Griswold MD, eds. The Sertoli cell. Clearwater, FL: Cache River Press; 538–549
46. **Dorrington JH, Bendell JJ, Khan SA** 1993 Interactions between FSH, estradiol-17 β and transforming growth factor-β regulate growth and differentiation in the rat gonad. J Steroid Biochem Mol Biol 44:441–447
47. **Cooke PS, Zhao YD, Bunick D** 1994 Triiodothyronine inhibits proliferation and stimulates differentiation of cultured neonatal Sertoli cells: possible mechanism for increased adult testis weight and sperm production induced by neonatal goitrogen treatment. Biol Reprod 51:1000–1005
48. **Pezzi V, Panno ML, Sirianni R, Forastieri P, Casaburi I, Lanzino M, Rago V, Giordano F, Giordano C, Carpino A, Ando S** 2001 Effects of tri-iodothyronine on alternative splicing events in the coding region of cytochrome P450 aromatase in immature rat Sertoli cells. J Endocrinol 170:381–393
49. **Ando S, Sirianni R, Forastieri P, Casaburi I, Lanzino M, Rago V, Giordano F, Giordano C, Carpino A, Pezzi V** 2001 Aromatase expression in prepuberal Sertoli cells: effect of thyroid hormone. Mol Cell Endocrinol 178:11–21
50. **Brendel C, Gelman L, Auwerx J** 2002 Multiprotein bridging factor-1 (MBF-1) is a cofactor for nuclear receptors that regulate lipid metabolism. Mol Endocrinol 16:1367–1377
51. **Kabe Y, Goto M, Shima D, Imai T, Wada T, Morohashi K, Shirakawa M, Hirose S, Handa H** 1999 The role of human MBF1 as a transcriptional coactivator. J Biol Chem 274:34196–34202
52. **Wang ZJ, Jeffs B, Ito M, Achermann JC, Yu RN, Hales DB, Jameson JL** 2001 Aromatase (Cyp19) expression is up-regulated by targeted disruption of Dax1. Proc Natl Acad Sci USA 98:7988–7993
53. **Suzuki T, Kasahara M, Yoshioka H, Morohashi K, Umesono K** 2003 LXXLL-related motifs in Dax-1 have target specificity for the orphan nuclear receptors Ad4BP/SF-1 and LRH-1. Mol Cell Biol 23:238–249
54. **Luo X, Ikeda Y, Parker KL** 1994 A cell-specific nuclear receptor is essential for adrenal and gonadal development and sexual differentiation. Cell 77:481–490

***Endocrinology* is published monthly by The Endocrine Society (http://www.endo-society.org), the foremost professional society serving the endocrine community.**

0021-972X/05/$15.00/0
Printed in U.S.A.

The Journal of Clinical Endocrinology & Metabolism 90(1):279–285

doi: 10.1210/jc.2004-0865

Corticotropin-Releasing Hormone Directly Stimulates Cortisol and the Cortisol Biosynthetic Pathway in Human Fetal Adrenal Cells

Rosa Sirianni, Khurram S. Rehman, Bruce R. Carr, C. Richard Parker, Jr., and William E. Rainey

Department of Obstetrics and Gynecology (R.S., K.S.R., B.R.C., W.E.R.), Division of Reproductive Endocrinology and Infertility, University of Texas Southwestern Medical Center, Dallas, Texas 75390; and Department of Obstetrics and Gynecology (C.R.P.), University of Alabama at Birmingham, Birmingham, Alabama 35233

Near term the human fetal adrenals (HFAs) initiate production of cortisol, which promotes organ maturation and acts to increase placental CRH biosynthesis. The objective of the present study was to determine whether CRH directly stimulates both cortisol production and expression of the steroidogenic enzymes in HFA-definitive zone cells. CRH stimulated the production of cortisol in a time- and dose-dependent manner, with an effective concentration of as low as 0.01 nM. In real-time RT-PCR experiments, CRH treatment increased the mRNA levels of steroidogenic acute regulatory protein and each of the enzymes needed to produce cortisol. CRH induced 3β-hydroxysteroid dehydrogenase type II (HSD3B2) by 34-fold, 21-hydroxylase (CYP21) by 55-fold, and 11β-hydroxylase by 41-fold. Induction of steroidogenic acute regulatory protein, cholesterol side chain cleavage (CYP11A), and 17α-hydroxylase (CYP17) mRNA by CRH was 6-, 4-, and 6-fold, respectively. We also demonstrated that submaximal concentrations of CRH (30 pM) and ACTH (30 pM) that are seen in fetal circulation were additive on cortisol biosynthesis and 3β-hydroxysteroid dehydrogenase type II mRNA induction. We suggest that CRH may play an important role in the late gestational rise in cortisol secretion from the HFAs, which may serve to augment placental CRH production and therefore participate in the endocrine cascade that is involved in fetal organ maturation and potentially in the timing of human parturition. (*J Clin Endocrinol Metab* 90: 279–285, 2005)

MORPHOLOGICALLY AND PHYSIOLOGICALLY, the human fetal adrenal glands are remarkable organs. At term they weigh the same as adult adrenal glands and represent the largest endocrine glands in the fetus. The daily production of steroids in the fetal adrenal glands near term may be 5-fold higher than that of adult adrenals at rest (1). Within the fetal adrenal, steroidogenic function and zonation are different from the adult. The key difference between the human fetal adrenal (HFA) and the adult adrenal is seen in the HFA in which a histologically distinct fetal zone accounts for the bulk of the gland (80–90%) during the second and third trimesters and is the source for steroid precursors that are used by the placenta to produce estrogens (2). The transient fetal zone is unique to humans and a few nonhuman primates. Functionally, the fetal zone is similar in many ways to the adult zona reticularis. The outer zone is called the definitive zone, and this zone is believed to give rise to the adult adrenal zona glomerulosa. A third transitional zone is present between the fetal and definitive zones and is believed to give rise to the postnatal zona fasciculata. Different studies demonstrated that these three zones have major differences in steroid-metabolizing enzyme expression (3, 4), providing important clues into the role of each zone in fetal adrenal steroidogenesis. Late in gestation, the definitive zone expresses the enzymes needed for the production of aldosterone, the transitional zone those for cortisol, and throughout gestation the fetal zone expresses enzymes and cofactors needed for high levels of dehydroepiandrosterone sulfate (DHEA-S) production, including cytochrome b_5 (5) and dehydroepiandrosterone sulfotransferase (6). The definitive and transitional zones together comprise the neocortex of the HFA and are distinct from the fetal zone in that during the second half of gestation, they begin to express 3β-hydroxysteroid dehydrogenase type II (HSD3B2), an enzyme that is almost absent in the fetal zone (7, 8).

Jaffe and colleagues (9–11) have shown that fetal adrenal cells respond to ACTH by secretion of growth factors that stimulate hyperplasia of the fetal zone. However, because of the substantial growth and capacity of the fetal adrenals for steroid synthesis during the latter stages of gestation at a time that fetal plasma ACTH levels decline slightly (12), there must be growth/steroidogenesis stimuli in addition to ACTH. Two observations make it extremely likely that factors secreted by the placenta play a key role in the regulation of steroidogenesis during the last part of gestation. First, the fact that ACTH levels do not increase during late gestation makes it likely that growth and differentiation of the fetal adrenal glands are influenced by placenta-derived factors. Second, the fact that the fetal zone of the adrenal undergoes rapid involution immediately after birth (13) when placenta-derived factors are no longer available further supports this hypothesis. Evidence suggests that CRH of placental origin is one of the critical components that facilitates fetal adrenal

First Published Online October 19, 2004

Abbreviations: CRH-BP, CRH-binding protein; Ct, threshold cycle; CYP, cytochrome P450; DHEA-S, dehydroepiandrosterone sulfate; DZ/TZ, definitive/transitional zone; HFA, human fetal adrenal; HSD3B2, 3β-hydroxysteroid dehydrogenase type II; StAR, steroidogenic acute regulatory protein.

hypertrophy and increased steroidogenesis before the onset of labor. Placental CRH, identical with maternal and fetal hypothalamic CRH, is synthesized in relatively large amounts. Unlike hypothalamic CRH, which is under glucocorticoid-negative feedback control (14), placental CRH production has been shown to be stimulated by cortisol both *in vitro* and *in vivo*, in humans and other primates (15–18). The ability of cortisol to stimulate placental CRH makes it possible to create a feed-forward endocrine cascade that does not end until separation of the fetus from the placenta at delivery. We and others have proposed that this cascade drives the rise in fetal CRH levels as well as fetal adrenal steroidogenesis in late gestation. Parker and colleagues (19) demonstrated that CRH can directly stimulate HFA cells to produce cortisol and DHEA-S. Jaffe and colleagues (20, 21) similarly have shown effects of CRH on fetal zone DHEA-S production as well as induction of cortisol synthesis. In this project we demonstrate that CRH stimulates both cortisol production and the cortisol biosynthetic pathway in isolated definitive/transitional zone cells from the HFA. In addition, we show that physiologic concentrations of CRH and ACTH can have additive effects on fetal adrenal cortisol biosynthesis, further supporting a combined role of these hormones in regulating the late gestational rise in fetal cortisol biosynthesis.

Materials and Methods

Cell culture

HFAs were obtained with informed consent from the pathological examination of elective pregnancy terminations performed between 18 and 24 wk of gestation. The definitive/transitional zone (DZ/TZ) was dissected from the fetal zone using sterile technique. The DZ/TZ was minced into small pieces and incubated in DME/F12 containing 1 mg/ml of collagenase-dispase and 0.25 mg/ml DNase-1. Digestion and mechanical dispersion were carried out twice for 30 min at 37 C, centrifuging cells between each digestion and combining them before plating. Cells were cultured initially for 4–6 d before use in DMEM/F12 medium containing 10% cosmic calf serum (HyClone, Logan, UT), 1% ITS+ (BD Biosciences, Bedford, MA), and antibiotics/antimycotics consisting of penicillin/streptomycin, gentamicin, kanamycin, and amphotericin B (complete medium). DZ/TZ cells were then plated onto 12-well culture dishes at a density of 1×10^5/well. Experimental treatments were applied 4–6 d later. The protocol was approved by the institutional review boards of the University of Texas Southwestern Medical Center and the University of Alabama at Birmingham.

Stimulation of steroid secretion and analysis of steroids

CRH (Sigma-Aldrich, St. Louis, MO) and ACTH (Organon, West Orange, NJ) were added to the cells and the treatment carried out at 37 C for the indicated times. Cortisol content of conditioned medium was determined using RIA kits (Diagnostic System Laboratories, Webster, TX). The inter- and intraassay coefficients of variation for cortisol are 8.4 and 9.1%, respectively (manufacturer's data).

RNA extraction, cDNA synthesis, and real-time RT-PCR

RNA was extracted from cells using the Ultraspec RNA isolation system (Biotecx Laboratories Inc., Houston, TX). All the RNA samples were DNase-1 treated (Ambion, Austin, TX), and purity and integrity of the RNA was checked spectroscopically and by gel electrophoresis before use. Two micrograms of total RNA was reverse transcribed in a final volume of 50 μl using the high-capacity cDNA archive kit (Applied Biosystems, Foster City, CA) and stored at −20 C. The nucleotide sequences of the primers and TaqMan probes are shown in Table 1, and sequences were based on the following GenBank accession no.: steroidogenic acute regulatory protein (StAR), NM_000349; cholesterol side chain cleavage (CYP11A), M14565; 17α-hydroxylase (CYP17), NM_000102; HSD3B2, NM_000198; 21-hydroxylase (CYP21), NM_000500; and 11β-hydroxylase (CYP11B1), NM_000498.

Real-time RT-PCRs were performed using the ABI Prism 7000 sequence detection system (Applied Biosystems) in a total volume of 30 μl reaction mixture following the manufacturer's protocol, using the SYBR Green universal 2 × PCR master mix (Applied Biosystems) and 0.1 μM of each primer using the dissociation protocol for the amplification of StAR, CYP11A, and CYP21; and the TaqMan 2 × PCR master mix and 0.1 μM of each primer and 0.1 μM of each probe using the emulation protocol for HSD3B2, CYP17, and CYP11B1. Negative controls contained water instead of first-strand cDNA. Each sample was normalized on the basis of its 18S rRNA content.

The 18S quantification was performed using a TaqMan rRNA reagent kit (Applied Biosystems) and using the manufacturer's protocol. Relative gene expression for each steroidogenic enzyme mRNA was normalized to a calibrator that was chosen to be the basal condition (untreated sample) for each time point. Results were calculated with the ΔΔCt method and expressed as n-fold differences in steroidogenic enzyme gene expression relative to 18S rRNA and calibrator and were determined as follows:

$$\text{n-fold} = 2^{-\Delta\Delta Ct}$$

$$(\Delta\Delta Ct = \Delta Ct \text{ sample} - \Delta Ct \text{ calibrator})$$

where the parameter Ct (threshold cycle) is defined as the fractional cycle number at which the PCR reporter signal passes a fixed threshold. ΔCt values of the sample and calibrator are determined by subtracting the average Ct value of the transcript under investigation from the average Ct value of the 18S rRNA gene, for each sample.

Data analysis and statistical methods

Data from two experiments run in triplicate, for a total of six independent observations for each condition, were pooled and analyzed using single-factor ANOVA with Fisher least significant differences multiple comparison method, using SigmaStat version 3.0 (SPSS, Chicago, IL). For experiments involving treatments with CRH and ACTH

TABLE 1. Oligonucleotide primer and probe sequences used for real-time RT-PCR

Gene	Oligonucleotide	Sequence (5′–3′)	TaqMan probe sequence (5′–3′)
StAR	Forward primer	CCACCCCTAGCACGTGGA	
	Reverse primer	TCCTGGTCACTGTAGAGAGTCTCTTC	
CYP11A	Forward primer	TCCAGAAGTATGGCCCGATT	
	Reverse primer	CATCTTCAGGGTCGATGACATAAA	
CYP17	Forward primer	TCTCTGGGCGGCCTCAA	TGGCAACTCTAGACATCGCGTCC
	Reverse primer	AGGCGATACCCTTACGGTTGT	
HSD3B2	Forward primer	GCGGCTAATGGGTGGAATCTA	TGATACCTTGTACACTTGTGCGTTAAGACCCA
	Reverse primer	CATTGTTGTTCAGGGCCTCAT	
CYP21	Forward primer	TCAGGTTCTTCCCCAATCCA	
	Reverse primer	TCCACGATGTGATCCCTCTTC	
CYP11B1	Forward primer	GGCAGAGGCAGAGATGCTG	TGCTGCACCATGTGCTGAAACACCT
	Reverse primer	TCTTGGGTTAGTGTCTCCACCTG	

alone and in combination (see Fig. 5), the six values obtained from three experiments run in duplicate were analyzed by single-factor ANOVA as described above. Whereas the single-factor ANOVA analysis was planned *a priori*, a factorial ANOVA was performed after the experimental data indicated a possible synergy between CRH and ACTH treatments. Thus, a two-factor ANOVA with Fisher's least significant differences multiple comparison testing was used to quantify the significance of interaction between these two treatments.

Results

Concentration- and time-dependent effects of CRH on DZ/TZ cell cortisol production and expression of steroid-metabolizing enzymes

DZ/TZ cells were isolated and placed in monolayer culture. Cells were treated with increasing concentrations of CRH (0.01–30 nM) and ACTH (10 nM) for 24 h. Media content of cortisol was determined by RIA (Fig. 1A). CRH caused a concentration-dependent increase in cortisol production with significant stimulation seen even at the dose of 0.03 nM ($P < 0.015$). Maximal stimulation of cortisol was observed with 10 nM CRH, which elicited a 14-fold increase over basal levels. ACTH at a dose of 10 nM caused a 27-fold increase in cortisol production. The time course of adrenocortical cell response to treatment with CRH (10 nM) or ACTH (10 nM) is shown in Fig. 1B. After 24 h of treatment, ACTH induced a 25-fold increase in cortisol levels over basal production, compared with a 10-fold increase for CRH.

Stimulation of adrenal steroid synthesis, regardless of the nature of the steroid, relies on an induction of cholesterol conversion to pregnenolone within the mitochondria. This rate-limiting step relies on the expression of StAR protein and the cholesterol side-chain cleavage enzyme (CYP11A). In dose-response experiments, we found that the low dose of 0.1 nM CRH induced a significant increase in StAR mRNA levels ($P < 0.009$). StAR transcripts were induced 7-fold by 10 nM CRH, 11-fold by 30 nM CRH, and 8-fold by 10 nM ACTH ($P < 0.001$, compared with basal) (Fig. 2A). All doses tested caused significant increases in CYP11A mRNA with an induction of 8-fold by 30 nM CRH and 5-fold by 10 nM ACTH ($P < 0.001$ under all different conditions) (Fig. 2A). Time-course analysis revealed a 6-fold induction of StAR mRNA by CRH ($P < 0.001$), 8-fold induction by ACTH at 24 h ($P < 0.001$) (Fig. 2B), and a 4-fold induction of CYP11A mRNA levels by both CRH ($P < 0.001$) and ACTH ($P < 0.001$) (Fig. 2B).

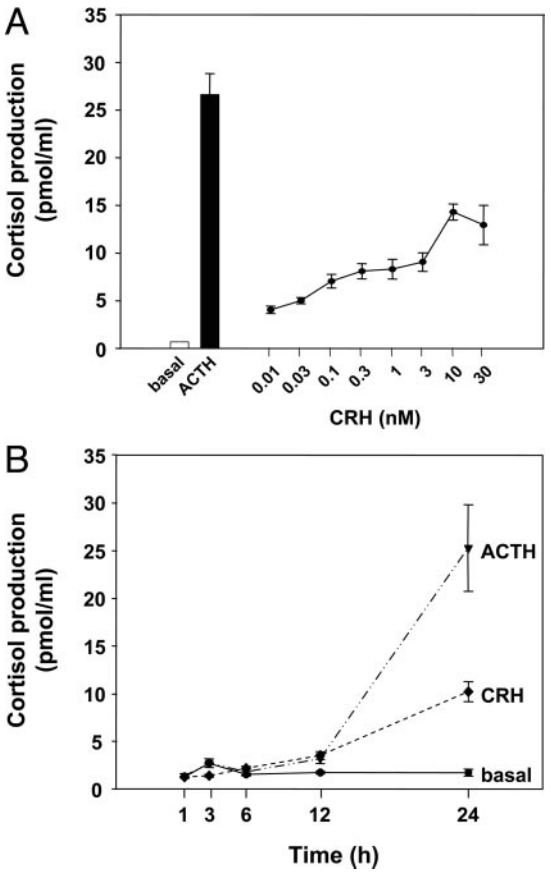

FIG. 1. Concentration- and time-dependent effects of CRH on cortisol production in human fetal adrenal DZ/TZ cells. A, DZ/TZ cells were treated for 24 h with ACTH (10 nM) or the indicated concentrations of CRH. B, Cells were incubated for the indicated times with ACTH (10 nM) or CRH (10 nM). Cortisol levels in the growth medium were determined by RIA; data points are the mean ± SE of values from two experiments run in triplicate and expressed as picomoles per milliliter.

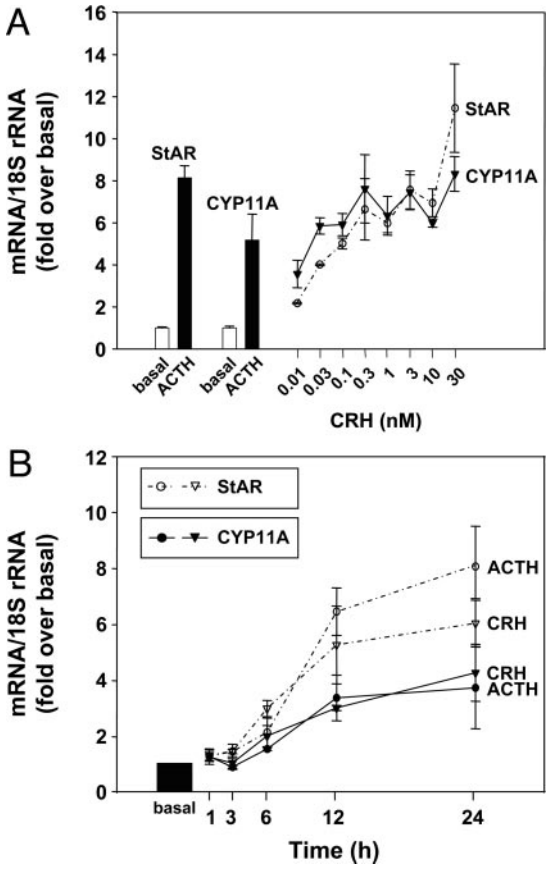

FIG. 2. Concentration- and time-dependent effects of CRH on StAR and CYP11A transcript levels in HFA DZ/TZ cells. Real-time RT-PCR was used to quantify mRNA levels of StAR and CYP11A in human fetal DZ/TZ cells. A, Cells were treated for 24 h with ACTH (10 nM) or the indicated concentrations of CRH. B, Cells were incubated for the indicated times with ACTH (10 nM) or CRH (10 nM). Data points are the values calculated with the ΔΔCt method as described in *Materials and Methods* and represent the mean ± SE of two independent RNA samples expressed as fold over basal.

Once pregnenolone is produced, it can be acted on by both CYP17 and HSD3B2, resulting in the production of 17α-hydroxyprogesterone. CRH stimulated the mRNA levels of CYP17 and HSD3B2 in a concentration- and time-dependent manner (Fig. 3, A and B). The dose of 0.1 nM CRH caused a significant increase in HSD3B2 mRNA, compared with basal levels ($P < 0.007$). HSD3B2 was induced 52-fold by 30 nM CRH and 78-fold by 10 nM ACTH ($P < 0.001$) (Fig. 3A). CYP17 mRNA was induced 7-fold by 10 nM CRH, 11-fold by 30 nM CRH, and 8-fold by 10 nM ACTH ($P < 0.001$) (Fig. 3A). HSD3B2 mRNA was induced significantly at 12 and 24 h of treatment (Fig. 3B). At 12 h, CRH produced a 10-fold induction ($P < 0.001$) and ACTH a 20-fold induction ($P < 0.001$). At 24 h, CRH produced a 34-fold induction ($P < 0.001$) and ACTH a 50-fold induction ($P < 0.001$). At 24 h CYP17 was induced 6-fold under both treatments ($P < 0.001$). Although this induction was modest, compared with the other enzymes studied, basal levels of CYP17 mRNA are already high in DZ/TZ cells.

Once 17α-hydroxyprogesterone is produced, it is converted to deoxycortisol by the enzymatic activity of CYP21 and then into cortisol by CYP11B1. CRH increased CYP21 and CYP11B1 mRNA levels in a time and concentration-dependent manner (Fig. 4). CYP21 was induced 64-fold by 30 nM CRH and 95-fold by 10 nM ACTH ($P < 0.001$) (Fig. 4A). CYP11B1 was induced 58-fold by 30 nM CRH and 36-fold by 10 nM ACTH ($P < 0.001$) (Fig. 4A). Both CYP21 and CYP11B1 were significantly induced at 12 and 24 h (Fig. 4B). CYP21 was induced 55-fold by CRH ($P < 0.001$) and 100-fold by ACTH at 24 h ($P < 0.001$) (Fig. 4B). CYP11B1 was induced 41-fold by CRH ($P < 0.001$) and 53-fold by ACTH at 24 h ($P < 0.001$) (Fig. 4B).

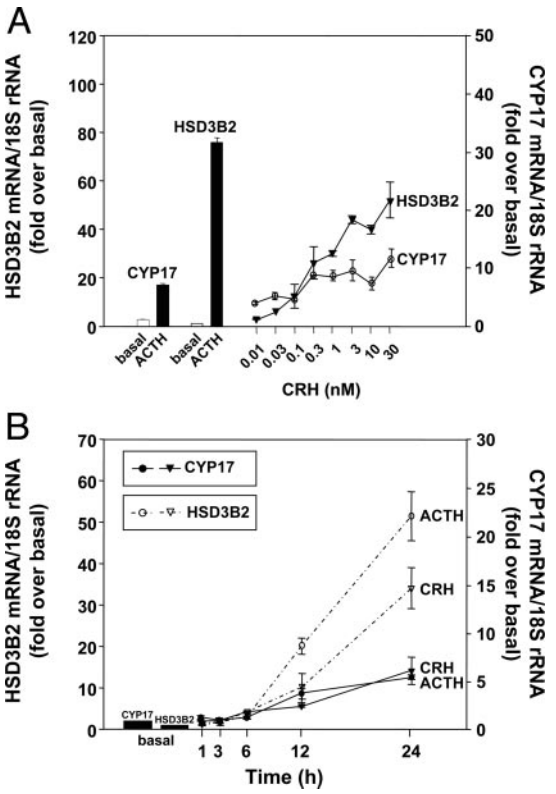

FIG. 3. Concentration- and time-dependent effects of CRH on CYP17 and HSD3B2 transcript levels in HFA DZ/TZ cells. Real-time RT-PCR was used to quantify mRNA levels of CYP17 and HSD3B2 in human fetal DZ/TZ cells. A, Cells were treated for 24 h with ACTH (10 nM) or the indicated concentrations of CRH. B, Cells were incubated for the indicated times with ACTH (10 nM) or CRH (10 nM). Data points are the values calculated with the $\Delta\Delta$Ct method as described in *Materials and Methods* and represent the mean ± SE of two independent RNA samples expressed as fold over basal.

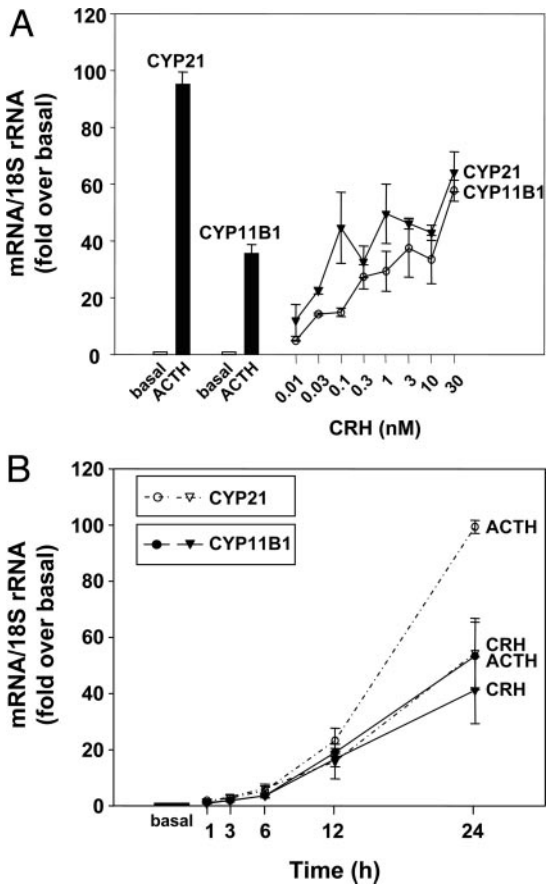

FIG. 4. Concentration- and time-dependent effects of CRH on CYP21 and CYP11B1 transcript levels in HFA DZ/TZ cells. Real-time RT-PCR was used to quantify mRNA levels of CYP21 and CYP11B1 in human fetal DZ/TZ cells. A, Cells were treated for 24 h with ACTH (10 nM) or the indicated concentrations of CRH. B, Cells were incubated for the indicated times with ACTH (10 nM) or CRH (10 nM). Data points are the values calculated with the $\Delta\Delta$Ct method as described in *Materials and Methods* and represent the mean ± SE of triplicate wells from two independent RNA samples expressed as fold over basal.

Synergistic effects between physiologic concentrations of CRH and ACTH on DZ/TZ cell cortisol production and HSD3B2 expression

Toward the end of gestation (after wk 34), the concentrations of CRH and ACTH measured in cord blood of human fetuses are both in the range of 30 pM. We wanted to investigate the effect of the combined presence of such physiologic doses of both agonists on cortisol production and HSD3B2 mRNA expression in DZ/TZ cells. Cells were treated for 24 h with ACTH 30 pM, CRH 30 pM, or the combined doses of both agonists (Fig. 5A). ACTH increased cortisol production 4.7-

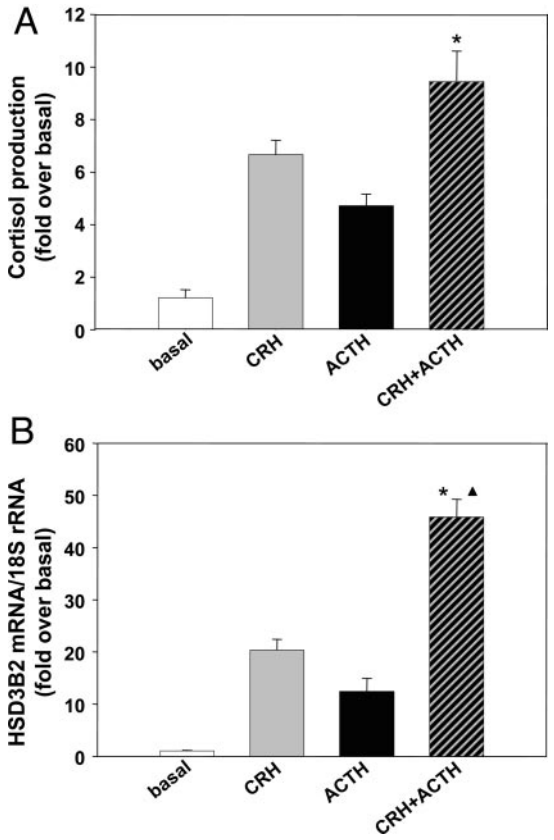

FIG. 5. Additive effect of physiologic doses of ACTH and CRH on cortisol production and HSD3B2 transcript levels in HFA DZ/TZ cells. Cells were incubated for 24 h with ACTH (30 pM), CRH (30 pM), and ACTH (30 pM) plus CRH (30 pM). A, Cortisol levels in the growth medium were determined by RIA; data points are the mean ± SE of values from three experiments run in duplicate and expressed as fold over basal. B, Real-time RT-PCR was used to quantify mRNA levels of HSD3B2. Data points are the values calculated with the ΔΔCt method as described in *Materials and Methods* and represent the mean ± SE of three independent RNA samples obtained from duplicate wells and expressed as fold over basal. (*, $P < 0.001$, compared with ACTH or CRH alone; ▲, $P = 0.007$ in the interaction between ACTH and CRH).

fold over basal ($P < 0.002$), whereas cortisol levels were increased 6.5-fold by CRH, compared with basal ($P < 0.001$). The presence of both CRH and ACTH caused an additive effect on cortisol production with a 9.8-fold increase over basal ($P < 0.001$) (Fig. 5A). The P value for the interaction between ACTH and CRH was not significant ($P = 0.69$), consistent with an additive rather than a synergistic effect. HSD3B2 mRNA was induced 20-fold over basal by CRH ($P < 0.001$), 12-fold over basal by ACTH ($P < 0.003$), and 45-fold over basal by combined treatments ($P < 0.001$) (Fig. 5B). The P value for the interaction between ACTH and CRH was highly significant ($P = 0.007$), indicating a synergistic effect between these factors. These data support the hypothesis that CRH and ACTH act together to increase cortisol biosynthesis in the HFAs.

Discussion

The initiation of cortisol production in the human fetus occurs in the second half of gestation and increases dramatically during the last month before birth (22). The late rise in cortisol production is important for fetal organ maturation and as a prerequisite for neonatal survival. The mechanisms responsible for the late gestational rise in fetal cortisol levels are not clear. Our results demonstrate that CRH stimulates fetal adrenal DZ/TZ cell production of cortisol and the expression of each of the mRNAs encoding the enzymes that comprise the cortisol biosynthetic pathway. We also demonstrated additive effects between physiologic concentrations of CRH and ACTH on stimulation of fetal adrenal cortisol production as a consequence of increased HSD3B2 expression. These data support a role for CRH in the rise in fetal cortisol biosynthesis seen in late gestation.

The 41-amino acid peptide CRH was the first hypothalamic releasing factor to be characterized, controlling ACTH release by the anterior pituitary, and thus cortisol and DHEA-S secretion by the adrenal cortex. By reflecting the set point of glucocorticoid-negative feedback at the hypothalamic level, CRH secretion defines the canonical endocrine-negative feedback loop of the hypothalamic-pituitary-adrenal axis for glucocorticoid production. The form of CRH that circulates in systemic blood during pregnancy is identical with maternal and fetal hypothalamic CRH but is likely derived mainly from the placenta (23, 24). Unlike hypothalamic CRH, which is under the control of glucocorticoid-negative feedback, placental CRH production has been found to be stimulated by cortisol both *in vitro* and *in vivo* in humans and other primates (18, 25, 26).

Maternal plasma CRH levels are low in the first trimester, rising from midgestation to term. In the last 12 wk of gestation, CRH plasma levels rise considerably, peaking during labor and then falling precipitously after delivery (15, 17). Umbilical cord blood and amniotic fluid levels of CRH are similarly increased in late gestation (16). Fetal CRH levels are lower than those in maternal circulation (50 *vs.* 1000 pM) but are still quite substantial, compared with levels in men and nonpregnant women, and increase during the latter stages of pregnancy. We propose that rising levels of placenta-derived CRH in the fetal plasma in late gestation directly stimulate human fetal adrenal steroidogenesis, working with ACTH to drive production of cortisol and DHEA-S.

The ability of CRH to increase fetal adrenal DHEA-S production has been noted in several studies (19–21). These investigators showed that CRH induces fetal adrenal DHEA-S biosynthesis as well as the levels of CYP17 and CYP11A mRNAs, supporting a role for this hormone in direct regulation of fetal zone production of DHEA-S. Thus, a hypothesis has developed that the late gestational rise in fetal CRH levels acts on fetal zone cells and is in part responsible for the dramatic increase in fetal DHEA-S production that occurs during the last weeks of gestation. This increase in fetal zone activity correlates with rising levels of maternal estrogen levels through the conversion of DHEA-S to estrogens within the placenta. The increase in the maternal estrogen to progesterone ratio may promote the expression of contraction-associated proteins in the myometrium, thus facilitating the initiation of parturition (27). Due to these reports, considerable focus has been placed on the ability of CRH to stimulate DHEA-S but not cortisol biosynthesis. Part of this focus was due to the observation that CRH treatment

of isolated fetal adrenal cells did not significantly enhance the level of HSD3B2 mRNA (19–21). The expression of this enzyme is a particularly important indicator of the capacity of the fetal adrenal to produce cortisol because during most of gestation, its expression is very low, thus limiting cortisol biosynthesis (6). The apparent lack of CRH effect on this enzyme would tend to diminish its role in cortisol biosynthesis. Our data, indicative of clear enhancement of HSD3B2 in fetal adrenal cells in response to CRH, would appear to conflict with this earlier report; however, the differences may be explained by different methods used for cell culture preparation and the study of HSD3B2 mRNA. In the earlier study, a mixed population of HFAs was used. It is important to remember that the fetal zone occupies 80–90% of the fetal adrenal cortex and expresses HSD3B2 at very low levels (7, 8), which makes it difficult to detect its mRNA with the use of Northern analysis. In our study, the fact that experiments were conducted on isolated human DZ/TZ cells, and the use of the more sensitive technique of real-time RT-PCR allowed us to detect HSD3B2 mRNA in the control cultures and cells treated with CRH or ACTH. Our report goes much further by showing that CRH actually increases the expression of mRNAs for all the enzymes needed for cortisol biosynthesis as well as the StAR protein, which is needed for cholesterol movement into the mitochondria. Thus, CRH would appear to be a potent secretagogue for fetal adrenal cortisol biosynthesis.

Unlike many species, human CRH is bound with high affinity to a specific serum binding protein, the CRH-binding protein (CRH-BP), with a concomitant reduction in its bioactivity (28, 29). Thus, any consideration of the possible physiologic role of CRH in the human fetus must take into account the concentrations of CRH present as well as CRH-BP. During most of pregnancy, it appears that CRH-BP binds the majority of circulating CRH in the fetal and maternal compartment, which likely serves to tightly control the bioactivity of placental-derived CRH (28). Although CRH-BP levels in pregnant women are high in the second trimester, they begin to fall and by wk 35 have decreased by 50%. CRH-BP levels in fetal plasma also decrease significantly in late gestation (30, 31). Decreased CRH-BP results in an increase in free, potentially biologically active CRH. It has been shown that in late gestation as much as 50% of fetal CRH circulates in the unbound form. Our dose-response studies suggest that physiologic bioactive levels of CRH are able to stimulate cortisol production. Perhaps more importantly, we show that the combination of physiologic levels of ACTH and CRH has an additive effect on the production of cortisol and a strong synergistic effect on HSD3B2 expression. The reason for the apparent additive effect on steroid production but synergistic effect on HSD3B2 expression may relate to the effects on early steps in steroid production. Specifically, in contrast to the effects on HSD3B2, the combined treatments (CRH plus ACTH) did not result in a synergistic StAR mRNA expression (data not shown). Because StAR expression may act to regulate cholesterol flux into cortisol, synergistic effects of the combined treatments on HSD3B2 mRNA or enzymatic activity may not be reflected in the absolute amount of cortisol produced. Thus, these data suggest that these hormones are likely to work together to increase the production of cortisol late in gestation.

The ability of CRH to stimulate both cortisol and DHEA-S is highly significant because it would allow the fetal adrenal to work with the placenta to create a feed-forward endocrine cascade that would not end until separation of the fetus from the placenta at delivery. Specifically, if CRH can stimulate fetal adrenals to produce cortisol, then the fetal-derived cortisol can stimulate placental CRH production via the unique glucorticoid-positive feedback system seen in the human placenta. This is in contrast to negative feedback of cortisol on fetal and maternal hypothalamic CRH production, and the placental effect may involve activation of different CRH receptor subtypes or through the initiation of a different cascade of events after binding to the receptor (18). This positive feedback cascade results in rising placental CRH and fetal cortisol production in the last trimester of human gestation. As noted, the rise in cortisol helps to promote maturation of fetal organs and this fetoplacental endocrine activation may also modulate the timing of the onset of human parturition (32).

In conclusion, this study further extends our knowledge of the mechanisms through which CRH activates the HFA in late gestation. Of note, we have demonstrated that CRH increases both cortisol secretion and the capacity to produce cortisol through an increase in mRNAs for all enzymes needed for its biosynthesis. In addition, these effects could be accomplished using physiologic concentrations of CRH, which were additive with ACTH. We thus hypothesize that placental CRH and fetal pituitary ACTH work together to cause the late gestational increase in fetal adrenal cortisol and DHEA-S production. By showing additive effects between physiologic concentrations of CRH and ACTH on fetal adrenal cortisol production, we now have *in vitro* evidence to support this hypothesis. The role of this fetoplacental endocrine cascade in the timing of human parturition merits more extensive study.

Acknowledgments

Received May 8, 2004. Accepted September 23, 2004.

Address all correspondence and requests for reprints to: William E. Rainey, Ph.D., Professor, Department of Obstetrics and Gynecology, University of Texas Southwestern Medical Center, 5323 Harry Hines Boulevard, Room J6.114, Dallas, Texas 75390-9032. E-mail: william.rainey@utsouthwestern.edu.

This work was supported by National Institutes of Health Grants T32 HD07190, HD11149, and DK43140 (to W.E.R.).

References

1. **Siiteri PK, MacDonald PC** 1966 Placental estrogen biosynthesis during human pregnancy. J Clin Endocrinol Metab 26:751–761
2. **Rehman KS, Carr BR, Rainey WE** 2003 Profiling the steroidogenic pathway in human fetal and adult adrenals. J Soc Gynecol Investig 10:372–380
3. **Freije WA, Pezzi V, Arici A, Carr BR, Rainey WE** 1997 Expression of 11β-hydroxylase (CYP11B1) and aldosterone synthase (CYP11B2) in the human fetal adrenal. J Soc Gynecol Investig 4:305–309
4. **Mesiano S, Coulter CL, Jaffe RB** 1993 Localization of cytochrome P450 cholesterol side-chain cleavage, cytochrome P450 17α-hydroxylase/17,20-lyase, and 3β-hydroxysteroid dehydrogenase isomerase steroidogenic enzymes in human and rhesus monkey fetal adrenal glands: reappraisal of functional zonation. J Clin Endocrinol Metab 77:1184–1189
5. **Dharia S, Slane A, Jian M, Conner M, Conley AJ, Parker Jr CR** 2004 Colocalization of P450c17 and cytochrome b5 in androgen-synthesizing tissues of the human. Biol Reprod 71:83–88

6. **Narasaka T, Suzuki T, Moriya T, Sasano H** 2001 Temporal and spatial distribution of corticosteroidogenic enzymes immunoreactivity in developing human adrenal. Mol Cell Endocrinol 174:111–120
7. **Parker Jr CR, Faye-Petersen O, Stankovic AK, Mason JI, Grizzle WE** 1995 Immunohistochemical evaluation of the cellular localization and ontogeny of 3 β-hydroxysteroid dehydrogenase/Δ5–4 isomerase in the human fetal adrenal gland. Endocr Res 21:69–80
8. **Doody KM, Carr BR, Rainey WE, Byrd W, Murry BA, Strickler RC, Thomas JL, Mason JI** 1990 3β-Hydroxysteroid dehydrogenase/isomerase in the fetal zone and neocortex of the human fetal adrenal gland. Endocrinology 126: 2487–2492
9. **Shifren JL, Mesiano S, Taylor RN, Ferrara N, Jaffe RB** 1998 Corticotropin regulates vascular endothelial growth factor expression in human fetal adrenal cortical cells. J Clin Endocrinol Metab 83:1342–1347
10. **Coulter CL, Goldsmith PC, Mesiano S, Voytek CC, Martin MC, Han VK, Jaffe RB** 1996 Functional maturation of the primate fetal adrenal *in vivo*: I. Role of insulin-like growth factors (IGFs), IGF-I receptor, and IGF binding proteins in growth regulation. Endocrinology 137:4487–4498
11. **Mesiano S, Jaffe RB** 1997 Role of growth factors in the developmental regulation of the human fetal adrenal cortex. Steroids 62:62–72
12. **Winters AJ, Oliver C, Colston C, MacDonald PC, Porter JC** 1974 Plasma ACTH levels in the human fetus and neonate as related to age and parturition. J Clin Endocrinol Metab 39:269–273
13. **Spencer SJ, Mesiano S, Lee JY, Jaffe RB** 1999 Proliferation and apoptosis in the human adrenal cortex during the fetal and perinatal periods: implications for growth and remodeling. J Clin Endocrinol Metab 84:1110–1115
14. **Jingami H, Matsukura S, Numa S, Imura H** 1985 Effects of adrenalectomy and dexamethasone administration on the level of prepro-corticotropin-releasing factor messenger ribonucleic acid (mRNA) in the hypothalamus and adrenocorticotropin/β-lipotropin precursor mRNA in the pituitary in rats. Endocrinology 117:1314–1320
15. **Goland RS, Wardlaw SL, Stark RI, Brown Jr LS, Frantz AG** 1986 High levels of corticotropin-releasing hormone immunoactivity in maternal and fetal plasma during pregnancy. J Clin Endocrinol Metab 63:1199–1203
16. **Lockwood CJ, Radunovic N, Nastic D, Petkovic S, Aigner S, Berkowitz GS** 1996 Corticotropin-releasing hormone and related pituitary-adrenal axis hormones in fetal and maternal blood during the second half of pregnancy. J Perinat Med 24:243–251
17. **Stalla GK, Bost H, Stalla J, Kaliebe T, Dorr HG, Pfeiffer D, von Werder K, Muller OA** 1989 Human corticotropin-releasing hormone during pregnancy. Gynecol Endocrinol 3:1–10
18. **Robinson BG, Emanuel RL, Frim DM, Majzoub JA** 1988 Glucocorticoid stimulates expression of corticotropin-releasing hormone gene in human placenta. Proc Natl Acad Sci USA 85:5244–5248
19. **Parker Jr CR, Stankovic AM, Goland RS** 1999 Corticotropin-releasing hormone stimulates steroidogenesis in cultured human adrenal cells. Mol Cell Endocrinol 155:19–25
20. **Smith R, Mesiano S, Chan EC, Brown S, Jaffe RB** 1998 Corticotropin-releasing hormone directly and preferentially stimulates dehydroepiandrosterone sulfate secretion by human fetal adrenal cortical cells. J Clin Endocrinol Metab 83:2916–2920
21. **Chakravorty A, Mesiano S, Jaffe RB** 1999 Corticotropin-releasing hormone stimulates P450 17α-hydroxylase/17,20-lyase in human fetal adrenal cells via protein kinase C. J Clin Endocrinol Metab 84:3732–3738
22. **Murphy BE** 1982 Human fetal serum cortisol levels related to gestational age: evidence of a midgestational fall and a steep late gestational rise, independent of sex or mode of delivery. Am J Obstet Gynecol 144:276–282
23. **Campbell EA, Linton EA, Wolfe CD, Scraggs PR, Jones MT, Lowry PJ** 1987 Plasma corticotropin-releasing hormone concentrations during pregnancy and parturition. J Clin Endocrinol Metab 64:1054–1059
24. **Petraglia F, Sawchenko P, Rivier J, Vale W** 1987 Evidence for local stimulation of ACTH by corticotropin-releasing hormone in human placenta. Nature 328: 717–719
25. **Jones SA, Brooks AN, Challis JR** 1989 Steroids modulate corticotropin-releasing hormone production in human fetal membranes and placenta. J Clin Endocrinol Metab 68:825–830
26. **Karalis K, Majzoub JA** 1995 Regulation of placental corticotropin-releasing hormone by steroids. Possible implications in labor initiation. Ann NY Acad Sci 771:551–555
27. **Mastorakos G, Ilias I** 2003 Maternal and fetal hypothalamic-pituitary-adrenal axes during pregnancy and postpartum. Ann NY Acad Sci 997:136–149
28. **Perkins AV, Wolfe CD, Eben F, Soothill P, Linton EA** 1995 Corticotrophin-releasing hormone-binding protein in human fetal plasma. J Endocrinol 146: 395–401
29. **Linton EA, Wolfe CD, Behan DP, Lowry PJ** 1988 A specific carrier substance for human corticotrophin releasing factor in late gestational maternal plasma which could mask the ACTH-releasing activity. Clin Endocrinol (Oxf) 28: 315–324
30. **Perkins AV, Linton EA** 1995 Identification and isolation of corticotrophin-releasing hormone-positive cells from the human placenta. Placenta 16: 233–243
31. **Petraglia F, Florio P, Simoncini T, Woods RJ, Giuntini A, Gremigni R, Serra GB, Genazzani AR, Lowry PJ** 1997 Cord plasma corticotropin-releasing factor-binding protein (CRF-BP) in term and preterm labour. Placenta 18:115–119
32. **Whittle WL, Patel FA, Alfaidy N, Holloway AC, Fraser M, Gyomorey S, Lye SJ, Gibb W, Challis JR** 2001 Glucocorticoid regulation of human and ovine parturition: the relationship between fetal hypothalamic-pituitary-adrenal axis activation and intrauterine prostaglandin production. Biol Reprod 64:1019–1032

JCEM is published monthly by The Endocrine Society (http://www.endo-society.org), the foremost professional society serving the endocrine community.

0021-972X/05/$15.00/0
Printed in U.S.A.

The Journal of Clinical Endocrinology & Metabolism 90(9):5393–5400

doi: 10.1210/jc.2005-0680

Corticotropin-Releasing Hormone (CRH) and Urocortin Act through Type 1 CRH Receptors to Stimulate Dehydroepiandrosterone Sulfate Production in Human Fetal Adrenal Cells

Rosa Sirianni, Bobbie A. Mayhew, Bruce R. Carr, C. Richard Parker, Jr., and William E. Rainey

Department of Obstetrics and Gynecology, Division of Reproductive Endocrinology and Infertility, University of Texas Southwestern Medical Center (R.S., B.A.M., B.R.C., W.E.R.), Dallas, Texas 75390; Department of Obstetrics and Gynecology, University of Alabama at Birmingham (C.R.P.), Birmingham, Alabama 35233

Context: Near term, the human fetal adrenal increases the production of cortisol and dehydroepiandrosterone sulfate (DHEAS). DHEAS, which acts as substrate for placental estrogen production, induces key changes involved in parturition.

Objective: The objective of this study was to determine quantitatively the effect of CRH on mRNA levels of enzymes needed for DHEAS production (steroidogenic acute regulatory protein, CYP11A, CYP17, and SULT2A1), to determine the CRH receptor (CRH-R) subtype(s) responsible for CRH action, and to determine the effect of CRH on CRH-R mRNA expression in human adrenal fetal zone (FZ) cells.

Design: Human adrenal FZ cells were treated with CRH, ACTH, urocortin (Unc), and CRH antagonists, and RNA was analyzed by microarray and real-time RT-PCR.

Setting: This study was performed at an academic research laboratory.

Main Outcome Measure: The main outcome measure was the expression of steroidogenic enzymes and CRH-R.

Results: Microarray analysis of human FZ cells treated for 24 h with CRH or ACTH showed increased mRNA expression levels of the genes needed for DHEAS production. Real-time RT-PCR analysis confirmed these data. Induction was lost in the presence of CRH-R1 antagonists, but not CRH-R2 antagonists. Stimulation was reproduced by Unc. The CRH-R1α mRNA splice variant was the only type 1 receptor isoform expressed in the fetal adrenal, and treatment with CRH up-regulates its mRNA levels.

Conclusions: CRH, Unc, and ACTH stimulate all elements of the DHEAS synthetic pathway and activate CRH-R1 as well. The resulting increased DHEAS levels can be used for placental estrogen synthesis and contribute to the process leading to parturition in humans. (***J Clin Endocrinol Metab* 90: 5393–5400, 2005**)

THE HIGH CIRCULATING levels of CRH in the human fetus and its rise in late gestation make this peptide an attractive candidate for regulation of fetal endocrine systems. We and others have shown that CRH can stimulate steroid hormone production by both definitive zone (DZ) and fetal zone (FZ) cells (1–4). Recently, we have shown that CRH increases the mRNA of all the steroidogenic enzymes needed for the production of cortisol in the definitive/transitional zones (DZ/TZ) of the human fetal adrenal (2). Cortisol secreted by the fetus may stimulate placental CRH production, creating a feed-forward endocrine cascade that would not end until the separation of the fetus from the placenta at delivery. CRH levels increased through this mechanism could also stimulate FZ cells to produce dehydroepiandrosterone sulfate (DHEAS). A number of investigators have shown that the fetal adrenal cortex is the principal source of placental estrogen precursors, namely DHEAS (5). This is consistent with the fact that women pregnant with an anencephalic fetus, which has atrophic adrenals that produce low levels of DHEAS, have decreased circulating estrogens (6). Estrogens produce many of the changes associated with parturition, such as the increase in oxytocin receptor and connexin-43 expression in the myometrium (7, 8). The increase in DHEAS would suggest that CRH is able to induce the enzymes needed for DHEAS biosynthesis. Jaffe and colleagues (1) showed that CRH activates 17α-hydroxylase (CYP17) and cholesterol side-chain cleavage (CYP11A) expression, albeit with less potency than ACTH. However, a detailed and quantitative analysis of the effects of CRH on all the enzymes needed for DHEAS production as well as the specific CRH receptor involved in adrenal regulation has not been performed.

Over the last few years the number of identified members of the CRH-related family of peptides, has expanded rapidly. The family includes not only CRH, but also urocortin (Ucn) Ucn II, and Ucn III as well as fish urotensin I and frog sauvagine (9–13). All the CRH family members exert their effects by binding to specific cell surface, G protein-coupled receptors. Two major CRH receptor subtypes are recognized, CRH-R1 and CRH-R2, which belong to the class II G protein-coupled receptor superfamily (14–16). These receptors share

First Published Online July 12, 2005

Abbreviations: CRH-R, CRH receptor; DHEAS, dehydroepiandrosterone sulfate; DZ/TZ, definitive/transitional zone; FZ, fetal zone; StAR, steroidogenic acute regulatory protein; Ucn, urocortin.

70% homology at the amino acid level, but have different binding properties for the members of the CRH family. CRH is able to activate both CRH-R1 and CRH-R2; Ucn activates both type 1 and 2, whereas Ucn II and Ucn III are selective ligands for CRH-R2. Several splice variants of the mRNA for CRH-R1 and -R2 have been found and should encode different sized proteins. CRH-R1 and -R2 have, respectively, eight and three mRNA splice variants. The human fetal adrenals have been shown to express both subtypes of the CRH receptor (17), but a detailed study to demonstrate the receptor isoform(s) expressed and responsible for CRH actions has not been performed. A number of specific inhibitors for CRH-R1 and -R2 have been recently developed, and these inhibitors have been useful tools to determine receptor subtype specificity of CRH effects in different cell types. Recently, the CRH-R1 promoter has been studied (18), and importantly, its activity in transient transfection experiments is up-regulated by CRH and Ucn. Therefore, in the present study we conducted experiments to determine quantitatively the effect of CRH on mRNA levels of all the enzymes needed for DHEAS production, determine the CRH-R subtype(s) responsible for CRH actions, and determine the effect of CRH on its own receptor mRNA expression in human adrenal FZ cells.

Materials and Methods

Cell culture

Human fetal adrenal glands were obtained with informed consent from the pathological examination of elective pregnancy terminations performed between 18 and 24 wk gestation. The DZ/TZ was dissected from the FZ using sterile technique. The FZ was minced into small pieces and incubated in DMEM/Ham's F-12 containing 1 mg/ml collagenase-dispase and 0.25 mg/ml deoxyribonuclease I. Digestion and mechanical dispersion were carried out twice for 30 min each time at 37 C, centrifuging cells between each digestion and combining them before plating. Cells were cultured initially for 4–6 d in DMEM/Ham's F-12 medium containing 10% Cosmic Calf Serum (HyClone, Logan, UT), 1% ITS$^+$ (BD Biosciences, Bedford, MA), and antibiotics/antimycotics consisting of penicillin/streptomycin, gentamicin, kanamycin, and amphotericin B (complete medium). Cells were then trypsinized, and aliquots of 3×10^6 cells were stored at −150 C for future use. FZ cells were then plated onto 12-well culture dishes at a density of 1×10^5/well. Experimental treatments were applied 4–6 d later. The protocol was approved by the institutional review boards of University of Texas Southwestern Medical Center (Dallas, TX) and University of Alabama (Birmingham, AL).

Stimulation of steroid secretion and analysis of steroids

CRH (Sigma-Aldrich Corp., St. Louis, MO), ACTH (Organon, West Orange, NJ), Ucn, Ucn II, and Ucn III (Sigma-Aldrich Corp.) were added to the cells, and treatment was carried out at 37 C for the indicated times. The CRH-R antagonists astressin (Sigma-Aldrich Corp.), astressin-2B (Sigma-Aldrich Corp.), and antalarmin (Sigma-Aldrich Corp.) were added to the plate 30 min before the addition of CRH.

The DHEAS content of experimental medium was determined using RIA kits (Diagnostic System Laboratories, Webster, TX).

Microarray analysis

RNA from adrenal FZ cells untreated (basal) or treated for 24 h with ACTH (10 nM) or CRH (10 nM) were hybridized to an Affymetrix human HG-U133plus oligonucleotide two-microarray set (Affymetrix, Inc., Santa Clara, CA) containing more than 54,000 probe sets representing over 38,500 independent human genes. The arrays were scanned at high resolution using an Affymetrix GeneChip Scanner 3000. Results were analyzed using GeneSpring version 6.1 software (Silicon Genetics, Redwood City, CA), and pure signal values were normalized using a list of 100 Normalization Control probe sets published by Affymetrix and used to identify genotypic differences between untreated and treated cells. Hierarchical clustering algorithms were used to determine steroidogenic gene expression patterns in the two treated samples.

Protein assay

Cells were lysed in 100 μl 1× Passive Lysis Buffer (Promega Corp., Madison, WI). The protein content of samples was then determined by the bicinchoninic acid protein assay using the BCA assay kit (Pierce Chemical Co., Rockford, IL).

RNA extraction, cDNA synthesis, and real-time RT-PCR

Adrenal glands from different fetuses were used to prepare cultures that were independently used for replicate experiments. RNA was extracted from cell cultures using the Ultraspec RNA isolation system (Biotecx Laboratories, Inc., Houston, TX). All RNA samples were treated with deoxyribonuclease I (Ambion, Austin, TX); the purity and integrity of the RNA were checked spectroscopically and by gel electrophoresis before use. Two micrograms of total RNA was reverse transcribed in a final volume of 50 μl using the High Capacity cDNA Archive Kit (Applied Biosystems, Foster City, CA) and stored at −20 C. The nucleotide sequences of the primers and TaqMan probes are shown in Table 1; sequences were based on the following GenBank accession numbers: steroidogenic acute regulatory protein (StAR), NM_000349; CYP11A1, M14565; CYP17, NM_000102; SULT2A1, NM_003167; and CRH-R1, NM_004382.

Real-time RT-PCRs were performed using the ABI PRISM 7000 Sequence Detection System (Applied Biosystems) in a total volume of 30 μl reaction mixture following the manufacturer's protocol, using the SYBR Green Universal 2× PCR Master Mix (Applied Biosystems) and

TABLE 1. Oligonucleotide primer and probe sequences used for real-time RT-PCR

Gene	Oligonucleotide	Sequence	TaqMan probe sequence
StAR	Forward primer	5′-CCACCCCTAGCACGTGGA-3′	
	Reverse primer	5′-TCCTGGTCACTGTAGAGAGTCTCTTC-3′	
CYP11A	Forward primer	5′-TCCAGAAGTATGGCCCGATT-3′	
	Reverse primer	5′-CATCTTCAGGGTCGATGACATAAA-3′	
CYP17	Forward primer	5′-TCTCTGGGCGGCCTCAA-3′	5′-TGGCAACTCTAGACATCGCGTCC-3′
	Reverse primer	5′-AGGCGATACCCTTACGGTTGT-3′	
SULT2A1	Forward primer	5′-TCGTGATAAGGGATGAAGATGTAATAA-3′	
	Reverse primer	5′-TGCATCAGGCAGAGAATCTCA-3′	
CRH-R1	Forward primer	5′-GAGGTCCACCAGAGCAACGT-3′	5′-GAAGTTGGTCACATGGAAGTAGTTGT-3′
	Reverse primer	5′-GAAGTTGGTCACATGGAAGTAGTTGT-3′	

0.1 μM of each primer using the dissociation protocol for the amplification of StAR, CYP11A, and SUL2A1, and the TaqMan 2× PCR Master Mix, 0.1 μM of each primer, and 0.1 μM of each probe using the emulation protocol for CYP17 and CRH-R1. Negative controls contained water instead of first-strand cDNA. Each sample was normalized on the basis of its 18S ribosomal RNA content.

The 18S quantification was performed with a TaqMan ribosomal RNA reagent kit (Applied Biosystems) using the manufacturer's protocol. Relative gene expression for each steroidogenic enzyme mRNA was normalized to a calibrator that was chosen to be the basal condition (untreated sample). Results were calculated with the ΔΔCt method; they were expressed as the *n*-fold differences in steroidogenic enzyme gene expression relative to 18S rRNA and calibrator and were determined as follows: $n\text{-fold} = 2^{-(\Delta Ct\ sample\ -\ \Delta Ct\ calibrator)}$, where the parameter Ct (threshold cycle) is defined as the fractional cycle number at which the PCR reporter signal passes a fixed threshold. ΔCt values of the sample and calibrator were determined by subtracting the average Ct value of the transcript under investigation from the average Ct value of the 18S rRNA gene for each sample.

Nested PCR

RT products (cDNA) from human tissues were used as template for the first round of PCR. Primers were previously described (19) that were designed to amplify fragments spanning exons 2–7. Products from the first-round PCR were used as template for a second PCR. PCR was performed in a total volume of 25 μl using 2 μl from the original first-strand cDNA synthesis. The PCR mix contained 2.5 mM $MgCl_2$, 0.25 mM of each deoxy-NTP, 0.4 μM of each primer, and 0.25 U platinum *Taq* polymerase (Invitrogen Life Technologies, Inc., Carlsbad, CA) Before PCR amplification, samples were denatured for 3 min at 94 C, then PCR was programmed for 35 cycles as follows: denaturing at 94 C for 50 sec, annealing at 65 C for 1 min, and extension at 72 C for 1 min. Two microliters of products of the first PCR served as a template for the second round of amplification reaction using the same conditions of the first-round PCR. As a negative control for all reactions, water was used in place of the cDNA (nontemplate control). The products of the second PCR were analyzed using 1% agarose gel electrophoresis.

Data analysis and statistical methods

Pooled results from triplicate experiments were analyzed by one-way ANOVA with Student-Newman-Keuls multiple comparison methods, using SigmaStat version 3.0 (SPSS, Inc., Chicago, IL).

Results

Comparison between CRH and ACTH on FZ cell DHEAS production and expression of steroid-metabolizing enzymes

FZ cells were isolated and placed in monolayer culture. Cells were treated with the same concentration of CRH or ACTH (10 nM) for 24 h. We used oligonucleotide microarray analysis to examine the transcript profile of steroidogenic enzymes needed for DHEAS production. Gene profiling was analyzed using GeneSpring software comparing treated with nontreated samples (Fig. 1). StAR, CYP11A, CYP17, and SULT2A1 were plotted against a total of 43 steroidogenic enzymes present on the Affymetrix microarray. ACTH and CRH had similar effects on the expression of steroidogenic enzymes. The effect of treatment with CRH or ACTH on DHEAS production or mRNA levels of steroidogenic enzymes needed for DHEAS production is shown in Fig. 2. The medium content of DHEAS was determined by RIA (Fig. 2A). ACTH was able to induce steroid production by 3-fold ($P < 0.001$), whereas CRH increased medium DHEAS by 4-fold ($P < 0.001$). StAR (Fig. 2B) and SULT2A1 (Fig. 2E) were induced by ACTH 6-fold ($P < 0.001$) and 5-fold ($P < 0.001$), respectively, and were induced 5-fold ($P < 0.05$) by CRH.

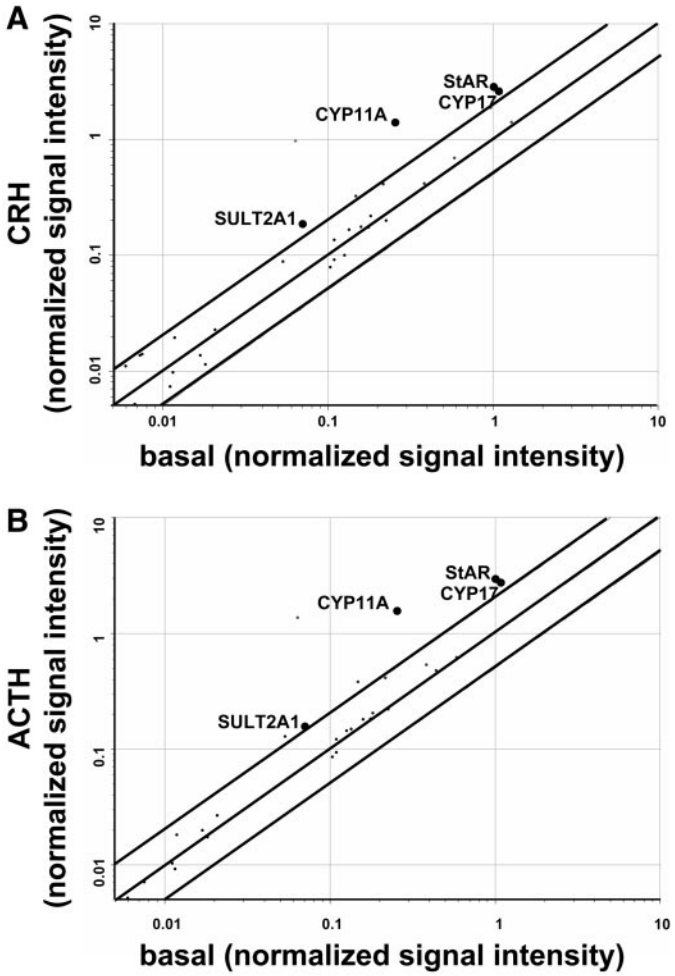

FIG. 1. Up-regulation of steroidogenic enzymes needed for DHEAS production in human FZ adrenal cells. Microarray analysis of adrenal cells treated for 24 h with 10 nM CRH *vs.* untreated (basal) cells (A) and cells treated for 24 h with 10 nM ACTH *vs.* basal cells (B). Global patterns of gene expression were identified using Affymetrix human HG-U133plus oligonucleotide GeneChip arrays. Each *dot* represents a unique sequence of steroidogenic enzyme genes, with a total of 43 genes from approximately 38,500 transcripts examined per array. Pure signal values were normalized to a list of 100 normalization control probe sets provided by Affymetrix. *Dots within parallel lines* represent mRNAs with less than 2-fold differences in expression; genes on the *middle line* have no differences in expression in the two compared conditions. The steroidogenic enzyme genes needed for DHEAS production are indicated.

CYP11A (Fig. 2C) and CYP17 (Fig. 2D) were induced 4-fold by CRH ($P < 0.001$), whereas ACTH increased CYP11A by 3.5-fold ($P < 0.001$) and CYP17 by 4-fold ($P < 0.001$). Taken together, these results indicate that ACTH and CRH both increase the production of DHEAS and the level of the mRNAs encoding the enzymes needed for DHEAS biosynthesis.

CRH effects are mediated through the CRH-R1

CRH actions rely on binding to CRH-Rs, existing as two different subtypes, R1 and R2. Each subtype has several isoforms. To determine which of the two CRH-R subtypes is responsible for CRH effects, we used specific inhibitors for the two receptor subtypes and measured DHEAS production

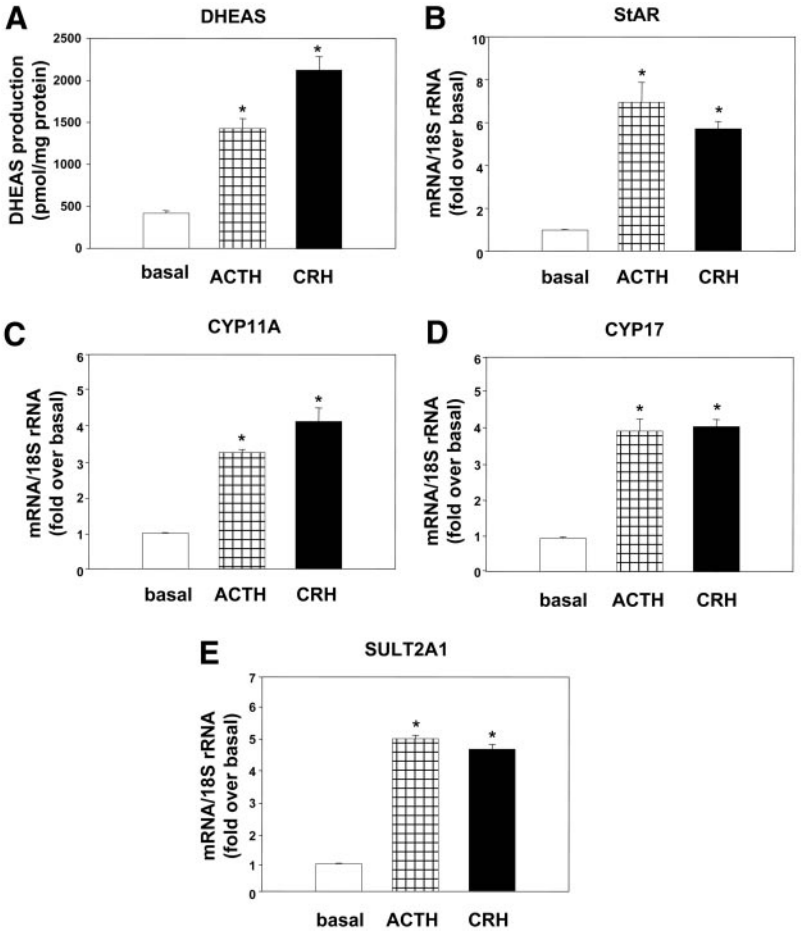

FIG. 2. Effects of CRH and ACTH on DHEAS production and transcript levels for StAR and the steroidogenic enzymes needed for DHEAS production in human FZ adrenal cells. Cells were treated for 24 h with ACTH (10 nM) or CRH (10 nM). RIA was used to measure levels of DHEAS production (A). The steroid content of the medium was normalized to the amount of cell protein on each tissue culture well. Real-time RT-PCR was used to quantify mRNA levels of StAR (B), CYP11A1 (C), CYP17 (D), and SULT2A1 (E) in human FZ cells. Data points are the values calculated with the ΔΔCt method as described in *Materials and Methods* and represent the mean ± SE of real-time data for cDNA from three RNA samples obtained from adrenals of three fetuses, expressed as the fold increase over the basal level. *, $P <$ 0.001 (compared with basal).

and steroidogenic enzymes mRNA expression in FZ cells. We used the CRH-R1-specific antagonist antalarmin, the CRH-R2-specific antagonist astressin-2B, and the CRH-R1/R2 nonselective antagonist astressin. As shown in Fig. 3A, astressin-2B was not able to block CRH-mediated induction of DHEAS production, whereas antalarmin and astressin decreased CRH-stimulated DHEAS levels by 50%. The effect produced by antalarmin and astressin on steroid production was a consequence of inhibition of CRH induction of mRNAs encoding steroidogenic enzymes (Fig. 3, B–E). CRH induced StAR and SULT2A1 by 5-fold ($P < 0.001$; Fig. 3B), whereas CYP11A (Fig. 3C) and CYP17 (Fig. 3D) were induced 4-fold ($P < 0.001$; Fig. 3E). Antalarmin and astressin blocked StAR induction by 56% and 64% respectively; CRH-R1 antagonists abolished induction of CYP11A by 60% ($P < 0.001$) and that of CYP17 and SULT2A1 by 70%. Astressin-2B had no effect on CRH induction of any of the investigated steroidogenic enzymes. Because CRH is not the only natural ligand for CRH-Rs, we decided to use the Ucns to confirm the data obtained with the receptor antagonists. Ucn is the only factor able to bind CRH-R1 and CRH-R2, whereas Ucn II and Ucn III can bind only the type 2 receptor. Ucn and CRH increased DHEAS production by 4-fold, whereas Ucn II and Ucn III did not have any effect (Fig. 4A). mRNA expression for StAR and the other three steroidogenic enzymes investigated in this study were not affected by Ucn II and Ucn III (Fig. 4, B–E). In contrast, Ucn increased StAR (Fig. 4B) and SULT2A1 (Fig. 4E) by 5-fold ($P < 0.001$) and increased CYP11A (Fig. 4C) and CYP17 (Fig. 4D) by 4-fold ($P < 0.05$).

Only the CRH-R1α isoform is expressed in fetal adrenal

Eight isoforms of CRH-R1 have been described; they derive from different intron/exon splicing, and a graphic depiction of the mRNA encoding these splice variants can be seen in Fig. 5. Because these splice variants appear to have different affinities for ligands and differing abilities to interact with G proteins, we used a nested RT-PCR protocol to screen for the presence of all eight splice variants in whole fetal adrenal, DZ/TZ, FZ, and adult adrenal gland (Fig. 5). The predicted sizes of PCR products were previously described (19). Adult and fetal adrenal tissues were both found to express CRH-R1α mRNA. RNA isolated from FZ and DZ/TZ both expressed only the CRH-R1α spliced form. The only variation in the expression pattern was for the adult adrenal, which also expressed the CRH-R1γ isoform.

CRH up-regulates CRH-R1 mRNA expression

After showing that CRH effects in FZ cells are mediated through the R1subtype and that only the R1α isoform is expressed in fetal adrenal, we next tested the hypothesis that ACTH, Ucn, and CRH regulate the expression of this receptor. As shown in Fig. 6 CRH up-regulated CRH-R1 mRNA

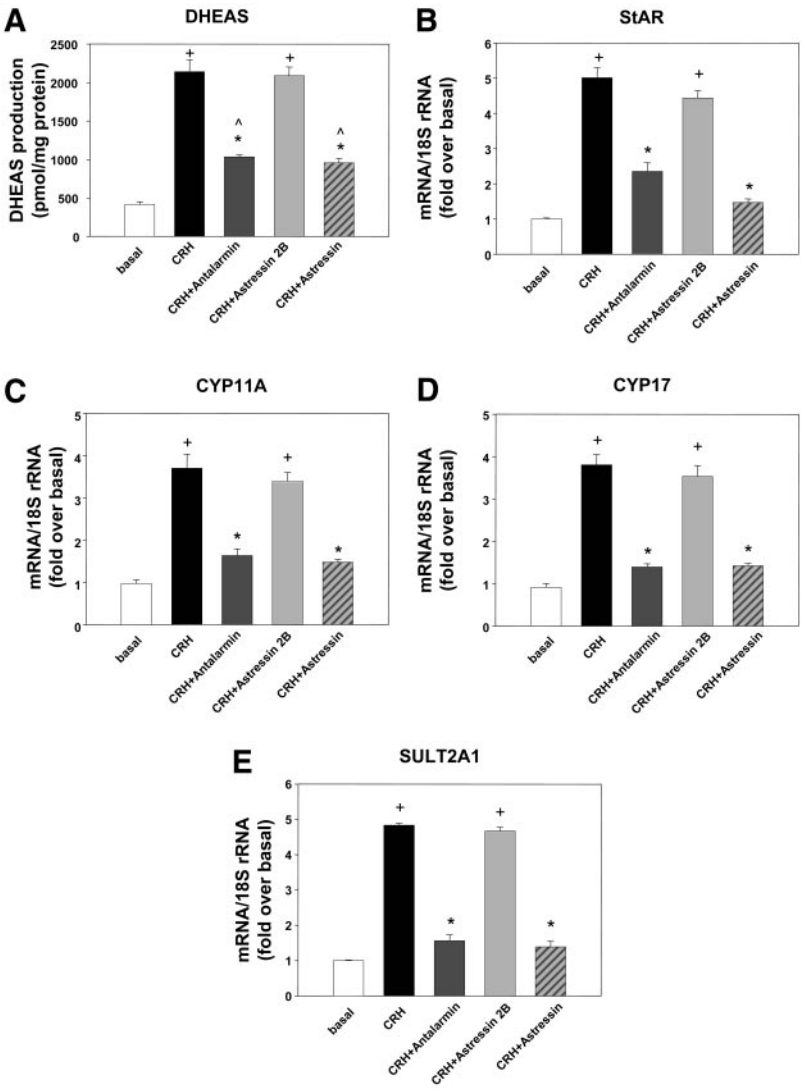

FIG. 3. Effects of CRH-R antagonists on CRH-induced DHEAS production and transcript levels for StAR and the steroidogenic enzymes needed for DHEAS production in human FZ adrenal cells. Cells were treated for 24 h with CRH (10 nM) alone or in combination with 10 μM CRH-R inhibitors. RIA was used to measure levels of DHEAS production (A). The steroid content of the medium was normalized to cell protein on each tissue culture well. Real-time RT-PCR was used to quantify mRNA levels of StAR (B), CYP11A (C), CYP17 (D), and SULT2A1 (E) in human FZ cells. Data points are the values calculated with the $\Delta\Delta$Ct method as described in *Materials and Methods* and represent the mean $\pm$ SE of real-time data for cDNA from three RNA samples obtained from adrenals of three fetuses, expressed as the fold increase over the basal level. *, $P < 0.001$ (compared with CRH). +, $P < 0.001$; ^, $P < 0.05$ (compared with basal).

expression by 3-fold ($P < 0.05$). A similar effect was obtained in the presence of ACTH or Ucn. The effects of CRH were again mediated through the R1 subtype, as shown by the ability of antalarmin or astressin to block transcript induction, whereas the type II receptor inhibitor astressin-2B did not have any effect.

Discussion

During the last trimester of gestation, the amount of DHEAS produced in the human fetal adrenal increases significantly. The DHEAS produced is then metabolized by the placenta to estrogens (20). The increase in adrenal activity occurs despite the fact that fetal ACTH levels do not significantly increase until the onset of parturition (21). This discrepancy of growing adrenal activity in the absence of increased circulating ACTH has led to speculation that factors other than ACTH are responsible for the third trimester growth and steroidogenesis of the fetal adrenal. There is now evidence that CRH may be the placental factor that directly regulates the fetal adrenal during the last weeks of gestation (2). In this study we investigated the effects of CRH on DHEAS and each of the mRNAs encoding the enzymes that comprise the DHEAS biosynthetic pathway. Our first approach to this study was to quantitatively evaluate the effect of CRH on DHEAS production in cultures of isolated FZ cells of the human adrenal. A previous study using a mixed population of fetal adrenal cells (1) reported that CRH is as potent as ACTH in inducing DHEAS production, but is less effective in inducing CYP17 expression. In this study we show that CRH induces all the enzymes needed for DHEAS production at levels similar to those seen with ACTH. We believe that the difference between our studies and the previous report can be explained by the different methods used for mRNA quantification. In the previous study (1) CYP17 mRNA was determined with the less sensitive and quantitative method of Northern analysis. Instead, we used the quantitative technique of real-rime RT-PCR. Also, we did not limit our analysis to two steroidogenic enzymes, but extended our study to all four enzymes required for DHEAS synthesis. Our results clearly support similar effects of ACTH and CRH on DHEAS production and induction of the mRNAs encoding the enzymes needed for its synthesis.

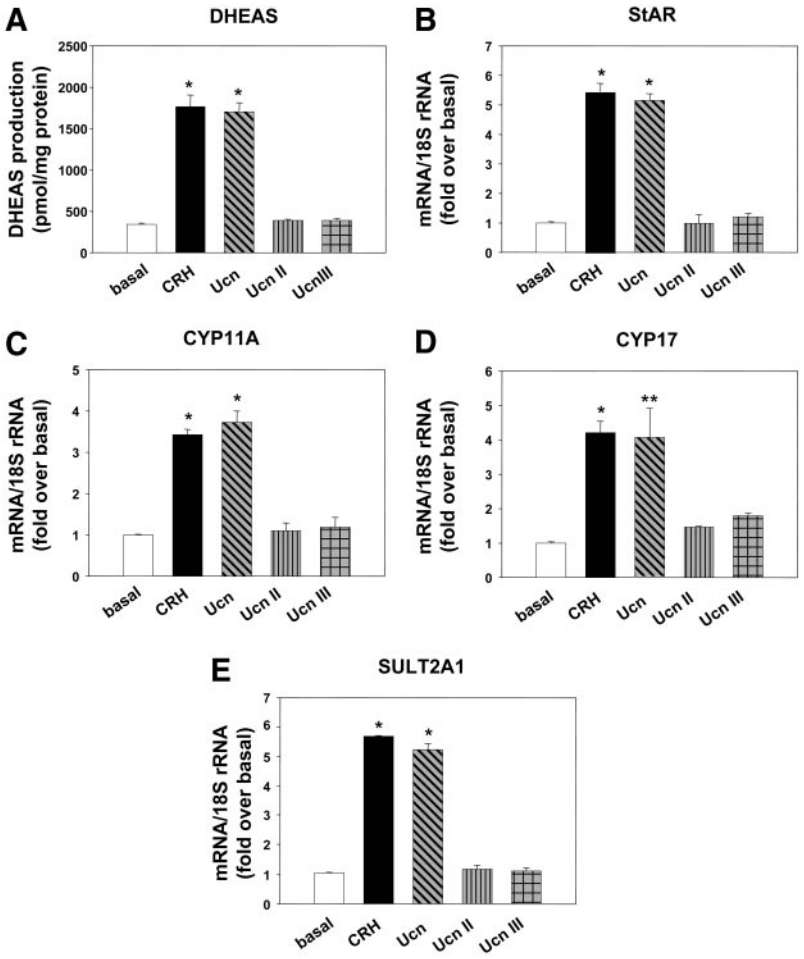

FIG. 4. Effect of CRH, Ucn, Ucn II, and Ucn III on transcript levels for StAR and the steroidogenic enzymes needed for DHEAS production in human FZ adrenal cells. Cells were treated for 24 h with CRH (10 nM), Ucn I (Ucn; 10 nM), Ucn II (10 nM), or Ucn III (10 nM). RIA was used to measure levels of DHEAS production (A). The steroid content of the medium was normalized to the amount of cell protein on each tissue culture well. Real-time RT-PCR was used to quantify mRNA levels of StAR (B), CYP11A (C), CYP17 (D), and SULT2A1 (E) in human FZ cells. Data points are the values calculated with the ΔΔCt method as described in *Materials and Methods* and represent the mean ± SE of real-time data for cDNA from three RNA samples obtained from adrenals of three fetuses, expressed as the fold increase over the basal value. *, $P < 0.001$; **, $P < 0.05$ (compared with basal).

Signals from CRH and CRH-related peptides are transduced via activation of two types of seven-transmembrane domain CRH receptors, CRH-R1 and -R2, with multiple subtypes (19, 22–27). Several splice variants of the mRNA for CRH-R1 have been found, and these should encode different sized proteins. The sequences would predict a variety of potential proteins, both membrane bound and soluble. The functions and exact expression levels of these isoforms have been difficult to determine due to the lack of available antibodies to the splice variants. Currently, eight isoforms of CRH-R1 have been identified, and these isoforms are termed R1α, R1β, R1c, R1d, R1e, R1f, R1γ, and R1h (19, 22, 28). CRH-R1α is the pituitary corticotrope cell receptor, but is also found in other brain regions, skin, and gastrointestinal and reproductive tracts (16, 27, 29). The CRH-R2 gene has three mRNA splice variants, encoding R2α, R2β, and R2γ receptor isoforms (24–26), with a unique tissue distribution (27). CRH-R2 is found in part of the hypothalamus, pituitary, heart, vascular endothelium and smooth muscle, skeletal muscle, skin, and gastrointestinal and reproductive tracts (24, 25, 30). Using specific CRH-R1 inhibitors (antalarmin) and agonists (Ucn), we showed that CRH works specifically through the type 1 receptor in fetal adrenal cells. Antalarmin, a type I receptor-specific antagonist, was able to inhibit CRH-induced DHEAS levels by 50%. It is possible that the dose of antalarmin was not high enough to completely block all the CRH-induced changes in expression of genes important to DHEAS synthesis. However, the extent of reduction in DHEAS secretion was statistically significant and was similar to the average effect of antalarmin on the various steroid synthetic enzyme genes. In addition, we show that the fetal adrenal only expresses the CRH-R1α isoform of the type 1 receptors. Our finding is in agreement with a previous report (17); however, the methods used for that study did not discriminate among R1α, R1d, and R1γ. Changes in the expression of the different CRH receptor isoforms have been found in the human placenta and myometrium. In the human placenta, CRH-R1 was localized in syncytiotrophoblast cells, chorionic trophoblast, and deciduas; CRH-R2 was found only in syncytiotrophoblast cells, cytotrophoblast within the structure of the villi, chorionic trophoblast, and decidual cells (31). Pregnant myometrium at term expresses the CRH-R isoforms 1α, 1β, 2α, and 2c (29, 32, 33). CRH-R1 mRNA is present at higher levels than CRH-R2 mRNA in both pregnant and nonpregnant women and is considerably up-regulated at the time of labor in the myometrium of the lower uterine segment (34). In sheep gestation, differences in CRH-R expression were found between immature and mature fetal and adult pituitary glands; CRH-R1 mRNA was decreased progressively at the different stages, and cortisol had a negative effect on receptor expression (35). Studies conducted on primary cultures of rat hypothalamic neurons

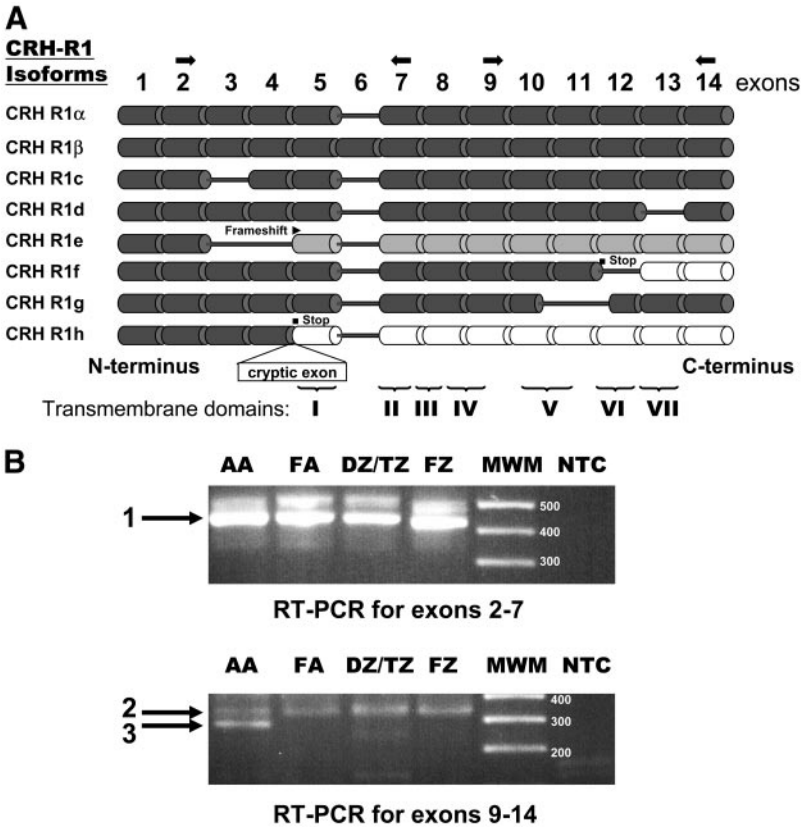

FIG. 5. Nested PCR amplification of the human CRH-R1 isoforms. CRH-R1 has eight different receptor isoforms (A). RNA extracted from adult adrenal (AA), fetal adrenal (FA), DZ/TZ, and FZ of the fetal adrenal was retrotranscribed and used in a PCR with two different sets of primers (B). Primers are indicated by *arrows* above A that go across exons 2–7 and 9–14. Amplification with the primers pair for exons 2–7 is specific for isoforms α, β, c, d, f, or g. Amplified bands indicated by *arrow 1* can only be α, d, f, or g isoforms. Amplification with the primers pair for exons 9–14 is specific for isoforms α, β, c, d, f, or g. Bands indicated with *arrow 2* are specific for isoforms α, β, or c; *arrow 3* indicates CRH-R1g. Bands that are not indicated with an *arrow* represent the cDNA from the first-round PCR that was used as template in the second reaction. Water was used as a negative control [nontemplate control (NTC)]. Molecular weight marker (MWM) is indicated. This schematic of receptor splice variants is based on Ref. 19.

revealed that CRH-R1 mRNA levels were significantly increased after incubation with CRH. This effect was blocked by the nonselective CRH-R1 and -R2 antagonist, α-helical CRF, demonstrating that CRH directly affects hypothalamic neurons to increase CRH-R1 mRNA expression (36). Up until now, a similar study on the fetal adrenal had not been performed. In this study we show that ACTH, CRH, and Ucn can increase the mRNA encoding CRH-R1, and that CRH works through the type I receptor in causing this effect. Although there are no data available on the expression patterns of Ucn II or Ucn III, Ucn is produced by the placenta (37, 38) and, acting through the type I receptor, could work with CRH to increase steroidogenic activity in the fetal adrenal. In sheep, the physiological importance of CRH, acting through CRH-R1, was determined by administration of CRH-R1 antagonists during pregnancy. Administration of antalarmin, a CRH-R1-specific antagonist, to pregnant sheep blocked the rise of fetal ACTH or cortisol levels seen in vehicle-infused sheep and delayed the onset of parturition (39). However, in the rat the use of another specific CRH-R1 antagonist did not affect the length of gestation, indicating that there is interspecies variation in the putative roles of CRH in different mammals (40). This confirms the necessity for studies using human tissues to investigate the endocrine mechanisms that may be important for human parturition.

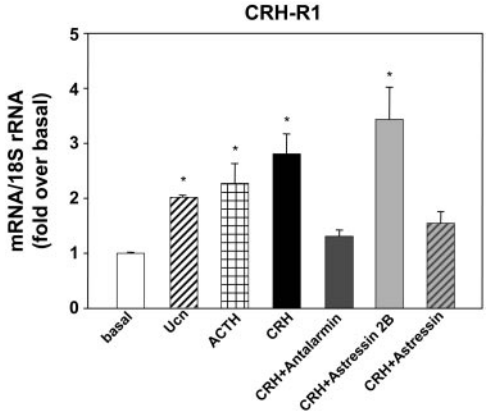

FIG. 6. Effects of agonists and CRH-R inhibitors on transcript levels for CRH-R1 in human FZ adrenal cells. Real-time RT-PCR was used to quantify mRNA levels of CRH-R1 in human FZ cells. Cells were treated for 24 h with ACTH (10 nM), Ucn (10 nM), or CRH (10 nM), alone or in combination with 10 μM CRH-R antagonists. Data points are the values calculated with the $\Delta\Delta$Ct method as described in *Materials and Methods* and represent the mean $\pm$ SE of real-time data for cDNA from five RNA samples obtained from adrenals of five fetuses, expressed as the fold increase over the basal level. *, $P < 0.05$ (compared with basal).

In conclusion, this study extends our knowledge of the mechanisms through which CRH activates the human fetal adrenal gland in late gestation. We thus hypothesize that both placental CRH and fetal ACTH are required for the late gestational increase in fetal adrenal cortisol and DHEAS production as a consequence of their effects on the DHEAS and cortisol biosynthetic pathway. CRH action is mediated through the type I receptor, specifically the isoform R1α, and CRH can induce the expression of its own receptor, creating a positive loop that contributes to maintain the increased expression of the enzymes necessary for DHEAS production. Although the type II receptor subtype does not seem to be

involved in CRH action, the expression pattern of CRH-R subtypes in the human fetal adrenal over the course of gestation merits additional study.

Acknowledgments

Received March 29, 2005. Accepted June 30, 2005.

Address all correspondence and requests for reprints to: Dr. William E. Rainey, Department of Physiology, Medical College of Georgia, 1130 15th Street CA 3094, Augusta, Georgia 30912. E-mail: wrainey@mail.mcg.edu.

This work was supported by National Institute of Health Grants T32-HD-07190, HD-11149, and DK-43140 (to W.E.R.).

References

1. **Smith R, Mesiano S, Chan EC, Brown S, Jaffe RB** 1998 Corticotropin-releasing hormone directly and preferentially stimulates dehydroepiandrosterone sulfate secretion by human fetal adrenal cortical cells. J Clin Endocrinol Metab 83:2916–2920
2. **Sirianni R, Rehman KS, Carr BR, Parker Jr CR, Rainey WE** 2005 Corticotropin-releasing hormone directly stimulates cortisol and the cortisol biosynthetic pathway in human fetal adrenal cells. J Clin Endocrinol Metab 90:279–285
3. **Parker Jr CR, Stankovic AM, Goland RS** 1999 Corticotropin-releasing hormone stimulates steroidogenesis in cultured human adrenal cells. Mol Cell Endocrinol 155:19–25
4. **Chakravorty A, Mesiano S, Jaffe RB** 1999 Corticotropin-releasing hormone stimulates P450 17α-hydroxylase/17,20-lyase in human fetal adrenal cells via protein kinase C. J Clin Endocrinol Metab 84:3732–3738
5. **Carr BR, Simpson ER** 1981 Lipoprotein utilization and cholesterol synthesis by the human fetal adrenal gland. Endocr Rev 2:306–326
6. **Tulchinsky D, Osathanondh R, Belisle S, Ryan KJ** 1977 Plasma estrone, estradiol, estriol and their precursors in pregnancies with anencephalic fetuses. J Clin Endocrinol Metab 45:1100–1103
7. **Adachi S, Oku M** 1995 The regulation of oxytocin receptor expression in human myometrial monolayer culture. J Smooth Muscle Res 31:175–187
8. **Chow L, Lye SJ** 1994 Expression of the gap junction protein connexin-43 is increased in the human myometrium toward term and with the onset of labor. Am J Obstet Gynecol 170:788–795
9. **Ichikawa T, McMaster D, Lederis K, Kobayashi H** 1982 Isolation and amino acid sequence of urotensin I, a vasoactive and ACTH-releasing neuropeptide, from the carp (*Cyprinus carpio*) urophysis. Peptides 3:859–867
10. **Lederis K, Letter A, McMaster D, Moore G, Schlesinger D** 1982 Complete amino acid sequence of urotensin I, a hypotensive and corticotropin-releasing neuropeptide from *Catostomus*. Science 218:165
11. **Vaughan J, Donaldson C, Bittencourt J, Perrin MH, Lewis K, Sutton S, Chan R, Turnbull AV, Lovejoy D, Rivier C** 1995 Urocortin, a mammalian neuropeptide related to fish urotensin I and to corticotropin-releasing factor. Nature 378:287–292
12. **Lewis K, Li C, Perrin MH, Blount A, Kunitake K, Donaldson C, Vaughan J, Reyes TM, Gulyas J, Fischer W, Bilezikjian L, Rivier J, Sawchenko PE, Vale WW** 2001 Identification of urocortin III, an additional member of the corticotropin-releasing factor (CRF) family with high affinity for the CRF2 receptor. Proc Natl Acad Sci USA 98:7570–7575
13. **Reyes TM, Lewis K, Perrin MH, Kunitake KS, Vaughan J, Arias CA, Hogenesch JB, Gulyas J, Rivier J, Vale WW, Sawchenko PE** 2001 Urocortin II: A member of the corticotropin-releasing factor (CRF) neuropeptide family that is selectively bound by type 2 CRF receptors. Proc Natl Acad Sci USA 98:2843–2848
14. **Richard D, Lin Q, Timofeeva E** 2002 The corticotropin-releasing factor family of peptides and CRF receptors: their roles in the regulation of energy balance. Eur J Pharmacol 440:189–197
15. **Grammatopoulos DK, Chrousos GP** 2002 Functional characteristics of CRH receptors and potential clinical applications of CRH-receptor antagonists. Trends Endocrinol Metab 13:436–444
16. **Slominski A, Wortsman J, Pisarchik A, Zbytek B, Linton EA, Mazurkiewicz JE, Wei ET** 2001 Cutaneous expression of corticotropin-releasing hormone (CRH), urocortin, and CRH receptors. FASEB J 15:1678–1693
17. **Karteris E, Randeva HS, Grammatopoulos DK, Jaffe RB, Hillhouse EW** 2001 Expression and coupling characteristics of the CRH and orexin type 2 receptors in human fetal adrenals. J Clin Endocrinol Metab 86:4512–4519
18. **Parham KL, Zervou S, Karteris E, Catalano RD, Old RW, Hillhouse EW** 2004 Promoter analysis of human corticotropin-releasing factor (CRF) type 1 receptor and regulation by CRF and urocortin. Endocrinology 145:3971–3983
19. **Pisarchik A, Slominski AT** 2001 Alternative splicing of CRH-R1 receptors in human and mouse skin: identification of new variants and their differential expression. FASEB J 15:2754–2756
20. **Rainey WE, Rehman KS, Carr BR** 2004 The human fetal adrenal: making adrenal androgens for placental estrogens. Semin Reprod Med 22:327–336
21. **Winters AJ, Oliver C, Colston C, MacDonald PC, Porter JC** 1974 Plasma ACTH levels in the human fetus and neonate as related to age and parturition. J Clin Endocrinol Metab 39:269–273
22. **Ross PC, Kostas CM, Ramabhadran TV** 1994 A variant of the human corticotropin-releasing factor (CRF) receptor: cloning, expression and pharmacology. Biochem Biophys Res Commun 205:1836–1842
23. **Grammatopoulos DK, Dai Y, Randeva HS, Levine MA, Karteris E, Easton AJ, Hillhouse EW** 1999 A novel spliced variant of the type 1 corticotropin-releasing hormone receptor with a deletion in the seventh transmembrane domain present in the human pregnant term myometrium and fetal membranes. Mol Endocrinol 13:2189–2202
24. **Valdenaire O, Giller T, Breu V, Gottowik J, Kilpatrick G** 1997 A new functional isoform of the human CRF2 receptor for corticotropin-releasing factor. Biochim Biophys Acta 1352:129–132
25. **Liaw CW, Lovenberg TW, Barry G, Oltersdorf T, Grigoriadis DE, de Souza EB** 1996 Cloning and characterization of the human corticotropin-releasing factor-2 receptor complementary deoxyribonucleic acid. Endocrinology 137:72–77
26. **Kostich WA, Chen A, Sperle K, Largent BL** 1998 Molecular identification and analysis of a novel human corticotropin-releasing factor (CRF) receptor: the CRF2γ receptor. Mol Endocrinol 12:1077–1085
27. **Lovenberg TW, Chalmers DT, Liu C, De Souza EB** 1995 CRF2α and CRF2β receptor mRNAs are differentially distributed between the rat central nervous system and peripheral tissues. Endocrinology 136:4139–4142
28. **Chen R, Lewis KA, Perrin MH, Vale WW** 1993 Expression cloning of a human corticotropin-releasing-factor receptor. Proc Natl Acad Sci USA 90:8967–8971
29. **Grammatopoulos D, Dai Y, Chen J, Karteris E, Papadopoulou N, Easton AJ, Hillhouse EW** 1998 Human corticotropin-releasing hormone receptor: differences in subtype expression between pregnant and nonpregnant myometria. J Clin Endocrinol Metab 83:2539–2544
30. **Kageyama K, Li C, Vale WW** 2003 Corticotropin-releasing factor receptor type 2 messenger ribonucleic acid in rat pituitary: localization and regulation by immune challenge, restraint stress, and glucocorticoids. Endocrinology 144:1524–1532
31. **Florio P, Franchini A, Reis FM, Pezzani I, Ottaviani E, Petraglia F** 2000 Human placenta, chorion, amnion and decidua express different variants of corticotropin-releasing factor receptor messenger RNA. Placenta 21:32–37
32. **Rodriguez-Linares B, Phaneuf S, Lopez Bernal A, Linton EA** 1998 Levels of corticotrophin-releasing hormone receptor subtype 1 mRNA in pregnancy and during labour in human myometrium measured by quantitative competitive PCR. J Mol Endocrinol 21:201–208
33. **Rodriguez-Linares B LEPS** 1998 Expression of corticotrophin-releasing hormone receptor mRNA and protein in the human myometrium. J Endocrinol 156:15–21
34. **Stevens MY, Challis JR, Lye SJ** 1998 Corticotropin-releasing hormone receptor subtype 1 is significantly up-regulated at the time of labor in the human myometrium. J Clin Endocrinol Metab 83:4107–4115
35. **Green JL, Figueroa JP, Massmann GA, Schwartz J, Rose JC** 2000 Corticotropin-releasing hormone type I receptor messenger ribonucleic acid and protein levels in the ovine fetal pituitary: ontogeny and effect of chronic cortisol administration. Endocrinology 141:2870–2876
36. **Konishi S, Kasagi Y, Katsumata H, Minami S, Imaki T** 2003 Regulation of corticotropin-releasing factor (CRF) type-1 receptor gene expression by CRF in the hypothalamus. Endocr J 50:21–36
37. **Petraglia F, Florio P, Benedetto C, Gallo C, Woods RJ, Genazzani AR, Lowry PJ** 1996 High levels of corticotropin-releasing factor (CRF) are inversely correlated with low levels of maternal CRF-binding protein in pregnant women with pregnancy-induced hypertension. J Clin Endocrinol Metab 81:852–856
38. **Clifton VL, Gu Q, Murphy VE, Schwartz J, Madsen G, Smith R, Qing G** 2000 Localization and characterization of urocortin during human pregnancy. Placenta 21:782–788
39. **Chan EC, Falconer J, Madsen G, Rice KC, Webster EL, Chrousos GP, Smith R** 1998 A Corticotropin-releasing hormone type I receptor antagonist delays parturition in sheep. Endocrinology 139:3357–3360
40. **Funai EF, O'Neill LM, Davidson A, Roque H, Finlay TH** 2000 A corticotropin releasing hormone receptor antagonist does not delay parturition in rats. J Perinat Med 28:294–297

JCEM is published monthly by The Endocrine Society (http://www.endo-society.org), the foremost professional society serving the endocrine community.

Antiestrogens upregulate estrogen receptor β expression and inhibit adrenocortical H295R cell proliferation

D Montanaro, M Maggiolini, A G Recchia, R Sirianni, S Aquila, L Barzon[1], F Fallo[2], S Andò and **V Pezzi**

Departments of Pharmaco-Biology and Cell Biology, University of Calabria, 87036 Arcavacata di Rende (CS), Italy

[1]Department of Histology, Microbiology and Medical Biotechnologies and [2]Department of Medical and Surgical Sciences, Clinica Medica 3, University of Padova, 35128 Padova, Italy

(Requests for offprints should be addressed to V Pezzi, Department of Pharmaco-Biology, University of Calabria, Arcavacata di Rende (CS) 87036, Italy; Email: v.pezzi@unical.it)

Abstract

The molecular mechanisms involved in adrenocortical tumorigenesis are still not completely understood. In this study, using the H295R cell line as a model system, we investigated the role of estrogens and estrogen receptor (ER) α and ERβ in the growth regulation of adrenocortical tumors. We demonstrated that H295R cells are able to convert androgens to estrogens by a constitutive expression of active cytochrome P450 aromatase protein and express ERβ to a greater extent than ERα. Moreover, physiological concentrations of 17β-estradiol (E_2) determined an increase of thymidine incorporation, suggesting the presence of an autocrine mechanism in maintaining H295R cell proliferation. Evaluating the response to ER antagonists like 4-hydroxytamoxifen (OHT) and ICI 182 780 (ICI), we observed an up-regulation of ERβ and a dose-dependent inhibition of H295R cell proliferation. Whereas ICI determined the growth arrest of H295R cells, OHT induced morphological changes that were characteristic of apoptosis. According to the above-mentioned observations, OHT but not ICI clearly induced a marked expression of FasL and the cleavage of both caspase-8 and caspase-3. Interestingly, the apoptotic effects of OHT in H295R cells may be consequent to the enhanced levels of ERβ which stimulate the expression of FasL interacting with activating protein (AP)-1 sites located within its promoter sequence. In conclusion, we have demonstrated that H295R cells are able to transform androgens to estrogens that activate an autocrine mechanism, mediated by their own receptors, and contribute to regulate the proliferation of these cells. Moreover, this study points towards a role for ERβ as an important mediator of the repressive effects exerted by antiestrogens on H295R cells; however, further studies are needed to clarify its role in the control of adrenocortical cell proliferation and on the potential benefits of antiestrogens for treatment of adrenocortical cancer.

Journal of Molecular Endocrinology (2005) **35,** 245–256

Introduction

Adrenocortical cancers are highly malignant and associated with a poor prognosis. The molecular mechanisms involved in adrenocortical tumorigenesis are still not completely understood. However, several studies have revealed an alteration of a wide variety of signaling pathways such as the mutation of the tumor-suppressor gene TP53 and *ras* gene family as well as the up-regulation of the insulin-like growth factor (IGF) II system (Logié *et al.* 1999, Barzon *et al.* 2001, Kirschner 2002).

The H295R adrenocortical carcinoma cell line (Rainey *et al.* 1994) was derived from H295 cells, which were established from a primary hormonally active adrenocortical carcinoma (Gazdar *et al.* 1990), and has been used as a model system to investigate the role of different signaling pathways in the growth regulation of adrenocortical tumors (Rossi *et al.* 1998, Logié *et al.* 1999, Bourcigaux *et al.* 2000). The IGF system has been well characterized (Weber *et al.* 2000): the IGF-II but not the IGF-I gene is strongly expressed in H295R cells as well as in human adrenocortical tumors and exhibits paternal isodisomy (loss of the maternal-derived allele and duplication of the IGF-II active paternal allele) or less frequently the loss of imprinting (Gicquel *et al.* 1997). IGF-II regulates the growth of adrenal cells by binding to the IGF receptor and inducing the activation of kinase systems as well as mitogen-activated protein kinases or protein kinase B/Akt (Kirschner 2002). Recently, in several tumoral cells the presence of a cross-talk has been reported between the IGF system and estrogens, which is able to activate the same pathway through the action of estrogen receptors (ERs; Hamelers & Steenbergh 2003).

It has been largely demonstrated that the effects of estrogens on target tissues are mediated by the ERα and ERβ, which act as transcription factors

DOI: 10.1677/jme.1.01806

Online version via http://www.endocrinology-journals.org

(Nilsson *et al.* 2001). In the human fetal adrenal gland the mRNA of ERβ was much more expressed than that of ERα and the ERβ protein was detected in the definitive zone of the adrenal cortex (Takeyama *et al.* 2001). The highly estrogenic environment during pregnancy has been reported to influence steroidogenesis of the primate fetal gland (Hirst *et al.* 1992, Albrecht *et al.* 1999) and it has been suggested that the effects of estrogens via ERβ may play an important role in modulating the development of both human and primate fetal adrenal glands (Albrecht *et al.* 1999, Takeyama *et al.* 2001). However, it remains to be elucidated whether estrogens can influence adrenocortical growth and function in the adult, and even tumorigenesis like that observed in other hormone-dependent tissues (Gao *et al.* 2002). A possible involvement of estrogens in adrenocortical tumor development is suggested by epidemiological and experimental studies. Adrenal tumors, and especially functioning tumors, are more frequently found in women than in men (Barzon *et al.* 2003). Moreover, adrenocortical cancers show a different distribution among genders, with functioning tumors, which represent about half of adrenocortical carcinomas, significantly more frequent in females, and non-functioning carcinomas more frequent in males. Interestingly, a case-control study demonstrated that use of estro-progestins was a risk-factor for the development of adrenocortical carcinomas (Hsing *et al.* 1996). Moreover, a recent study on H295R cells (Somjen *et al.* 2003) has shown that these cells are sensitive to low doses of estrogens in terms of proliferation and that they express mRNA of both ER isoforms.

In the present study, using the H295R cell as a model system, we investigated the involvement of estrogen and ERs in the growth regulation of adrenocortical carcinoma. We have demonstrated that H295R cells are able to transform androgens to estrogens that activate an autocrine mechanism, mediated by their own receptors, and contribute to the regulation of proliferation of these cells. Moreover, for the first time we have revealed that in H295R cells antiestrogens such as 4-hydroxytamoxifen (OHT) and ICI 182,780 (ICI) exert relevant growth-inhibitory effects through different pathways. For instance, OHT induces apoptosis in H295R cells, up-regulating the expression of FasL and determining the autocrine activation of caspases.

Materials and methods

Reagents

Forskolin (FSK), 17β-estradiol (E_2) and OHT were purchased from Sigma (St Louis, MO, USA), ICI was a gift from Astra-Zeneca (Italy) and Letrozole was a gift from Novartis Pharma AG (Basel, Switzerland). All these reagents were dissolved in dimethylsulfoxide (DMSO).

Cell cultures

H295R cells, a cell line established from a human adrenocortical carcinoma, was obtained from Dr W E Rainey (University of Texas Southwestern Medical Center, Dallas, TX, USA) and cultured in Dulbecco's modified Eagle's medium/Ham's F12 (DMEM/F12; 1:1; Eurobio, Les Ulis, France) supplemented with 1% ITS Liquid Media Supplement (100×; Sigma), 10% calf serum and antibiotics (Eurobio), at 37 °C in an atmosphere of humidified air containing 5% CO_2. MCF-7 breast cancer cells were incubated in the same conditions but maintained in DMEM/F12 supplemented with 10% calf serum.

Plasmids and *in vitro* transcription/translation

The coding regions of ERα and ERβ were excised from their vector and subcloned into the pcDNA3·1 zeo(+) expression plasmid (Invitrogen, Carlsbad, CA, USA). 1 μg each plasmid was used for *in vitro* transcription/translation using T7 RNA polymerase in the rabbit reticulocyte system following manufacturer's protocol for the TNT kit (Promega, Madison, WI, USA) in a final volume of 50 μl.

Aromatase activity assay

The aromatase activity in subconfluent H295R cell culture medium was measured by tritiated water-release assay using 0·5 μM [1β-^{3}H(N)]androst-4-ene-3,17-dione (25·3 Ci/mmol; DuPont NEN, Boston, MA, USA) as a substrate (Lephart & Simpson 1991). Incubations were performed at 37 °C for 2 h under a 95%:5% air/CO_2 atmosphere. The results obtained were expressed as pmol/h and normalized to milligram of protein (pmol/h per mg protein).

Estradiol measurement

Subconfluent H295R cells, seeded in 12-well/plates at the concentration of 5×10^5 cells/well, were washed twice with PBS and grown in medium without serum. After 24 h, cells were washed again with PBS and grown in 0·5 ml/well fresh medium without serum for 48 and 72 h. The experiment was performed three times in sextuplicate. Total E_2 was measured in the supernatant of H295R cells by competitive immunoassays on ADVIA Centaur (Bayer Diagnostics, Tarrytown, NY, USA).

RNA isolation and reverse transcriptase (RT)-PCR

Total cellular RNA was extracted from H295R cells with Trizol reagent (Invitrogen, Life Technologies, San Giuliano Milanese, Italy) according to the protocol provided by the manufacturer. All the RNA was

DNase-treated using the DNA-free™ kit (Ambion, Austin, TX, USA), and purity and integrity of the RNA was checked spectroscopically and by gel electrophoresis before carrying out the analytical procedures. The evaluation of gene expression was performed by semiquantitative RT-PCR (Maggiolini *et al.* 1999). For cytochrome P450 aromatase (henceforth called P450 aromatase), ERβ and internal control gene 36B4 the primers were 5′-CTGGAAGAATGTATGGACTT-3′ (P450 aromatase forward), 5′-GATCATTTCCAGCAT GTTTT-3′ (P450 aromatase reverse), 5′-CAGCATTC CCAGCAATGTCAC-3′ (ERβ forward), 5′-GCAGAA GTGAGCATCCCTCTTTG-3′ (ERβ reverse), 5′-CTC AACATCTCCCCCTTCTC-3′ (36B4 forward) and 5′-CAAATCCCATATCCTCGTCC-3′ (36B4 reverse), to yield products of 660, 281 and 408 bp, respectively, with 30, 20 and 15 PCR cycles of 1 min at 95 °C for all genes, 1 min at 64 °C for P450 aromatase, 1 min at 58 °C for ERβ and 1 min at 57 °C for 36B4, followed by 1 min at 72 °C for all genes.

Western-blot analysis

Total cell protein extracts from H295R and MCF-7 cells were lysed in ice-cold Ripa buffer containing protease inhibitors (20 mM Tris, 150 mM NaCl, 1% Igepal, 0·5% sodium deoxycholate, 1 mM EDTA, 0·1% SDS, 1 mM PMSF, 0·15 units/ml aprotinin and 10 μM leupeptin). Nuclear extracts were prepared from H295R and MCF-7 as previously described (Andrews & Faller 1991). Briefly, cells plated onto 60 mm^2 dishes were scraped into 1·5 ml cold PBS. Cells were pelleted for 10 s and resuspended in 400 μl cold buffer A, containing protease inhibitors, 10 mM Hepes, pH 7·9, 1·5 mM $MgCl_2$, 10 mM KCl, 0·5 mM dithiothreitol, 0·2 mM PMSF, 10 μM leupeptin and 0·15 units/ml aprotinin, by flicking the tube. The cells were allowed to swell on ice for 10 min and then vortexed for 10 s. Samples were centrifuged for 10 s and the supernatant fraction discarded. The pellet was resuspended in 50 μl cold buffer C (20 mM Hepes, pH 7·9, 25% glycerol, 1·5 mM $MgCl_2$, 420 mM NaCl, 0·2 mM EDTA, 0·5 mM dithiothreitol, 0·2 mM PMSF, 10 μM leupeptin and 0·15 units/ml aprotinin) and incubated on ice for 20 min for high-salt extraction. Cellular debris was removed by centrifugation for 2 min at 4 °C and the supernatant fraction (containing DNA-binding proteins) was stored at −70 °C. The yield was determined by Bradford method (Bradford 1976). The proteins were separated on 11% SDS/polyacrylamide gel and then electroblotted onto a nitrocellulose membrane. The blots were incubated overnight at 4 °C with (1) mouse anti-(human P450 aromatase) antibody, raised against a conserved epitope within P450 aromatase (1:1000; Serotec, Oxford, UK), (2) anti-ERβ antibody against the C-terminal region of the ERβ (1:500; Serotec), (3) anti-ERα (F-10) antibody against the N-terminal region of the ERα (1:1000; Santa Cruz Biotechnology, Santa Cruz, CA, USA), (4) anti-caspase-8 1C12 monoclonal antibody (1:1000; Cell Signaling Technology, Celbio, Milan, Italy), (5) anti-caspase-3 antibody (1:1000; Cell Signaling Technology), (6) anti-Fas (FL-335) antibody (1:1000; Santa Cruz Biotechnology) and (7) anti-FasL antibody (1:1000; DB Transduction Laboratories, Lexington, KY, USA). The antigen–antibody complexes were detected by incubation of the membranes at room temperature with goat anti-mouse IgG coupled to peroxidase, developed using the ECL Plus Western-blotting detection system (Amersham Biosciences, Cologno Monzese, Italy). As a loading control, membranes were stripped and reprobed with β-actin antiserum.

Cell-proliferation assay

A total of 1×10^6 cells were seeded onto six-well plates in complete medium, for proliferative analysis. After 3 days the medium was replaced with DMEM lacking Phenol Red as well as serum and ITS Liquid Media Supplement and treated with different concentrations of E_2, ICI 182 780 and OHT alone or in combination for 96 h. Control cells were treated with the same amount of vehicle alone (DMSO) that never exceeded the concentration of 0·01% (v/v).

[^{3}H]Thymidine incorporation was evaluated after a 24-h incubation period with 1 μCi [^{3}H]thymidine (PerkinElmer Life Sciences, Boston, MA, USA) per well. Cells were washed once with 10% trichloroacetic acid, twice with 5% trichloroacetic acid and lysed in 1 ml 0·1 M NaOH at 37 °C for 30 min. The total suspension was added to 10 ml optifluor fluid and was counted in a scintillation counter.

Staining for apoptosis detection

The apoptotic cells were stained using Hoechst 33342 staining (Sigma). H295R cells, plated on chamber slides, were fixed with 4% paraformaldehyde and stained with Hoechst 33342 dye to a final concentration of 5 μg/ml (150 μM) for 20 min at room temperature. Following washing with PBS, the cells were observed under an Olympus BX51 fluorescence microscope.

Chromatin immunoprecipitation (ChIP)

This assay was performed using the ChIP assay kit from Upstate Biotechnology (Lake Placid, NY, USA; http://www.nature.com/cgi-taf/DynaPage.taf?file=/onc/journal/v23/n45/full/1208014a.html-bib23#bib23) with minor modifications in the protocol. H295R cells were grown in 100 mm plates. Confluent cultures (90%) were treated for 24 h with 10 nM E_2, 10 μM OHT or 10 μM ICI. Control cells were treated with the same amount of

vehicle alone (DMSO) that never exceeded 0·01% (v/v). Following treatment DNA–protein complexes were cross-linked with 1% formaldehyde at 37 °C for 10 min. Next, cells were collected and resuspended in 400 µl SDS lysis buffer (Upstate Biotechnology) and left on ice for 10 min. Cells were sonicated four times for 10 s at 30% maximal power (Vibra Cell VCX 500; Sonics & Material, Inc. Newtown, CT, USA) and collected by centrifugation at 4 °C for 10 min at 11 000 ***g***. Of the supernatants 20 µl were kept as input (starting material, to normalize results) and 100 µl were diluted 1:10 in 900 µl ChIP dilution buffer (Upstate Biotechnology) and immunocleared with 80 µl sonicated salmon sperm DNA–Protein A agarose (Upstate Biotechnology) for 6 h at 4 °C. The precleared chromatin was immunoprecipitated overnight with 2 µg specific anti-ERβ antibody. The following day 60 µl salmon sperm DNA–Protein A agarose was added and precipitation was continued at 4 °C until the day after. After pelleting, precipitates were washed sequentially for 5 min with the following buffers: High Salt Immune Complex Wash Buffer, Low Salt Immune Complex Wash Buffer, LiCl Immune Complex Wash Buffer and then twice with TE buffer (all buffers are contained in the kit). The immune complexes were eluted with elution buffer (1% SDS and 0·1 M $NaHCO_3$). The eluates and the 20 µl input were reverse cross-linked by heating at 65 °C overnight and digested with proteinase K (0·5 mg/ml) at 45 °C for 1 h. DNA was recovered by phenol/chloroform extractions. A 2 µl aliquot of 10 mg/ml yeast tRNA was added to each sample and DNA was precipitated with ethanol for 1 h at − 20 °C and then resuspended in 50 µl TE buffer. A 5 µl volume of each sample and 2 µl of input were used for PCR using the following FasL promoter primers (GenBank accession no. AF035584): sense, 5′-AAACTG AGGCAGGAGGATGT-3′, and antisense, 5′-TCG TAGTTAACTGCAGCCTC-3′. The PCR conditions were 1 min at 94 °C, 1 min at 55 °C and 2 min at 72 °C for 30 cycles. The amplification products of 200 bp were analyzed on a 1% agarose gel and visualized by ethidium bromide staining. In control samples, nonimmune rabbit IgG was used instead of the specific antibody.

Statistical analysis

Statistical analysis was performed using one-way ANOVA. Data were analyzed using software from STATPAC (Minneapolis, MN, USA).

Results

Estradiol production and aromatase activity in H295R cells

We initially examined whether H295R cells, used as a model system, were able to synthesize estrogens. H295R cells were cultured for 48 and 72 h in serum-free medium; E_2 content was measured with a competitive immuno assay and revealed a time-dependent increase. E_2 medium content was 512 ± 36 pg/ml at 48 and 834 ± 67 pg/ml at 72 h.

We next investigated the expression and the activity of P450 aromatase in the absence or presence of the adenylate cyclase activator FSK. A 24-h treatment with FSK significantly increased aromatase mRNA expression (Fig. 1A and B) and protein levels (Fig. 1C and D). This behavior was reproduced with aromatase activity, which was 7·43 ± 0·4 pmol/h per mg protein in basal conditions and increased to 23·28 ± 2·5 pmol/h per mg protein after incubating cells for 24 h with FSK. The presence of the aromatase inhibitor Letrozole, used 1 h before and during the incubation with the tritiated aromatase substrate, inhibited basal and, in particular, FSK-induced aromatase activity to 1·087 ± 0·1 pmol/h per mg protein (Fig. 1E).

Expression of ERα and ERβ in H295R cells

Since the effects of estrogens on target tissues are mediated by the estrogen receptors (ERα and ERβ), we next investigated the expression of these factors in H295R cells. We subcloned the ERα and ERβ genes into the expression vectors pcDNA3·1 zeo(+) and used these vectors for *in vitro* transcription, and the synthetized proteins were utilized as a standard curve for ERα and ERβ in Western-blot analysis. Standard points were obtained using increasing amounts of the synthetized proteins (0·5, 1, 3 and 6 µl). Densitometric analysis, reference band intesities to the curve where the standard point with the lowest concentration was taken as 100%, indicated that in H295R cells ERβ is significantly higher than ERα. We also used MCF-7 human breast cancer cells, a known ERα-positive cell type, as a control, and found as expected a high expression of the ERα isoform, whereas ERβ was barely detectable (Fig. 2). Based on these results we focused our attention on the role of ERβ in mediating estrogen signaling in this adrenal cancer cell line.

E_2 enhances while antiestrogens and the aromatase inhibitor Letrozole inhibit the proliferation of H295R cells

We then aimed to investigate the effects of E_2 on the proliferation of H295R cells assayed using thymidine incorporation. Treatment with different concentrations of E_2 (0·1–1000 nM) for 96 h exhibited a slight but significative increase of thymidine incorporation (Fig. 3A), while shorter exposures (24, 48 and 72 h) did not determine significant effects on DNA synthesis (data not shown). To demonstrate the involvement of ERs, we also investigated the effects of antiestrogens on H295R

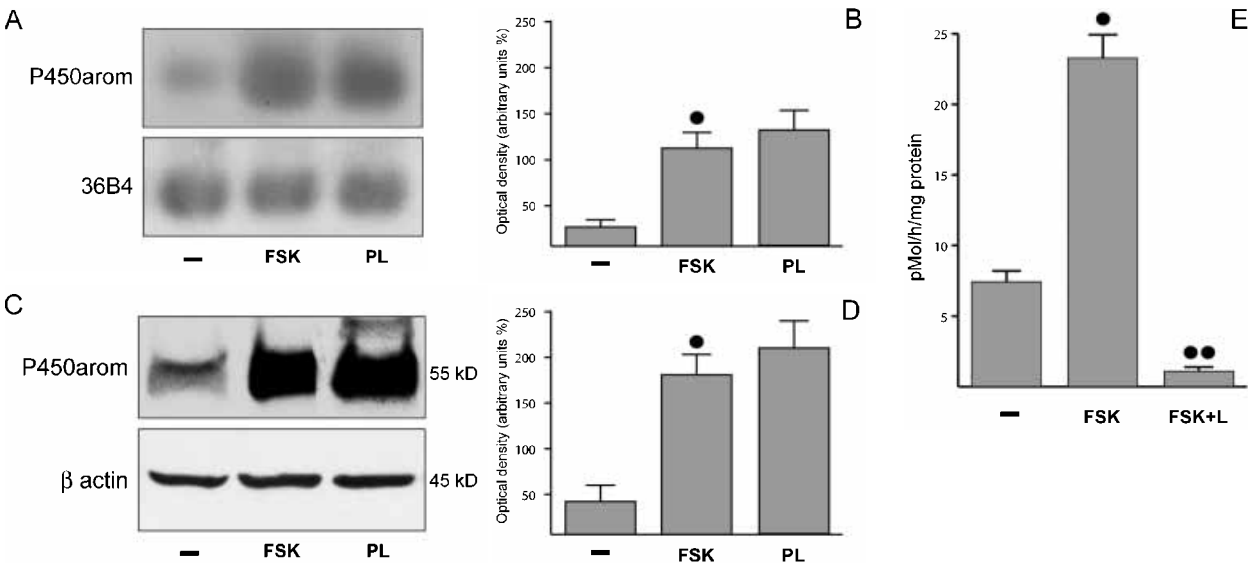

Figure 1 Effects of FSK on P450 aromatase expression and activity in cultured H295R cells. (A) P450 aromatase mRNA expression in H295R cells in the absence (–) or presence of FSK for 24 h was determined by semi-quantitative RT-PCR. Human placenta RNA (PL) was used as a positive control. 36B4 mRNA levels (lower panel) were also determined as a loading control. (B) Quantitative representation of data (means±S.E.M.) from three independent RT-PCR experiments after densitometry and correction for 36B4 expression. (C) Protein expression of P450 aromatase in H295R cells in the absence (–) or presence of FSK for 24 h. Whole-cell extracts (50 μg) were subjected to Western-blot analysis using anti-(human P450 aromatase) antibody (upper panel) and anti-actin antibody (lower panel) as a loading control. (D) Quantitative representation of data (means±S.E.M.) of three independent Western-blot experiments after densitometry and correction for β-actin expression. (E) Aromatase activity in H295R cells. The cells were cultured for 24 h in DMEM/F12 in the absence (–) or presence of FSK (25 μM), or FSK (25 μM) combined with Letrozole (4 μM; FSK+L). Aromatase activity was assessed using the modified tritiated water method. The results obtained were expressed as pmol [^{3}H]water released per h and were normalized for mg protein (pmol/h per mg protein). Values represent the means±S.E.M. from three different experiments, each performed with triplicate samples. ●, $P<0{\cdot}01$ compared with untreated cells (–); ●●, $P<0{\cdot}01$ compared with cells treated with FSK alone.

proliferation. Treatment with increasing amounts of ICI (0·1–10 μM) or OHT (0·1–10 μM) determined a dose-dependent inhibition of thymidine incorporation both under the basal conditions and in the presence of E_2 (10 nM) (Fig. 3B). To further confirm that H295R growth depends on estrogens we investigated the effect of aromatase inhibitor Letrozole on cell proliferation. As shown in Fig. 3C treatment with increasing amounts of Letrozole (1–10 μM) determined a dose-dependent inhibition of thymidine incorporation.

Antiestrogens modulate ERβ expression

The above results prompted us to evaluate whether ERβ expression can be modulated by E_2 and/or antiestrogens such as ICI and OHT. Performing a semiquantitative RT-PCR we observed that a 24-h exposure to ICI or OHT was clearly able to up-regulate the mRNA levels of ERβ, which were not modified by E_2 (10 nM) treatment (Fig. 4A and B). In fact, E_2 dose-response (0·1–1000 nM) or time-course (12, 24 and 48 h) experiments did not reveal any significant differences with respect to controls (data not shown). Besides, Western-blot analysis revealed an increase in ERβ protein levels after a 96-h exposure to antiestrogens (Fig. 4C and D), which paralleled the evaluation of cell proliferation.

Antiestrogens up-regulate FasL protein expression and induce activation of caspase pathway in H295R cells

Microscopic observation of H295R cells treated with 10 μM OHT and stained with Hoechst 33342 showed morphological changes characteristic of apoptosis after only 24 h (Fig. 5). These changes were not observed in cells treated with estradiol or ICI (data not shown).

These results led us to ascertain the involvement of the Fas/FasL pathway in the OHT-promoted apoptosis of H295R cells. Fas protein was expressed but not modulated by E_2, ICI or OHT in H295R cells (Fig. 6A and D), however the expression of FasL was up-regulated only by OHT (Fig. 6B and E). The autocrine mechanism of apoptosis in H295R cells by the Fas/FasL system was further supported by the expression of the active forms of caspase-8 (p43/45 and p28) and caspase-3 (p20 and p17) induced only by OHT treatment (Fig. 7).

ERβ binds the activating protein (AP)-1 site on the FasL promoter

Since for several ER-dependent genes transcription has been shown to be regulated through ER binding to the AP-1 complex, we used chromatin immunoprecipitation analysis to show ERβ binding to the AP-1 site on the FasL promoter in H295R cells. Samples were immunoprecipitated with the ERβ antibody and the FasL promoter region containing the AP-1 site was amplified with specific primers. The results obtained show that ERβ is able to interact with the protein complex bound to the AP-1 site in basal conditions and that this binding is maintained in treated cells (Fig. 8). Bands are specific as shown by the lack of amplification in samples immunoprecipitated with nonimmune rabbit IgG.

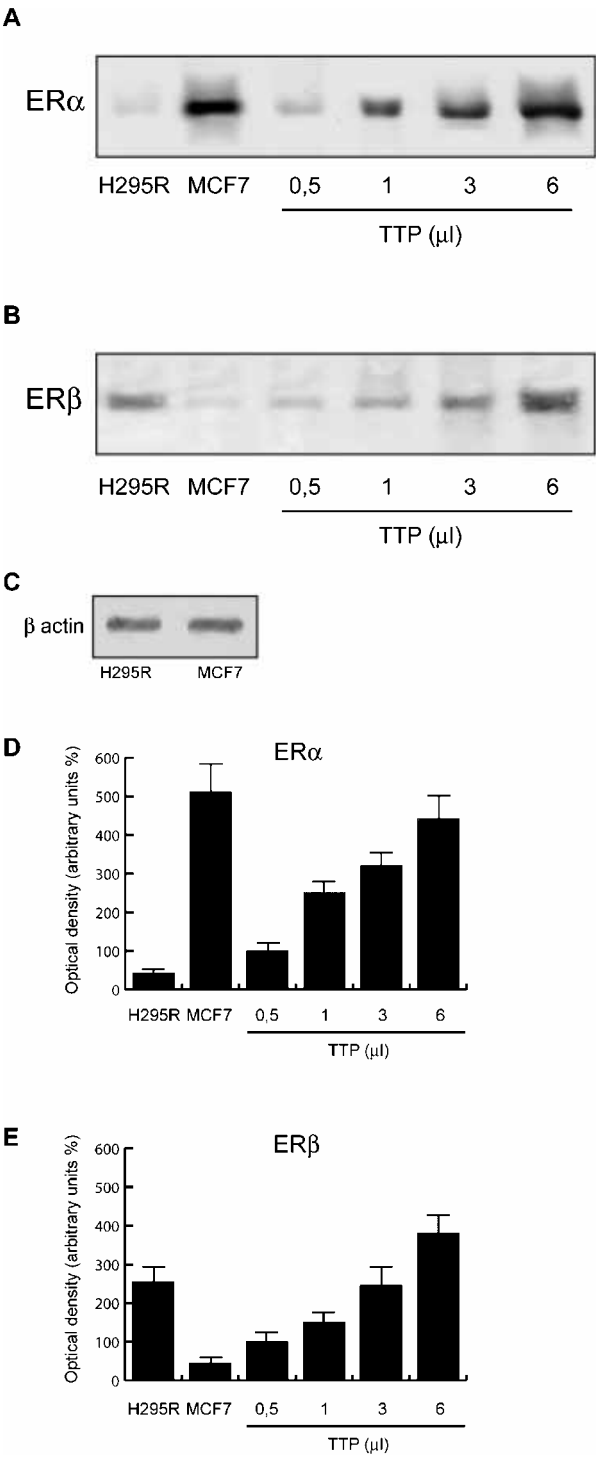

Discussion

In the present study we have shown that H295R adrenocortical carcinoma cells are able to convert androgens to estrogens, which, through a short autocrine loop, mediated by their own receptors, contribute to enhance H295R cell proliferation. Furthermore, both antiestrogens ICI and OHT up-regulate ERβ expression and dose-dependently inhibit basal and E_2-induced H295R cell proliferation by activating different pathways. In fact, whereas ICI determines the growth arrest of H295R cells, OHT treatment activates the Fas/FasL pathway which in turn induces apoptosis.

Androgens and estrogens determine various biological activities on mammalian tissues controlling cellular growth and differentiation through different signal transduction pathways. Previous studies have demonstrated that androgens inhibit H295R cell proliferation through the androgen receptor (Rossi *et al.* 1998), whereas the role of estrogens and ERs in both normal adult and malignant adrenocortical cells remains to be elucidated. Our results give a functional emphasis to recent studies which revealed that the H295R cell line is able to transform androgens into estrogens (Watanabe & Nakaijn 2004) and express ERα and ERβ mRNA (Somjen *et al.* 2003). We demonstrated that high levels of basal aromatase activity are present in H295R cells, allowing these cells to produce E_2. Moreover, H295R cells also express both ER protein isoforms, with a

Figure 2 Expression of ERα and ERβ in H295R cells. Western-blot analysis was performed on total proteins from H295R or MCF-7 cells (50 μg) and on *in vitro*-transcribed and -translated protein (TTP) ERα and ERβ; (synthesized as described in the Materials and methods section) utilized as a standard curve at the indicated volumes. Anti-ERα (F10) (A), anti-ERβ (B) and anti-β actin (C) antibodies were used. These results are representative of those obtained in three independent experiments. (D and E) Quantitative represention of data (means±S.E.M.) from three independent Western-blot experiments performed after densitometry and correction for β-actin expression. For densitometric analysis, standard point with the lowest concentration was taken as 100% and band intesities were referred to the curve.

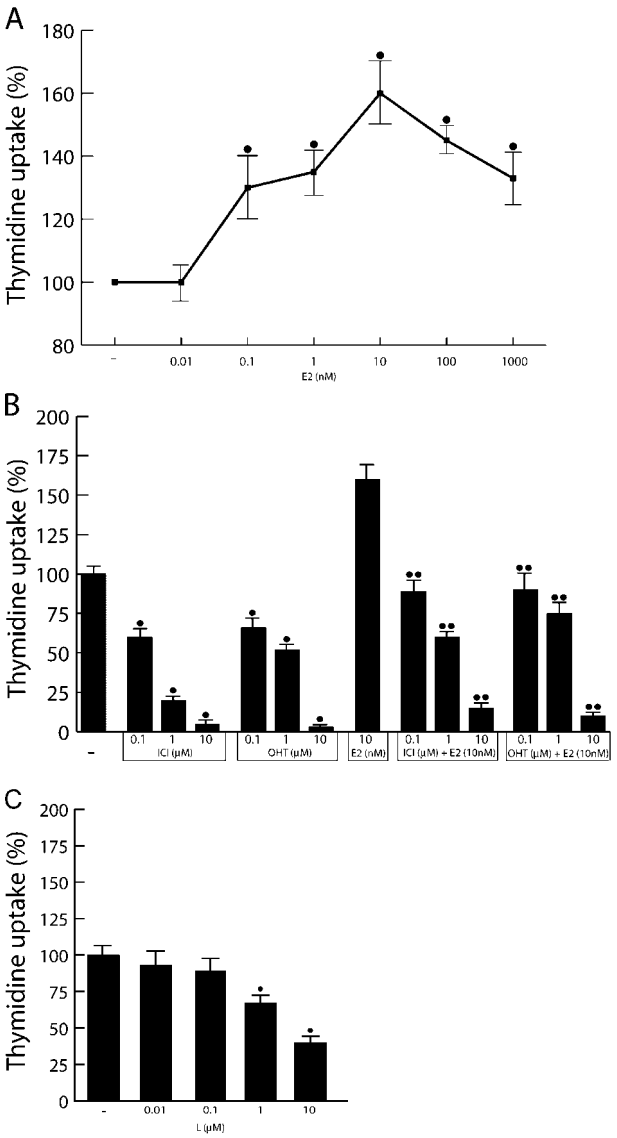

Figure 3 Proliferative analysis in H295R cells. Proliferation was evaluated by [^{3}H]thymidine incorporation analysis. (A) H295R cells were cultured for 96 h in DMEM in the absence or presence of E_2 at the indicated concentrations. (B) H295R cells were cultured for 96 h in DMEM in the absence or presence of E_2, ICI, OHT, E_2+ICI or E_2+OHT at the indicated concentrations. Control cells were treated with the same amount of vehicle alone (DMSO) that never exceeded 0·01% (v/v). (C) H295R cells were cultured for 96 h in DMEM in the absence or presence of Letrozole (L) at the indicated concentrations. Values expressed as percentages of untreated cells (100%); means±S.E.M. from three independent experiments each performed with triplicate samples. ●, $P<0·01$ compared with untreated cells (–); ●●, $P<0·01$ compared with E_2-treated cells (E_2).

prevalence of ERβ, thus reproducing the same ER ratio present in the fetal adrenal gland (Takeyama *et al.* 2001). The exposure to a physiological concentration of E_2 determined a slight but significant increase of thymidine incorporation, confirming the results of a previous study (Somjen *et al.* 2003) and revealing the presence of an autocrine mechanism which could contribute to H295R cell proliferation. The observation that both antiestrogens and the aromatase inhibitor Letrozole determined a dose-dependent arrest of these proliferative effects supports this hypothesis. However, only OHT was responsible for the morphological changes associated with apoptosis as observed in previous studies performed on MCF-7 breast cancer cells using tamoxifen and its analogs (Bardon *et al.* 1987, Warri *et al.* 1993, Wilson *et al.* 1995). On the contrary, apoptotic events were shown to be induced also by ICI in ER-positive primary breast cancer cells (Ellis *et al.* 1997). Moreover a study performed on six malignant rhabdoid tumor cell lines revealed that OHT but not ICI induced apoptosis (Koshida *et al.* 2002). To explain these apparently controversial data we have to take into account that the pharmacological potency elicited by antiestrogens is dependent on the cellular context as well as on the interaction of these molecules with the two different ER isoforms. This hypothesis is supported by studies which have shown that ER agonists and antagonists are able to induce distinct conformations and biological activity of both ER isoforms (Van Den Bemd *et al.* 1999). A study using a fingerprint assay clearly indicates that OHT determines, for both ERα and ERβ, the exposure of unique peptide-binding surfaces that are not exposed in the presence of ICI (Paige *et al.* 1999). So, different ER–ligand complexes may be able to recruit different coactivator and corepressor proteins within the cell, and the overall biological response is determined by unique combinations of protein–protein interactions that occur in a given cell and promoter context (Jones *et al.* 1999). The present study contributes to the understanding of the biological activity of OHT and ICI, extending to adrenocortical cancer cells the different response to antiestrogens.

We ascertained that the antiestrogens OHT and ICI were able to induce the up-regulation of ERβ, whereas E_2 did not show any change in our experimental conditions. What is the molecular mechanism by which antiestrogens can enhance ERβ expression and what is the biological counterpart of this response? It is worth noting that Paech *et al.* (1997) reported an antiestrogen-dependent transcriptional activity of ERβ at AP-1 sites which were demonstrated to be located within the promoter region of ERβ gene (Li *et al.* 2000). In line with these findings, our data may provide new insight on ERβ autologous regulation by antiestrogens as displayed even in H295R cells. Moreover, could this up-regulation of ERβ mediate the above reported down-regulatory effects of ICI and OHT on H295R cell proliferation? This question opens an additional intriguing area of research that we are investigating currently.

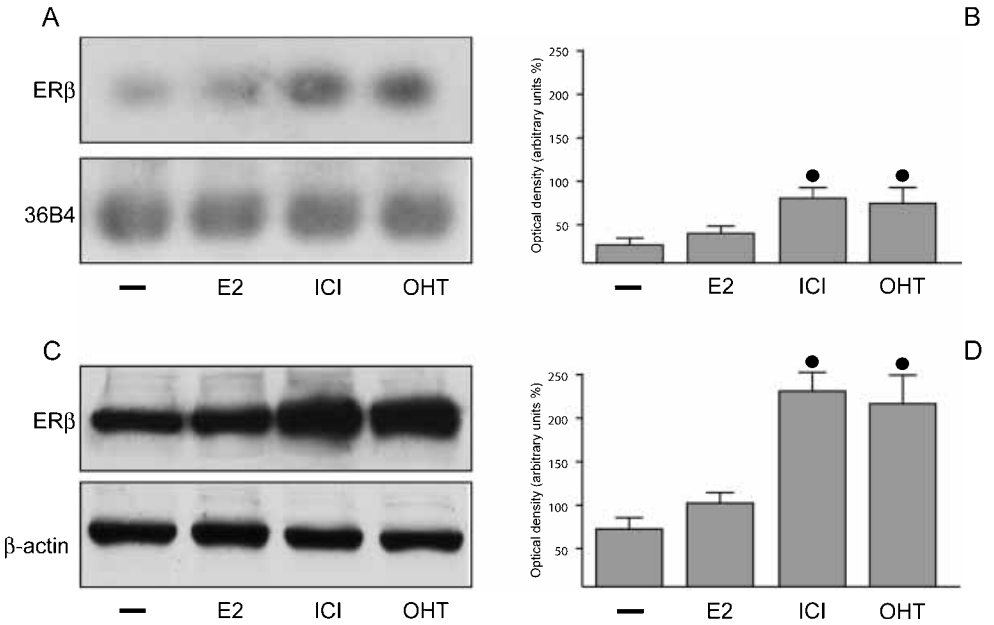

Figure 4 Effects of antiestrogens on ERβ expression in H295R cells. (A) ERβ mRNA expression in H295R cells in the absence (–) or presence of E_2 (10 nM), ICI (10 μM) or OHT (10μM) for 24 h was determined by semi-quantitative RT-PCR (upper panel). 36B4 mRNA levels (lower panel) were used as a loading control. (B) Quantitative representation of data (means±S.E.M.) from three independent RT-PCR experiments after densitometry and correction for 36B4 expression. (C) ERβ protein expression in H295R cells in the absence or presence of E_2 (10 nM), ICI (10 μM) or OHT (10 μM) for 96 h was determined by Western blotting (upper panel); β-actin was also used as a loading control (lower panel). (D) Quantitative representation of data (means±S.E.M.) of three independent Western-blot experiments after densitometry and correction for β-actin expression. ●, $P<0{\cdot}01$ compared with untreated cells (–).

In H295R cells we also observed that ICI determined a dose-dependent inhibition of proliferation. This cytostatic effect could be explained by the inhibitory effects exerted by ICI on the IGF signaling pathway, which is activated strongly in H295R cells by the autocrine action of IGF-II through the type 1 IGF receptor (IGF-1R; Logié *et al.* 1999). In fact, in mammary tissue it has been demonstrated that the effect of estrogen on cell growth is mediated by the up-regulation of IGF-1R (Stewart *et al.* 1990), insulin receptor substrate (IRS)-1 and IRS-2 (Lee *et al.* 1999) expression and/or by the down-regulation of the inhibitory IGF-binding protein 3 (IGFBP-3; Huynh *et al.* 1996), while ICI reduced basal phosphorylation of IGF-1R, IRS-1, IRS-2, Akt-1 and the p85 subunit of phosphoinositide 3-kinase (Chan *et al.* 2001). These observations indicate that inhibition of cell growth by ICI may not only be attributable to competition between estrogens and ICI for ER but also to the interruption of the IGF signaling pathway. By doing so, ICI may also block a possible cross-talk between the ER and IGF-1R signaling pathways (Dupont *et al.* 2000). The molecular mechanism determining the cytostatic effect of ICI on H295R cells is currently under investigation, but preliminary results seem to confirm this hypothesis.

Interestingly, we demonstrated the involvement of the Fas/FasL system as a signal transduction pathway mediating the OHT-induced apoptosis. FasL is a membrane protein belonging to the tumor necrosis factor family (Suda *et al.* 1993), which is able to induce apoptosis by cross-linking with the Fas receptor (Takahashi *et al.* 1994). FasL is normally expressed on activated cells of the immune system and is used for killing cells infected with viruses or cancer cells expressing Fas (Suda *et al.* 1993). It has also been demonstrated that tumor cells can express FasL by which they kill Fas-positive immune cells evading the immune system (Walker *et al.* 1997, Nagarkatti 2000). Recently, it has been described that, in certain Fas-positive tumor cells, OHT induces apoptotic effects by up-regulating FasL (Nagarkatti & Davis 2003). Our study recalls these observations since we have shown that H295R cells are Fas-positive and that OHT is able to increase the expression of FasL which may activate pro-apoptotic events. This autocrine mechanism is further substantiated by the cleavage of caspase-8 and caspase-3 observed upon OHT treatment. Notably,

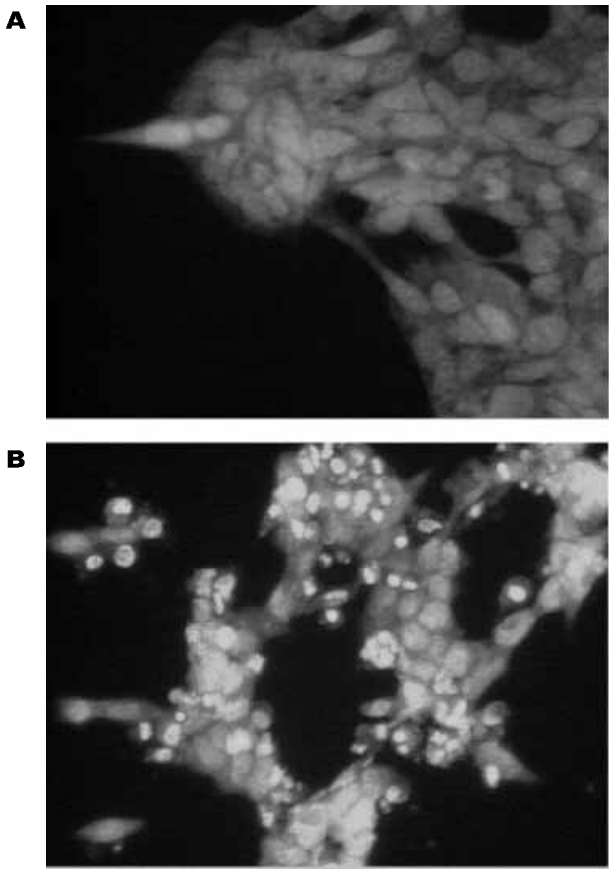

Figure 5 Induction of apoptosis in H295R cells by OHT. H295 cells were cultured for 24 h in the absence (A) or presence (B) of 10 μM OHT. Control cells were treated with the same amount of vehicle alone (DMSO) that never exceeded 0·01% (v/v). The cells were stained subsequently with Hoechst 33342. These results are representative of those obtained in three independent experiments.

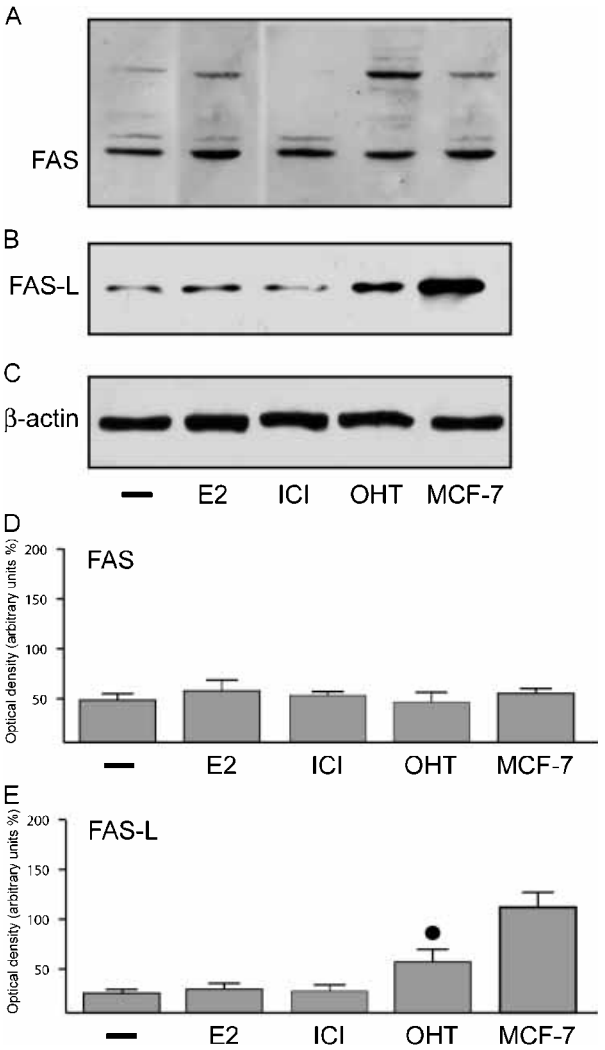

Figure 6 Expression of Fas and FasL in H295R cells. Western blots of Fas (A) and FasL (B) on H295R whole-cell extracts (50 μg) after 24 h of treatment with E_2 (10 nM), ICI (10 μM) or OHT (10 μM). (C) β-Actin was used as a loading control. (D) Quantitative representation of data (means±S.E.M.) from three independent Western-blot experiments using antibody anti-Fas after densitometry and correction for β-actin expression. (E) Quantitative representation of data (means±S.E.M.) from three independent Western-blot experiments using antibody anti-FasL after densitometry and correction for β-actin expression. MCF-7 whole cell extracts were used as positive controls. ●, $P<0·01$ compared with untreated cells (–).

these phenomena could be consequent to the interaction of the ERβ–OHT complex with the promoter of FasL, which contains a complete AP-1 sequence (Mor *et al.* 2000), while in our cellular context the ERβ–ICI complex seems to be unable to activate FasL transcription.

A previous study (Mor *et al.* 2000) reported that OHT inhibits the expression of FasL in MCF-7 and in T47D breast tumor cells through ERα. In contrast, other authors showed that OHT is able to up-regulate FasL in T47D cells (Nagarkatti & Davis 2003), depending on the concentrations of treatments and culture conditions. A role for ERβ in the regulation of FasL has been hypothesized by a study on neuronal cells demonstrating that ERβ mediates apoptosis induction in cells expressing Fas/FasL proteins, while ERα has antiapoptotic and neuroprotective effects (Nilsen *et al.* 2000). Mechanisms controlling the activation of ER-dependent genes through AP-1 sites are not completely clear. ERβ shows a unique capacity to enhance AP-1 activity in response to selective antiestrogens (Paech *et al.* 1997, Weatherman & Scanlan 2001); this is due to ERβ interactions with corepressors, as such interactions are inhibited by antiestrogens and increased by agonists (Webb *et al.* 2003, Uht *et al.* 2004). Our data show that ERβ is able to interact with the proteins bound to the

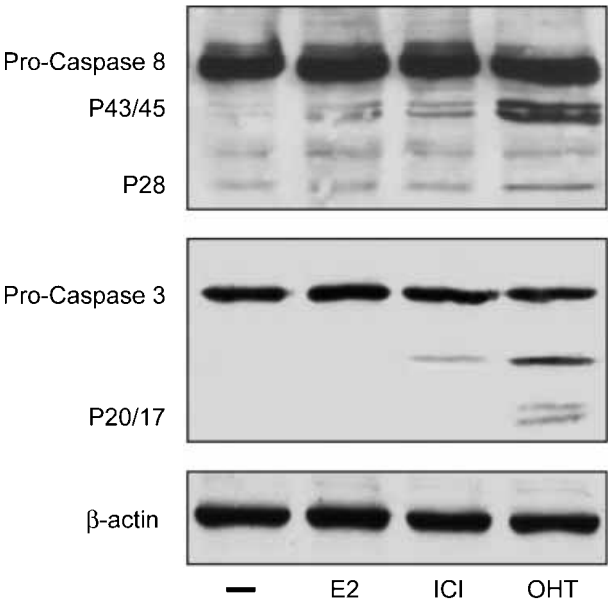

Figure 7 OHT induces caspase-8 and caspase-3 activation in H295R cells. The effect of E_2 (10 nM), ICI (10 μM) or OHT (10 μM) on caspase-8 and caspase-3 activation was evaluated by Western-blot analysis. Active forms of caspase-8 (p43/45 and p28; upper panel) and caspase-3 (p20 and p17; middle panel) were revealed only after OHT treatment for 24 h; β-actin was used as a loading control (lower panel). These results are representative of those obtained in three independent experiments.

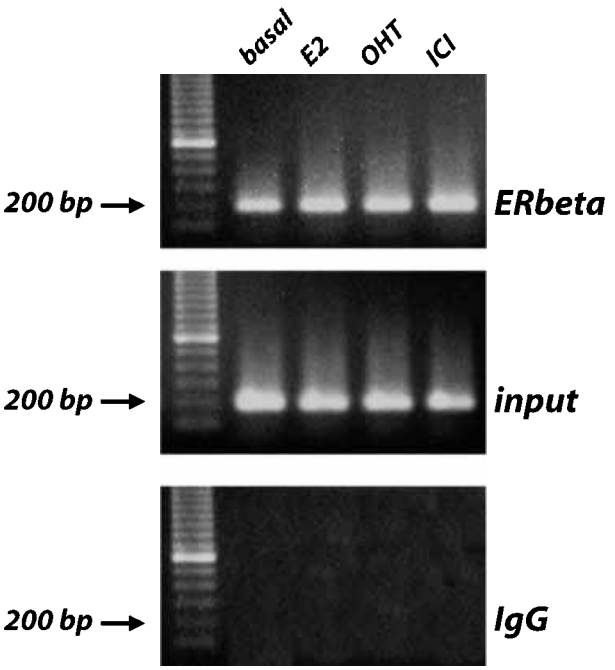

Figure 8 ERβ is recruited to the FasL promoter. H295R cells were incubated for 24 h with E2 (10 nM), OHT (10 μM) or ICI (10 μM). Control cells were treated with the same amount of vehicle alone (DMSO) that never exceeded 0·01% (v/v). *In vivo* binding of ERβ to the FasL promoter was examined using ChIP assay. Immunoprecipitated (ERβ, IgG) and total (10% input) DNA were subject to PCR using specific primers. These results are representative of those obtained in three independent experiments.

AP-1 complex on human FasL promoter and confirm that transcriptional activity does not depend only on ERβ binding to the promoter but instead depends on ERβ's ability to recruit specific cofactors. In our cellular context, the interaction between ERβ and OHT may be able to recruit corepressors bound to the AP-1 complex determining the activation of FasL expression that in turn promotes apoptosis. Nevertheless we cannot exclude that high doses of OHT are also able to induce apoptosis involving other factors such as p53 or c-Myc in a direct manner (Mandlekar & Kong 2001). Whatever the mechanism involved, what clearly emerges from this study is that the H295R adrenocortical cancer cell line exhibits estrogen-sensitive proliferation which can be inhibited by exposure to antiestrogens ICI and OHT or the aromatase inhibitor Letrozole. The present findings and our preliminary observations (Barzon *et al.*, unpublished observations), which clearly reveal (by real-time PCR and western-blot analysis) the expression of ERβ in human adrenocortical carcinoma tissues, open new perspectives on the potential therapeutic benefits of antiestrogens as pharmacological agents in antagonizing adrenocortical carcinoma cell growth and progression. However, further studies are needed to clarify the role for ERβ as a possible mediator of adrenocortical cell proliferation.

Acknowledgements

We thank Astra-Zeneca Italia for providing us with ICI 182,780 and Novartis Pharma AG (Basel, Switzerland) for providing us with Letrozole. This work was supported by MIUR (ex 60%) (Italy). The authors declare that there is no conflict of interest that would prejudice the impartiality of this scientific work.

References

Albrecht ED, Babischkin JS, Davies WA, Leavitt MG & Pepe GJ 1999 Identification and developmental expression of the estrogen receptor alpha and beta in the baboon fetal adrenal gland. *Endocrinology* **140** 5953–5961.

Andrews NC & Faller DV 1991 A rapid micropreparation technique for extraction of DNA-binding proteins from limiting numbers of mammalian cells. *Nucleic Acids Research* **19** 2499.

Bardon S, Vignon F, Montcourrier P & Rochefort H 1987 Steroid receptor-mediated cytotoxicity of an antiestrogen and an antiprogestin in breast cancer cells. *Cancer Research* **47** 1441–1448.

Barzon L, Chilosi M, Fallo F, Martignoni G, Montagna L, Palu G & Boscaro M 2001 Molecular analysis of CDKN1C and TP53 in sporadic adrenal tumors. *European Journal of Endocrinology* **145** 207–212.

Barzon L, Sonino N, Fallo F, Palu G & Boscaro M 2003 Prevalence and natural history of adrenal incidentalomas. *European Journal of Endocrinology* **149** 273–285.

Bourcigaux N, Gaston V, Logié A, Bertagna X, Le Bouc Y & Gicquel C 2000 High expression of cyclin E and G1 CDK and loss of function of $p57^{KIP2}$ are involved in proliferation of malignant sporadic adrenocortical tumors. *Journal of Clinical Endocrinology and Metabolism* **85** 322–330.

Bradford MM 1976 A rapid and sensitive method for the quantitation of microgram quantities of protein utilizing the principle of protein-dye binding. *Analytical Biochemistry* **72** 248–254.

Chan TW, Pollak M & Huyunh H 2001 Inhibition of insulin-like growth factor signaling pathways in mammary gland by pure antiestrogen ICI 182,780. *Clinical Cancer Research* **7** 2545–2554.

Dupont J, Karas M & LeRoith D 2000 The potentiation of estrogen on insulin-like growth factor I action in MCF-7 human breast cancer cells includes cell cycle components. *Journal of Biological Chemistry* **275** 35893–35901.

Ellis PA, Saccani-Jotti G, Clarke R, Johnston SRD, Anderson E, Howell A, A'Hern R, Salter J, Detre S, Nicholson R *et al.* 1997 Induction of apoptosis by tamoxifen and ICI 182780 in primary breast cancer. *International Journal of Cancer* **72** 608–613.

Gao X, Loggie BW & Nawaz Z 2002 The roles of sex steroid receptor coregulators in cancer. *Molecular Cancer* **1** 7.

Gazdar AF, Oie HK, Shackleton CH, Chen TR, Triche TJ, Myers CE, Chrousos GP, Brennan MF, Stein CA & La Rocca RV 1990 Establishment and characterization of a human adrenocortical carcinoma cell line that expresses multiple pathways of steroid biosynthesis. *Cancer Research* **50** 5488–5496.

Gicquel C, Raffin-Sanson M, Gaston V, Bertagna X, Plouin P, Schlumberger M, Louvel A, Luton J & Le Bouc Y 1997 Structural and functional abnormalities at 11p15 are associated with the malignant phenotype in sporadic adrenocortical tumors. Study on a series of 82 tumors. *Journal of Clinical Endocrinology and Metabolism* **87** 2559–2565.

Hamelers IHL & Steenbergh PH 2003 Interactions between estrogen and insulin-like growth factor signaling pathways in human breast tumor cells. *Endocrine-related Cancer* **10** 331–345.

Hirst JJ, West NB, Brenner RM & Novy MJ 1992 Steroid hormone receptors in the adrenal glands of fetal and adult rhesus monkeys. *Journal of Clinical Endocrinology and Metabolism* **75** 308–314.

Hsing AW, Nam JM, Co Chien HT, McLaughlin JK & Fraumeni Jr JF 1996 Risk factors for adrenal cancer: an exploratory study. *International Journal of Cancer* **65** 432–436.

Huynh H, Yang X & Pollak M 1996 Estradiol and antiestrogens regulate a growth inhibitory insulin-like growth factor binding protein 3 autocrine loop in human breast cancer cells. *Journal of Biological Chemistry* **271** 1016–1021.

Jones PS, Parrott E & White IN 1999 Activation of trascription by estrogen receptor alpha and beta is cell type- and promoter-dependent. *Journal of Biological Chemistry* **274** 32008–32014.

Kirschner LS 2002 Signaling pathways in adrenocortical cancer. *Annals of the New York Academy of Sciences* **968** 222–239.

Koshida S, Narita Tsutomu, Kato H, Yoshida S, Taga T, Ohta S & Takeuchi Y 2002 Estrogen receptor expression and estrogen receptor-independent cytotoxic effects of tamoxifen on malignant rhabdoid tumor cells in vitro. *Japanese Journal of Cancer Research* **93** 1351–1357.

Lee AV, Jackson JG, Gooch JL, Hilsenbeck SG, Coronado-Heinsohn E, Osborne CK & Yee D 1999 Enhancement of insulin-like growth factor signaling in human breast cancer: estrogen regulation of insulin receptor substrate-1 expression *in vitro* and *in vivo*. *Molecular Endocrinology* **13** 787–796.

Lephart ED & Simpson ER 1991 Assay of aromatase activity. *Methods in Enzymology* **206** 477–483.

Li LC, Yeh CC, Nojima D & Dahiya R 2000 Cloning and caracterization of human estrogen receptor β promoter. *Biochemistry and Biophysics Research Communications* **275** 682–689.

Logié A, Boulle N, Gaston V, Perin L, Boudou P, Le Bouc Y & Gicquel C 1999 Autocrine role of IGF-II in proliferation of human adrenocortical carcinoma NCI H295R cell line. *Journal of Molecular Endocrinology* **23** 23–32.

Maggiolini M, Donzè O & Picard D 1999 A non-radioactive method for inexpensive quantitative RT-PCR. *Biological Chemistry* **380** 695–697.

Mandlekar S & Kong AN 2001 Mechanisms of tamoxifen-induced apoptosis. *Apoptosis* **6** 469–477.

Mor G, Kohen F, Garcia-Velasco J, Nilsen J, Brown W, Song J & Naftolin F 2000 Regulation of Fas ligand expression in breast cancer cells by estrogen: functional differences between estradiol and tamoxifen. *Journal of Steroid Biochemistry and Molecular Biology* **73** 185–194.

Nagarkatti N 2000 Tumor-derived FasL induces toxicity in lymphoid organs and plays an important role in successful chemotherapy. *Cancer Immunology and Immunotherapy* **49** 46–55.

Nagarkatti N & Davis BA 2003 Tamoxifen induces apoptosis in Fas+ tumor cells by upregulating the expression of Fas ligand. *Cancer Chemotherapy and Pharmacology* **51** 284–290.

Nilsen J, Mor G & Naftolin F 2000 Estrogen-regulated developmental neuronal apoptosis is determined by estrogen receptor subtype and the Fas/Fas ligand system. *Journal of Neurobiology* **43** 64–78.

Nilsson S, Makela S, Treuter E, Tujague M, Thomsen J, Andersson G, Enmark E, Pettersson K, Warner M & Gustafsson JA 2001 Mechanisms of estrogen action. *Physiology Reviews* **81** 1535–1565.

Paech K, Webb P, Kuiper GGJM, Nilsson S, Gustafsson JÅ, Kushner PJ & Scanlan TS 1997 Differential ligand activation of estrogen receptor ERα and ERβ at AP1 sites. *Science* **277** 1508–1510.

Paige LA, Christensen DJ, Gron H, Norris JD, Gottlin EB, Padilla KM, Chang CY, Ballas LM, Hamilton PT, McDonnell DP & Fowlkes DM 1999 Estrogen receptor (ER) modulators each induce distinct conformational changes in ER alpha and ER beta. *PNAS* **96** 3999–4004.

Rainey WE, Bird IM & Mason JI 1994 The NCI-H295 cell line: a pluripotent model for human adrenocortical studies. *Molecular and Cellular Endocrinology* **100** 45–50.

Rossi R, Zatelli MC, Valentini A, Cavazzini P, Fallo F, del Senno L & degli Uberti EC 1998 Evidence for androgen receptor gene expression and growth inhibitory effect of dihydrotestosterone on human adrenocortical cells. *Journal of Endocrinology* **159** 373–380.

Somjen D, Stern N, Knoll E, Sharon O, Gayer B, Kulik T & Kohen F 2003 Carboxy derivatives of isoflavones as affinity carriers for cytotoxic drug targeting in adrenocortical H295R carcinoma cells. *Journal of Endocrinology* **179** 395–403.

Stewart AJ, Johnson MD, May FE & Westley BR 1990 Role of insulin-like growth factors and the type I insulin-like growth factor receptor in the estrogen-stimulated proliferation of human breast cancer cells. *Journal of Biological Chemistry* **265** 21172–21178.

Suda T, Takahashi T, Golstein P & Nagata S 1993 Molecular cloning and expression of the Fas ligand, a novel member of the tumor necrosis factor family. *Cell* **75** 1169–1178.

Takahashi T, Tanaka M, Brannan CI, Jenkins NA, Copeland NG, Suda T & Nagata S 1994 Generalized lymphoproliferative disease in mice, caused by a point mutation in the Fas ligand. *Cell* **76** 969–976.

Takeyama J, Suzuki T, Inoue S, Kaneko C, Nagura H, Harada N & Sasano H 2001 Expression and cellular localization of estrogen receptors alpha and beta in the human fetus. *Journal of Clinical Endocrinology and Metabolism* **86** 2258–2262.

Uht RM, Webb P, Nguyen P, Price Jr RH, Valentine C, Favre H & Kushner PJ 2004 A conserved lysine in the estrogen receptor DNA binding domain regulates ligand activation profiles at AP-1 sites, possibly by controlling interactions with a modulating repressor. *Nuclear Receptor* **2** 2.

Van Den Bemd JG, Kuiper GG, Pols HA & Van Leeuwen JP 1999 Distinct effects on the conformation of estrogen receptor alpha and beta by both the antiestrogens ICI 164,384 and ICI 182,780 leading to opposite effects on receptor stability. *Biochemistry and Biophysics Research Communications* **261** 1–5.

Walker PR, Saas P & Dietrich PY 1997 Role of Fas ligand (CD95 L) in immune escape: the tumor cell strikes back. *Journal of Immunology* **158** 4521–4524.

Warri AM, Huovinen RL, Laine AM, Martikainen PM & Harkonen K 1993 Apoptosis in toremifene-induced growth inhibition of human breast cancer cells in vivo and in vitro. *Journal of the National Cancer Institute* **85** 1412–1418.

Watanabe M & Nakaijn S 2004 Forskolin up-regulates aromatase (CYP19) activity and gene transcripts in the human adrenocortical carcinoma cell line H295R. *Journal of Endocrinology* **180** 125–133.

Weatherman RV & Scanlan TS 2001 Unique protein determinants of the subtype-selective ligand responses of the estrogen receptors (ERalpha and ERbeta) at AP-1 sites. *Journal of Biological Chemistry* **276** 3827–3832.

Webb P, Valentine C, Nguyen P, Price Jr RH, Marimuthu A, West BL, Baxter JD & Kushner PJ 2003 ERbeta binds N-CoR in the presence of estrogens via an LXXLL-like motif in the N-CoR C-terminus. *Nuclear Receptor* **1** 4.

Weber MM, Fottner C & Wolf E 2000 The role of the insulin-like growth factor system in adrenocortical tumourigenesis. *European Journal of Clinical Investigation* **30** 69–75.

Wilson JW, Wakeling AE, Morris ID, Hickman JA & Dive C 1995 MCF-7 human mammary adenocarcinoma cell death in vitro in response to hormone-withdrawal and DNA damage. *International Journal of Cancer* **61** 502–508.

Received 25 May 2005
Accepted 14 June 2005
Made available online as an Accepted Preprint 23 June 2005

Submitted to Molecular and Cellular Biology, November 2006 manuscript # MCB03022-06

The AP-1 complex: a negative regulator of CYP17 transcription in adrenal cells

Rosa Sirianni[1], Mary H. Bassett[1], Bruce R. Carr[1], Takashi Suzuki[2], Vincenzo Pezzi[3], Sebastiano Andò[3] and William E. Rainey[4*]

[1]Department of Obstetrics & Gynecology, University of Texas Southwestern Medical Center, Dallas, Texas; [2]Departments of Pathology Tohoku University School of Medicine, Sendai, Japan; [3]Faculty of Pharmacy, Department of Cell Biology, University of Calabria, Arcavacata di Rende (CS) Italy; [4]Department of Physiology, Medical College of Georgia, Augusta, Georgia.

Running title: The AP-1 complex represses CYP17 transactivation.

***Corresponding author.**
Mailing address: Department of Physiology
Medical College of Georgia
1130 15th Street CA 3094
Augusta, GA 30912
Phone: 706-721 7665
Email: wrainey@mcg.edu

ABSTRACT

Steroid production by the adrenal zona glomerulosa is under the control of Angiotensin II (Ang II), which upon binding to its receptor activates protein kinase C (PKC) within the cell. PKC is a potent inhibitor of CYP17, an enzyme expressed in the zona fasciculata but absent from the zona glomerulosa. Herein we determined the molecular mechanism responsible for the inhibitory effect of PKC on CYP17 expression. We demonstrated that MAP kinases ERK-1 and -2 are downstream of PKC and that their activation was necessary for inhibition of CYP17. We also determined the genes most responsive to Ang II and TPA; which include members of the AP-1 family of transcription factors. Importantly Fos expression was limited to the zona glomerulosa and blocking fos expression eliminated PKC-mediated inhibition of CYP17. Dimers of Jun and Fos blocked SF-1 induced transcription of CYP17 and this inhibition was mediated through a direct interaction between SF-1 and Fos that prevented binding of cofactors necessary for SF-1 transcriptional activity. Collectively these results explain at least one of the molecular mechanisms responsible for zone-specific expression of CYP17 in the adrenal cortex.

INTRODUCTION

Each zone of the adrenal cortex is characterized by the production of specific steroids based on a distinct pattern of expression of specific steroid-metabolizing enzymes (39). In particular the zona glomerulosa produces mineralocorticoids, mainly aldosterone, whose levels are regulated primarily by Angiotensin II (Ang II) and potassium (8). The zona glomerulosa is characterized by high expression levels of aldosterone synthase (CYP11B2) and 3β-hydroxysteroid dehydrogenase type II (HSD3B2), and extremely low expression levels of 17α-hydroxylase 17,20-lyase (CYP17) (8). The absence of CYP17 in the zona glomerulosa is necessary for production of aldosterone

since this enzyme competes with HSD3B2 for substrate metabolism. On the other hand CYP17 transcript levels are high in the zona fasciculata and zona reticularis where expression of this enzyme is necessary for production of cortisol and adrenal androgens respectively. Presumably the zone-specific expression of CYP17 depends on *trans*-acting factors that are differentially expressed or regulated in the glomerulosa and fasciculata. These factors, which remain poorly defined, would interact with specific elements in the promoter of this gene either activating or repressing transcription.

Protein kinase C (PKC), which is part of a common pathway activated by many growth factors and by Ang II (31,50), has been shown to have a potent inhibitory effect on CYP17 mRNA expression (5,9,32,33,36) and enzymatic activity (42). Various isoforms of PKC are capable of directly activating a cascade of phosphorylation events that lead to the phosphorylation and thus activation of ERKs (10,11,50). Extracellular-Regulated Kinase-1 and -2 (ERK-1/2) are two members of the mitogenic-activated protein kinase (MAPK) family. ERK-1/2 have been shown to be activated by a variety of receptors including the G protein-coupled receptors (GPCRs). In particular it has been shown that Ang II is able to activate ERKs in smooth muscle cells (3), in bovine adrenals (12) and in H295R cells (53). It has recently been shown that silencing of ERK-1/2, using the inhibitor PD98059, increases CYP17 expression in the H295R adrenal cell model (46). Also, studies conducted on the rat adrenal showed that ERKs are localized in the zona glomerulosa and the medulla, but absent from the zonae fasciculata and reticularis (34). Once activated, ERK-1 and ERK-2 phosphorylate numerous substrates in all cellular compartments including various membrane proteins, cytoskeletal proteins and nuclear substrates such as SRC-1, Elk-1, MEF2, c-Myc, STAT3 and c-Fos (43).

c-Fos belongs to the activator protein-1 (AP-1) family of transcription factors. This family is composed of the Jun family members (Jun, JunB and JunD) and the Fos family members (Fos, FosB, Fra1 and Fra2) (15). Fos and Jun family proteins function as dimeric transcription factors that bind with the highest affinity to an asymmetric heptanucleotide recognition sequence TGA(C/G)TCA (AP-1 site) in the promoter of numerous mammalian genes (15). The Jun family members can form homo- and hetero-dimers among them and can also heterodimerize with the Fos family members, which do not homodimerize but instead require heterodimerization to bind DNA. Most AP-1 transcription factors are present at low levels in cells but are rapidly induced and activated in response to specific stimuli. Ang II has been shown to increase mRNA of c-fos, c-jun and junB in primary cultures of bovine and ovine adrenal cells (13,51).

Despite the intense effort to analyze the regulation and function of the jun and fos families in many different cell types, only a few studies have analyzed the regulation of these factors in the human adrenal and their involvement in regulation of steroidogenic enzyme expression. Based on the potential involvement of these factors in steroidogenesis we want to determine which AP-1 members are present and regulated by Ang II in adrenal cells, which pathway leads to their activation and if a specific AP-1 dimer is capable of blocking expression of CYP17. Herein, we tested the hypothesis that Ang II repression of CYP17 occurs through PKC and subsequent ERK-1/2 activation, leading to increase in expression of AP-1 members. If confirmed, this would explain, at least in part, the molecular mechanism for repressed CYP17 expression in the adrenal zona glomerulosa.

MATERIALS AND METHODS

Cell culture. NCI-H295R (H295R) cells were cultured in Dulbecco's modified Eagle's and Ham's F-12 (DMEM/F12) medium (GIBCO, BRL; Gaithersburg, MD), supplemented with 10%

cosmic calf serum (Hyclone, Logan, UT), and antibiotics. Cell monolayers were subcultured onto 100 mm culture dishes for nuclear extract preparation ($10x10^6$ cells/plate), 30 mm dishes for protein or RNA extraction ($4x10^6$ cells/plate) and 12 well culture dishes for steroid measurement and transfection experiments ($4x10^5$ cells/well) and used for experiments 48 h later.

Stimulation of steroid secretion and analysis of steroids. Prior to experiments, cells were maintained overnight in DMEM/F12 medium containing 0·1% cosmic calf serum (Hyclone) and antibiotics (low-serum medium). TPA (Sigma-Aldrich, St Louis, MO), Forskolin (Sigma-Aldrich, Saint Louis, MO) or both were added to the cells in fresh low-serum medium and the treatment carried out at 37°C for 24 h. DHEAS or aldosterone content of conditioned medium was determined using radioimmunoassay kits (Diagnostic System Laboratories, Webster, TX). Results of steroid assays were normalized to the cellular protein content in each well and expressed as pmol/mg cell protein.

Expression vectors. Expression vectors containing the full length sequence for the human v-jun (GenBank acc no. BC006175), junB (GenBank acc no. BC004250), v-fos (GenBank acc no. BC004490), fosL1 (GenBank acc no. BC016648) and fosL2 (GenBank acc no. BC022791) were originally purchased from ATCC (Manassas, VA 20108 USA) and junD (GenBank acc no NM_005354) plasmid was a gift from Dr. Marcello Maggiolini (University of Calabria, Italy) (52). Coding sequences for the genes were excised from their original vectors and subcloned into pcDNA3.1 zeo(+) (Invitrogen, Carlsbad, CA, USA). The coding sequence for FosB (GenBank acc no. NM_006732) was amplified in a PCR reaction using as a template cDNA obtained after reverse transcription of mRNA from H295R cells, following the same protocol indicated in the real time RTPCR section. Primers for the amplification were based on the published sequence of the FosB gene Forward: 5'-TGTGCCCAGGGAAATGTTTCAGGC-3' Reverse: 5'-

AATCCTCCTGTCCGATGGCAGTGGC-3', which gave a 1202 bp fragment. PCR product was cloned into TOPO II vector (Invitrogen), digested with EcoRI and finally subcloned into pcDNA3.1 zeo (+). Human SF-1 was provided by Dr Meera Ramayya (University of Washington, Seattle, WA, USA) (55), SRC-1 plasmid was provided by Dr Bert O'Malley (Baylor College of Medicine, Houston, TX) (38). Coding sequence for the SF-1 and SRC-1 plasmids was excised from their vector and subcloned into the pcDNA3.1 zeo(+) expression plasmid.

Transfection assay. The preparation of the hCYP17 promoter construct has been described previously (20). Transfections were carried out for 6 h using the transfection reagent Transfast (Promega, Madison, WI) according to manufacturer's directions. For co-transfection experiments, indicated amounts of expression plasmids were included in the transfection reaction, and the total amount of DNA was kept constant by addition of carrier DNA (empty expression vector, pcDNA3.1 zeo(+)). To normalize luciferase activity cells were co-transfected with 50 ng of pSV β-galactosidase control vector (Promega). Following transfection, cells were incubated with 2.0 ml low serum medium for 18–24 h to allow for recovery and expression of foreign DNA. Cells were then lysed and assayed for enzyme activity using the luciferase assay system (Promega) and β-galatosidase assay system (Tropix, Applied Biosystems, Foster City, CA).

Protein assay and western blot analysis. Cells were lysed in passive lysis buffer (Promega). The protein content of samples was then determined by the bicinchoninic acid protein assay, using the BCA assay kit (Pierce; Rockford, IL). Polyacrylamide gel electrophoresis was carried out on samples using the Novex gel electrophoresis system with 4-12 % bis-tris NuPage gels (Invitrogen). Proteins were electrophoretically transferred onto PVDF membranes by wet transfer for 1 hr at 25 V. Following transfer, membranes were incubated overnight at 4°C with antibody against the phosphorylated form of ERK1/2 (New England Biolabs, England UK) or with antibody against

Fos (sc-52) and Jun (sc-45) (Santa Cruz Biotechnology Inc.). The p-ERK-1/2 and the Fos and Jun antibodies were applied at a 1:1000, 1:500 and 1:500 dilution respectively. To assure equal loading of nuclear proteins membranes were stripped and incubated overnight with antibody against Lamin B1 (sc-6216) (Santa Cruz Biotechnology) at a 1:1000 dilution overnight at 4°C. Membranes were incubated with horseradish peroxidase (HRP)-conjugated secondary antibodies (Amersham Pharmacia Biotech, Piscataway, NJ) and immunoreactive bands were visualized with the ECL western blotting detection system (Amersham Pharmacia Biotech).

Real-time RTPCR. Prior to experiments, cells were maintained overnight in low serum medium. Cells were then treated for the indicated times and RNA was extracted from cells using the Ultraspec RNA isolation system (Biotecx Laboratories Inc., Houston TX). All RNA was treated with DNase I (Ambion, Austin, TX), and purity and integrity of the RNA was confirmed spectroscopically and by gel electrophoresis prior to use. Two μg of total RNA was reverse transcribed in a final volume of 50 μl using the High Capacity cDNA Archive Kit (Applied Biosystems, Foster City, CA), cDNA was diluted 1:5 in nuclease free water, aliquoted and stored at –20°C. Primers for the amplification were based on published sequences for the human AP-1 and CYP17 genes. The nucleotide sequences of the primers for CYP17 have been previously published (49). For the AP-1 factors amplification was accomplished using the following primers Jun: forward 5'-AGCTGGAGCGCCTGATAATC-3' and reverse 5'-CTCCTGCTCATCTGTCACGTTCT-3' and Fos: forward 5'-AGGAGGGAGCTGACTGATACACT-3' and reverse 5'-TTTCCTTCTCCTTCAGCAGGTT-3'.

PCR reactions were performed in the ABI Prism 7000 Sequence Detection System (Applied Biosystems), using 0.1 μM of each primer, in a total volume of 30 μL reaction mixture following the manufacturer's recommendations. SYBR Green Universal PCR Master Mix (Applied

Biosystems) for the dissociation protocol was used for the AP-1 members and TaqMan Master Mix was used for CYP17. Negative controls contained water instead of first-strand cDNA. Each sample was normalized on the basis of its 18S ribosomal RNA content. The 18S quantification was performed using a TaqMan Ribosomal RNA Reagent kit (Applied Biosystems) following the method provided in the TaqMan Ribosomal RNA Control Reagent kit (Applied Biosystems). The relative AP-1 gene expression levels were normalized to a calibrator that was chosen to be the basal, untreated sample. Final results were expressed as *n*-fold differences in AP-1 gene expression relative to 18S rRNA and calibrator, calculated following the ΔΔCt method, as follows:

$$n\text{-fold} = 2^{-(\Delta Ct_{sample} - \Delta Ct_{calibrator})}$$

where ΔCt values of the sample and calibrator were determined by subtracting the average Ct value of the 18S rRNA reference gene from the average Ct value of the different genes analyzed.

Microarray analysis. RNA from H295R cells untreated (basal) or treated for 1 h with TPA (10 nM) or Ang II (100 nM) were hybridized to an Affymetrix human HG-U133plus oligonucleotide two-microarray set containing more than 54,000 probe sets representing over 38,500 independent human genes (Affymetrix, Santa Clara, CA). The arrays were scanned at high resolution using an Affymetrix GeneChip Scanner 3000. Results were analyzed using GeneSpring version 6.1 software (Silicon Genetics, Redwood City CA). Pure signal values were normalized using a list of 100 normalization control probe sets published by Affymetrix and used to identify genotypic differences between untreated and treated cells. Hierarchical clustering algorithms were used to determine steroidogenic genes expression patterns in the two treated samples.

Chromatin Immunoprecipitation (ChIP). This assay was performed using the ChIP assay kit from Upstate (Lake Placid, NY) with minor modifications in the protocol. H295R cells were grown in 100 mm plates. Confluent cultures (90 %) were treated for 1 h with 10 nM TPA, 100 nM

Ang II or with PD98059 for 30 min before stimulation with 10 nM TPA or left untreated. Following treatment DNA/protein complexes were crosslinked with 1 % formaldehyde at 37 °C for 10 min. Next, cells were collected and resuspended in 400 μl of SDS lysis buffer (Upstate) and left on ice for 10 min. Then, cells were sonicated four times for 10 sec at 20 % of maximal power and collected by centrifugation at 4 °C for 10 min at 14 000 rpm. Of the supernatants 10 μl were kept as input (starting material, to normalize results) while 100 μl were diluted 1:10 in 900 μl of ChIP dilution buffer (Upstate) and immunocleared with 80 μl of sonicated salmon sperm DNA/protein A agarose (Upstate) for 6 h at 4 °C. Immunocomplex was formed using 2 μg of specific antibodies, anti-fos (sc-253) and anti-jun (sc-44) (Santa Cruz Biotechnology) overnight at 4 °C. Immunoprecipitation with salmon sperm DNA/protein A agarose was continued at 4 °C until the day after. DNA/protein complexes were reverse crosslinked overnight at 65 °C. Extracted DNA was resuspended in 20 μl of TE buffer. 4 μl volume of each sample and 2 μl of input were used for PCR using CYP17 promoter primers. The PCR conditions were 1 min at 94 °C, 1 min at 50 °C and 2 min at 72 °C for 30 cycles using the following primers: forward, 5'-CCTTTAACAGTCCCTGCTACTTG-3'; reverse, 5'-GGGCACAAGGAGGCCTTTTA-3'. The amplification products of 400 bp were analyzed on a 1 % agarose gel and visualized by ethidium bromide staining. In control samples, nonimmune rabbit IgG was used instead of specific antibodies.

Immunohistochemistry. Nonpathologic human adult adrenal tissues were retrieved from autopsy files of Tohoku University Hospital, Sendai, Japan. These tissues were fixed in 10 % formalin and embedded in paraffin-wax. Histological examinations revealed no significant pathologic abnormalities including nodules or neoplasms. Review of the charts revealed that those patients had not received any form of adrenocortical steroids prior to their demise. The rabbit

polyclonal antibody for c-Fos (Ab-2) was purchased from Calbiochem, and the rabbit polyclonal antibody for P450c17 has been described in detail previously (45). A Histofine Kit (Nichirei, Tokyo, Japan), which employs the streptavidin-biotin amplification method was used in this study. Antigen retrieval for c-Fos immunostaining was performed by heating the slides in an autoclave at 120 ˚C for 5 min in citric acid buffer (2 mM citric acid and 9 mM trisodium citrate dehydrate, pH 6.0). Dilutions of primary antibodies used in this study were c-Fos; 1/500 and P450c17 1/2000. The antigen-antibody complex was visualized with 3.3'-diaminobenzidine (DAB) solution (1 mM DAB, 50 mM Tris-HCl buffer pH 7.6 and 0.006 % H_2O_2), and counterstained with hematoxylin. For a negative control, the sections were incubated with normal rabbit IgG instead of the primary antibodies, and no specific immunoreactivity was detected in these sections.

RNA interference. Fos *SMART*pool® siRNA and scrambled siRNA were purchased from Upstate Biotechnology. Twenty-four hours after plating cells into 30 mm dishes at 4×10^6 cells, siRNAs were transfected to a final concentration of 100 nM using the RNAiFect Transfection Reagent (Qiagen Inc., Valencia, CA) according to manufacturer's instructions. For RNA extraction, the day after transfection the medium was replaced with low serum medium and TPA (10 nM) was added to the cells and treatment allowed for 24 h. For protein extraction, two days after transfection cells were treated for 1 h with TPA (10 nM), fos specific knock-down was detected by western analysis.

Data Analysis and Statistical Methods. Pooled results from triplicate experiments were analyzed using one-way ANOVA with Student-Newman-Keuls multiple comparison methods, using SigmaStat version 3.0 (SPSS, Chicago, IL).

RESULTS

Activation of PKC promotes glomerulosa-like phenotype in H295R cells.

The zona glomerulosa of the human adrenal gland does not express CYP17. The human H295R adrenal cell line is a pluripotent model, producing steroids characteristic of each adrenocortical zone (40). However H295R can become a glomerulosa-like cell line by activating the PKC pathway. In fact, as can be seen in Figure 1A, activation of PKC, using TPA, results in a reduction of CYP17 mRNA expression by 73 % ($P < 0.05$). Forskolin (FSK), a PKA pathway agonist, increases CYP17 expression more than 2-fold, but the simultaneous activation of both PKC (with TPA) and PKA (with FSK) pathways, causes an inhibition of FSK-induced gene expression by 85 % (Fig. 1A), thus making the cells, resemble a glomerulosa-like cell line. The inhibitory effect of TPA on CYP17 is paralleled by a 40 % inhibition of DHEAS levels in the culture medium (Fig.1 B). As expected FSK stimulated DHEAS production by 2-fold while the addition of TPA along with FSK blocked DHEAS stimulation by 46 % compared to FSK alone ($P < 0.001$). In contrast TPA increased aldosterone production in the culture medium by 3.1-fold respectively ($P < 0.05$). The presence of both TPA and FSK resulted in a 6.6-fold ($P < 0.05$) increase in aldosterone production.

ERK-1/2 are activated by Ang II and mediate the PKC-dependent inhibition of CYP17.

Ang II increases ERK-1/2 activity in adrenal cells (53). We measured ERK activity in response to Ang II by examing the amounts of these phosphorylated kinases in H295R cells. Cells were treated with Ang II for different times, and western blot showed a time-dependent increase in phosphorylation of ERK-1/2 with a peak 5 min after treatment (Fig. 2A). Since Ang II exerts its effects by binding to specific receptors, the AT-1 and AT-2 receptor isoforms, we treated cells with specific inhibitors for both receptors before stimulating with Ang II. Activation of ERK-1/2 is

specifically mediated by the type 1 receptor as shown by the ability of the AT-1 inhibitor Dup753 to block the production of p-ERK1/2 (Fig. 2B). Ang II positively regulates expression of all the genes for steroidogenic enzymes required for production of aldosterone in adrenal zona glomerulosa (6,7,14). This zone is characterized by high expression of CYP11B2 (17,37) and very low levels of CYP17 (16). Since Ang II, upon binding to the AT-1 receptor, causes an increase in cellular calcium and an activation of PKC, we tested the effect of the PKC activator TPA and the calcium ionophore ionomycin on CYP17 expression in H295R cells. As previously shown TPA inhibited CYP17 expression by 75 % observed at 24 h while ionomycin increased CYP17 gene expression by 1.6-fold ($p<0.001$) (Fig. 3A). Ang II, by stimulating both calcium and PKC activity, did not change levels of CYP17 mRNA (Fig. 3A). However treatments with Ang II in the presence of the CaM kinase inhibitor KN93 decreased CYP17 mRNA levels by 75 % (Fig. 3B). Treatments with Ang II plus the PKC inhibitor GF109203X, resulted in a significant increase in CYP17 gene expression ($p<0.001$) (Fig. 3B). In addition the presence of the PKC inhibitor GF109203X blocked the Ang II induced activation of ERKs, while the presence of the CaM kinase inhibitor KN93 had no effect on Ang II mediated activation of ERK-1/2 (Fig. 3C). Importantly TPA inhibition of CYP17 was blocked by the addition of the ERK inhibitor PD98059 (Fig. 3D), while TPA induced phosphorylation of ERK-1/2 was prevented by the presence of PD98059 (Fig. 3E).

Ang II and TPA induce AP-1 mRNA and protein synthesis in adrenal cells.

The inhibition of CYP17 mRNA by TPA occurred in a time dependent manner and was completely abolished by the presence of the protein synthesis inhibitor cycloheximide (Fig. 4A), indicating that synthesis of new proteins was necessary for the down-regulatory effect that TPA has on CYP17 mRNA. Since ERK-1/2 are involved in the activation of several genes, we used microarray analysis to screen a large number of genes of the human genome. Microarray analyses

of mRNA from H295R cells untreated (basal) or treated with either Ang II or TPA, are shown in Figure 4B and 4C. Most of the AP-1 family members examined were upregulated by AngII and TPA (Figs 4B and 4C). The greatest increases, following treatment with AngII or TPA, were observed for fos (300- and 194-fold respectively) and fosB (500- and 65-fold respectively) followed by junB (14- and 9-fold respectively), jun (4.2- and 2-fold respectively) and junD (2-fold each). While both fra-1 and fra-2 increased 2-fold following treatment with AngII, only fra-1 was increased by TPA treatment (2-fold). Basal and treated cells demonstrated that the AP-1 genes are differentially expressed. Interestingly under basal conditions fos and fosB are present at very low levels compared to jun or junD. However cells treated with Ang II or TPA show fos and fosB expression similar to jun. Using real-time RTPCR analysis as an alternative approach to measure mRNA expression of specific genes, we confirmed that both fos and jun mRNA were increased rapidly in a time dependent manner (Fig. 5A, 5B). Ang II induction of both fos and jun mRNA was maximal after 30 min of treatment, with fos induced 300-fold and jun 4-fold. Prolonged exposure of cells to Ang II led to a decline in gene induction (Fig. 5A and B) but induction was maintained above basal levels. The situation in the presence of TPA was slightly different, with maximum levels of fos observed 1 h after stimulation (200-fold) and with a gradual decrease in expression at the other two time points analyzed (Fig. 5A). jun mRNA levels were induced 2-fold at 1 h and remained relatively constant at the other two time points (Fig. 5B). Induction of fos mRNA was paralleled by an increase in protein levels in the presence of either Ang II or TPA (Fig. 5C). Levels of jun protein did not significantly change in the presence of the two agonists (Fig. 5D) as determined by intensity of western bands with densitometric analysis and normalized to lamin B content. Fos was induced 50-fold by Ang II and 12-fold by TPA (Fig. 5C lower panel) while Jun was induced 2.5- and 1.5-fold by Ang II and TPA respectively (Fig. 5D lower panel). To confirm

the importance of ERK-1/2 in the activation of the AP-1 genes by TPA, we treated cells with PD98059 prior to TPA stimulation and measured mRNA expression of fos and jun (Fig. 6A and B). Induction of fos by TPA was 200-fold over basal and this was reduced by 70 % ($p<0.001$) in the presence of the ERK-1/2 inhibitor PD98059 (Fig. 6A). Fos protein expression was also inhibited by PD98059 (Fig. 6C). Conversely the ERK inhibitor had no significant effect on the regulation of jun mRNA and protein (Fig. 6B and D).

Fos expression is limited to the zona glomerulosa and mediates CYP17 repression.

Immunohistochemical analyses showed that Fos (brown cells) expression (Fig. 7A top panel) is localized to the zona glomerulosa where CYP17 expression is absent (Fig. 7A middle panel). Using siRNA for fos it was possible to knock-down expression of Fos in H295R cells (Fig. 7B) and show that the presence of this factor is necessary for PKC mediated inhibition of CYP17 (Fig. 7C). TPA inhibited CYP17 mRNA expression by 65 %, but when Fos expression was blocked this inhibition was only 25 % (Fig. 7C).

AP-1 proteins regulate gene transcription by binding to specific consensus sequences in the gene promoter (AP-1 sites). Sequence analysis of the CYP17 promoter identified several potential AP-1 sites. We used chromatin immunoprecipitation analysis to show functional binding of AP-1 proteins to the CYP17 promoter. Both Fos and Jun binding was induced by treatment with Ang II and TPA (Fig. 8A). However binding of Fos, but not Jun, was reduced by blocking ERK-1/2 activation using the inhibitor PD98059 (Fig. 8A). Since Fos family members bind promoters only as dimers we first transfected a 381 bp fragment of the hCYP17 promoter/reporter construct with Fos plus the different Jun family members (Fig. 8B). Dimers formed with Fos and any of the Jun family members were able to significantly repress CYP17 basal transcription by 40 to 45 % ($p<0.001$).

Since human CYP17 transcription is enhanced by SF-1 (20) we tested the effect of Fos or the Jun family members on the SF-1 induced transcription of CYP17 and found that none of the factors interfered with SF-1 mediated transcription (Fig. 8C). We then tested the effect of dimers formed between Fos and the different Jun family members on the SF-1 induced transcription of CYP17 (Fig. 8D). SF-1 induced CYP17 transcription by 7.5-fold and Jun/Fos dimers inhibited SF-1 activated transcription by 68 % ($p<0.001$). JunB/Fos caused a 50 % inhibition ($p<0.001$) while JunD/Fos dimers were able to decrease SF-1 induction of CYP17 by 45 % ($p<0.001$). Since the presence of the Fos members seem to be critical for CYP17 transcription, we tested the effect of increasing doses of the Fos members in combination with constant doses of Jun (Fig. 8E). Fos caused a dose-dependent inhibition of SF-1 activated transcription of CYP17 with a significant inhibition observed in the presence of as little as 1 ng of expression vector, 50 % inhibition was observed in the presence of 10 ng of Fos and 100 ng inhibited SF-1 activation by 80 % (Fig. 8E).

Fos represses CYP17 through direct interaction with SF-1.

Fos mediated repression of CYP17 was overcome by cotransfection with increasing amounts of SF-1 (Fig. 9A). Addition of the highest dose of SF-1 reversed AP-1 inhibition by 80 %. These results suggested competition between the two proteins. Therefore we examined the potential for a direct interaction between Fos and SF-1. To investigate this hypothesis we tested if SF-1 would co-immunoprecipitate with Fos using an anti-Fos antiserum. As shown in Figure 9B western analysis for SF-1 revealed its presence in Fos immunoprecipitates, and this interaction increased if cellular Fos levels were increased after treatment with Ang II or TPA (see Fig. 5).

SF-1 transcriptional activity depends on binding of co-activators, so we hypothesized that the competition for common co-activators like CREB binding protein (CBP) or steroid receptor coactivator-1 (SRC-1) could be the mechanism responsible for the inhibition of CYP17

transcription. To evaluate this hypothesis H295R cells were co-transfected with a CYP17 reporter construct and increasing amounts of expression vectors for CBP and SRC-1 (Fig. 9C). Overexpression of both factors was able to completely overcome Fos-mediated inhibition, and when the two factors were added simultaneously at the concentration of 0.3 μg, the final effect was a significant induction of gene transcription of 2-fold over SF-1 alone ($p < 0.05$).

DISCUSSION

The human adrenal cortex consists of three zones: the glomerulosa, fasciculata and reticularis. Each zone is characterized by the production of specific hormones. The zona glomerulosa synthesizes aldosterone, the zona fasciculata produces cortisol and the reticularis produces DHEA and DHEAS. Hormone production in each zone depends on the relative activities of specific steroidogenic enzymes. The steroidogenic enzymes needed for aldosterone production are cholesterol side-chain cleavage (CYP11A), 3β-hydroxysteroid dehydrogenase type 2 (HSD3B2), 21-hydroxylase (CYP21) and aldosterone synthase (CYP11B2). Importantly the zona glomerulosa lacks the expression of 17α-hydroxylase (CYP17). This enzyme is not involved in aldosterone production and, indeed, if CYP17 was present it would decrease glomerulosa aldosterone production by competing for steroid precursors (16). The molecular mechanisms causing the zonal pattern of CYP17 expression within the adrenal cortex are not known.

Aldosterone production is controlled by Ang II and it appears possible that the lack of CYP17 expression in the aldosterone-producing zona glomerulosa is under the control of factor(s) activated by Ang II. Supporting a key role for Ang II is the observation that type 1 Ang II receptors (AT-1 receptors) are expressed primarily in the zona glomerulosa and not in the fasciculata or reticularis where expression of CYP17 is high (19). The nuclear receptor

Steroidogenic Factor-1 (SF-1) is known to be a positive regulator of CYP17 and its transcriptional activity can be blocked by the orphan nuclear receptor DAX-1 (20). Like SF-1, DAX-1 is expressed throughout the different zones of the human adrenal (48). Thus based on its expression pattern DAX-1 does not appear to be the factor controlling zone specific CYP17 expression in the adrenal.

Glomerulosa cells respond to Ang II activation of the AT-1 receptor by increasing intracellular calcium and activation of PKC. It has long been our hypothesis that the expression of CYP17 can be inhibited by PKC (4,5,7,30,41). The inhibitory effect of PKC activation on adrenal cell CYP17 expression has been confirmed by several laboratories (9,32,36). We confirm and extend those observations in the current study by dissecting the relative role of calcium (as an activator of CYP17) and PKC (as an inhibitor of CYP17 expression). We demonstrate these opposing roles through the use of agonists for each pathway: TPA to activate PKC and inhibit CYP17 or ionomycin to increase cellular calcium and activate CYP17. Further support is provided through the use of the specific antagonist of PKC (GF109203X) which then permitted Ang II to become an activator of CYP17 expression. In addition we show that blocking CaM Kinases with the antagonist KN93 allowed Ang II to be a more potent inhibitor of CYP17 expression.

To further determine the downstream signaling events that inhibit CYP17 we tested the hypothesis that ERK-1/2 inhibit CYP17 expression. We have previously shown that activation of ERK-1/2 is part of the Ang II activated pathway in H295R cells (53). Here we demonstrate that Ang II activates ERK-1/2 in a time-dependent manner, that this activation is mediated by the AT-1 receptor, that activation can be blocked by PKC inhibition (but not by inhibition of CaM kinase activity) and finally that the selective activator of PKC, TPA, is a potent activator of ERK-1/2. These events were well coordinated with the inhibitory effect on CYP17 mRNA levels in that

ERK-1/2 activation results in a decrease in CYP17 expression. This is in agreement with previous reports showing that silencing of ERK-1/2, using the inhibitor PD98059, increases CYP17 expression in the H295R adrenal (46). Furthermore, adrenocorticotropin (ACTH), which is a known positive regulator of CYP17, decreases ERK activity in the adrenal cortex in vivo and in the mouse adrenal Y1 cell line (54). These previous data, together with ours, support the hypothesis that ERK activation is involved in the down-regulation of CYP17.

Our microarray data indicated that the members of the AP-1 family are differentially expressed in the human adrenal and are up-regulated by treatments with Ang II or TPA. Fos appears to be the most highly elevated early response gene in response to both Ang II and TPA treatments. Our immunohistochemical analysis shows that Fos expression is limited to the zona glomerulosa, where CYP17 is absent, and that Fos is low in the fasciculata and reticularis where CYP17 is highly expressed. This inverse correlation between Fos and CYP17 made us hypothesize that Fos was the factor responsible for CYP17 down-regulation in the zona glomerulosa. To confirm our hypothesis we used an siRNA to down-regulate fos expression in the H295R adrenal cell line. The knock-down of this gene was able to significantly block the ability of TPA to inhibit CYP17 expression, demonstrating that inhibition of CYP17 through PKC activation depends on the increased expression of Fos.

Transcription of the human CYP17 gene is regulated through binding to specific sites of SF-1 (20), GATA (22) and Sp1 (18). An analysis of the human CYP17 promoter revealed the presence of AP-1 sites located inbetween the SF-1 sites. To better define the mechanisms of Fos inhibition of CYP17 expression we show that AP-1 factors are present on the CYP17 promoter *in vivo*. Also our transfection experiments demonstrate that AP-1 dimers can result in an inhibition of SF-1 mediated activation of CYP17. A similar effect was observed for the rat StAR promoter (47). In

that study the authors showed that over-expression of Fos interfered with SF-1 for StAR activation, and mutation of an AP-1 site did not reverse the inhibition but decreased SF-1 mediated induction, leading the authors to suggest a more complex interaction between AP-1 and SF-1.

In an attempt to explain the molecular mechanism of AP-1 inhibition of CYP17 transactivation we mutated the putative AP-1 sites present on the CYP17 promoter. As in the case of the rat StAR promoter our mutational studies resulted in a decrease in SF-1 mediated transcription of CYP17 and double mutants completely blocked the ability of SF-1 to activate gene expression (data not shown). These results led us to examine the interaction between SF-1 and AP-1 factors. It has been shown by *in vitro* studies that SF-1 and Fos can interact (29). Based on the position of the AP-1 and SF-1 sites on the CYP17 promoter it is a likely possibility that a similar interaction occurs in our model. A previous study has shown that all three SF-1 sites are necessary for maximal activation of CYP17 transcription and that mutation of any one of the three SF-1 binding cis-elements reduces activity by approximately 70 % compared to the wild type promoter (20). The apparent need for both the SF-1 and AP-1 cis-elements led us to test the hypothesis that the factors binding these elements cooperate through cofactor sharing. Based on their relative abundance it is possible that under basal condition the AP-1 sites are bound by dimers of the Jun family members and they work with SF-1 to activate transcription. Importantly ACTH, a positive regulator of CYP17, activates SAPK (also called JNK kinase) which is responsible for phosphorylation and activation of Jun (54). With transfection experiments we were able to demonstrate that the cofactors, CREB binding protein (CBP) and Steroid Receptor Coactivator-1 (SRC-1), allow SF-1 to become a more potent activator of CYP17 if Jun is present (data not shown). After activation of the Ang II pathway and the rapid induction of Fos it is possible that the Jun homodimer is replaced with a Jun/Fos heterodimer. Studies on the capacity of the Jun or Fos protein family members to

bind DNA have revealed that the different dimers have different binding affinities. Specifically for homodimers, Jun has the stronger affinity, followed by JunD and finally JunB (44). Importantly, heterodimers of any of the Jun with any of the Fos family members have a greatly enhanced binding activity compared to homodimers. It is possible that the Jun/Fos dimers do not allow cooperation with the three SF-1 sites. This is a valid possibility since it has been demonstrated that the composition of the AP-1 dimers plays an important role in determining the final effect on gene transcription. In fact it has been observed that the AP-1 dimers upon binding to the promoter induces a conformational change of the promoter (24,25). It is possible that the Jun/Fos dimer modifies the conformation of the CYP17 promoter in such a way so that the three SF-1 proteins cannot share cofactors or that a RNA polymerase complex cannot be formed. Therefore we tested the possibility that the AP-1 dimers interfere with SF-1 binding to DNA. ChIP assay determined that at the same times that Ang II and TPA increased AP-1 binding to CYP17 promoter SF-1 binding to DNA was not altered (data not shown). Our next step was to determine if SF-1 and Fos had a direct interaction. We assessed this using an immunoprecipitation assay, which showed an interaction that increased with increasing amounts of Fos, as is seen following stimulation of H295R cells with TPA or Ang II.

Based on the observed interaction between SF-1 and Fos we investigated the possibility that Fos might prevent cofactors from binding to SF-1, which should lead to a decrease in its transcriptional activity. CBP and SRC-1 have been described as cofactors for AP-1 (1,2,26), various nuclear receptor proteins including SF-1, and certain other transcription factors and is required for their transactivation properties (21,23,27,28). Therefore, we proposed CBP and/or SRC-1 as common limiting cofactors that can account for inhibition of SF-1-dependent gene expression by AP-1. It has been demonstrated that CBP interacts with SF-1 in the H295R cell

model and that it potentiates SF-1 activated transcription of CYP11A (35). In the above mentioned study the authors proposed that the interaction of SF-1 with CBP could influence the interaction of CBP with other factors to trigger RNA polymerase II-dependent transcription and suggested that SF-1 mediated CYP17 gene expression was also up-regulated by the presence of CBP in NCI-H295 cells. We contransfected CYP17 promoter vector, SF-1 and AP-1 together with CBP and/or SRC-1. By increasing the amounts of CBP and/or SRC-1 we were able to rescue SF-1 induced activation of CYP17 transcription from the inhibition caused by the presence of AP-1 dimers. The presence of both cofactors had a more potent effect, not only in rescuing CYP17 from the inhibition, but in activating transcription to levels higher than with SF-1 alone.

In conclusion we show for the first time the cellular pathway that is activated by Ang II and is responsible for the down-regulation of CYP17 in the human adrenal cells (Fig. 10). In this pathway Ang II activates PKC resulting in phosphorylation of ERK1/2; which then leads to an increase in Fos levels. We also demonstrate that the increase in Fos is responsible for repression of CYP17 transcription. In this proposed mechanism Fos heterodimerizes with Jun and replaces Jun homodimers on the CYP17 promoter. The Jun/Fos heterodimer prevents the cofactors CBP and SRC-1 from binding SF-1 resulting in a repression of CYP17 gene transcription. These data further our understanding of the mechanisms contributing to the functional zonation of the human adrenal gland.

REFERENCES

1. **Arias, J., A. S. Alberts, P. Brindle, F. X. Claret, T. Smeal, M. Karin, J. Feramisco, and M. Montminy.** 1994. Activation of cAMP and mitogen responsive genes relies on a common nuclear factor. Nature **370**:226-229.

2. **Benkoussa, M., C. Brand, M. H. Delmotte, P. Formstecher, and P. Lefebvre**. 2002. Retinoic Acid Receptors Inhibit AP1 Activation by Regulating Extracellular Signal-Regulated Kinase and CBP Recruitment to an AP1-Responsive Promoter. Mol.Cell.Biol. **22**:4522-4534.

3. **Berk, B. C., and M. A. Corson.** 1997. Angiotensin II Signal Transduction in Vascular Smooth Muscle : Role of Tyrosine Kinases. Circ Res **80**:607-616.

4. **Bird, I. M., R. R. Magness, J. I. Mason, and W. E. Rainey.** 1992. Angiotensin-II acts via the type 1 receptor to inhibit 17 alpha-hydroxylase cytochrome P450 expression in ovine adrenocortical cells. Endocrinology **130**:3113-3121.

5. **Bird, I. M., J. I. Mason, and W. E. Rainey.** 1998. Battle of the kinases: integration of adrenal responses to cAMP, DG and Ca2+ at the level of steroidogenic cytochromes P450 and 3betaHSD expression in H295R cells. Endocr Res **24**:345-354.

6. **Bird, I. M., J. I. Mason, and W. E. Rainey.** 1998. Protein kinase A, protein kinase C, and Ca(2+)-regulated expression of 21-hydroxylase cytochrome P450 in H295R human adrenocortical cells. J Clin Endocrinol Metab **83**:1592-1597.

7. **Bird, I. M., M. M. Pasquarette, W. E. Rainey, and J. I. Mason.** 1996. Differential control of 17 alpha-hydroxylase and 3 beta-hydroxysteroid dehydrogenase expression in human adrenocortical H295R cells. J Clin Endocrinol Metab **81**:2171-2178.

8. **Bird, I. M., N. A. Hanley, R. A. Word, J. M. Mathis, J. L. McCarthy, J. I. Mason, and W. E. Rainey**. 1993. Human NCI-H295 adrenocortical carcinoma cells: a model for angiotensin-II-responsive aldosterone secretion. Endocrinology **133**:1555-1561.

9. **Brentano, S. T., J. Picado-Leonard, S. H. Mellon, C. C. Moore, and W. L. Miller.** 1990. Tissue-specific, cyclic adenosine 3',5'-monophosphate-induced, and phorbol ester-repressed transcription from the human P450c17 promoter in mouse cells. Mol Endocrinol **4**:1972-1979.

10. **Cacace, A. M., M. Ueffing, A. Philipp, E. K. Han, W. Kolch, and I. B. Weinstein.** 1996. PKC epsilon functions as an oncogene by enhancing activation of the Raf kinase. Oncogene **13**:2517-2526.

11. **Cai, H., U. Smola, V. Wixler, I. Eisenmann-Tappe, M. T. Diaz-Meco, J. Moscat, U. Rapp, and G. M. Cooper**. 1997. Role of diacylglycerol-regulated protein kinase C isotypes in growth factor activation of the Raf-1 protein kinase. Mol.Cell.Biol. **17**:732-741.

12. **Cherradi, N., B. Pardo, A. S. Greenberg, F. B. Kraemer, and A. M. Capponi**. 2003. Angiotensin II Activates Cholesterol Ester Hydrolase in Bovine Adrenal Glomerulosa Cells through Phosphorylation Mediated by p42/p44 Mitogen-Activated Protein Kinase. Endocrinology **144**:4905-4915.

13. **Clark, A. J., T. Balla, M. R. Jones, and K. J. Catt.** 1992. Stimulation of early gene expression by angiotensin II in bovine adrenal glomerulosa cells: roles of calcium and protein kinase C. Mol Endocrinol. **6**:1889-1898.

14. **Clark, B. J., V. Pezzi, D. M. Stocco, and W. E. Rainey.** 1995. The steroidogenic acute regulatory protein is induced by angiotensin II and K+ in H295R adrenocortical cells. Mol Cell Endocrinol **115**:215-219.

15. **Curran, T., and B. R. Jr. Franza.** 1988. Fos and Jun: the AP-1 connection. Cell **55**:395-397.

16. **Dharia, S., A. Slane, M. Jian, M. Conner, A. J. Conley, and C. R. Parker Jr**. 2004. Co-localization of P450c17 and cytochrome b5 in androgen-synthesizing tissues of the human. Biol Reprod **71**:83-88.

17. **Domalik, L. J., D. D. Chaplin, M. S. Kirkman, R. C. Wu, W. W. Liu, T. A. Howard, M. F. Seldin, and K. L. Parker.** 1991. Different isozymes of mouse 11 beta-hydroxylase produce mineralocorticoids and glucocorticoids. Mol Endocrinol **5**:1853-1861.

18. **Fluck, C. E., and W. L. Miller.** 2004. GATA-4 and GATA-6 modulate tissue-specific transcription of the human gene for P450c17 by direct interaction with SP1. Mol Endocrinol **18**:1144-1157.

19. **Frei, N., J. Weissenberger, A. G. Beck-Sickinger, M. Hofliger, J. Weis, and H. Imboden**. 2001. Immunocytochemical localization of angiotensin II receptor subtypes and angiotensin II with monoclonal antibodies in the rat adrenal gland. Regulatory Peptides **101**:149-155.

20. **Hanley, N. A., W. E. Rainey, D. I. Wilson, S. G. Ball, and K. L. Parker.** 2001. Expression profiles of SF-1, DAX1, and CYP17 in the human fetal adrenal gland: potential interactions in gene regulation. Mol Endocrinol **15**:57-68.

21. **Ito, M., R. N. Yu, and J. L. Jameson**. 1998. Steroidogenic Factor-1 Contains a Carboxy-Terminal Transcriptional Activation Domain That Interacts with Steroid Receptor Coactivator-1. Molecular Endocrinology **12**:290-301.

22. **Jimenez, P., K. Saner, B. Mayhew, and W. E. Rainey.** 2003. GATA-6 is expressed in the human adrenal and regulates transcription of genes required for adrenal androgen biosynthesis. Endocrinology **144**:4285-4288.

23. **Kamei, Y., L. Xu, T. Heinzel, J. Torchia, R. Kurokawa, B. Gloss, S. C. Lin, R. A. Heyman, D. W. Rose, C. K. Glass, and M. G. Rosenfeld.** 1996. A CBP integrator

complex mediates transcriptional activation and AP-1 inhibition by nuclear receptors. Cell **85**:403-414.

24. **Kerppola, T. K., and T. Curran.** 1993. Selective DNA bending by a variety of bZIP proteins. Mol Cell Biol **13**:5479-5489.

25. **Kerppola, T. K., and T. Curran.** 1997. The transcription activation domains of Fos and Jun induce DNA bending through electrostatic interactions. EMBO J. **16**:2907-2916.

26. **Lee, S. K., H. J. Kim, S. Y. Na, T. S. Kim, H. S. Choi, S. Y. Im, and J. W. Lee**. 1998. Steroid Receptor Coactivator-1 Coactivates Activating Protein-1-mediated Transactivations through Interaction with the c-Jun and c-Fos Subunits. J.Biol.Chem. **273**:16651-16654.

27. **Liu, Z., and E. R. Simpson.** 1997. Steroidogenic factor-1 (SF-1) and SP1 are required for regulation of bovine CYP11A gene expression in bovine luteal cells and adrenal Y1 cells. Mol Endocrinol **11**:127-137.

28. **Lund, J., B. Borud, G. Mellgren, R. Aesoy, T. Hoang, A. L. Jacob, and M. Bakke.** 2002. Differential regulation of SF-1-cofactor interactions. Endocr Res **28**:505-513.

29. **Manna, P. R., D. W. Eubank, and D. M. Stocco**. 2004. Assessment of the Role of Activator Protein-1 on Transcription of the Mouse Steroidogenic Acute Regulatory Protein Gene. Molecular Endocrinology **18**:558-573.

30. **Mason, J. I., B. R. Carr, and W. E. Rainey.** 1986. The action of phorbol ester on steroidogenesis in cultured human fetal adrenal cells. Endocr Res **12**:447-467.

31. **Mazzocchi, G., L. K. Malendowicz, G. Gottardo, P. Rebuffat, and G. Nussdorfer.** 1997. Angiotensin-II stimulates DNA synthesis in rat adrenal zona glomerulosa cells: receptor subtypes involved and possible signal transduction mechanism. Endocr Res. **23**:191-203.

32. **McAllister, J. M., and P. J. Hornsby.** 1988. Dual regulation of 3 beta-hydroxysteroid dehydrogenase, 17 alpha- hydroxylase, and dehydroepiandrosterone sulfotransferase by adenosine 3',5'-monophosphate and activators of protein kinase C in cultured human adrenocortical cells. Endocrinology **122**:2012-2018.

33. **McGee, E. A., A. Nguyen, J. I. Mason, W. E. Rainey, and B. R. Carr.** 1996. Protein kinase A and protein kinase C differentially regulate steroidogenesis in human ovarian thecal tumor cells. Endocrine **4**:151-157.

34. **McNeill, H., J. R. Puddefoot, and G. P. Vinson.** 1998. MAP kinase in the rat adrenal gland. Endocr Res **24**:373-380.

35. **Monte, D., F. DeWitte, and D. W. Hum.** 1998. Regulation of the human P450scc gene by steroidogenic factor 1 is mediated by CBP/p300. J Biol Chem **273**:4585-4591.

36. **Naseeruddin, S. A., and P. J. Hornsby.** 1990. Regulation of 11 beta- and 17 alpha-hydroxylases in cultured bovine adrenocortical cells: 3', 5'-cyclic adenosine monophosphate, insulin-like growth factor-i, and activators of protein kinase c. Endocrinology **127**:1673-1681.

37. **Ogishima, T., H. Suzuki, J. Hata, F. Mitani, and Y. Ishimura.** 1992. Zone-specific expression of aldosterone synthase cytochrome P-450 and cytochrome P-45011 beta in rat adrenal cortex: histochemical basis for the functional zonation. Endocrinology **130**:2971-2977.

38. **Onate, S. A., S. Y. Tsai, M. J. Tsai, and B. W. O'Malley.** 1995. Sequence and characterization of a coactivator for the steroid hormone receptor superfamily. Science **270**:1354-1357.

39. **Rainey W. E.** 1999. Adrenal zonation: clues from 11beta-hydroxylase and aldosterone synthase. Mol Cell Endocrinol **151**:151-160.

40. **Rainey, W. E., I. M. Bird, and J. I. Mason**. 1994. The NCI-H295 cell line: a pluripotent model for human adrenocortical studies. Mol Cell Endocrinol **100**:45-50.

41. **Rainey, W. E., D. Naville, and J. I. Mason.** 1991. Regulation of 3 beta-hydroxysteroid dehydrogenase in adrenocortical cells: effects of angiotensin-II and transforming growth factor beta. Endocr Res **17**:281-296.

42. **Rainey, W. E., K. Oka, R. R. Magness, and J. I. Mason.** 1991. Ovine fetal adrenal synthesis of cortisol: regulation by adrenocorticotropin, angiotensin II and transforming growth factor-beta. Endocrinology **129**:1784-1790.

43. **Roux, P. P., and J. Blenis**. 2004. ERK and p38 MAPK-Activated Protein Kinases: a Family of Protein Kinases with Diverse Biological Functions. Microbiol.Mol.Biol.Rev. **68**:320-344.

44. **Ryseck, R. P., and R. Bravo.** 1991. c-JUN, JUN B, and JUN D differ in their binding affinities to AP-1 and CRE consensus sequences: effect of FOS proteins. Oncogene **6**:533-542.

45. **Sasano, H., J. I. Mason, and N. Sasano.** 1989. Immunohistochemical study of cytochrome P-45017 alpha in human adrenocortical disorders. Hum Pathol **20**:113-117.

46. **Sewer, M. B., and M. R. Waterman.** 2003. cAMP-dependent protein kinase enhances CYP17 transcription via MKP-1 activation in H295R human adrenocortical cells. J Biological Chem **278**:8106-8111.

47. **Shea-Eaton, W., T. W. Sandhoff, D. Lopez, D. B. Hales, and M. P. McLean**. 2002. Transcriptional repression of the rat steroidogenic acute regulatory (StAR) protein gene by the AP-1 family member c-Fos. Mol.Cell.Endocrinol. **188**:161-170.

48. **Shibata, H., Y. Ikeda, T. Mukai, K. i. Morohashi, I. Kurihara, T. Ando, T. Suzuki, S. Kobayashi, M. Murai, I. Saito, and T. Saruta**. 2001. Expression Profiles of COUP-TF, DAX-1, and SF-1 in the Human Adrenal Gland and Adrenocortical Tumors: Possible Implications in Steroidogenesis. Molecular Genetics and Metabolism **74**:206-216.

49. **Sirianni, R., K. S. Rehman, B. R. Carr, C. R. Parker, Jr., and W. E. Rainey**. 2005. Corticotropin-Releasing Hormone Directly Stimulates Cortisol and the Cortisol Biosynthetic Pathway in Human Fetal Adrenal Cells. J Clin Endocrinol Metab **90**:279-285.

50. **Tian, Y., R. D. Smith, T. Balla, and K. J. Catt**. 1998. Angiotensin II activates Mitogen-Activated Protein Kinase via Protein Kinase C and Ras/Raf-1 kinase in bovine adrenal glomerulosa cells. Endocrinology **139**:1801-1809.

51. **Viard, I., C. Jaillard, R. Ouali, and J. M. Saez.** 1992. Angiotensin-II-induced expression of proto-oncogene (c-fos, jun-B and c-jun) mRNA in bovine adrenocortical fasciculata cells (BAC) is mediated by AT-1 receptors. FEBS Lett. **313**:43-46.

52. **Vinciguerra, M., A. Vivacqua, G. Fasanella, A. Gallo, C. Cuozzo, A. Morano, M. Maggiolini, and A. M. Musti**. 2004. Differential Phosphorylation of c-Jun and JunD in Response to the Epidermal Growth Factor Is Determined by the Structure of MAPK Targeting Sequences. J.Biol.Chem. **279**:9634-9641.

53. **Watanabe, G., R. J. Lee, C. Albanese, W. E. Rainey, D. Batlle, and R. G. Pestell.** 1996. Angiotensin II activation of cyclin D1-dependent kinase activity. J Biol Chem **271**:22570-22577.

54. **Watanabe, G., P. Pena, C. Albanese, L. D. Wilsbacher, J. B. Young, and R. G. Pestell.** 1997. Adrenocorticotropin induction of Stress-activated Protein Kinase in the adrenal cortex in vivo. J Biological Chem **272**:20063-20069.

55. **Wong, M., M. S. Ramayya, G. P. Chrousos, P. H. Driggers, and K. L. Parker.** 1996. Cloning and sequence analysis of the human gene encoding steroidogenic factor 1. J Mol Endocrinol **17**:139-147.

FIGURE LEGEND

FIG.1. Activation of PKC represses expression of CYP17 and promotes a glomerulosa-like phenotype in H295R cells. Real-time RTPCR was used to quantify CYP17 transcript levels (A) while steroid assays were employed to measure medium levels of DHEAS (B) or aldosterone (C). Basal (untreated) cells were used as control. Cells were incubated for 24 h with forskolin (FSK) (10 μM), TPA (10 nM) or FSK (10 μM) plus TPA (10 nM). For real-time RTPCR data represent the mean ± SEM of three independent RNA samples from H295R cultures and are expressed as relative difference from basal (calibrator) as indicated in the Material and Methods section. Steroid content of the medium was determined by RIA and normalized to the amount of cell protein present in each tissue culture well. Steroid data points are the mean ± SEM of values from three experiments each performed in triplicate and expressed as pmol steroid/mg protein. (* $P < 0.05$ compared with basal; ^ $P < 0.05$ compared with FSK; ** $P < 0.001$ compared with basal; ++ $P < 0.001$ compared with FSK; + $P < 0.05$ compared with FSK or TPA).

FIG. 2. Activation of ERK-1/2 in H295R cells. H295R cells were maintained in low serum overnight and then treated as indicated. The phosphorylated forms of ERK-1 and -2 were examined by immunoblot analysis using equivalent amounts of protein from total cellular lysate. Basal (untreated) cells were used as control. (A) Cells were incubated for the indicated times with Ang II (100 nM). (B) Cells were either untreated (basal) or preincubated for 30 min with the AT1 receptor inhibitor Dup 753 (10 μM) or the AT2 receptor inhibitor PD123319 (10 μM) and then incubated for 5 min with Ang II (100 nM). Western analyses shown represent data from three independent experiments.

FIG. 3. CYP17 mRNA expression depends on the status of ERK1/2 activation. Real-time RTPCR was used to quantify CYP17 transcript levels in H295R cells. The phosphorylated forms of ERK-1 and -2 were examined by immunoblot analysis using equivalent amounts of protein from total cellular lysate. Basal (untreated) cells were used as control. (A) CYP17 expression in H295R cells incubated for 24 h with Ang II (100 nM), TPA (10 nM) or Ionomycin (1 μM). (B) CYP17 expression in H295R cells incubated for 24 h with Ang II (100 nM), with Ang II plus the PKC inhibitor GF109203X (GF) (5 μM) or Ang II plus the Cam kinase inhibitor KN93 (5 μM). (C) ERK-1/2 phosphorylation in cells untreated (basal) or incubated for 5 min with Ang II (100 nM), Ang II plus the PKC inhibitor GF109203X (GF) (5 μM) or Ang II plus the Cam kinase inhibitor KN93 (5 μM). (D) CYP17 expression in H295R cells incubated for 24 h with TPA (10 nM) alone or in the presence of ERK-1/2 inhibitor PD98059 (10 μM). (E) ERK-1/2 phosphorylation in cells incubated with TPA (10 nM) for 5 min or preincubated for 30 min PD98059 (10 μM) before 5 min incubation with TPA (10 nM). Western analyses shown represent data from three independent experiments. Real-time data represent the mean ± SEM of three independent RNA samples from H295R cultures and are expressed as relative difference from basal (calibrator) as indicated in the Material and Methods section. (*, $P < 0.001$ compared with basal).

FIG. 4. TPA-induced inhibition of CYP17 mRNA is dependent on protein synthesis. (A) H295R cells were incubated for the indicated times with TPA (10 nM) alone or in the presence of cycloheximide (10 μM). Real-time RTPCR analysis was used to quantify CYP17 transcript levels. Data represent the mean ± SEM of three independent RNA samples from H295R cultures and are expressed as relative difference from basal (calibrator). (*, $P < 0.001$ compared with basal). (B) Microarray analysis of H295R cells treated for 1 h with 100 nM Ang II vs basal (untreated) cells and (C) cells treated for 1 h with 10 nM TPA vs basal cells. Each spot represents a unique sequence with a total of approximately 38,500 transcripts examined per array. Pure signal were normalized to a list of 100 normalization control probe sets provided by Affymetrix. Spots outside of the parallel lines represent mRNAs with greater than 2-fold differences in expression. AP-1 family member genes are indicated.

FIG. 5. Effect of Ang II and TPA on expression of jun and fos. H295R cells were incubated for the indicated times with TPA (10 nM) or with Ang II (100 nM). Real-time RTPCR was used to quantify fos (A) and jun (B) transcript levels. Data represent the mean ± SEM of three independent RNA samples from H295R cultures and are expressed as relative difference from basal (calibrator). Cells were incubated with TPA (10 nM) or Ang II (100 nM) for 1 h. Fos (C) and Jun (D) protein levels were examined by immunoblot analysis using equivalent amounts of nuclear extracts. Graphs depicted below western blots were obtained by densitometric analysis. Protein expression in each lane was normalized to the lamin B content, and expressed as relative difference from basal levels. Western analyses shown represent data from three independent experiments.

FIG. 6. Effect of PD98059 on TPA-mediated induction of fos and jun. H295R cells were incubated for 1 h with TPA (10 nM) alone or in the presence of PD98059 (10 μM). Total RNA was extracted and real-time RTPCR was used to quantify fos (A) and jun (B) transcript levels. Data represent the mean ± SEM of three independent RNA samples from H295R cultures and are expressed as relative difference from basal (calibrator). Fos (C) and Jun (D) protein levels were examined by immunoblot analysis using equivalent amounts of nuclear extracts. Graphs depicted below western blots were obtained by densitometric analysis. Protein expression in each lane was normalized to the lamin B content, and expressed as relative difference from basal levels. Western analyses shown represent data from three independent experiments. (*, $P < 0.001$ compared with basal; **, $P < 0.001$ compared with TPA).

FIG. 7. An inverse correlation exists between Fos and P450c17 expression in human adrenal. (A) Immunohistochemical analysis of Fos (top panel) and P450c17 (middle panel) in human adult adrenals. Lower panel is the negative control for Fos expression. Immunoreactivity is indicated with brown staining; hematoxylin was used as counterstaining which gave a blue coloring. Each panel is of a serial section of the same field. G, Glomerulosa; F, Fasciculata. *Bar* = 100 μm. (B) H295R cells were grown for 2 days in the presence of siRNA for Fos and then treated for 1 h with TPA (10 nM). Western blot analysis for Fos protein in H295R cells following siRNA gene silencing was performed. (C) Real-time RTPCR for CYP17 in H295R following siRNA gene silencing for Fos. Cells were grown for 1 day in the presence of siRNA for Fos and then treated for

24 h with TPA (10 nM). Data represent the mean ± SEM of two independent RNA samples from H295R cultures and are expressed as relative difference from cells untreated and transfected with scrambled siRNA (basal) (calibrator). (*, $P < 0.001$ compared with basal; **, $P < 0.001$ compared with TPA).

FIG. 8. Jun and Fos proteins are recruited to the CYP17 promoter and repress its transcription. (A) H295R cells were untreated (basal) or incubated for 1 h with Ang II (100 nM), TPA (10 nM) alone or in the presence PD98059 (10 μM). *In vivo* binding of Jun and Fos to the CYP17 promoter was examined using ChIP assay. Immunoprecipitated (Jun, Fos, IgG) and total (10% input) DNA were subject to PCR using specific primers. (B-E) H295R cells were transfected with the luciferase promoter construct containing 381 bp of the promoter region of the human CYP17 gene. (B) Cells were cotransfected with 0.1 μg of expression vector for AP-1 family members. (C-D) Cells were cotransfected with 0.3 μg of SF-1 expression vector, 0.1 μg of expression vector for the human jun and fos family members. (E) Effect of increasing doses of Fos (0.3, 1, 3, 10, 30, 100 ng) on constant amount of SF-1 (0.3 μg) and Jun (0.1 μg) expression plasmids. Data were normalized to coexpressed β-gal. Results represent the mean ± SEM of data from 2 to 3 independent experiments, each performed in triplicate. (*, $P < 0.001$ compared with SF-1; and ^, $P < 0.001$ compared with basal).

FIG. 9. Direct interaction between SF-1 and Fos. (A) H295R cells were transfected with the luciferase promoter construct containing 381 bp of the promoter region from the human CYP17 gene. Cells were cotransfected with increasing doses of SF-1 expression vector as indicated and 0.1 μg of expression vector for the human jun and fos. Results represent the mean ± SEM of data from 2 independent experiments, each performed in triplicate. (B) H295R cells were treated for the indicated times with Ang II (100 nM) or TPA (10 nM). Nuclear extracts were immunoprecipitated (IP) with an anti-Fos antibody, and then used for immunoblot analysis (WB) using an anti-SF-1 antibody. Western analyses shown represent data from three independent experiments. (C) H295R cells were transfected with the luciferase promoter construct containing 381 bp of the promoter region of the human CYP17 gene, in the presence of expression vector for SF-1 (0.3 μg), Jun (0.1 μg), Fos (0.1 μg), CBP (1 μg), SRC-1 (1 μg) or increasing doses of SRC-1, CBP, or SRC-1 plus CBP as indicated by the table under the graph. Results represent the mean ± SEM of data from 3 independent experiments, each performed in triplicate. (*, $P < 0.001$ and **, $P < 0.05$ compared with SF-1+Jun/Fos); ^, $P < 0.05$ compared with SF-1).

FIG. 10. Schematic model showing Ang II regulation of hCYP17 expression. One of the three adjacent AP1 and SF1-binding *cis*-elements in the CYP17 promoter are indicated. Ang II, acting through the type 1 Ang II receptor (AT1) activates PKC, which, in turn, activates ERK1/2. ERK1/2 activate fos transcription. Fos heterodimerizes with Jun and the Jun/Fos dimers bind to the CYP17 AP-1 *cis*-elements. The bound AP-1 complexes repress CYP17 gene expression as a consequence of decreased binding of the co-activators SRC-1 and CBP to the SF-1 protein. This decreased CYP17 transcription characterizes the glomerulosa phenotype and allows zonal production of aldosterone.

FIG.1

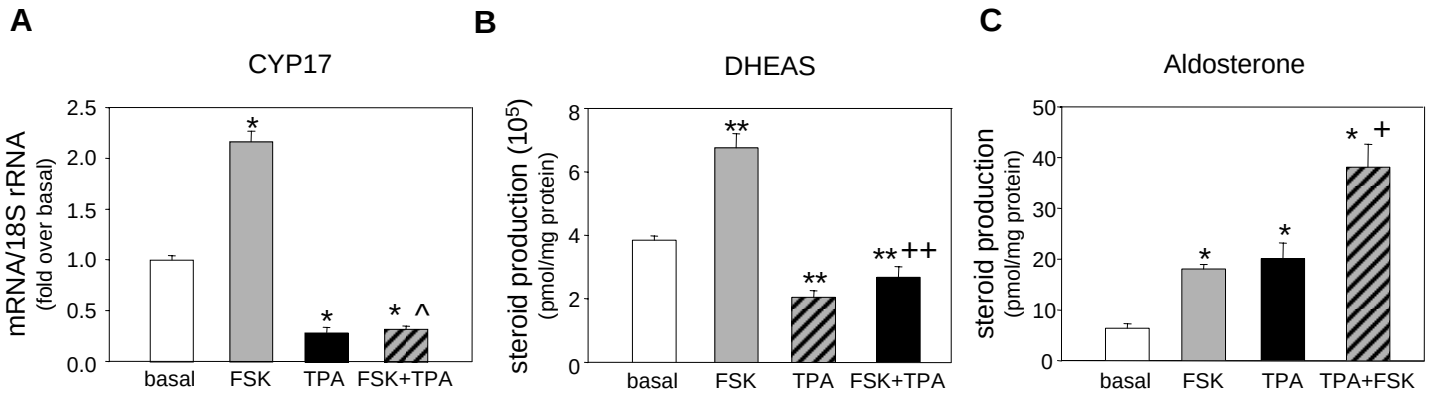

FIG.1. Activation of PKC represses expression of CYP17 and promotes a glomerulosa-like phenotype in H295R cells. Real-time RTPCR was used to quantify CYP17 transcript levels (A) while steroid assays were employed to measure medium levels of DHEAS (B) or aldosterone (C). Basal (untreated) cells were used as control. Cells were incubated for 24 h with forskolin (FSK) (10 μM), TPA (10 nM) or FSK (10 μM) plus TPA (10 nM). For real-time RTPCR data represent the mean ± SEM of three independent RNA samples from H295R cultures and are expressed as relative difference from basal (calibrator) as indicated in the Material and Methods section. Steroid content of the medium was determined by RIA and normalized to the amount of cell protein present in each tissue culture well. Steroid data points are the mean ± SEM of values from three experiments each performed in triplicate and expressed as pmol steroid/mg protein. (* $P < 0.05$ compared with basal; ^ $P < 0.05$ compared with FSK; ** $P < 0.001$ compared with basal; ++ $P < 0.001$ compared with FSK; + $P < 0.05$ compared with FSK or TPA).

FIG. 2

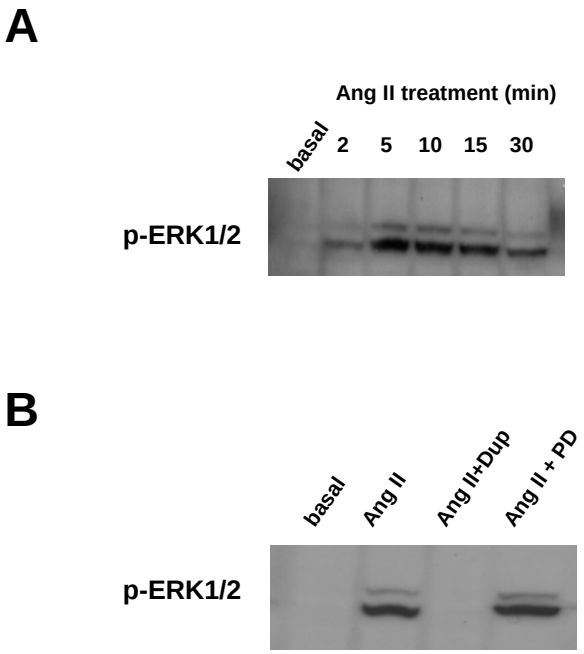

FIG. 2. Activation of ERK-1/2 in H295R cells. H295R cells were maintained in low serum overnight and then treated as indicated. The phosphorylated forms of ERK-1 and -2 were examined by immunoblot analysis using equivalent amounts of protein from total cellular lysate. Basal (untreated) cells were used as control. (A) Cells were incubated for the indicated times with Ang II (100 nM). (B) Cells were either untreated (basal) or preincubated for 30 min with the AT1 receptor inhibitor Dup 753 (10 μM) or the AT2 receptor inhibitor PD123319 (10 μM) and then incubated for 5 min with Ang II (100 nM). Western analyses shown represent data from three independent experiments.

FIG. 3

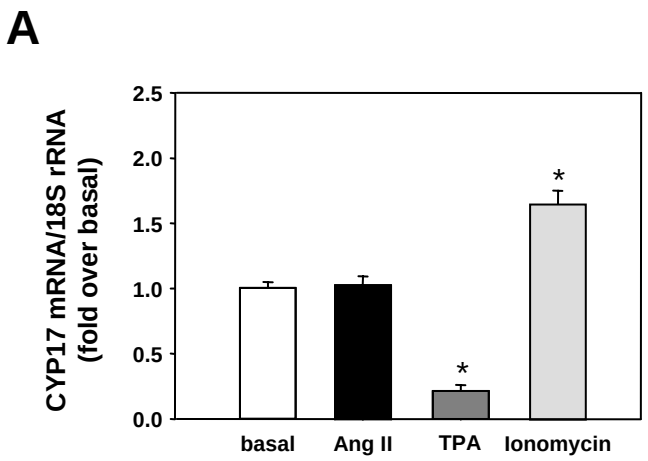

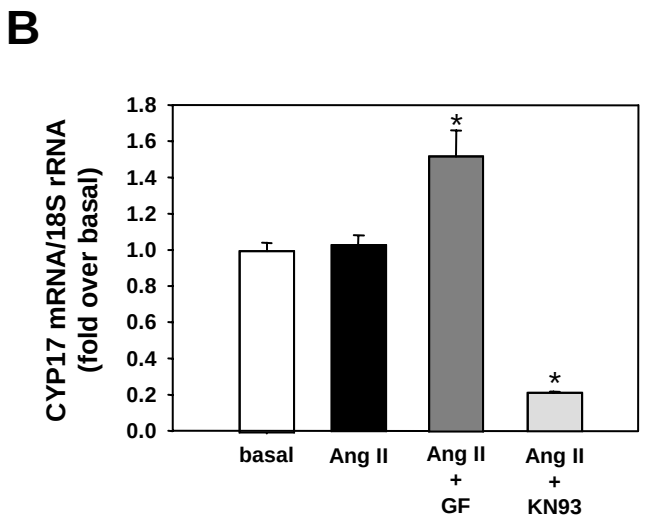

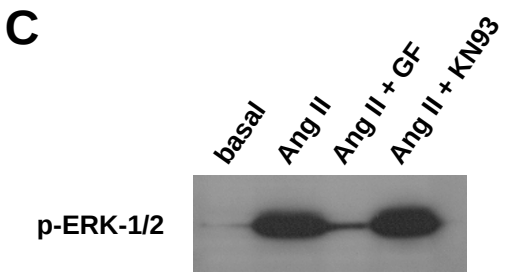

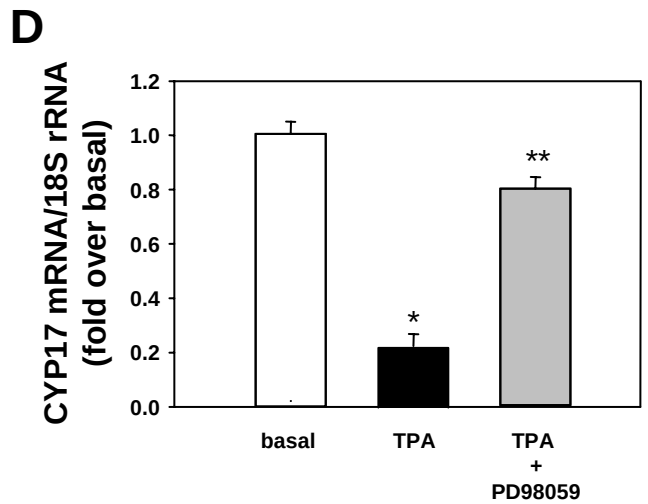

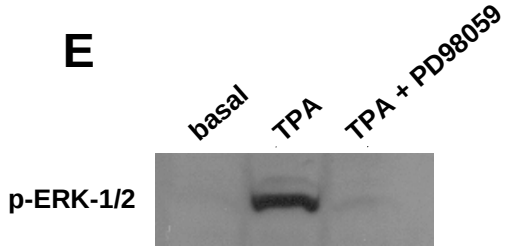

FIG. 3. CYP17 mRNA expression depends on the status of ERK1/2 activation. Real-time RTPCR was used to quantify CYP17 transcript levels in H295R cells. The phosphorylated forms of ERK-1 and -2 were examined by immunoblot analysis using equivalent amounts of protein from total cellular lysate. Basal (untreated) cells were used as control. (A) CYP17 expression in H295R cells incubated for 24 h with Ang II (100 nM), TPA (10 nM) or Ionomycin (1 μM). (B) CYP17 expression in H295R cells incubated for 24 h with Ang II (100 nM), with Ang II plus the PKC inhibitor GF109203X (GF) (5 μM) or Ang II plus the Cam kinase inhibitor KN93 (5 μM). (C) ERK-1/2 phosphorylation in cells untreated (basal) or incubated for 5 min with Ang II (100 nM), Ang II plus the PKC inhibitor GF109203X (GF) (5 μM) or Ang II plus the Cam kinase inhibitor KN93 (5 μM). (D) CYP17 expression in H295R cells incubated for 24 h with TPA (10 nM) alone or in the presence of ERK-1/2 inhibitor PD98059 (10 μM). (E) ERK-1/2 phosphorylation in cells incubated with TPA (10 nM) for 5 min or preincubated for 30 min PD98059 (10 μM) before 5 min incubation with TPA (10 nM). Western analyses shown represent data from three independent experiments. Real-time data represent the mean ± SEM of three independent RNA samples from H295R cultures and are expressed as relative difference from basal (calibrator) as indicated in the Material and Methods section. (*, $P < 0.001$ compared with basal).

FIG. 4

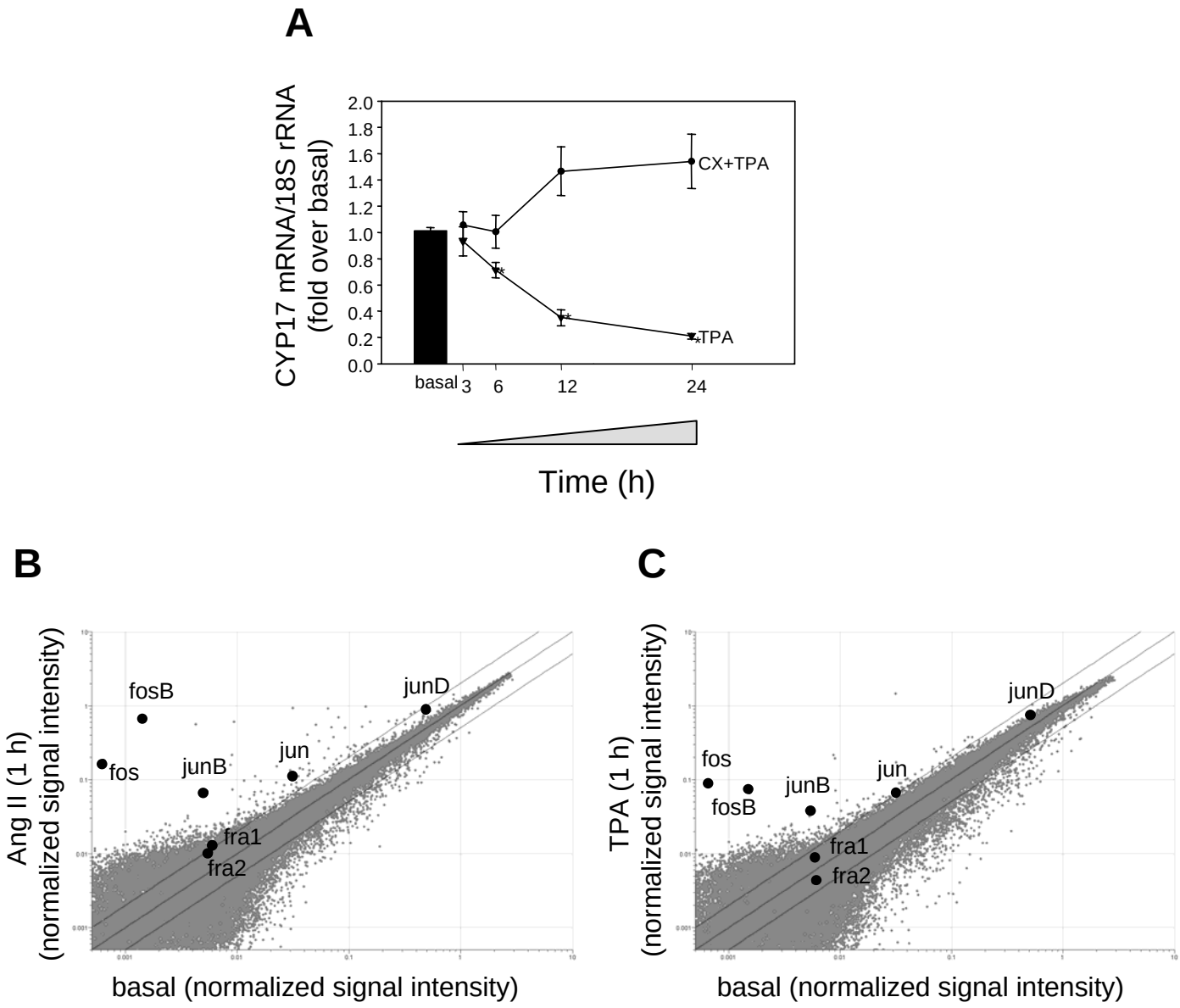

FIG. 4. TPA-induced inhibition of CYP17 mRNA is dependent on protein synthesis. (A) H295R cells were incubated for the indicated times with TPA (10 nM) alone or in the presence of cycloheximide (10 μM). Real-time RTPCR analysis was used to quantify CYP17 transcript levels. Data represent the mean ± SEM of three independent RNA samples from H295R cultures and are expressed as relative difference from basal (calibrator). (*, $P < 0.001$ compared with basal). (B) Microarray analysis of H295R cells treated for 1 h with 100 nM Ang II vs basal (untreated) cells and (C) cells treated for 1 h with 10 nM TPA vs basal cells. Each spot represents a unique sequence with a total of approximately 38,500 transcripts examined per array. Pure signal were normalized to a list of 100 normalization control probe sets provided by Affymetrix. Spots outside of the parallel lines represent mRNAs with greater than 2-fold differences in expression. AP-1 family member genes are indicated.

FIG. 5

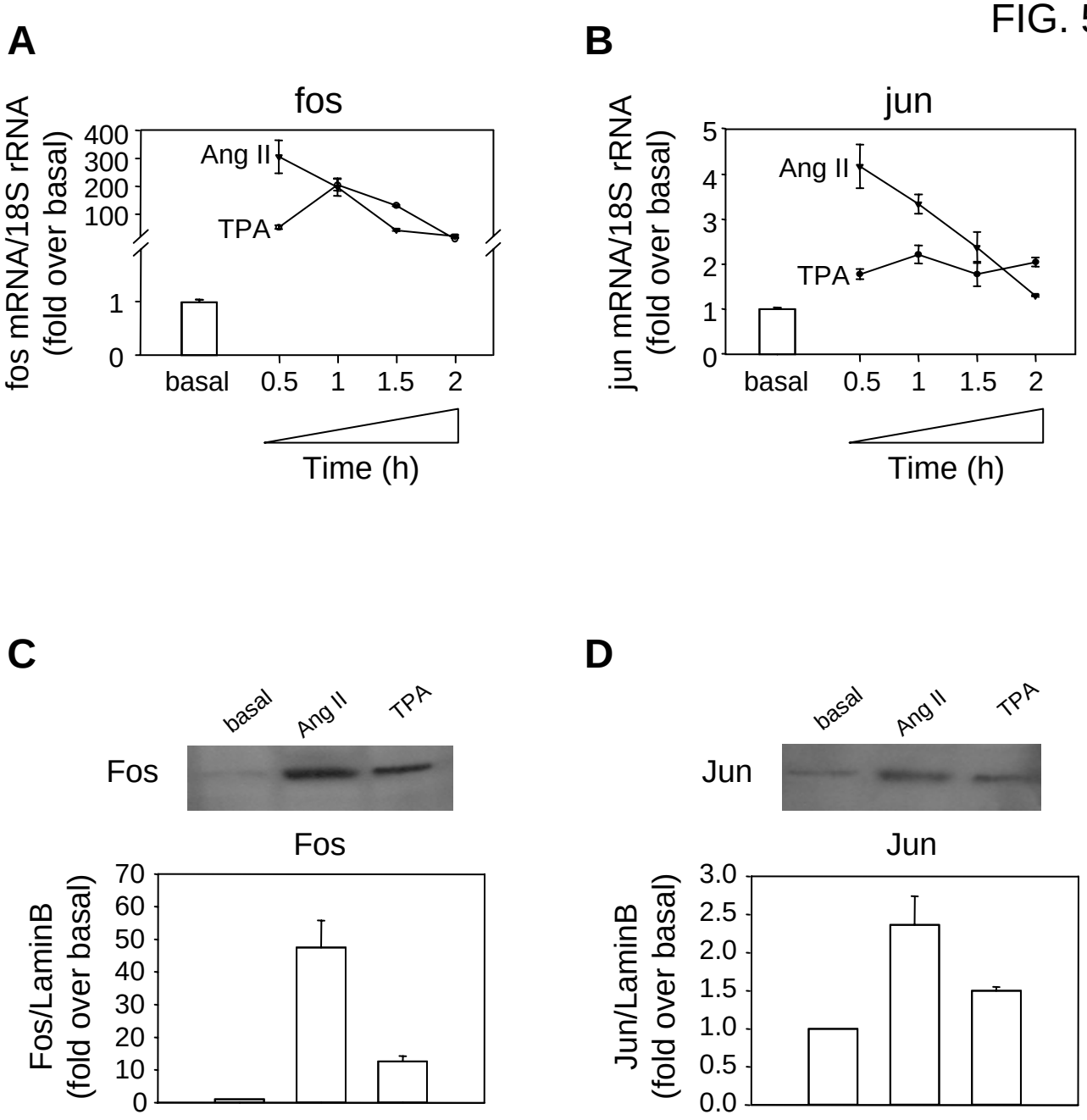

FIG. 5. Effect of Ang II and TPA on expression of jun and fos. H295R cells were incubated for the indicated times with TPA (10 nM) or with Ang II (100 nM). Real-time RTPCR was used to quantify fos (A) and jun (B) transcript levels. Data represent the mean ± SEM of three independent RNA samples from H295R cultures and are expressed as relative difference from basal (calibrator). Cells were incubated with TPA (10 nM) or Ang II (100 nM) for 1 h. Fos (C) and Jun (D) protein levels were examined by immunoblot analysis using equivalent amounts of nuclear extracts. Graphs depicted below western blots were obtained by densitometric analysis. Protein expression in each lane was normalized to the lamin B content, and expressed as relative difference from basal levels. Western analyses shown represent data from three independent experiments.

FIG. 6

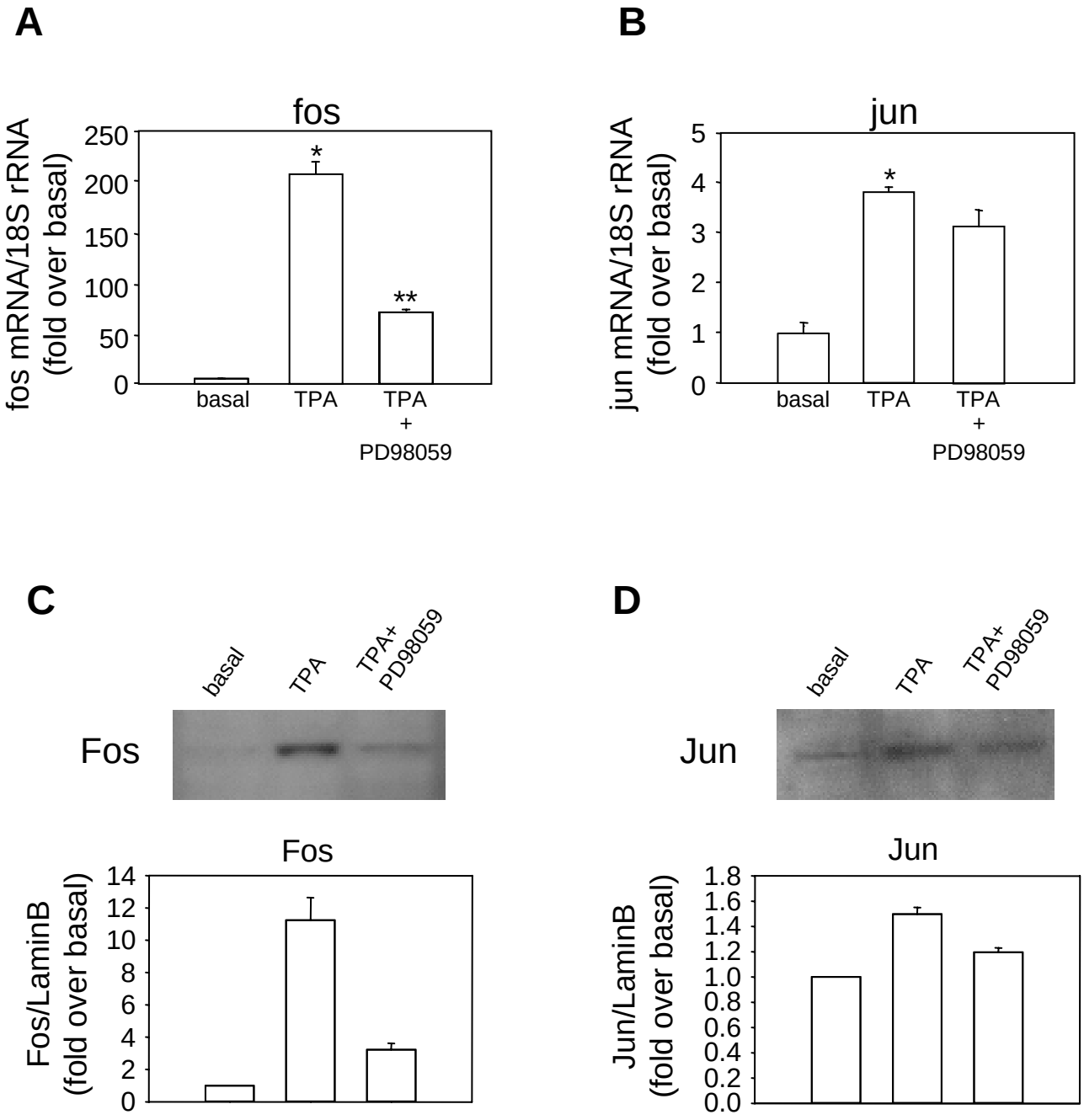

FIG. 6. Effect of PD98059 on TPA-mediated induction of fos and jun. H295R cells were incubated for 1 h with TPA (10 nM) alone or in the presence of PD98059 (10 μM). Total RNA was extracted and real-time RTPCR was used to quantify fos (A) and jun (B) transcript levels. Data represent the mean ± SEM of three independent RNA samples from H295R cultures and are expressed as relative difference from basal (calibrator). Fos (C) and Jun (D) protein levels were examined by immunoblot analysis using equivalent amounts of nuclear extracts. Graphs depicted below western blots were obtained by densitometric analysis. Protein expression in each lane was normalized to the lamin B content, and expressed as relative difference from basal levels. Western analyses shown represent data from three independent experiments. (*, $P < 0.001$ compared with basal; **, $P < 0.001$ compared with TPA).

FIG. 7

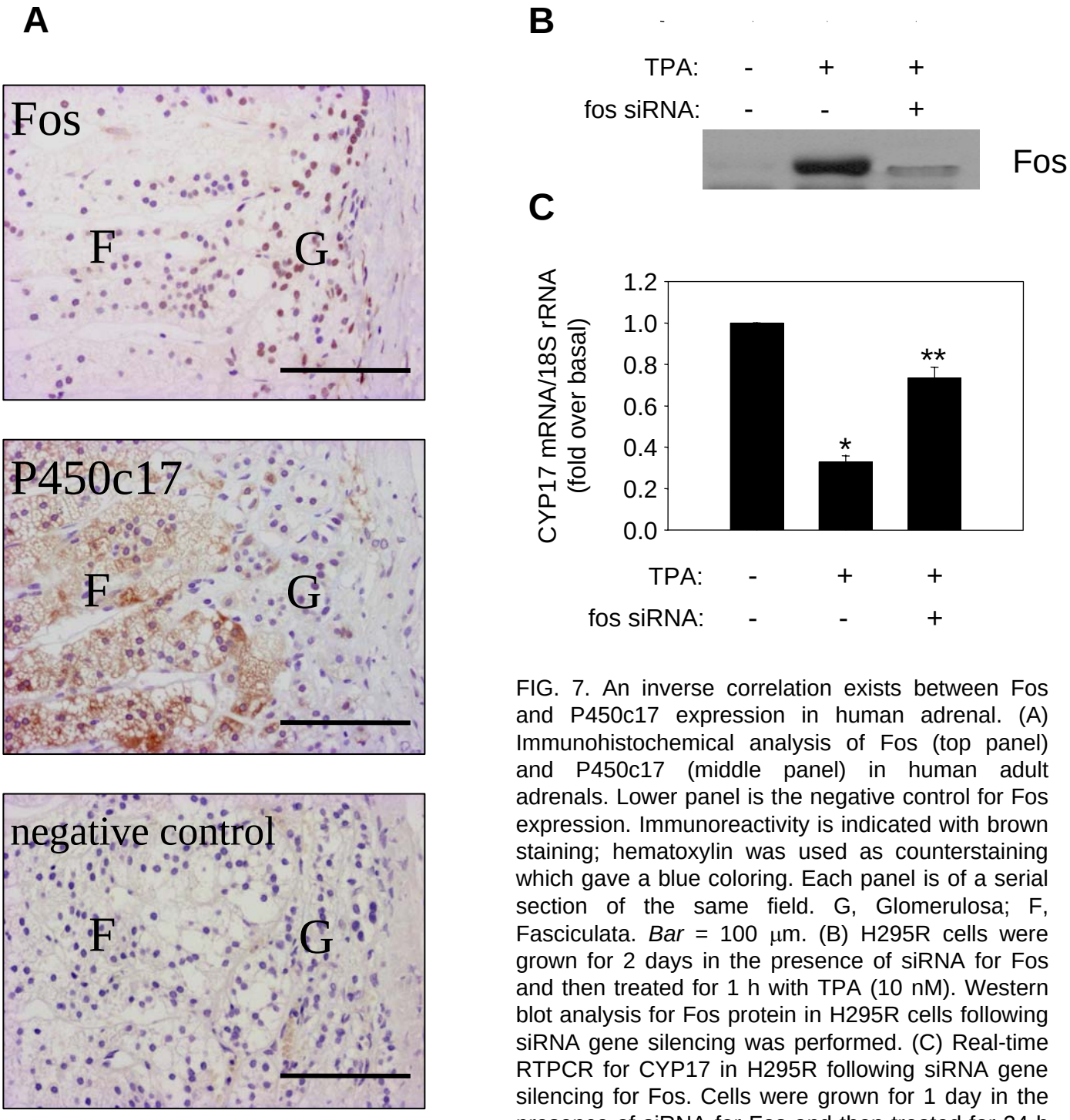

FIG. 7. An inverse correlation exists between Fos and P450c17 expression in human adrenal. (A) Immunohistochemical analysis of Fos (top panel) and P450c17 (middle panel) in human adult adrenals. Lower panel is the negative control for Fos expression. Immunoreactivity is indicated with brown staining; hematoxylin was used as counterstaining which gave a blue coloring. Each panel is of a serial section of the same field. G, Glomerulosa; F, Fasciculata. *Bar* = 100 μm. (B) H295R cells were grown for 2 days in the presence of siRNA for Fos and then treated for 1 h with TPA (10 nM). Western blot analysis for Fos protein in H295R cells following siRNA gene silencing was performed. (C) Real-time RTPCR for CYP17 in H295R following siRNA gene silencing for Fos. Cells were grown for 1 day in the presence of siRNA for Fos and then treated for 24 h with TPA (10 nM). Data represent the mean ± SEM of two independent RNA samples from H295R cultures and are expressed as relative difference from cells untreated and transfected with scrambled siRNA (basal) (calibrator). (*, $P < 0.001$ compared with basal; **, $P < 0.001$ compared with TPA).

FIG. 8

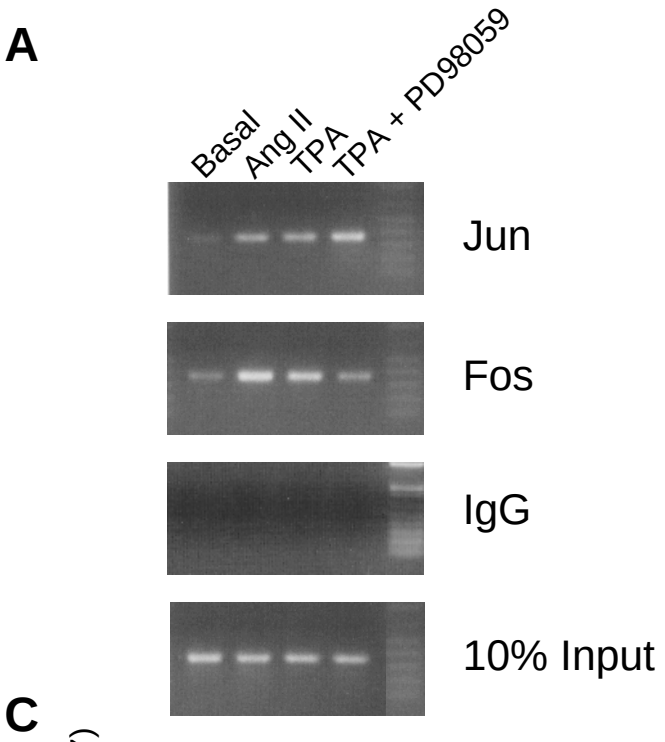

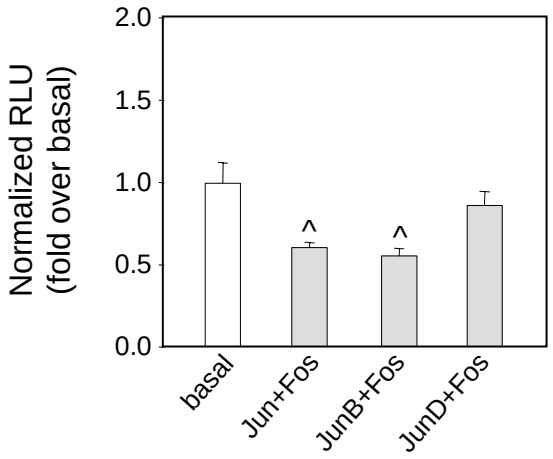

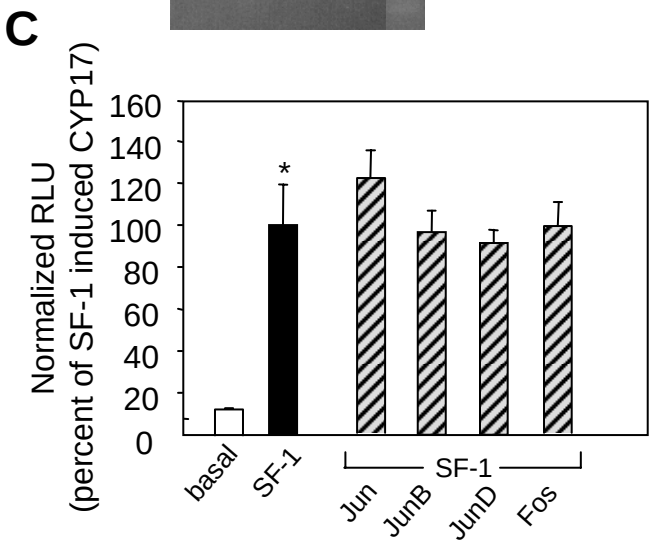

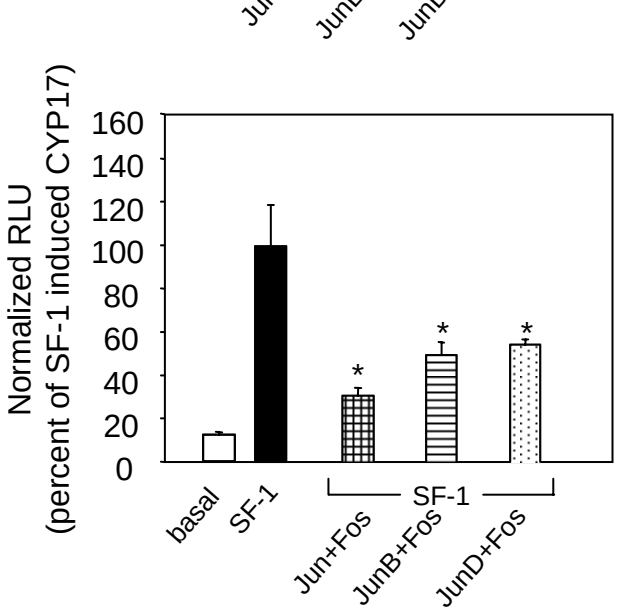

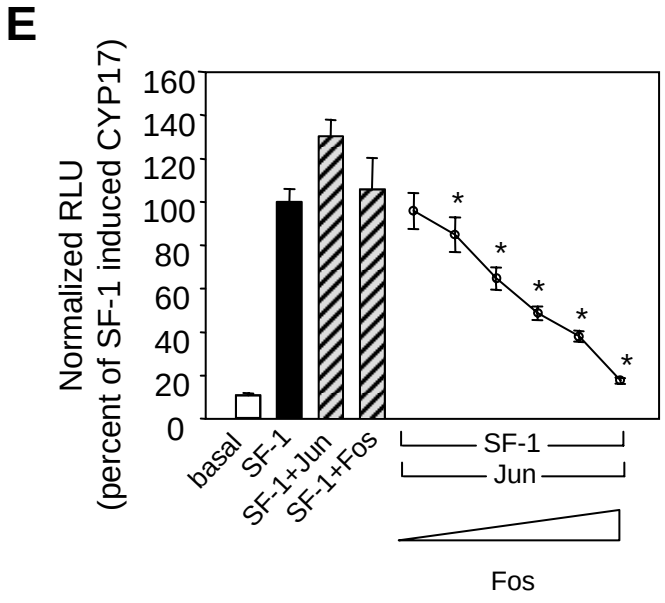

FIG. 8. Jun and Fos proteins are recruited to the CYP17 promoter and repress its transcription. (A) H295R cells were untreated (basal) or incubated for 1 h with Ang II (100 nM), TPA (10 nM) alone or in the presence PD98059 (10 μM). *In vivo* binding of Jun and Fos to the CYP17 promoter was examined using ChIP assay. Immunoprecipitated (Jun, Fos, IgG) and total (10% input) DNA were subject to PCR using specific primers. (B-E) H295R cells were transfected with the luciferase promoter construct containing 381 bp of the promoter region of the human CYP17 gene. (B) Cells were cotransfected with 0.1 μg of expression vector for AP-1 family members. (C-D) Cells were cotransfected with 0.3 μg of SF-1 expression vector, 0.1 μg of expression vector for the human jun and fos family members. (E) Effect of increasing doses of Fos (0.3, 1, 3, 10, 30, 100 ng) on constant amount of SF-1 (0.3 μg) and Jun (0.1 μg) expression plasmids. Data were normalized to coexpressed β-gal. Results represent the mean ± SEM of data from 2 to 3 independent experiments, each performed in triplicate. (*, $P < 0.001$ compared with SF-1; and ^, $P < 0.001$ compared with basal).

FIG. 9

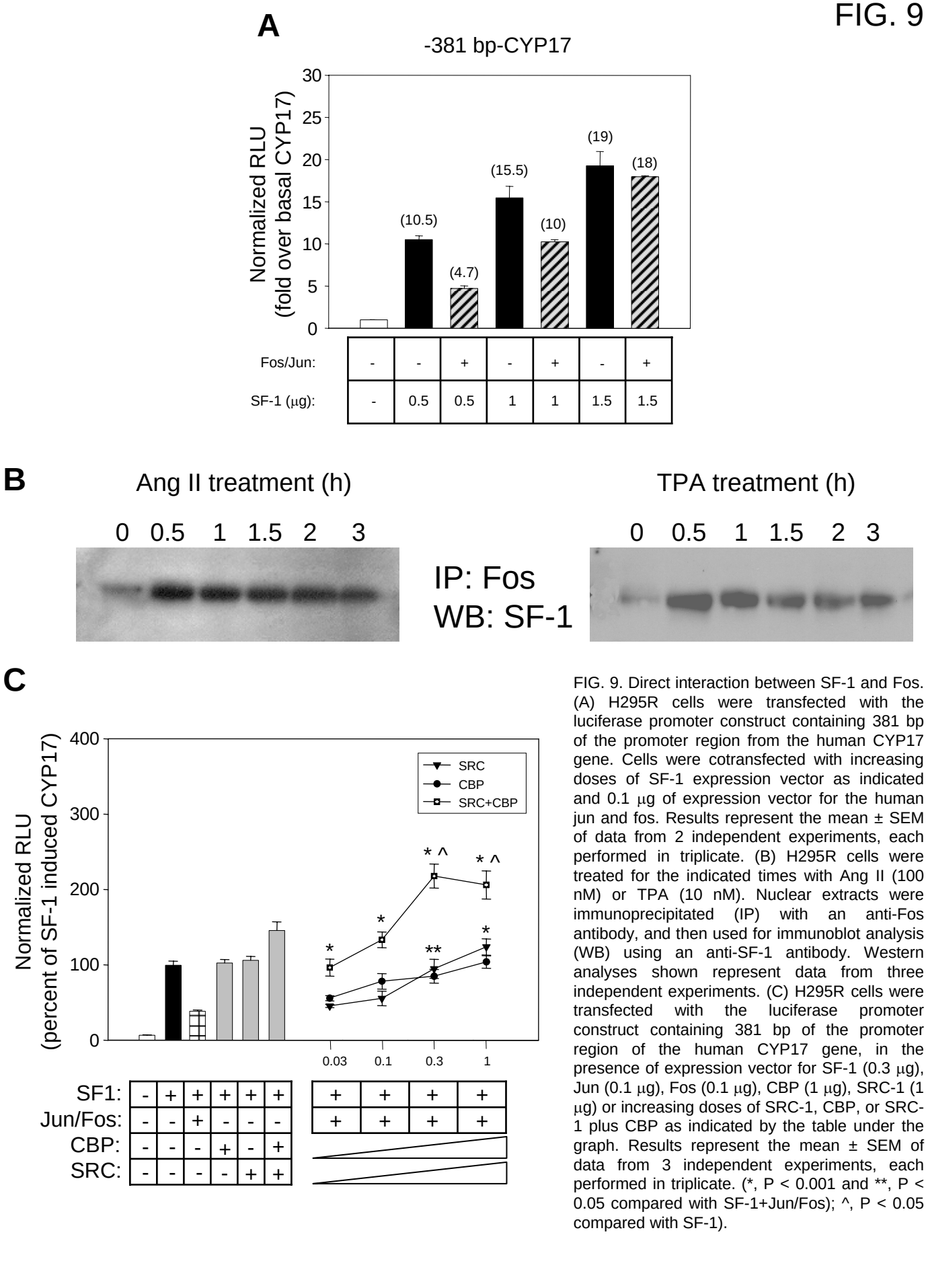

FIG. 9. Direct interaction between SF-1 and Fos. (A) H295R cells were transfected with the luciferase promoter construct containing 381 bp of the promoter region from the human CYP17 gene. Cells were cotransfected with increasing doses of SF-1 expression vector as indicated and 0.1 μg of expression vector for the human jun and fos. Results represent the mean ± SEM of data from 2 independent experiments, each performed in triplicate. (B) H295R cells were treated for the indicated times with Ang II (100 nM) or TPA (10 nM). Nuclear extracts were immunoprecipitated (IP) with an anti-Fos antibody, and then used for immunoblot analysis (WB) using an anti-SF-1 antibody. Western analyses shown represent data from three independent experiments. (C) H295R cells were transfected with the luciferase promoter construct containing 381 bp of the promoter region of the human CYP17 gene, in the presence of expression vector for SF-1 (0.3 μg), Jun (0.1 μg), Fos (0.1 μg), CBP (1 μg), SRC-1 (1 μg) or increasing doses of SRC-1, CBP, or SRC-1 plus CBP as indicated by the table under the graph. Results represent the mean ± SEM of data from 3 independent experiments, each performed in triplicate. (*, $P < 0.001$ and **, $P < 0.05$ compared with SF-1+Jun/Fos); ^, $P < 0.05$ compared with SF-1).

FIG. 10

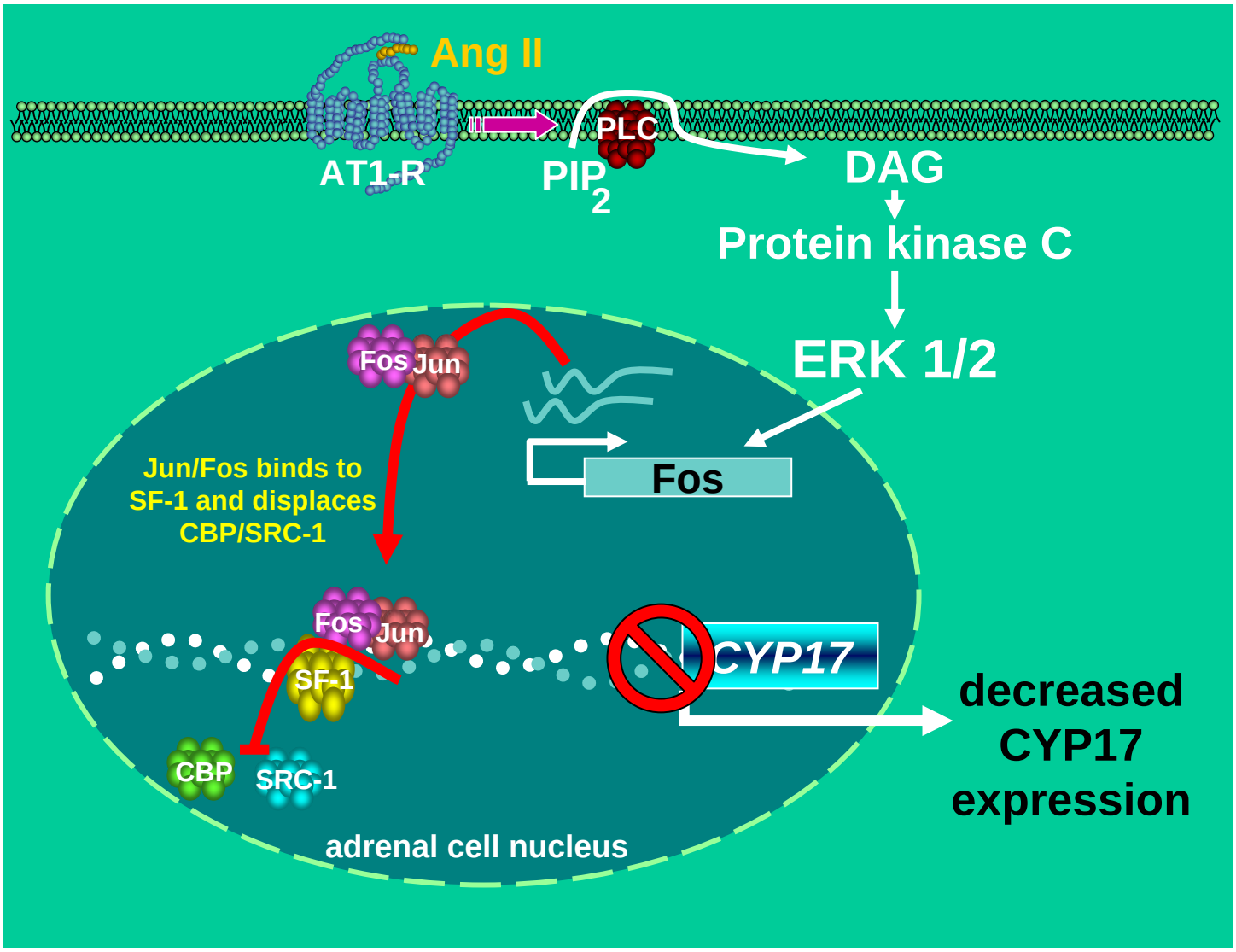

FIG. 10. Schematic model showing Ang II regulation of hCYP17 expression. One of the three adjacent AP1 and SF1-binding *cis*-elements in the CYP17 promoter are indicated. Ang II, acting through the type 1 Ang II receptor (AT1) activates PKC, which, in turn, activates ERK1/2. ERK1/2 activate fos transcription. Fos heterodimerizes with Jun and the Jun/Fos dimers bind to the CYP17 AP-1 *cis*-elements. The bound AP-1 complexes repress CYP17 gene expression as a consequence of decreased binding of the co-activators SRC-1 and CBP to the SF-1 protein. This decreased CYP17 transcription characterize the glomerulosa phenotype and allows zonal production of aldosterone.

Submitted to Cancer Research November 2006 manuscript #CAN 06-4064

IGF-I regulating aromatase expression through SF-1, supports estrogen-dependent tumor Leydig cell proliferation

Rosa Sirianni[1]*, Adele Chimento[1]*, Rocco Malivindi[1], Ignazio Mazzitelli[1], Sebastiano Andò[2], and Vincenzo Pezzi[1].

Departments of [1]Pharmaco-Biology and [2]Cell Biology University of Calabria Arcavacata di Rende (CS) Italy.

* These authors contributed equally to this work.

Running title: IGF-I and estrogen-dependent tumor Leydig cell proliferation
Key words: Leydig cell tumor, IGF-I, aromatase, estrogen

Requests for reprints:
Prof. Vincenzo Pezzi
Department of Pharmaco-Biology
Università della Calabria
87036 RENDE (CS) - ITALY
Tel.: +39 - 0984 - 493157
Fax: +39 - 0984 - 493271
E-Mail: v.pezzi@unical.it

This work was supported by PRIN-MIUR N°2004067227

Abstract

Aim of this study was to investigate the role of estrogens in Leydig cell tumor proliferation. We used rat R2C Leydig tumor cells and testicular samples from Fischer rats with a developed Leydig tumor (FRTT). Both experimental models express high levels of aromatase and Estrogen Receptor alpha (ERα). Treatment with exogenous E2 induced proliferation of R2C cells and upregulation of cell cycle regulators cyclin D1 and E, that were blocked by addition of antiestrogens. These observations leaded us to suppose an E2/ERα dependent mechanism for Leydig cell tumor proliferation. Determining the molecular mechanism responsible for aromatase overexpression, we found that total and phosphorylated levels of transcription factors CREB and SF-1 were higher in tumor samples. Moreover, we found that R2C cells produce also high levels of IGF-I that increased aromatase mRNA, protein and activity as a consequence of increased total and phosphorylated SF-1 levels and that specific inhibitors for IGF-I receptor, Protein Kinase C and Phosphoinositol-3-kinase determined a reduction in SF1 and consequently in aromatase expression and activity. The same inhibitors were also able to inhibit the IGF-1 dependent-SF-1 recruitment to the aromatase PII promoter as shown with ChIP assays. We conclude that one of the molecular mechanims determining Leydig cell tumorogenesis is an excessive estrogen production stimulating a short autocrine loop determining cell proliferation. In addition, cell produced IGF-I amplifies estrogen signaling through a SF-1-dependent up-regulation of aromatase expression. The finding of this new molecular mechanism will be helpful in defining new therapeutic approaches of Leydig cell tumor.

Introduction

The etiology and pathogenesis of human testicular tumors are poorly defined. Several studies have demonstrated how in human exposure to an excess of estrogens in prenatal and perinatal periods (1, 2) or in the adulthood In addition exposure to an excess of estrogens in the adulthood, as it occurs in gynecomastia (3), estrogenic treatment of prostate cancer (4) or in the case of occupational contact with xenoestrogen (5-6) appear linked to a higher risk for testicular cancer. Moreover it has been reported that estrogen serum levels are elevated in patients with testicular germ cell cancer as a consequence of increased local estrogen production reflecting an higher aromatase activity present in Sertoli and Leydig cells (7, 8). Ninety-five percent of all human testicular neoplasms arise from germinal cells while Leydig cell tumors are the most common tumors of the gonadal stroma (9).

In rodents, reproductive system tumors in general are uncommon, with the few exceptions of Leydig cell and ventral prostatic neoplasms in some rat strains (10) or in non-inbred mice (11), however analogously to the human, chronic administration of estrogens induced testicular tumors (12).

A useful model utilized to investigated if an excess of estrogens might have a central role in the mechanism leading to testicular tumorogenesis are transgenic mice overexpressing aromatase and presenting enhancement of E2 circulating levels (13). About half of these male mice were infertile and/or had enlarged testis and showed Leydig cell hyperplasia and Leydig cell tumors (13) while the female of these mice revealed mammary glands hyperplasia associated with an altered expression of proteins involved in apoptosis, cell cycle, growth and tumor suppression (14). Whereas the effects of estrogen on mammary gland tumorogenesis in human and in rodents is well known, the role of aromatase overexpression and in situ estrogen production in testicular tumorogenesis is not clearly defined. In this study we have investigated the molecular mechanisms causing aromatase overexpression and the effect of estradiol (E2) overproduction on rat Leydig cell tumor proliferation. As experimental model we used rat R2C Leydig tumor cell line and to validate our in vitro data in an in

vivo model we used Leydig cell tumors from old Fisher rat testes in which the incidence of the spontaneous neoplasm is exceptionally high in aged animals (15).

Aromatase activity is regulated primarily at the level of gene expression and is present in testis somatic cells and along the maturative phases of male germ cells (16, 17). The CYP19 gene that encodes aromatase has at least 8 unique promoters that are used in a tissue-specific manner (18). The proximal promoter II regulates aromatase expression in human fetal and adult testis, R2C and H540 rat Leydig tumour cells and purified preparations of rat Leydig, Sertoli and germ cells (19, 20). Specific sequences appear to be mainly involved in aromatase expression: a sequence that contains an half-site binding nuclear receptors (AGGTCA) in position -90 in the rat binding SF-1 (21) and CRE-like sequences binding CREB/ATF protein families (22, 23) localized upstream respect the first one [in the rat in position -169 (TGCACGTCA) -335 (TGAACTCA) e -231 (TGAAATCA)] (24). Similar responsive elements (binding CRE and SF-1) have been reported on Steroidogenic Acute Regulatory (StAR) protein gene promoter (25) whose expression is regulated by IGF-1 signaling in Leydig cells. As StAR protein is involved in the transfer of cholesterol from the outer to the inner mitochondrial membrane, the rate-limiting and regulated step in steroidogenesis, IGF-I plays an important role on the regulation of testicular steroid biosynthesis.

For these reasons we investigated the role of Insulin-like growth factor-I (IGF-I) a peptide also demonstrated to have a role in testicular growth and development, control of Leydig cell number (26). IGF-I is produced locally in the testis, in Sertoli, Leydig and peritubular cells derived from the immature rat testis and cultured in vitro (27, 28). The crucial role of IGF-I in the development and function of Leydig cells was highlighted by studies on IGF-I gene knock-out mice (29, 30). The failure of adult Leydig cells to mature and the reduced capacity for T production is caused by deregulated expression of testosterone (T) biosynthetic and metabolizing enzymes (31). Expression levels of all

mRNA species associated with T biosynthesis were lower in the absence of IGF-I. However, this study didn't investigate the effect on aromatase expression, even though an effect could be supposed.

Starting from these findings, in this study we investigate if a testicular overproduction of IGF-I could be one of the mechanisms determining aromatase overexpression in rat tumor Leydig cells through the activation of specific transcriptional factors. The high related Leydig cells E2 production through an autocrine/paracrine mechanism mediated by their own receptors, could contribute to the hormone dependence of testicular tumorogenesis stimulating Leydig tumor cell proliferation.

Materials and Methods

Cell cultures and animals. TM3 cells (mouse Leydig cell line) were cultured in D-MEM/F-12 medium supplemented with 5% HS, 2.5% FBS and antibiotics (Invitrogen, S.R.L., San Giuliano Milanese, Italy); R2C cells (rat Leydig tumor cell line) were cultured in Ham/F-10 medium supplemented with 15% HS, 2.5% FBS and antibiotics (Invitrogen, S.R.L., San Giuliano Milanese, Italy). Male Fischer 344 rats (a generous gift of Sigma-Tau Pomezia, Italy), 6 (FRN) and 24 (FRT) months of age were used for studies. 24 months old animals presented spontaneously developed Leydig cell tumors absent in younger animals. Testes of all animals were surgically removed by qualified, specialized animal care staff in accordance with the Guide for Care and Use of Laboratory Animals (National Institutes of Health) and used for experiments.

Aromatase activity assay. The aromatase activity in subconfluent R2C cell culture medium was measured by tritiated water-release assay using 0.5 μM [1β-^{3}H(N)]androst-4-ene-3,17-dione (DuPont NEN, Boston, MA, USA) as a substrate (32). Incubations were performed at 37 °C for 2 h under a 95%:5% air/CO2 atmosphere. Obtained results were expressed as pmol/h and normalized to milligram of protein (pmol/h per mg protein).

Radioimmunoassay. Prior to experiments, TM3 cells were maintained overnight in DME/F12 medium and R2C cells in Ham/F-10 (medium only). The Estradiol content of medium recovered from each well was determined against standards prepared in low serum medium using a radioimmunoassay kit (DSL 43100; Diagnostic System Laboratories, Webster, TX, USA). Results assay were normalized to the cellular protein content per well and expressed as pmol per mg cell protein. IGF-I content in medium recovered from each well of R2C and TM3 cells was determined following extraction and assay protocols provided with the mouse/rat IGF-I radioimmunoassay kit (DSL 2900; Diagnostic System Laboratories, Webster, TX, USA).

Chromatin Immunoprecipitation (ChIP). This assay was performed using the ChIP assay kit from Upstate (Lake Placid, NY) with minor modifications in the protocol. R2C cells were grown in 100 mm plates. Confluent cultures (90 %) were treated for 24 h with AG1024 (Sigma St Louis, MO, USA), PD98059 (Calbiochem, VWR International S.R.L. Milano), LY294002 (Calbiochem, VWR International S.R.L. Milano), GF109203X (Calbiochem, VWR International S.R.L. Milano) or for increasing times with 100 ng/ml IGF-I (Sigma St Louis, MO, USA) or left untreated. Following treatment DNA/protein complexes were crosslinked with 1 % formaldehyde at 37 °C for 10 min. Next, cells were collected and resuspended in 400 µl of SDS lysis buffer (Upstate Technology, Lake Placid, NJ) and left on ice for 10 min. Then, cells were sonicated four times for 10 sec at 30 % of maximal power and collected by centrifugation at 4 °C for 10 min at 14 000 rpm. Of the supernatants 10 µl were kept as input (starting material, to normalize results) while 100 µl were diluted 1:10 in 900 µl of ChIP dilution buffer (Upstate Technology, Lake Placid, NJ) and immunocleared with 80 µl of sonicated salmon sperm DNA protein A agarose (Upstate) for 6 h at 4 °C. Immunocomplex was formed using 1 µl of 1:5 dilution of specific antibody anti-SF-1 (provided by Prof. Ken-ichirou Morohashi, Division for Sex Differentiation, National Institute for Basic Biology, National Institutes of Natural Sciences,

Myodaiji-cho, Okazaki, Japan) overnight at 4 °C. Immunoprecipitation with salmon sperm DNA protein A agarose was continued at 4 °C until the day after. DNA/protein complexes were reverse crosslinked overnight at 65 °C. Extracted DNA was resuspended in 20 µl of TE buffer. 3 µl volume of each sample and input were used for PCR using CYP19 promoter II specific primers. The PCR conditions were 1 min at 94 °C, 1 min at 50 °C and 2 min at 72 °C for 30 cycles using the following primers: forward, 5'-TCAAGGGTAGGAATTGGGAC-3'; reverse, 5'-GGTGCTGGAATGGACAGATG-3'. Amplification products were analyzed on a 1 % agarose gel and visualized by ethidium bromide staining. In control samples, non immune rabbit IgG was used instead of specific antibodies.

Real-time RTPCR. Prior to experiments, cells were maintained overnight in low serum medium. Cells were then treated or the indicated times and RNA was extracted from cells using the TRiazol RNA isolation system (Invitrogen). TRiazol was also used to homogenize total tissue of normal (FRNT) and tumor (FRTT) Fisher rat testes for RNA extraction. Each RNA sample was treated with DNase I (Ambion, Austin, TX), and purity and integrity of the RNA was confirmed spectroscopically and by gel electrophoresis prior to use. One µg of total RNA was reverse transcribed in a final volume of 30 µl using the ImProm-II Reverse transcription system kit (Promega, Promega Italia S.R.L. Milano, Italy), cDNA was diluted 1:3 in nuclease free water, aliquoted and stored at –20°C. Primers for the amplification were based on published sequences for the rat CYP19, rat CREB and rat SF-1 genes. The nucleotide sequences of the primers for CYP19 were: forward 5'-GAGAAACTGGAAGACTGTATGGAT-3' and reverse 5'-ACTGATTCACGTTCTCCTTTGTCA-3'. For CREB amplification were used the following primers: forward 5'-AATATGCACAGACCACTGATGGA-3' and reverse 5'-TGCTGTGCGAATCTGGTATGTT-3'; for SF-1 amplification primers have been previously published (33). PCR reactions were performed in the

iCycler iQ Detection System (Biorad Hercules, CA, USA), using 0.1 μM of each primer, in a total volume of 30 μL reaction mixture following the manufacturer's recommendations. SYBR Green Universal PCR Master Mix (Biorad Hercules, CA, USA) with the dissociation protocol was used for gene amplification, negative controls contained water instead of first-strand cDNA. Each sample was normalized on the basis of its 18S ribosomal RNA content. The 18S quantification was performed using a TaqMan Ribosomal RNA Reagent kit (Applied Biosystems, Applera Italia, Monza, Milano, Italy) following the method provided in the TaqMan Ribosomal RNA Control Reagent kit (Applied Biosystems, Applera Italia, Monza, Milano, Italy). The relative gene expression levels were normalized to a calibrator that was chosen to be the basal, untreated sample. Final results were expressed as *n*-fold differences in gene expression relative to 18S rRNA and calibrator, calculated following the ΔΔCt method, as follows:

$$n\text{-fold} = 2^{-(\Delta Ct\text{sample} - \Delta Ct\text{calibrator})}$$

where ΔCt values of the sample and calibrator were determined by subtracting the average Ct value of the 18S rRNA reference gene from the average Ct value of the different genes analyzed.

Western-blot analysis. R2C and TM3 cells or total tissue of FRNT and FRTT were lysed in ice-cold Ripa buffer containing protease inhibitors (20 mM Tris, 150 mM NaCl, 1% Igepal, 0.5% sodium deoxycholate, 1 mM EDTA, 0·1% SDS, 1 mM PMSF, 0.15 units/ml aprotinin and 10 μM leupeptin) for protein extraction. The protein content was determined by Bradford method (34). The proteins were separated on 11% SDS/polyacrylamide gel and then electroblotted onto a nitrocellulose membrane. Blots were incubated overnight at 4 °C with 1. anti-human P450 aromatase antibody (1:50) (Serotec, Oxford, UK, MCA 2077), 2. anti-ERα (F-10) antibody (1:500) (Santa Cruz Biotechnology, Santa Cruz,

CA, USA, sc8002), 3. anti-ERβ (H-150) (1:1000) (Santa Cruz Biotechnology, Santa Cruz, CA, USA, sc8974), 4. anti-cyclin D1 (M-20) antibody (1:1000) (Santa Cruz Biotechnology, Santa Cruz, CA, USA, sc718), 5. anti-cyclin E (M-20) antibody (1:1000) (Santa Cruz Biotechnology, Santa Cruz, CA, USA, sc481), 6. anti-CREB antibodies (1:1000) (48H2, Cell Signaling Technology, Celbio, Milan, Italy) and (1:1000) (AHO0842Biosource Inc. Camarillo CA USA); 7. anti-pCREB ser133 (87G3) (1:1000) (Cell Signaling Technology, Celbio, Milan, Italy) or anti-pCREB Ser129/133 (1:1000) (Biosource Inc. Camarillo CA USA, 44-297G), 8. anti SF-1 (1:1000) provided by Prof. Ken-ichirou Morohashi, Division for Sex Differentiation, National Institute for Basic Biology, National Institutes of Natural Sciences, Myodaiji-cho, Okazaki, Japan), 9. anti-pSF-1 (1:1000) provided by Dr Holly A. Ingraham Department of Physiology, University of California, San Francisco, San Francisco, California 94143-0444, USA), 10. anti-actin (C-2) antibody (1:1000) (Santa Cruz Biotechnology, Santa Cruz, CA, USA, sc8432). Membranes were incubated with horseradish peroxidase (HRP)-conjugated secondary antibodies (Amersham Pharmacia Biotech, Piscataway, NJ) and immunoreactive bands were visualized with the ECL western blotting detection system (Amersham Biosciences, Cologno Monzese, Italy). To assure equal loading of proteins membranes were stripped and incubated overnight with β-actin antiserum.

Cell-proliferation assay. For proliferative analysis a total of $1x10^5$ cells were seeded onto 12-well plates in complete medium and let grow for 2 days. Prior to experiments, cells were maintained overnight in Ham/F-10 medium and the day after treated with ICI 182780, a gift from Astra-Zeneca (Basiglio, Milano, Italy), 4-hydroxytamoxifen (OHT) (Sigma St Louis, MO, USA) and Letrozole, a gift from Novartis Pharma AG (Basel, Switzerland) and 17β-estradiol (E2) (Sigma St Louis, MO, USA). Control (basal) cells were treated with the same amount of vehicle alone (DMSO) that never exceeded the concentration of 0.01% (v/v). [3H]Thymidine incorporation was evaluated after a 24-h incubation

period with 1 μCi [^{3}H]thymidine (PerkinElmer Life Sciences, Boston, MA, USA) per well. Cells were washed once with 10% trichloroacetic acid, twice with 5% trichloroacetic acid and lysed in 1 ml 0.1 M NaOH at 37°C for 30 min. The total suspension was added to 10 ml optifluor fluid and was counted in a scintillation counter.

Data Analysis and Statistical Methods. Pooled results from triplicate experiments were analyzed using one-way ANOVA with Student-Newman-Keuls multiple comparison methods, using SigmaStat version 3.0 (SPSS, Chicago, IL).

Results

Estradiol induces Leydig cell tumor proliferation through an autocrine mechanism. We performed our study utilizing as model system R2C Leydig tumor cells. These cells have been demonstrated to have high aromatase expression and, consequently, activity (21), while we used another Leydig cell line, TM3 cells, as a normal control. We also analyzed testes from older and younger Fischer rats. Aged animals have a high incidence of spontaneous neoplasm of Leydig cells (15, 35), a phenomenon not observed in younger animals, allowing us to use them as a good *in vivo* model to confirm results obtained in cell lines. Our first step was to measure estradiol content in culture medium of R2C and TM3 cells maintained in culture for increasing time. While E2 levels in TM3 medium were extremely low (data not shown) in R2C cells E2 levels after 24 h were 0.5 pmol/mg protein and increased by 7-fold at 96 h (Fig. 1A). This production was dependent on high constitutive active aromatase activity, since the presence of aromatase inhibitor Letrozole was able to decrease E2 production at all time points tested (Fig. 1B). E2 levels after 24 h treatment with Letrozole were still detectable, but were completely knock down when we removed the medium after 24 h and renewing the treatment for an additional 24 h. The same effect was maintained for the other two time points

investigated (Fig. 1B). Once estradiol is produced it can exert its actions binding to specific receptors, the estrogen receptors α e β (ERα and ERβ). Analysis of the two receptor protein isoforms in our models demonstrated that tumor Leydig cells express both isoform of ERs (Fig. 2). Particularly the α isoform seems to be more expressed in R2C cells respect to TM3 and in FRTT respect to the its control FRNT (Fig. 2A) where ERβ is more expressed (Fig. 2B). In R2C as well as in FRTT was observed an increase in ERα/ERβ ratio (Fig. 2E). Moreover aromatase protein content is extremely high in tumoral samples (13) (Fig. 2C).

Our next experiments demonstrated that estrogen receptors are required for proliferation through a short autocrine loop maintained by endogenous E2 production in Leydig tumor cells. For instance, the use of both antiestrogens OHT and ICI and the use of aromatase inhibitor Letrozole determined a dose-dependent inhibition of cell proliferation (Fig. 3A). Among the different doses tested the highest dose of OHT (10 μM) was able to inhibit cell proliferation by 90%, ICI 10 μM by 86% and letrozole by 70%. In the same vein, starving cells for prolonged time and changing the medium every day in order to remove local E2 production, we found that addition of 1, 10 and 100 nM E2 stimulated Leydig tumor cell proliferation (Fig. 3B), and partially abrogated the inhibition induced by Letrozole (Fig. 3C). The stimulatory effect of E2 was concomitant with the increased levels of cell cycle regulator cyclin D1 and E, whose expression was inhibited by pure antiestrogen ICI (Fig. 3D). All these results address how the classic E2/ERalpha signalling may control Leydig cell tumor growth and proliferation similarly to what observed in other estrogen-dependent tumors.

Aromatase overexpression is determined by constitutive activation of transcription factors SF-1 and CREB. Aromatase gene transcription in rat Leydig cells is driven by the PII promoter, which is principally regulated through three CRE-like sites and one NRE site binding SF-1 and LRH-1 (21, 33). Constitutive active levels of CREB have been previously demonstrated in R2C cells (36). Here we confirmed these data and demonstrated high phosphorylated status of CREB together with enhanced

phosphorylation of SF-1 in FRTT (Fig. 4). Furthermore we demonstrated the presence of high expression levels of SF-1 with the protein present in a phosporylated status in R2C but not in TM3.

IGF-I is produced by R2C cells and induces aromatase expression through PI3K- and PKC-mediated activation of SF-1. Starting from previous findings demonstrating that SF-1 and CREB are activated by IGF-I and lead to an increase in StAR transcription and then steroidogenesis (25, 37), we investigated the role of this factor locally produced in the testis in regulation of aromatase. Determination of IGF-I content in TM3 and R2C culture medium by RIA revealed a significant difference in the growth factor production with R2C cells producing about 4-fold higher IGF-I (Fig. 5). Upon binding to its receptor, IGF-IR, IGF-I activates three major transductional pathways: Ras/Raf/MAPK, PI3K/AKT, PLC/PKC, to demonstrate involvement of IGF-I transductional pathways in modulating aromatase expression in Leydig cell tumors, we used specific inhibitors: of IGF-I receptor (IGF-IR) [AG1024 (AG)], of ERK1/2 [PD98059 (PD)], of PI3K [LY294002 (LY)] and of PKC [GF109203X (GFX)]. IGF-I receptor inhibitor was able to inhibit aromatase activity in R2C cells by 85% (Fig. 6), LY determined 65 % inhibition, PD 35 % and GFX 61 %. The same inhibitory pattern was observed also on aromatase mRNA (fig. 7A) and protein content (Fig. 8). Parallely all of the different inhibitors but PD were able to reduce SF-1 mRNA, while CREB remained unchanged (Fig. 7). For SF-1 inhibition was 75% with AG, 90 % with LY and 80 % with GFX (Fig. 7). Analysis of protein levels by western blot confirmed the data on mRNA (Fig. 8). Treatments with increasing doses of AG, LY and GFX but not PD were able to induce a dose-dependent inhibition of total and phosphorylated levels of SF-1, on the other hand CREB was not affected by the presence of any of the inhibitors (Fig. 8).

IGF-I induces aromatase expression and activity in R2C cells. To further demonstrate the prevalent role of SF-1 in IGF-I induced aromatase expression in Leydig cell tumor, we monitored the effect of IGF-I on CYP19 and SF-1 expression. Addition of exogenous amounts of IGF-I were able to

induce aromatase activity by 1.8-fold (Fig. 9A). A significant effect of IGF-I treatment was seen also on CYP19 mRNA levels (Fig. 9B). IGF-I was able to induce a significant increase of 2- and 3.8-fold in aromatase mRNA at 12h and 24h, respectively (Fig. 9B). Aromatase protein levels under the same treatments reflected mRNA data (Fig. 9C). Analysis of expression levels of total and phosphorylated forms of transcription factors SF-1 and CREB showed an increase in SF-1 and pSF-1 in the presence of IGF-I after 4h while no difference was observed for CREB at any of the investigated times (Fig. 9C).

Changes in IGF-I pathway activation status lead to changes in SF-1 binding to the aromatase PII promoter. Finally we performed CHIP assay to investigate how IGF-I stimulation influence per se binding of transcription factors to the aromatase PII promoter. We evidenced how in basal condition all the different inhibitors but not PD reduced the amount of bound SF-1 reflecting changes in SF-1 protein amount (Fig. 10 A). The increase in SF-1 protein content seen under IGF-I treatment (Fig. 9C) reflected an increase in SF-1 binding to the PII promoter (Fig. 10B).

Discussion

The current study was aimed to explain the molecular mechanism responsible for aromatase overexpression in tumor Leydig cells with a consequent excess of estradiol *in situ* production sustaining tumor cell growth and proliferation.

Mammalian testis is capable of estrogen synthesis, whose production is regulated by different factors at different ages. In mature animals, aromatization of testosterone to estradiol is enhanced by LH/chorionic gonadotropin (CG) and not by FSH. The site of this synthesis appears to be age-dependent, at least in some species, such as the rat (38). Leydig cells are an elective target site of LH/CG which controls testosterone biosynthesis as well as its conversion to estradiol through aromatase activity. Leydig cell is also known to be the site of estrogen synthesis in several species, including mice (39), humans (40), suine (41), and sheep (42). Alterations in local estrogen synthesis

may have significant consequences in malignancy of these cells. In the present study we observed that manteinance of R2C cells in the absence of serum induces a cospicous release of E2 from cellular storage in a time dependent manner. This synthesis was abrogated by treatment with Letrozole, an aromatase inhibitor, addressing how estrogen production is dependent on high constitutive aromatase activity. A strongly increased aromatase expression was observed in R2C cells respect to the normal cell line control TM3 as well as in FRTT respect to FRNT. These findings concord with a previous study on human tissues showing that the increase in estrogen synthesis, as a consequence of a more intense aromatase activity, is higher in Leydig cell tumor fraction than in normal tissue surrounding the tumor of the same patient (43).

Mediators of the physiological effects of estrogens are the estrogen receptors (ER) α and β. ERα appears to be confined to Leydig cells in testicular tissue (44), while ERβ has been detected immunohistochemically in several rat testicular cell types, including Sertoli cells, germ cells, and peritubular cells (45). An enhanced expression of ERα, resulting in an increased ERα/ERβ, ratio was observed in R2C compared to TM3 cell line as well as in FRTT respect to FRNT. This is in agreement with previous reports demonstrating that transgenic mice overexpressing aromatase have an enhanced occurrence of breast and Leydig cell tumors together with an enhanced expression of ERα in the tumoral tissue (13). The latter findings address reasonably how an estrogen short autocrine loop may be involved in breast and testicular tumorogenesis in the presence of an excess of locally produced estradiol. Indeed, an arrest of cell growth was observed following abrogation of local E2 production with Letrozole or after addition of ERα inhibitors ICI or OHT. Besides, only after remotion of medium every day along with prolonged R2C starvation abolishing local steroid production, we observed how exogenous E2 was able to display proliferative effects.

One mechanism through which estrogens induce cell proliferation is by increasing protein levels of G1 regulatory cyclins A, B1, D1, D3, and E in target cells (46). In our study we showed that the

expression of two of the most important regulators of Leydig cell cycle, cyclin D1 and E can be increased by E2 and downregulated by treatment with antiestrogens. These data further confirm that aromatase overexpression and the consequent E2 production may be the cause of altered cell cycle regulation of Leydig tumor cells.

In the attempt to explain the molecular mechanism determining aromatase overexpression in our tumor cell line, we focused our attention on expression levels of transcription factors identified as crucial regulators of aromatase gene expression: CREB and SF-1. In the adult testis SF-1 is predominantly expressed in Leydig cells (47). The increase of total and/or phosphorylated protein can potentiate SF-1 transcriptional activity (48). In R2C cells and in FRTT compared to the normal controls we found higher SF-1 phosphorylated protein levels as a consequence of elevated protein content. Total CREB levels were similar in all samples but highly phosphorylated in tumor samples. Starting from these observations we investigated which pathways could be involved in the activation of these transcription factors.

The most important signal that initiates steroidogenesis in Leydig cells is the binding of LH to the LH receptor (49). It has been demonstrated that LH/LHreceptor signaling pathway is constitutively active in R2C cells and makes the phenotype of these cells constitutively steroidogenic (50). For instance in the presence of a specific PKA inhibitor, constitutive synthesis of *Star* mRNA and steroids were significantly inhibited (51). These observations fit well with our findings evidencing how the presence of PKA inhibitor determined a strong decrease in aromatase activity together with a drop in CREB phosphorylation (data not shown). In the presence of a specific PKC inhibitor no effects were elicited on phosphorylation of CREB, while SF-1 dropped dramatically.

It has been shown that CREB in mouse Leydig cells can be phosphorylated also through the PKC pathway, activated by IGF-I (50). In this study we have revealed that R2C tumor Leydig cells release higher levels of IGF-I in the culture medium respect to TM3 cells. However, the exposure to IGF-I as

well as the treatment with inhibitors of IGF-I signalling did not affect CREB phosphorylative status but decreased SF-1 phosphorylation, postulating a separate mechanism controlling CREB and SF-1 activation in modulating aromatase activity.

These findings led us to suppose that the IGF-I derived from tumor Leydig cells could act through an autocrine mechanism in activating aromatase expression. IGF-I receptors have previously been identified in Leydig cells of several species (52-55). It has been hypothesized that changes in IGF-RI expression can influence tumor cell progression. However in our cellular models, we did not reveal differences in IGF-RI expression between normal and tumor cells (data not shown), indicating that IGF-I level may be the determining factor in potentiating IGF-I signalling. A previous study investigating the effects of long term IGF-I treatment on Leydig cells did not reveal alterations in DNA synthesis, indicating that IGF-I may act as a differentiation factor rather than a mitogenic factor (56). In fact, expression levels of all mRNA species associated with T biosynthesis were shown to be lower in the absence of IGF-I, while treatment with IGF-I/insulin has been found to stimulate steroidogenesis and StAR expression in Leydig cells through a process that does not require cAMP signaling (26, 57, 58). In the same vein we may reasonable hypothesize that IGF-I could sustain, through an autocrine/paracrine mechanism, the elevated aromatase expression/activity in tumor Leydig cells. To verify this hypothesis we studied the various signalling pathways initiated by IGF-I through IGF-IR. Binding of IGF-I to its receptor causes receptor autophosphorylation and the activation of intrinsic tyrosine kinase that acts on various substrates including the insulin receptor substrate (IRS) and Shc adaptor proteins. These activated proteins recruit other factors, leading to activation of multiple signalling pathways including the phosphatidyl inositol 3-kinase (PI3K)/Akt and the mitogen-activated protein (MAP) kinase cascade. In addition, it has been shown that IGF-I can activate also the phospholipase C (PLC)/protein kinase C (PKC) pathway (25, 59). To demonstrate a role for IGF-I in mediating aromatase activation we used specific inhibitors for IGF-I signaling [AG1024 (AG)],

ERK1/2 [PD98059 (PD)], PI3K [LY294002 (LY)] and PKC [GF109203X (GFX)] and showed a reduction of aromatase activity with all of them. Together these data confirm a role for IGF-I in mediating aromatase activation in tumor Leydig cells. All of the different inhibitors but PD were able to produce a similar inhibitory pattern on both aromatase and SF-1 mRNA and protein expression. Furthermore by ChIP assay we evidenced that SF-1 binding to the aromatase promoter II that was reduced by AG, LY, GFX but not by PD indicating a central role of this transcription factor in regulating aromatase gene transcription in tumor Leydig cells. This is the first report of a direct link between SF-1 transcription and IGF-I signalling pathway in regulating aromatase expression.

Furthermore, addition of IGF-I itself was able to increase aromatase activity and expression. These events were due to an increase in the amount of total and phosphorylated SF-1 levels whose binding to the aromatase promoter was shown to be rapidly augmented. So we postulate that an enhanced endogenous IGF-I local production may contribute to maintain an elevated aromatase activity sustained by a direct stimulatory effect of SF-1. For instance the inhibition of IGF-I signalling through inhibition of either PI3K/AKT and PLC/PKC pathways were able to block SF-1 expression and protein phoshorylation. Particularly treatment with AG blocked SF-1 phosphorylation more efficiently than the separate treatment of PI3K or PKC, addressing how both pathways may synergize in upregulating SF-1 activity. In the presence of PD, SF-1 expression remained unchanged together with unaffected aromatase mRNA and protein levels. Importantly aromatase activity appeared decreased in the presence of PD suggesting a potential stimulatory role of ERK1/2 on the enzyme at a post-transcriptional level. From our findings then emerges a double mechanism inducing enhanced expression of aromatase: 1. a constitutive activation of LH/cAMP/PKA pathway which determines CREB activation; 2. an enhanced IGF-I signaling potentiating SF-1 action. The enhanced expression of SF-1 may be maintained by the lack of DAX-1 (Dosage-Sensitive Sex Reversal, Adrenal Hypoplasia Congenita, Critical Region on the X Chromosome, Gene-1) in R2C cells (36). DAX-1 is a specific co-

repressor of SF-1 (60-64) and inhibits StAR expression and steroidogenesis by 40-60% when overexpressed in R2C cells (36). The lack of DAX-1 expression in R2C cells may be due to the constitutive active PKA signalling, in fact since in a mouse Leydig cell line was shown a marked decrease of DAX-1 mRNA within 3 h after addition of LH or forskolin (63). Then, the activation of LH/LHr/PKA pathway at the same time decreases DAX-1 expession and promotes SF-1 activity.

Remains to explain which molecular mechanism(s) is responsible for the elevated IGF-I production in tumor Leydig cells. In vivo, administration of hCG increases IGF-I mRNA levels in rat Leydig cells (65). LH deprival determines a decrease in the BrdU incorporation as well as a decrease in mRNA levels of IGF-I and IGF-I receptor. These observations together with our data showing a decrease in IGF-I basal production after treatment with a PKA inhibitor (data not shown) suggest the possibility that LH can mediate its proliferative effects also by regulating IGF-I and its receptor in Leydig cells and that the altered LH/LHreceptor activated pathway in R2C cells could be the cause of IGF-I overproduction (66).

Moreover the observation that in murine Leydig cells IGF-I is able to increase the LHr mRNA stability (67) together with data showing that the presence of an IGF-I antibody reduced the steroidogenic responsiviness to LH/hCG (68) suggest also the possibility of an IGF-I action in sustaining LH/LHr signalling. If the constitutive activation of LH/LHr/PKA signalling in R2C cells may be involved in upregulation of IGF-I expression remains also to be explored.

In conclusion, in this study we demonstrated that in tumor Leydig cells aromatase overexpression determines an excessive local estradiol production able to stimulate the expression of genes involved in cycle regulation and sustaining cell proliferation. Aromatase overexpression appears to be induced by the combined enhanced LH/LHr and IGF-I signalling (Fig. 11).

Particularly, LH/LHr signaling determines a constitutive active CREB phosphorylation on aromatase gene promoter while IGF-I overproduction stimulates through an autocrine mechanism SF-1

binding on the same promoter. The observation that antiestrogens and aromatase inhibitors as well as IGF-I signalling blockers are able to reduce R2C proliferation opens new perspectives on the adjuvant therapeutic approach of testicular cancer.

Acknowledgments

We thank Dr. V. Cunsulo (Biogemini Sas, Catania, Italy) for generously providing us with the RIA kits. We also thank Dr Ken-ichirou Morohashi and Dr Holly A. Ingraham for providing us respectively with anti SF-1 and anti pSF-1 antibodies. This work was supported by PRIN-MIUR, AIRC.

References

1. Weir HK, Marrett LD, Kreiger N, Darlington GA, Sugar L. Pre-natal and peri-natal exposures and risk of testicular germ-cell cancer. Int J Cancer 2000;87:438-443.

2. Dieckmann KP, Endsin G, Pichlmeier U. How valid is the prenatal estrogen excess hypothesis of testicular germ cell cancer? A case control study on hormone-related factors. Eur Urol 2001;40:677-683.

3. Olsson H, Bladstrom A, Alm P. Male gynecomastia and risk for malignant tumours - a cohort study. BMC Cancer 2002;2:26.

4. Hem E, Attramadal A, Tveter KJ. Synchronous bilateral primary germ cell tumors in patient receiving estrogen therapy. Urology 1988;31:70-71.

5. Fleming LE, Bean JA, Rudolph M, Hamilton K. Cancer incidence in a cohort of licensed pesticide applicators in Florida. J Occup Environ Med 1999;41:279-288.

6. Ohlson CG, Hardell L. Testicular cancer and occupational exposures with a focus on xenoestrogens in polyvinyl chloride plastics. Chemosphere 2000;40:1277-1282.

7. Carroll PR, Whitmore WF Jr, Herr HW et al. Endocrine and exocrine profiles of men with testicular tumors before orchiectomy. J Urol 1987;137:420-423.

8. Uysal Z, Bakkaloglu M. Serum estradiol as a tumour marker for non-seminomatous germinal cell tumours (NSGCT) of the testis. Int Urol Nephrol 1987;19:415-418.

9. Hawkins C, Miaskowski C. Testicular cancer: a review. Oncol Nurs Forum 1996;23:1203-1211.

10. Mostofi FK, Sesterhenn IA, Bresler VM. Pathology of tumours in laboratory animals. Tumours of the rat. Tumours of the testis. IARC Sci Publ 1990;(99):399-419 1990;99:399-419.

11. Horn HA, Stewart HL. A review of some spontaneous tumors in noninbred mice. J Natl Cancer Inst 1952;13:591-603.

12. Bosland MC. Hormonal factors in carcinogenesis of the prostate and testis in humans and in animal models. Prog Clin Biol Res 1996;394:309-352.

13. Fowler KA, Gill K, Kirma N, Dillehay DL, Tekmal RR. Overexpression of aromatase leads to development of testicular Leydig cell tumors: an in vivo model for hormone-mediated testicular cancer. Am J Pathol 2000;156:347-353.

14. Kirma N, Gill K, Mandava U, Tekmal RR. Overexpression of aromatase leads to hyperplasia and changes in the expression of genes involved in apoptosis, cell cycle, growth, and tumor suppressor functions in the mammary glands of transgenic mice. Cancer Res 2001;61:1910-1918.

15. Coleman GL, Barthold W, Osbaldiston GW, Foster SJ, Jonas AM. Pathological changes during aging in barrier-reared Fischer 344 male rats. J Gerontol 1977;32:258-278.

16. Aquila S, Sisci D, Gentile M et al. Towards a physiological role for cytochrome P450 aromatase in ejaculated human sperm. Hum Reprod 2003;18:1650-1659.

17. Inkster S, Yue W, Brodie A. Human testicular aromatase: immunocytochemical and biochemical studies. J Clin Endocrinol Metab 1995;80:1941-1947.

18. Simpson ER, Mahendroo MS, Means GD et al. Aromatase cytochrome P450, the enzyme responsible for estrogen biosynthesis. Endocr Rev 1994;15:342-355.

19. Young M, Lephart ED, McPhaul MJ. Expression of aromatase cytochrome P450 in rat H540 Leydig tumor cells. J Steroid Biochem Mol Biol 1997;63:37-44.

20. Lanzino M, Catalano S, Genissel C et al. Aromatase messenger RNA is derived from the proximal promoter of the aromatase gene in leydig, sertoli, and germ cells of the rat testis. Biol Reprod 2001;64:1439-1443.

21. Young M, McPhaul MJ. A Steroidogenic factor-1-binding site and cyclic adenosine 3',5'-monophosphate response element-like elements are required for the activity of the rat aromatase promoter in rat Leydig tumor cell lines. Endocrinology 1998;139:5082-5093.

22. Fitzpatrick SL, Richards JS. Identification of a cyclic adenosine 3',5'-monophosphate-response element in the rat aromatase promoter that is required for transcriptional activation in rat granulosa cells and R2C leydig cells. Mol Endocrinol 1994;8:1309-1319.

23. Carlone DL, Richards JS. functional interactions, phosphorylation, and levels of 3',5'-cyclic adenosine monophosphate-regulatory element binding protein and steroidogenic factor-1 mediate

hormone-regulated and constitutive expression of aromatase in gonadal cells. Mol Endocrinol 1997;11:292-304.

24. Fitzpatrick SL, Richards JS. cis-acting elements of the rat aromatase promoter required for cyclic adenosine 3',5'-monophosphate induction in ovarian granulosa cells and constitutive expression in R2C Leydig cells. Mol Endocrinol 1993;7:341-354.

25. Manna PR, Chandrala SP, King SR et al. molecular mechanisms of insulin-like growth factor-I mediated regulation of the steroidogenic acute regulatory protein in mouse Leydig cells. Mol Endocrinol 2006;20:362-378.

26. Saez JM. Leydig cells: endocrine, paracrine, and autocrine regulation. Endocr Rev 1994;15:574-626.

27. Casella SJ, Smith EP, van Wyk JJ et al. Isolation of rat testis cDNAs encoding an insulin-like growth factor I precursor. DNA 1987;6:325-330.

28. Zhou J, Bondy C. Anatomy of the insulin-like growth factor system in the human testis. Fertil Steril 1993;60:897-904.

29. Baker J, Hardy MP, Zhou J et al. Effects of an Igf1 gene null mutation on mouse reproduction. Mol Endocrinol 1996;10:903-918.

30. Liu JP, Baker J, Perkins AS, Robertson EJ, Efstratiadis A. Mice carrying null mutations of the genes encoding insulin-like growth factor I (Igf-1) and type 1 IGF receptor (Igf1r). Cell 1993;75:59-72.

31. Wang GM, O'Shaughnessy PJ, Chubb C, Robaire B, Hardy MP. Effects of Insulin-Like Growth Factor I on Steroidogenic Enzyme Expression Levels in Mouse Leydig Cells. Endocrinology 2003;144:5058-5064.

32. Lephart ED, Simpson ER. Assay of aromatase activity. Methods Enzymol 1991;206:477-483.

33. Pezzi V, Sirianni R, Chimento A et al. differential expression of steroidogenic factor-1/adrenal 4 binding protein and liver receptor homolog-1 (LRH-1)/fetoprotein transcription factor in the rat testis: LRH-1 as a potential regulator of testicular aromatase expression. Endocrinology 2004;145:2186-2196.

34. Bradford MM. A rapid and sensitive method for thequantitation of microgram quantities of protein utilizing theprinciple of protein-dye binding. Analytical Biochemistry 1976;72:248-254.

35. Jacobs BB, Huseby RA. Neoplasms occurring in aged Fischer rats, with special reference to testicular, uterine and thyroid tumors. J Natl Cancer Inst 1967;39:303-309.

36. Jo Y, Stocco DM. regulation of steroidogenesis and steroidogenic acute regulatory protein in R2C cells by DAX-1 (dosage-sensitive sex reversal, adrenal hypoplasia congenita, critical region on the X chromosome, gene-1). Endocrinology 2004;145:5629-5637.

37. LaVoie HA, Garmey JC, Veldhuis JD. Mechanisms of insulin-like growth factor I augmentation of follicle-stimulating hormone-induced porcine steroidogenic acute regulatory protein gene promoter activity in granulosa cells. Endocrinology 1999;140:146-153.

38. Pomerantz D. Developmental changes in the ability of follicle stimulating hormone to stimulate estrogen synthesis in vivo by the testis of the rat. Biol Reprod 1980;23:948-954.

39. Kmicikiewicz I, Krezolek A, Bilinska B. The effects of aromatase inhibitor on basal and testosterone-supplemented estradiol secretion by Leydig cells in vitro. Exp Clin Endocrinol Diabetes 1997;105:113-118.

40. Payne AH, Kelch RP, Musich SS, Halpern ME. Intratesticular site of aromatization in the human. J Clin Endocrinol Metab 1976;42:1081-1087.

41. Raeside JI, Renaud RL. Estrogen and androgen production by purified Leydig cells of mature boars. Biol Reprod 1983;28:727-733.

42. Bilinska B, Lesniak M, Schmalz B. Are ovine Leydig cells able to aromatize androgens?. Reprod Fertil Dev 1997;9:193-199.

43. Valensi P, Coussieu C, Pauwles A et al. Feminizing Leydig cell tumor: endocrine and incubation studies. J Endocrinol Invest 1987;10:187-193.

44. Fisher JS, Millar MR, Majdic G et al. Immunolocalization of oestrogen receptor-a within the testis and excurrent ducts of the rat and marmoset monkey from perinatal life to adulthood. J Endocrinol 1997;153:485-495.

45. Saunders PT, Fisher JS, Sharpe RM, Millar MR. Expression of oestrogen receptor beta (ER beta) occurs in multiple cell types, including some germ cells, in the rat testis. J Endocrinol 1998;156:R13-R17.

46. Prall OWJ, Sarcevic B, Musgrove EA, Watts CKW, Sutherland RL. Estrogen-induced activation of Cdk4 and Cdk2 during G1-S phase progression is accompanied by increased cyclin D1 expression and decreased cyclin-dependent kinase inhibitor association with cyclin E-Cdk2. J Biol Chem 1997;272:10882-10894.

47. Hatano O, Takayama K, Imai T et al. Sex-dependent expression of a transcription factor, Ad4BP, regulating steroidogenic P-450 genes in the gonads during prenatal and postnatal rat development. Development 1994;120:2787-2797.

48. Desclozeaux M, Krylova IN, Horn F, Fletterick RJ, Ingraham HA. Phosphorylation and intramolecular stabilization of the ligand binding domain in the nuclear receptor steroidogenic factor 1. Mol Cell Biol 2002;22:7193-7203.

49. Dufau ML, Winters CA, Hattori M et al. Hormonal regulation of androgen production by the Leydig cell. J Steroid Biochem 1984;20:161-173.

50. Jo Y, King SR, Khan SA, Stocco DM. Involvement of protein kinase c and cyclic adenosine 3',5'-monophosphate-dependent kinase in steroidogenic acute regulatory protein expression and steroid biosynthesis in Leydig cells. Biol Reprod 2005;73:244-255.

51. Rao RM, Jo Y, Leers-Sucheta S et al. Differential regulation of steroid hormone biosynthesis in R2C and MA-10 Leydig tumor cells: role of SR-B1-mediated selective cholesteryl ester transport. Biol Reprod 2003;68:114-121.

52. Vannelli BG, Barni T, Orlando C et al. Links Insulin-like growth factor-I (IGF-I) and IGF-I receptor in human testis: an immunohistochemical study. Fertil Steril 1988;49:666-669.

53. Saez JM, Chatelain PG, Perrard-Sapori MH, Jaillard C, Naville D. Differentiating effects of somatomedin-C/insulin-like growth factor I and insulin on Leydig and Sertoli cell functions. Reprod Nutr Dev 1988;28:989-1008.

54. Nagpal ML, Wang D, Calkins JH, Chang WW, Lin T. Human chorionic gonadotropin up-regulates insulin-like growth factor-I receptor gene expression of Leydig cells. Endocrinology 1991;129:2820-2826.

55. Hasegawa T, Cohen P, Hasegawa Y, Fielder PJ, Rosenfeld RG. Characterization of the insulin-like growth factors (IGF) axis in a cultured mouse Leydig cell line (TM-3). Growth Regul 1995;5:151-159.

56. Lin T, Haskell J, Vinson N, Terracio L. Characterization of insulin and insulin-like growth factor I receptors of purified Leydig cells and their role in steroidogenesis in primary culture: a comparative study. Endocrinology 1986;119:1641-1647.

57. Lin T, Wang D, Hu J, Stocco DM. Upregulation of human chorionic gonadotrophin-induced steroidogenic acute regulatory protein by insulin-like growth factor-I in rat Leydig cells. Endocrine 1998;8:73-78.

58. Gelber SJ, Hardy MP, Mendis-Handagama SM, Casella SJ. Effects of insulin-like growth factor-I on androgen production by highly purified pubertal and adult rat Leydig cells. J Androl 1992;13:125-130.

59. Kojima I, Mogami H, Shibata H, Ogata E. Role of calcium entry and protein kinase C in the progression activity of insulin-like growth factor-I in Balb/c 3T3 cells. J Biol Chem 1993;268:10003-10006.

60. Bae DS, Schaefer ML, Partan BW, Muglia L. Characterization of the mouse DAX-1 gene reveals evolutionary conservation of a unique amino-terminal motif and widespread expression in mouse tissue. Endocrinology 1996;137:3921-3927.

61. Yazawa T, Mizutani T, Yamada K et al. Involvement of cyclic adenosine 5'-monophosphate response element-binding protein, steroidogenic factor 1, and Dax-1 in the regulation of gonadotropin-inducible ovarian transcription factor 1 gene expression by follicle-stimulating hormone in ovarian granulosa cells. Endocrinology 2003;144:1920-1930.

62. Osman H, Murigande C, Nadakal A, Capponi AM. Repression of DAX-1 and induction of sf-1 expression. two mechanisms contributing to the activation of aldosterone biosynthesis in adrenal glomerulosa cells. J Biol Chem 2002;277:41259-41267.

63. Song KH, Park YY, Park KC et al. The atypical orphan nuclear receptor DAX-1 interacts with orphan nuclear receptor Nur77 and represses its transactivation. Mol Endocrinol 2004;18:1929-1940.

64. Tamai KT, Monaco L, Alastalo TP et al. Hormonal and developmental regulation of DAX-1 expression in Sertoli cells. Mol Endocrinol. 1996;10:1561-1569.

65. Moore A, Chen CL, Davis JR, Morris ID. Insulin-like growth factor-I mRNA expression in the interstitial cells of the rat testis. J Mol Endocrinol 1993;11:319-324.

66. Sriraman V, Rao VS, Sairam MR, Rao AJ. Effect of deprival of LH on Leydig cell proliferation: involvement of PCNA, cyclin D3 and IGF-1. Molecular and Cellular Endocrinology 2000;162:113-120.

67. Zhang FP, El-Hafnawy T, Huhtaniemi I. Regulation of luteinizing hormone receptor gene expression by insulin-like growth factor-I in an immortalized murine leydig tumor cell line (BLT-1). Biol Reprod 1998;59:1116-1123.

68. Le Roy C, Lejeune H, Chuzel F, Saez JM, Langlois D. Autocrine regulation of Leydig cell differentiated functions by insulin-like growth factor I and transforming growth factor beta. J Steroid Biochem Mol Biol 1999;69:379-384.

FIGURE LEGENDS

Figure 1. E2 production in R2C cells. (**A**) Cells were cultured for the indicated times in serum free medium. (**B**) Cells were treated for the indicated times in HAM-F10 in the absence (-) or presence of aromatase inhibitor Letrozole (0.1, 1, 10 μM). Every 24h, before renewing treatment, cell culture medium was removed and analyzed for steroid content. E2 content was determined by RIA and normalized to the cell culture well protein content. Data represent the mean ± SEM of values from three separate cell culture wells expressed as pmol/mg protein.

Figure 2. Expression of estrogen receptors and Aromatase in R2C cells. ERα (**A**) ERβ (**B**) and aromatase (**C**) western blot analysis was performed on 50 μg of total proteins extracted from TM3 and R2C cells or from total tissue of normal (FRNT) and tumor (FRTT) Fisher rat testes. Results are representative of three independent experiments. β-actin (**D**) was used as loading control. Graphs depicted near western blots were obtained by averaging densitometric analyses of the three independent experiments. Protein expression in each lane was normalized to the β-actin content, and expressed as fold over control. (**E**) Graph was obtained calculating ERα/ERβ ratio of normalized optical density. (*,$P < 0.001$ and **,$P < 0.05$ compared with basal).

Figure 3. Effects of antiestrogens, aromatase inhibitor Letrozole and estradiol on R2C cell proliferation. (**A**) Cells were treated for 96h in HAM-F10 in the absence (-) or presence of antiestrogens hydroxytamoxifen (OHT) or ICI 182,760 (ICI) or aromatase inhibitor Letrozole at the indicated concentrations. (**B**) Cells were cultured for 48h in serum-free HAM-F10, every 24 h cell culture medium was removed and renewed. Cells were then treated for 24 h with estradiol at the indicated concentrations. (**C**) Cells were cultured for 24h in serum-free HAM-F10, cells were then treated for 48 h with letrozole (1μM) changing the culture medium and renewing treatment every 24h. For additional 24h cells were treated with letrozole (1μM) in combination with estradiol at the indicated concentrations. Proliferation was evaluated by [3H] Thymidine incorporation analysis. Values expressed as percent of untreated (basal) cells (100%) represent the mean ± SEM of three independent experiments each performed in triplicate. (*) $P < 0.05$ compared with basal cells. (**D**) R2C cells were cultured for 48h in serum-free HAM-F10, every 24 h cell culture medium was removed and renewed. Cells were then treated for 24 h in the absence (basal) or in the presence with estradiol (1nM) and ICI (1μM) before extracting total proteins. Western blot analysis of Cyclin D1 and Cyclin E was performed on 50 μg of total proteins extracted from R2C cells. Blots are representative of three independent experiments with similar results. β-actin was used as loading control. Graphs depicted below western blots were obtained by averaging densitometric analyses of the three independent experiments. Protein expression in each lane was normalized to the β-actin content, and expressed as relative fold over basal. (*,$P < 0.05$ and **,$P < 0.01$ compared with basal).

Figure 4. Expression of total and phosphorylated forms of SF-1 and CREB. Western blot analysis was performed on 50 μg of total proteins extracted from TM3 and R2C cells or from total tissue of normal (FRNT) and tumor (FRTT) Fisher rat testes. Blots are representative of three independent experiments with similar results. β-actin was used as loading control. Graphs depicted near western blots were obtained by averaging densitometric analyses of the three independent experiments. Protein expression in each lane was normalized to the β-actin content, and expressed as relative difference from controls. (*,$P < 0.001$ compared with basal).

Figure 5. IGF-I production in Leydig cells. IGF-I levels in culture medium of TM3 and R2C cells by RIA. TM3 and R2C cells were cultured for 24 h in serum free medium and IGF-I content was normalized to the cell culture well protein content. Data represent the mean ± SEM of values from three separate cell culture wells expressed as pmol/mg protein. (*) $P< 0.01$ compared with basal conditions.

Figure 6. Aromatase activity in R2C cells in response to inhibitors of IGF-I pathways. Cells were treated with AG (20μM), LY (10 μM), PD (20 μM) and GFX (20 μM). Aromatase activity was assessed by using the modified tritiated water method. Results obtained are expressed as pmoles of [3H]H2O released per hour and are normalized to the well protein content (pmol/h/mg protein). Values represent the mean ± SEM of three independent experiments each performed with triplicate samples. * $P < 0.01$ compared to basal.

Figure 7. Effects of inhibitors of IGF-I pathways on mRNA expression of CYP19, SF-1 and CREB in R2C cells. Total RNA was extracted from R2C cells untreated (bs) or treated for 24h with AG (20μM), LY (10 μM), PD (20 μM) and GFX (20 μM). Real time RT-PCR was used to analyze mRNA levels of CYP19, SF-1, and CREB. Data represent the mean ± SEM of values from three separate RNA samples. Each sample was normalized to its 18S ribosomal RNA content. Final results are expressed as n-fold differences of gene expression relative to calibrator (basal) calculated with the ΔΔCt method. * $P < 0.001$ compared to basal.

Figure 8. Effects of inhibitors of IGF-I pathways on expression of Aromatase, total and phosphorylated forms of SF-1 and CREB in R2C cells. Western blot analyses were performed on 50 μg of total proteins extracted from R2C cells untreated (bs) or treated for 24h with the indicated doses of AG (**A**), LY (**B**), PD (**C**) and GFX (**D**). Blots are representative of three independent experiments with similar results. β-actin was used as loading control. Graphs depicted near western blots were obtained by averaging densitometric analyses of the three independent experiments. Protein expression in each lane was normalized to the β-actin content, and expressed as relative difference from basal. (*,$P < 0.01$ compared with basal).

Figure 9. Aromatase activity and expression in R2C cells in response to IGF-I. (A) Cells were treated with IGF-I (100 ng/ml) for 24h. Aromatase activity was assessed by using the modified tritiated water method. Results obtained are expressed as pmoles of [3H]H2O released per hour and are normalized to the well protein content (pmol/h/mg protein). Values represent the mean ± SEM of three independent experiments each performed with triplicate samples. *$P<0.05$ compared to basal. (B) Total RNA was extracted from R2C cells untreated (bs) or treated for the indicated times with IGF-I (100

ng/ml). Real time RT-PCR was used to analyze mRNA levels of CYP19. Data represent the mean ± SEM of values from three separate RNA samples. Each sample was normalized to its 18S ribosomal RNA content. Final results are expressed as n-fold differences of gene expression relative to calibrator (basal) calculated with the ΔΔCt method. *P<0.01 and **P<0.001compared to basal. (C) Western blot analyses were performed on 50 μg of total proteins extracted from R2C cells untreated (basal) or treated for the indicated times with IGF-I (100 ng/ml). Blots are representative of three independent experiments with similar results. β-actin was used as loading control. Graphs depicted below western blots were obtained by averaging densitometric analyses of the three independent experiments.. Protein expression in each lane was normalized to the β-actin content, and expressed as relative difference from controls. (*,P < 0.01 compared with basal).

Figure 10. IGF-I increases SF-1 recruitment to the aromatase PII promoter through PI3K and PKC. (A) R2C cells were incubated for 24 h with AG (20μM), LY (10 μM), PD (20 μM) and GFX (20 μM). Untreated cells (basal, bs) were treated with the same amount of vehicle alone (DMSO) that never exceeded 0·01% (v/v). (B) R2C cells were incubated for the indicated times with IGF-I (100 ng/ml). *In vivo* binding of SF-1 to the aromatase PII promoter was examined using ChIP assay. Immunoprecipitated (SF-1) and total (10% input) DNA were subject to PCR using specific primers. Similar results were obtained in two additional experiments.

Figure 11. Schematic model showing the mechanism of tumor Leydig cell proliferation. IGF-I overproduced by tumor Leydig cell activates PI3K/AKT and PLC/PKC. This transductional pathways activate transcription and phosphorylation of SF-1 which in turn activates CYP19 gene expression together with pCREB activated by a PKA dependent pathway. The high aromatase activity determines an excessive estrogen production stimulating a short autocrine loop ER mediated activating cell cycle regulators as cyclin D1 and E and then cell proliferation.

FIG. 1

A

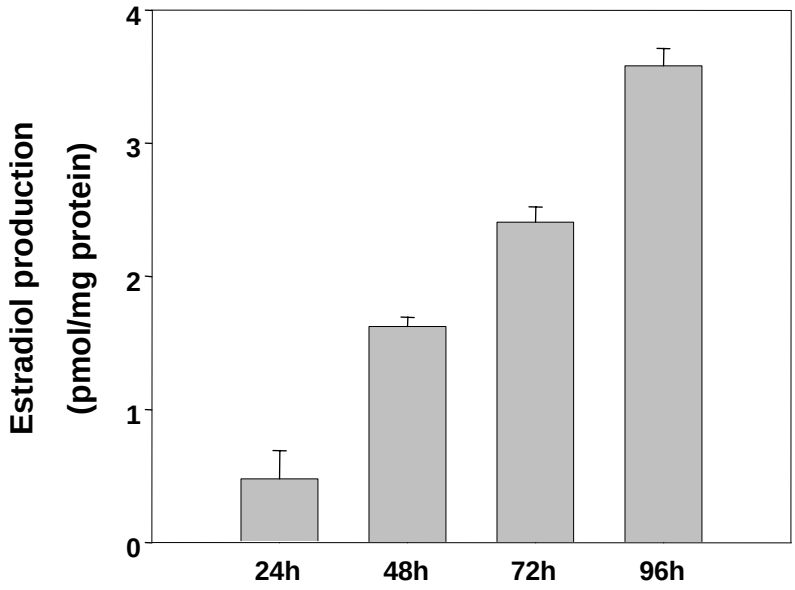
Estradiol production
(pmol/mg protein)
4
3
2
1
0
24h
48h
72h
96h

B

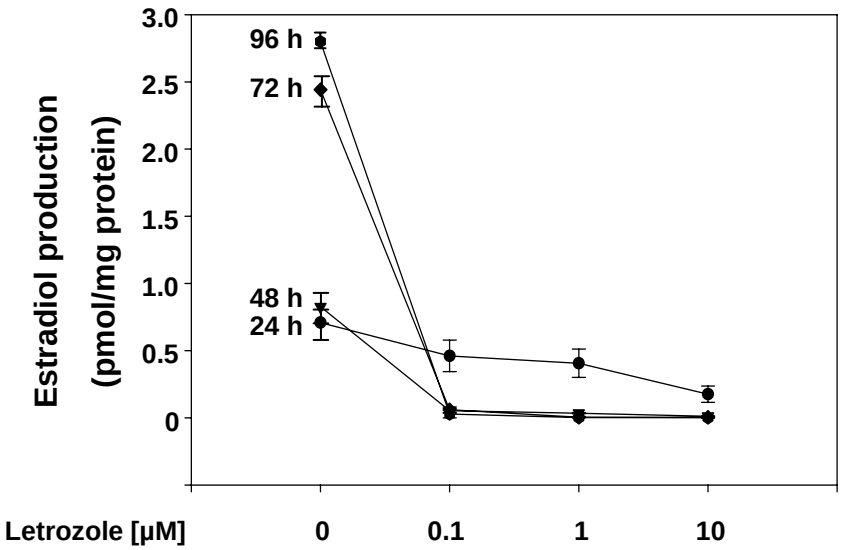
Estradiol production
(pmol/mg protein)
3.0
2.5
2.0
1.5
1.0
0.5
0
96 h
72 h
48 h
24 h
Letrozole [µM]
0
0.1
1
10

FIG. 2

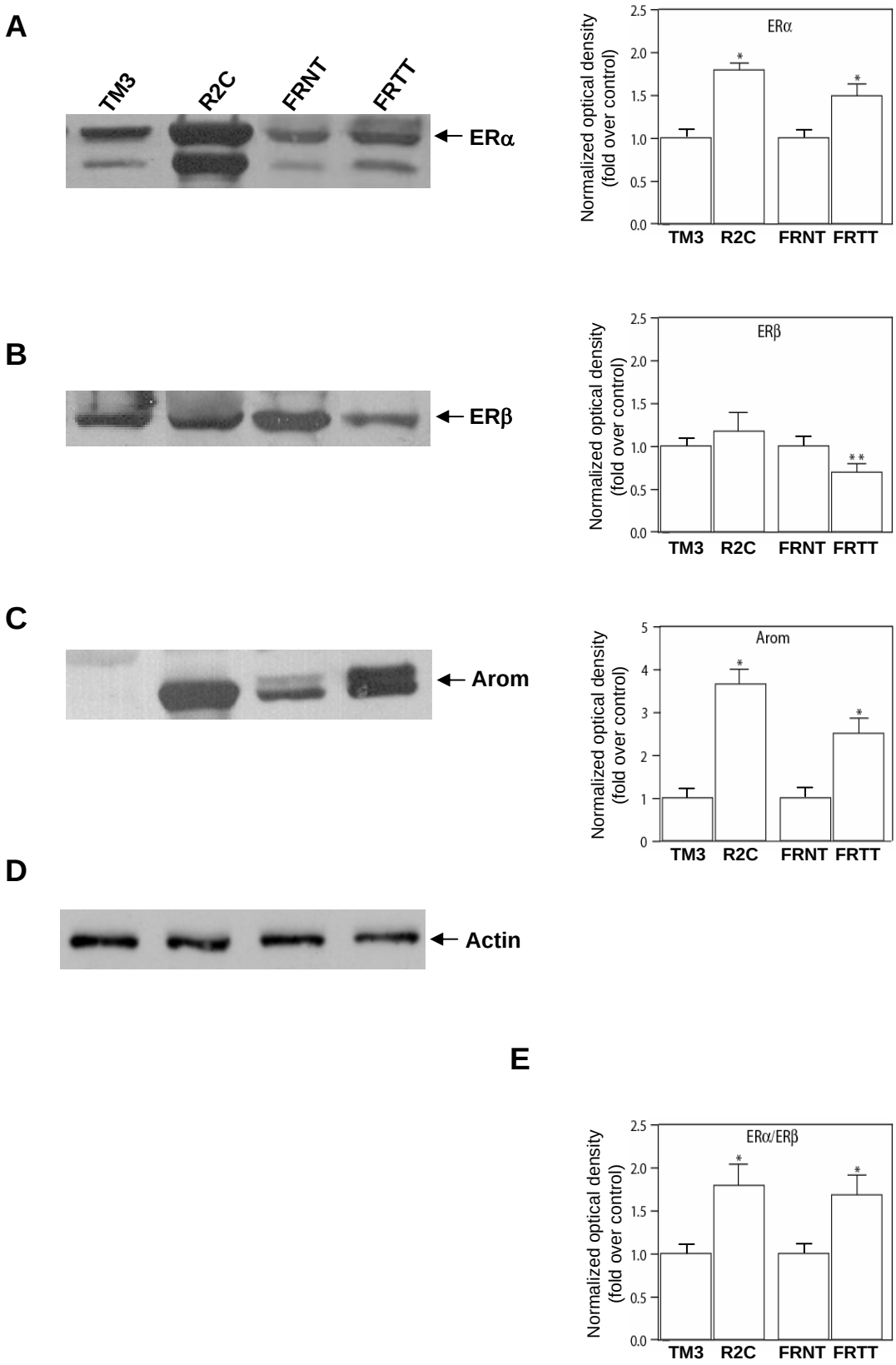
A
TM3
R2C
FRNT
FRTT
ERα
Normalized optical density (fold over control)
ERα
TM3 R2C FRNT FRTT
B
ERβ
Normalized optical density (fold over control)
ERβ
TM3 R2C FRNT FRTT
C
Arom
Normalized optical density (fold over control)
Arom
TM3 R2C FRNT FRTT
D
Actin
E
Normalized optical density (fold over control)
ERα/ERβ
TM3 R2C FRNT FRTT

FIG. 3

A

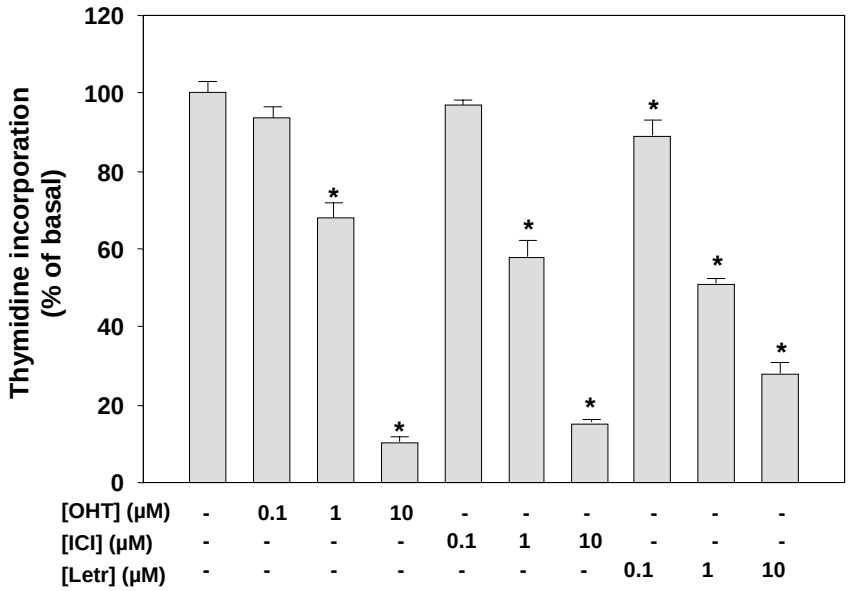
Thymidine incorporation
(% of basal)
120
100
80
60
40
20
0
*
[OHT] (μM) - 0.1 1 10 - - - - - -
[ICI] (μM) - - - - 0.1 1 10 - - -
[Letr] (μM) - - - - - - - 0.1 1 10

B

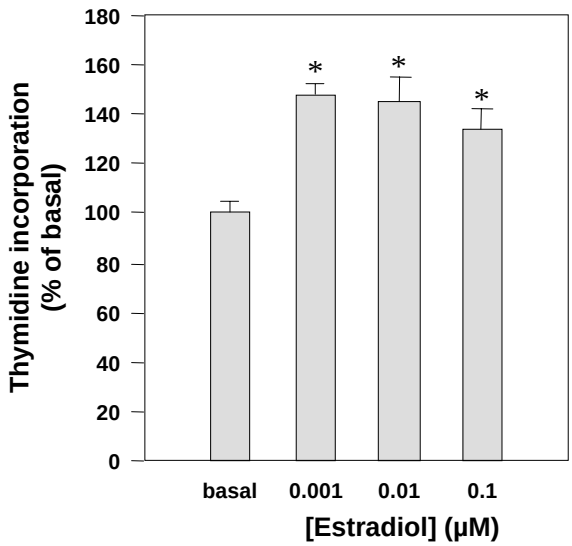
Thymidine incorporation
(% of basal)
180
160
140
120
100
80
60
40
20
0
*
basal
0.001
0.01
0.1
[Estradiol] (μM)

FIG. 3

C

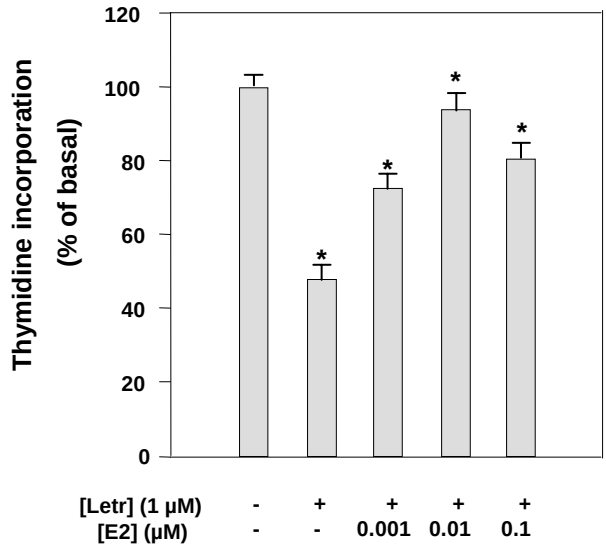
Thymidine incorporation
(% of basal)
120
100
80
60
40
20
0
*
*
*
*
[Letr] (1 μM) - + + + +
[E2] (μM) - - 0.001 0.01 0.1

D

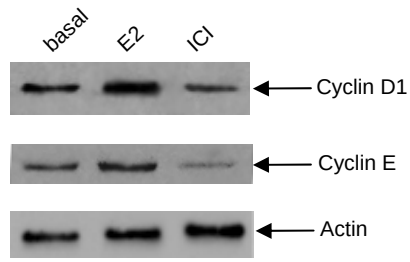
basal
E2
ICI
Cyclin D1
Cyclin E
Actin

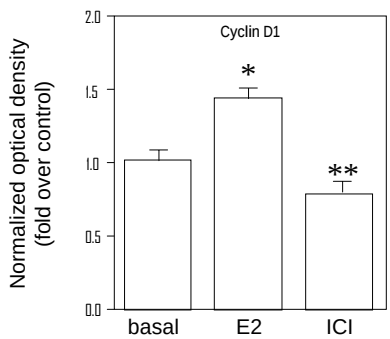
Cyclin D1
Normalized optical density
(fold over control)
2.0
1.5
1.0
0.5
0.0
*
**
basal
E2
ICI

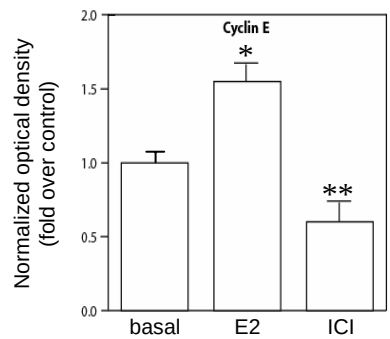
Cyclin E
Normalized optical density
(fold over control)
2.0
1.5
1.0
0.5
0.0
*
**
basal
E2
ICI

FIG. 4

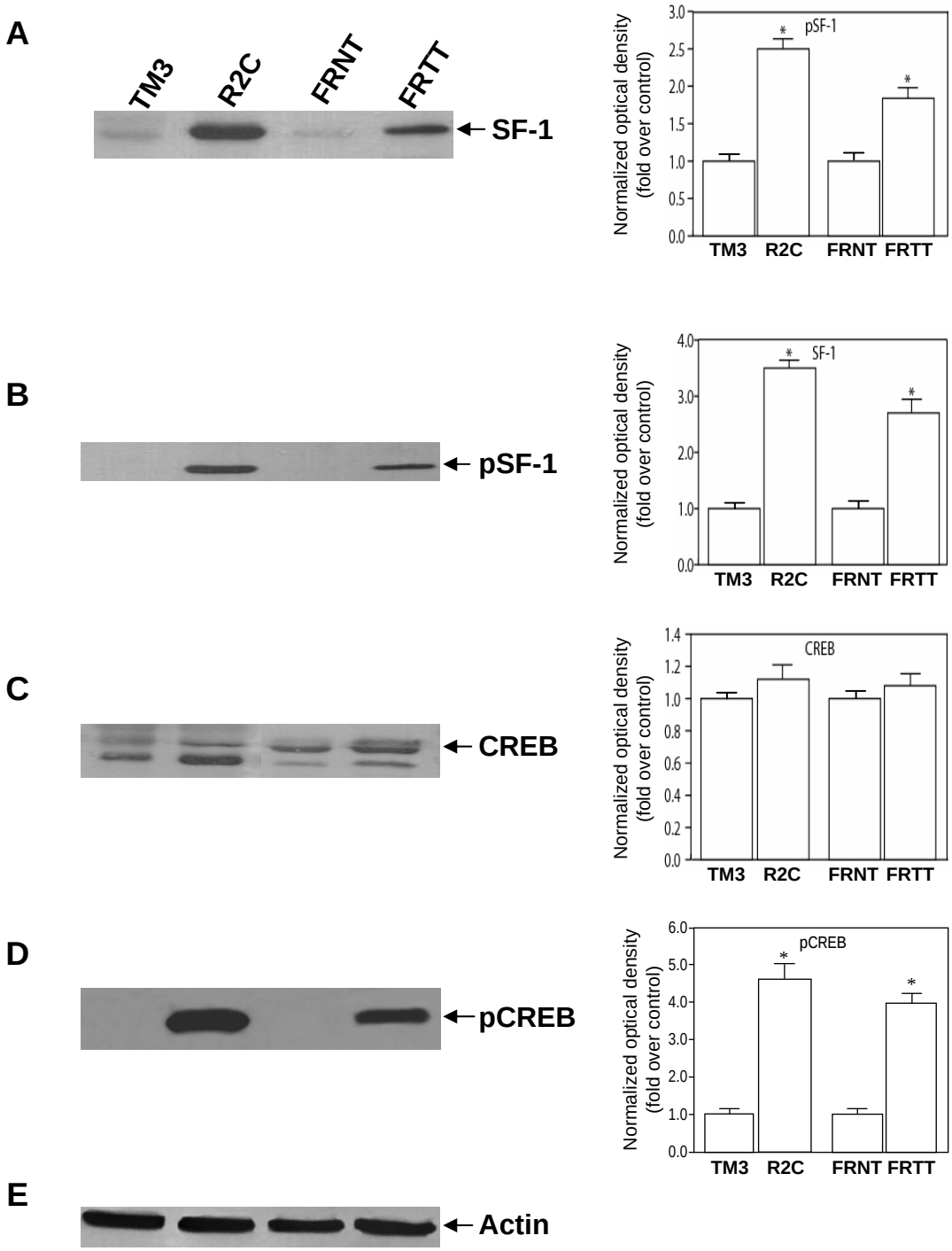
A
TM3
R2C
FRNT
FRTT
SF-1
pSF-1
Normalized optical density (fold over control)
TM3 R2C FRNT FRTT
B
pSF-1
SF-1
C
CREB
D
pCREB
E
Actin

FIG. 5

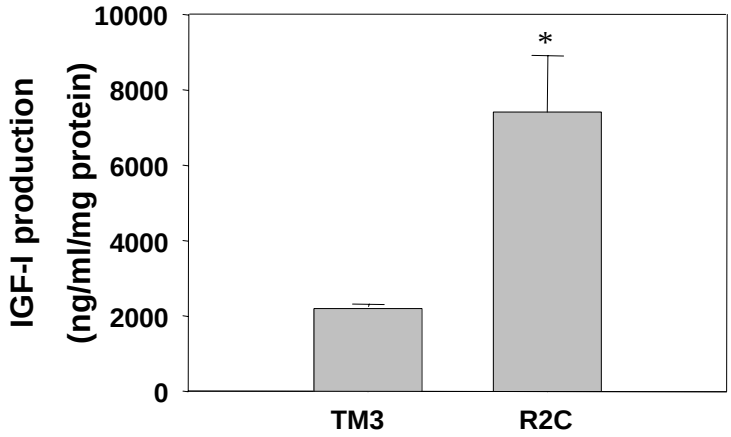
IGF-I production
(ng/ml/mg protein)
10000
8000
6000
4000
2000
0
*
TM3
R2C

FIG. 6

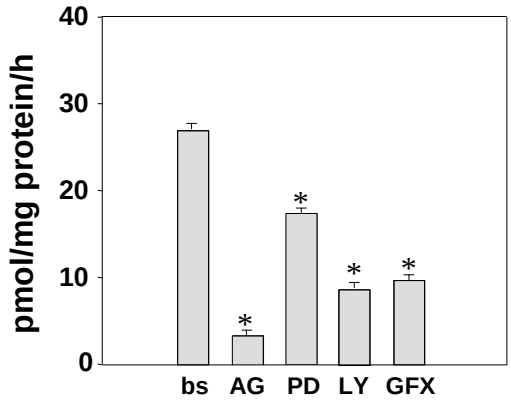

FIG. 7

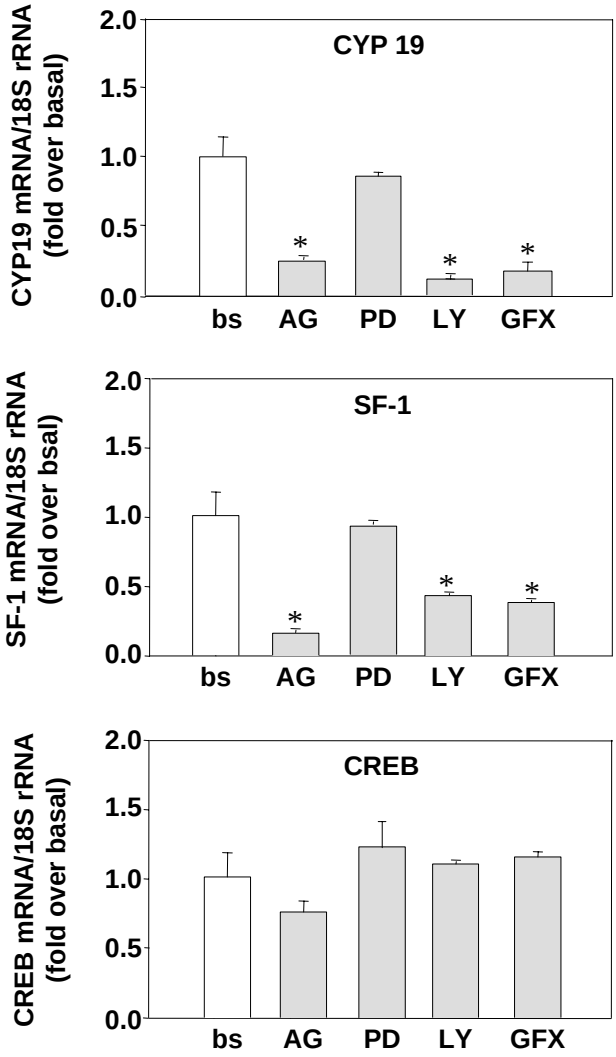
CYP 19
CYP19 mRNA/18S rRNA (fold over basal)
2.0
1.5
1.0
0.5
0.0
bs
AG
PD
LY
GFX
SF-1
SF-1 mRNA/18S rRNA (fold over bsal)
CREB
CREB mRNA/18S rRNA (fold over basal)

FIG. 8

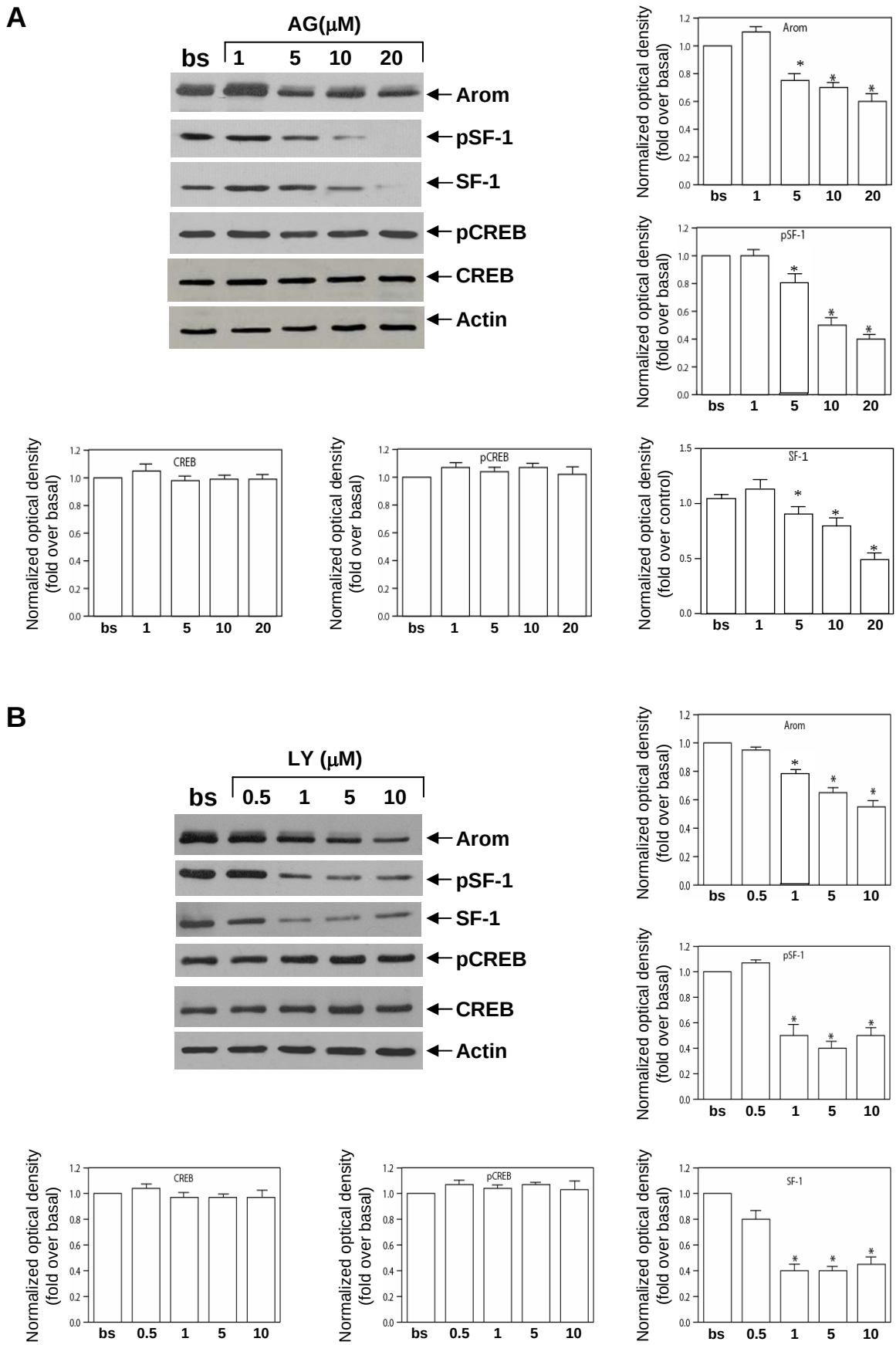
A
AG(μM)
bs
1
5
10
20
Arom
pSF-1
SF-1
pCREB
CREB
Actin
Normalized optical density (fold over basal)
Normalized optical density (fold over control)
B
LY (μM)
0.5

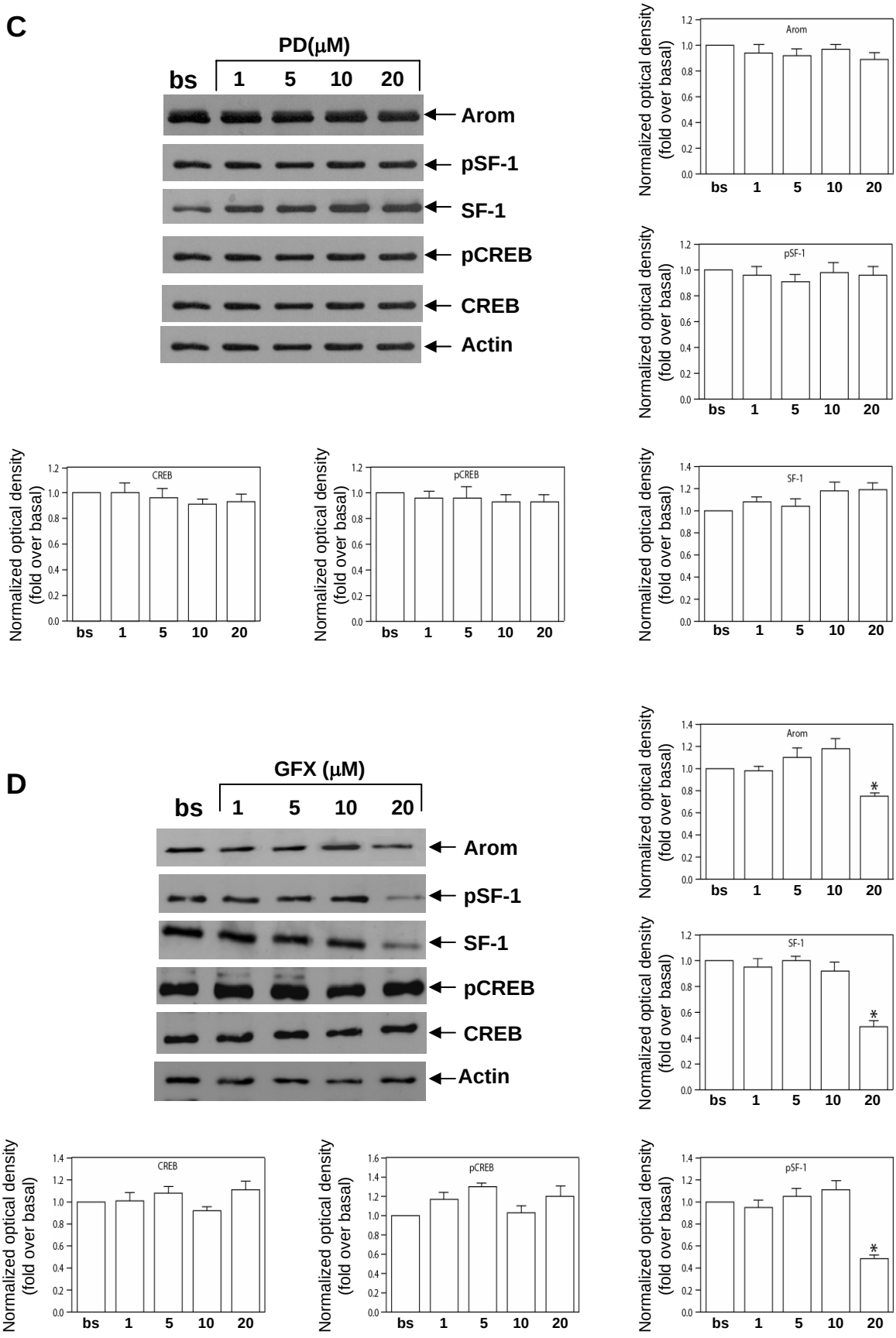
C
PD(μM)
bs
1
5
10
20
Arom
pSF-1
SF-1
pCREB
CREB
Actin
Normalized optical density (fold over basal)
Arom
pSF-1
CREB
pCREB
SF-1
D
GFX (μM)
bs
1
5
10
20
Arom
pSF-1
SF-1
pCREB
CREB
Actin
Normalized optical density (fold over basal)
Arom
SF-1
CREB
pCREB
pSF-1
*

FIG. 9

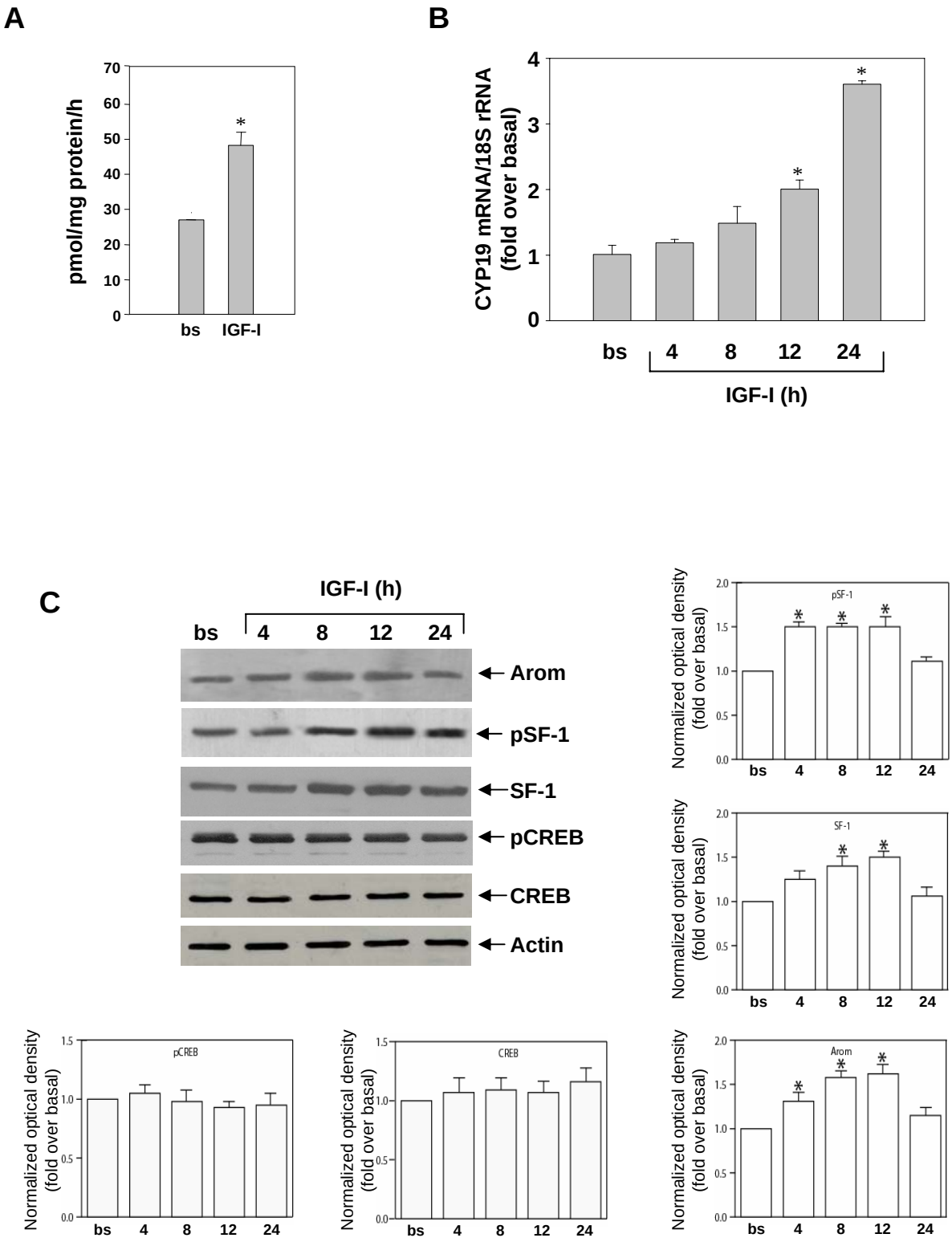
A
pmol/mg protein/h
70
60
50
40
30
20
10
0
*
bs
IGF-I
B
CYP19 mRNA/18S rRNA
(fold over basal)
4
3
2
1
0
*
*
bs
4
8
12
24
IGF-I (h)
C
IGF-I (h)
bs
4
8
12
24
Arom
pSF-1
SF-1
pCREB
CREB
Actin
Normalized optical density
(fold over basal)
pSF-1
SF-1
pCREB
CREB
Arom
2.0
1.5
1.0
0.5
0.0
bs
4
8
12
24

FIG. 10

A

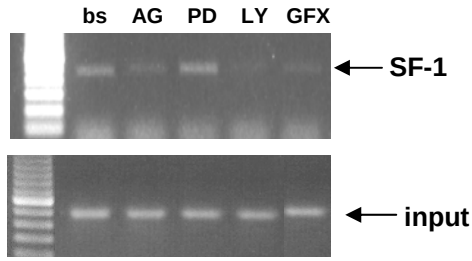

B

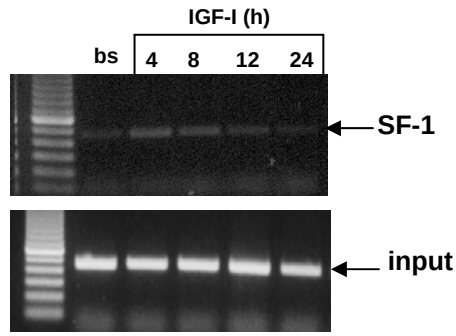

FIG. 11

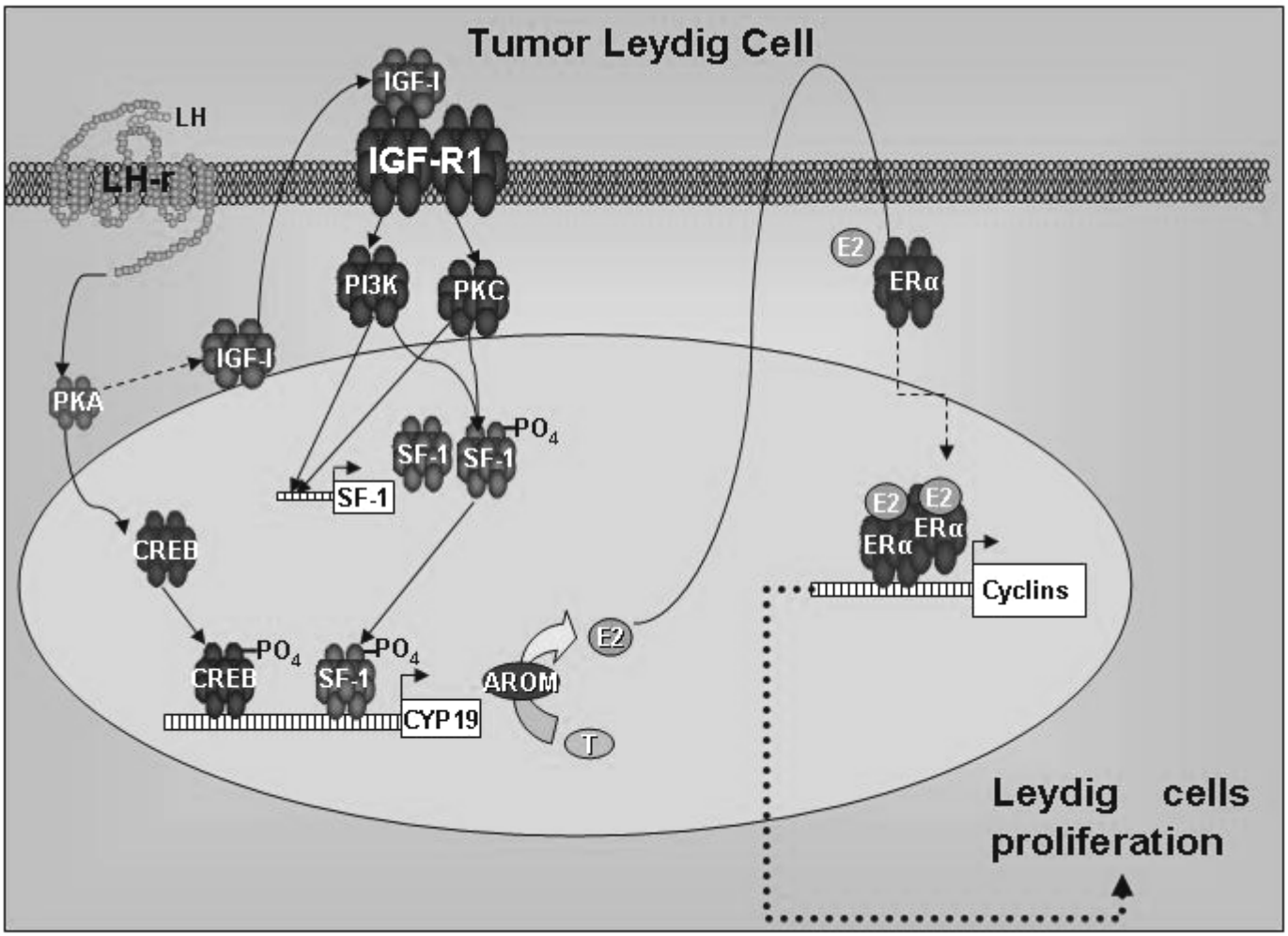
Tumor Leydig Cell
IGF-I
LH
IGF-R1
LH-r
PI3K
PKC
E2
ERα
IGF-I
PKA
SF-1
SF-1
PO4
SF-1
CREB
E2
E2
ERα
ERα
Cyclins
CREB
PO4
SF-1
PO4
AROM
E2
CYP19
T
Leydig cells proliferation